U. S. Department
of Transportation
**United States
Coast Guard**

Report of the International Ice Patrol in the North Atlantic

Marine Biological Laboratory
LIBRARY
AUG 30 1989
Woods Hole, Mass.

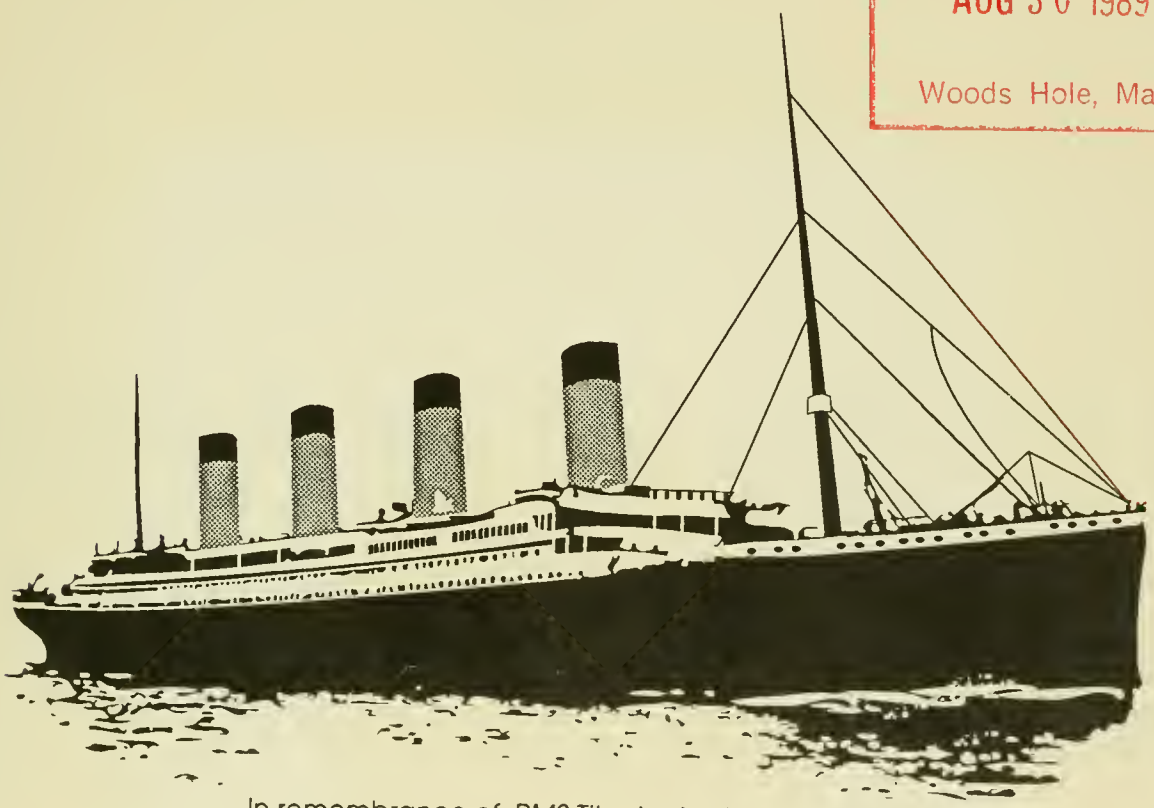

In remembrance of *RMS Titanic* April 14-15, 1912.

1987 Season
Bulletin No. 73
CG-188-42

Bulletin No. 73

REPORT OF THE INTERNATIONAL ICE PATROL SERVICES IN THE NORTH ATLANTIC OCEAN

Season of 1987

CG-188-42

Marine Biological Laboratory
LIBRARY
AUG 30 1989
Woods Hole, Mass.

FOREWARD

Forwarded herewith is bulletin No. 73 of the International Ice Patrol describing the Patrol's services, ice observations and conditions during the 1987 season.

R. T. NELSON
Chief, Office of Navigation Safety
and Waterway Services

DISTRIBUTION - SDL No. 126

	a	b	c	d	e	f	g	h	i	j	k	l	m	n	o	p	q	r	s	t	u	v	w	x	y	z
A																										
B	*3	*1	*1		2					1				2	2		1									
C	*1																*1									
D																							60			
E																										
F																										
G																										
H																										

Non-Standard Distribution: *B:a G-NIO only, *B:b LANTAREA (5), B:b PACAREA (1), B:c First, Fifth Districts Only, *C:a Elizabeth City only, *C:q LANATAREA only, SML CG-4

Introduction

This is the 73rd annual report of the International Ice Patrol Service in the North Atlantic. This report contains information on Ice Patrol operations, environmental conditions, and ice conditions for 1987. The U.S. Coast Guard conducts the International Ice Patrol Service in the North Atlantic under the provisions of U.S. Code, Title 46, Sections 738, 738a through 738d, and the International Convention for the Safety of Life at Sea (SOLAS), 1974, regulations 5-8. This service was initiated shortly after the sinking of the RMS TITANIC on April 15, 1912.

Commander, International Ice Patrol, working under Commander, Coast Guard Atlantic Area, directs the International Ice Patrol from offices located at Groton, Connecticut. The International Ice Patrol analyzes ice and environmental data, prepares the daily ice bulletins and facsimile charts, and replies to any requests for special ice information. It also controls the aerial Ice Reconnaissance Detachment and any surface patrol cutters when assigned, both of which patrol the southeastern, southern, and southwestern limits of the Grand Banks of Newfoundland for icebergs. The International Ice Patrol makes twice-daily radio broadcasts to warn mariners of the limits of iceberg distribution.

Vice Admiral D. C. Thompson was Commander, Atlantic Area, and LCDR S. R. Osmer was Commander, International Ice Patrol, during the 1987 ice season.

Summary of Operations, 1987

From March 12 to July 31, 1987, the International Ice Patrol (IIP), a unit of the U.S. Coast Guard, conducted the International Ice Patrol Service, which has been provided annually since the sinking of the RMS TITANIC on April 15, 1912. During past years, Coast Guard ships and/or aircraft have been patrolling the shipping lanes off Newfoundland within the area delineated by 40°N - 52°N, 39°W - 57°W, detecting icebergs, and warning mariners of these hazards. During 1987, Coast Guard HC-130 aircraft flew 53 ice reconnaissance sorties, logging over 368 flight hours. The AN/APS-135 Side-Looking Airborne Radar (SLAR), which was introduced into Ice Patrol duty during the 1983 season, again proved to be an excellent all-weather tool for the detection of both icebergs and sea ice.

Aircraft deployments were made on January 25 to February 4 and February 27 to March 6 to determine the pre-season iceberg distribution. For the first time, these pre-season surveys were made jointly with the Ice Branch of the Atmospheric Environment Service (AES) of Canada. This was the first season since 1978 that IIP has conducted a pre-season census of icebergs north of 52°N and the first pre-season census ever done using SLAR. Figures 1 and 2 show the iceberg distribution north of 52°N from these two surveys. This cooperative census with SLAR allowed a wider look at the pre-season iceberg distribution than in

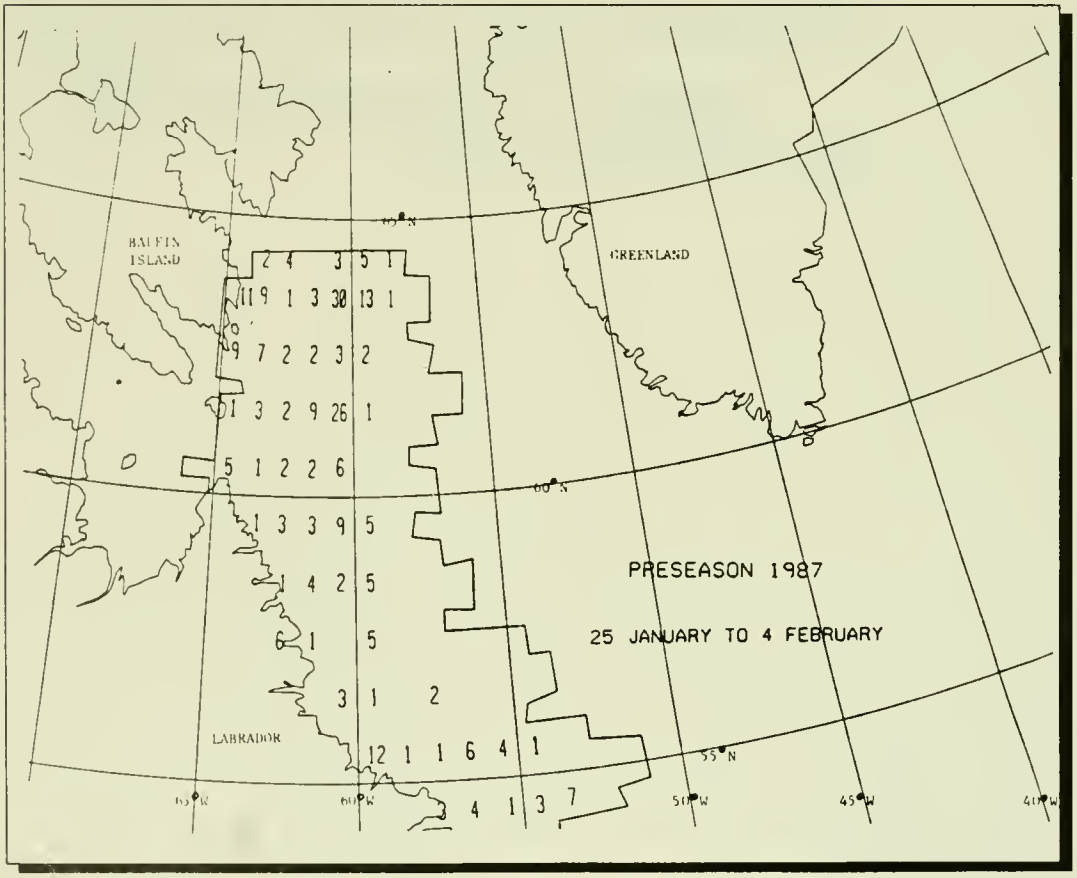

Figure 1. Area of iceberg census and iceberg count January 25 to February 4, 1987. Numbers shown are number of icebergs per 1° latitude by 1° longitude square.

previous years. These AES-IIP joint surveys will continue in the future whenever it is mutually beneficial.

Based on the second pre-season deployment, the 1987 season opened on March 12 and regular aircraft deployments started on March 18. From the later date until August 2, 1987, an aerial Iceberg Reconnaissance Detachment (ICERECDET) operated from Gander, Newfoundland, one week out of every two. The season officially closed on July 31, 1987.

Watchstanders at IIP's Operations Center in Groton, Connecticut, analyze the iceberg sighting information from the ICERECDET, along with sighting information from commercial shipping and AES sea ice/iceberg reconnaissance flights. Only those iceberg sightings within IIP's operations area (40°N - 52°N, 39°W - 57°W) are entered into the IIP iceberg drift prediction computer model (ICEPLOT). The watchstanders determine whether each sighting is a resight of an iceberg IIP already has on ICEPLOT, or whether the sighting is a sighting of a new iceberg which had not been previously reported. Iceberg sightings near the Newfoundland coast are not entered into the computer model due to lack of current information in the model in these areas to drift the icebergs. Each sighting is labelled in the computer model as either a resight or a new sighting. During the 1987 ice year, 755 icebergs were sighted in IIP's operations area (south of 52°N), compared to 415 icebergs in the 1986 ice year.

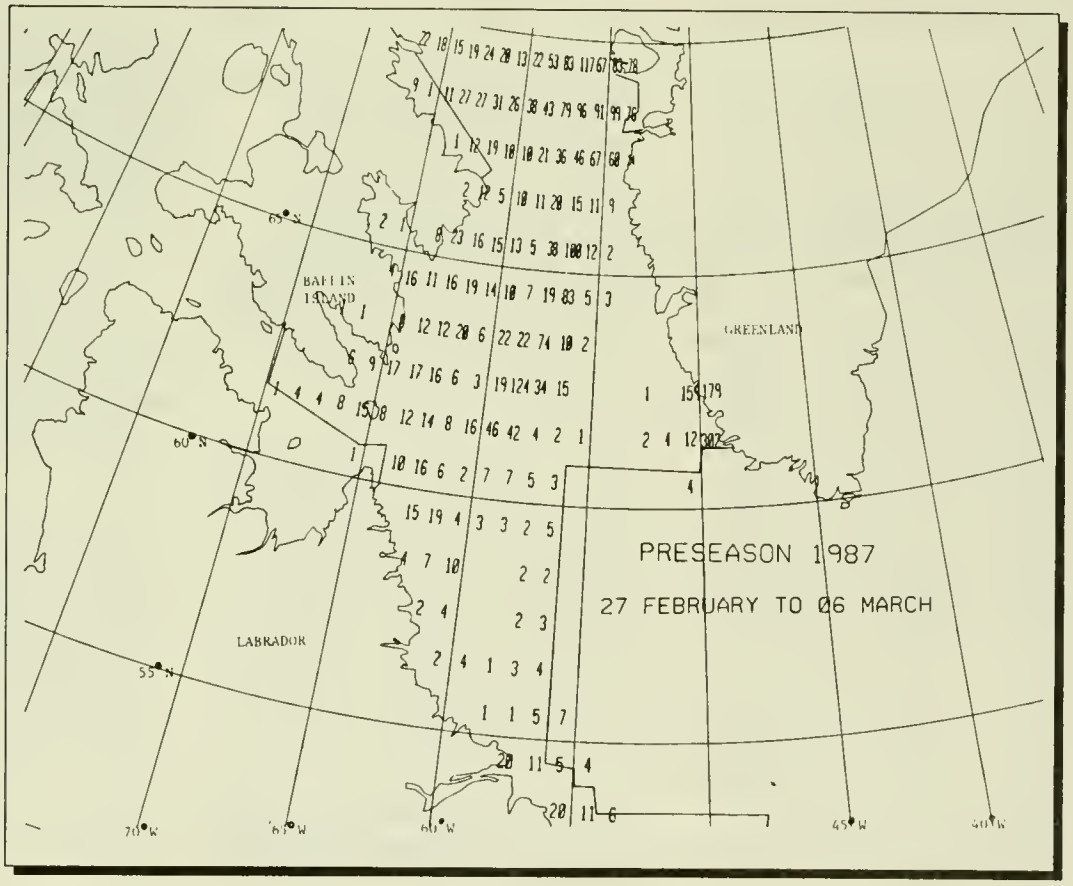

Figure 2. Area of iceberg census and iceberg count February 7 to March 6, 1987. Numbers shown are number of icebergs per 1° latitude by 1° longitude square.

Table 1. Source of International Ice Patrol Iceberg Reports by Size.

Sighting Source	Growler	Small	Medium	Large	Radar Target	Total	Percent of Total
Coast Guard SLAR	29	94	82	30	12	247	12.9
Coast Guard Visual	40	94	85	26	0	245	12.8
CanadianSLAR	2	34	23	12	245	316	16.6
Canadian Visual	11	253	124	49	0	437	22.9
Ship Radar	5	5	18	3	49	80	4.2
Ship Visual	43	95	195	61	0	394	20.6
Offshore Oil Industry	9	35	24	8	4	80	4.2
Lighthouse/Shore	0	0	1	0	0	1	0.1
DOD Sources	0	14	53	34	0	101	5.3
Other	0	4	1	0	3	8	0.4
Total	139	628	606	223	313	1909	100.0

IIP's computer model consists of a routine which predicts the drift of each iceberg, and a routine which predicts the deterioration of each iceberg. The drift prediction program uses a historical current data file to drift the icebergs. This historical data file is modified weekly using satellite-tracked ocean drifting buoy data to take into account local, short-term current fluctuations. Murphy and Anderson (1985) describe the IIP drift model in more detail, along with an evaluation of the model which was conducted in 1985.

The IIP iceberg deterioration program uses daily wind, sea surface temperature, and wave height information from the U.S. Navy Fleet Numerical Oceanography Center to melt the icebergs. Anderson (1983) describes the IIP deterioration model in detail. It is the ability of the SLAR to detect icebergs in all weather, and the IIP's computer models to estimate iceberg drift and deterioration, which has enabled IIP to reduce its ICERECDET operations from weekly deployments to every other week deployments.

Table 1 shows the total iceberg sightings reported to IIP in 1987 (including re-sights), broken down by the sighting source and iceberg size. The number of iceberg sightings shown in Table 1 are only those which were in IIP's operations area and away from the Newfoundland coast. For example, more than one iceberg sighting was received from the Canadian lighthouses, but since most were nearshore, only one was entered into IIP's computer model. Appendix A lists all iceberg sightings received from commercial shipping, regardless of the sighting location.

The SLAR continued to be an important instrument in iceberg detection in 1987. IIP and Canadian (AES) SLAR observations accounted for 29.5 percent of all 1987 iceberg reports (Table 1). Visual and SLAR observations from Canadian (AES) sea ice/iceberg reconnaissance flights accounted for 39.5 percent of all 1987 iceberg reports. This is a significant increase from the past, representing greater emphasis on iceberg reporting by AES, and again indicating the increased mutually-beneficial cooperation between IIP and AES.

Table 2 shows monthly estimates of the total number of icebergs that crossed 48°N for the pre-International Ice Patrol era, and for the ship, aircraft visual, and aircraft SLAR reconnaissance eras. Table 3 compares the estimated number of icebergs crossing 48°N for each month of 1987 with the monthly mean number of icebergs crossing 48°N for each of the four different eras.

During the 1987 ice year, an estimated 318 icebergs drifted south of 48°N latitude, compared to 204 icebergs drifting south of 48°N during 1986. The number of icebergs crossing 48°N during 1987 was less than the SLAR reconnaissance era average. It is important to note, however, that this average is based on only four years of data. The average number of icebergs drifting south of 48°N from 1913 to 1987 is 395 icebergs (Appendix B). With 318 icebergs drifting south of 48°N, 1987 was deemed an intermediate or average ice year (Appendix B).

April 15, 1987, marked the 75th anniversary of the sinking of the RMS TITANIC. A memorial wreath was placed near the site of the sinking during an ice reconnaissance patrol to commemorate the nearly 1500 lives lost.

Table 2. Total Icebergs South of 48° N - The four periods shown are pre-International Ice Patrol (1900-1912), ship reconnaissance (1913-1945), aircraft visual reconnaissance (1946-1982), and SLAR reconnaissance (1983-1986).

	Total 1900-12	Total 1913-45	Total 1946-82	Total 1983-86	1987
OCT	27	80	2	3	0
NOV	13	93	4	11	0
DEC	38	42	11	9	5
JAN	33	87	65	11	2
FEB	79	372	273	225	14
MAR	898	1204	1172	394	48
APR	1537	3308	3131	1560	76
MAY	1611	5472	2993	1213	29
JUN	1004	2514	1865	666	127
JUL	423	773	489	552	15
AUG	160	229	100	136	2
SEP	58	188	10	41	0
Total	5,881	14,362	10,115	4,821	318

Table 3. Average Number of Icebergs South of 48° N - The four periods shown are pre-International Ice Patrol (1900-1912), ship reconnaissance (1913-1945), aircraft visual reconnaissance (1946-1982), and SLAR reconnaissance (1983-1986).

	Avg 1900-12	Avg 1913-45	Avg 1946-82	Avg 1983-86	1987
OCT	2	2	0	1	0
NOV	1	3	0	3	0
DEC	3	1	0	2	5
JAN	2	3	2	3	2
FEB	6	11	7	56	14
MAR	69	36	32	98	48
APR	118	100	85	390	76
MAY	124	166	81	303	29
JUN	77	76	50	166	127
JUL	32	23	13	138	15
AUG	12	7	3	34	2
SEP	4	6	0	10	0
Era Average	452	435	273	1204	318

From March 23-25, IIP participated in the Labrador Ice Margin EXperiment (LIMEX) '87. This international experiment involved four remote sensing aircraft and a surface vessel. LIMEX '87 was a pilot study for the full experiment effort scheduled for 1989. The three objectives of LIMEX '87 were the verification of remote sensing algorithms for active and passive microwave sensors with the aim of applying these to future satellite-borne sensors, the investigation of oceanographic conditions in the marginal ice zone, and the determination of the characteristics of the Labrador ice pack in the region of maximum southerly advance. The IIP aircraft provided SLAR mosaics of the pack ice and the ice edge which were collected during the course of regular reconnaissance patrols.

Eleven satellite-tracked oceanographic drifters were deployed to provide operational data for IIP's iceberg drift model. Six of these drifters belonged to AES and were deployed by IIP. AES and IIP each had access to the data these eleven drifters provided. The drifters' data are discussed in Appendix C.

No U. S. Coast Guard cutters were deployed to act as surface patrol vessels this year. Two cruises were performed during the 1987 season to conduct oceanographic research for the Ice Patrol. The first was conducted from U.S. Coast Guard Cutter (USCGC) BITTERSWEET (WLB-389) during the period April 27 through May 26. The primary objective of this cruise was to study water mass and frontal boundary identification in conjunction with the SLAR. The second cruise was conducted from USCGC TAMAROA (WMEC-166) during the period June 8-27. The primary objectives of this cruise were to compare the environmental inputs to the IIP's iceberg drift and deterioration model with observed conditions, and evaluate any errors in the model. The results of these studies are presented in Appendices D, E, and F.

These cruises were the first deployments of IIP's transportable oceanographic equipment, including a Mobile Oceanographic Laboratory, portable hydrographic winch, and A-frame platform. This transportable equipment allows IIP to perform oceanographic research from many types of Coast Guard cutters. Alles and Alfultis (1988) discuss the assembly and operation of this system in detail.

Iceberg Reconnaissance and Communications

During the 1987 Ice Patrol year (from October 1, 1986, through September 30, 1987), 80 aircraft sorties were flown in support of the International Ice Patrol. These included pre-season flights, ice reconnaissance flights during the season, post-season flights, and logistics flights. Pre-season flights determined iceberg concentrations north of 48°N. These iceberg concentrations were needed to estimate when icebergs would threaten the North Atlantic shipping lanes in the vicinity of the Grand Banks of Newfoundland. During the active season, ice reconnaissance flights located the southwestern, southern, and southeastern limits of icebergs. Logistics flights were necessary to support patrol aircraft with aircraft maintenance problems. Post-season flights were made to check on the iceberg distribution, to retrieve parts and equipment from Gander, and to close out all business transactions from the season.

U.S. Coast Guard aircraft, deployed from Coast Guard Air Station Elizabeth City, North Carolina, conducted all the aircraft missions. Aerial ice reconnaissance was conducted solely with SLAR-equipped HC-130H aircraft. HC-130H and HU-25A aircraft were used on logistics flights. Table 4 shows aircraft use during the 1987 season.

Table 4. Aircraft use during the 1987 IIP Year (October 1, 1986 - September 30, 1987)

Aircraft Deployment	Sorties	Flight Hours
Pre-season	14	69.9
Regular Season	58	370.2
Post season	8	38.0
Total	80	478.1

Iceberg Reconnaissance Sorties by Month

Month	Sorties	Flight Hours
Jan	1	4.7
Feb	2	13.5
Mar	11	81.4
Apr	6	43.4
May	13	90.3
Jun	10	69.3
Jul	7	46.8
Aug	3	19.5
Total	53	368.9

Table 5. Iceberg and SST Reports.

Number of ships furnishing Sea Surface Temperature (SST) reports	91
Number of SST reports received	416
Number of ships furnishing ice reports	256
Number of ice reports received	505
First Ice Bulletin	120000Z MAR87
Last Ice Bulletin	311200Z JUL 87
Number of facsimile charts transmitted	141

The IIP prepares the ice bulletin warning mariners of the southwestern, southern, and southeastern limits of icebergs twice a day for broadcast at 0000Z and 1200Z. The IIP also prepares a facsimile chart graphically depicting these limits for broadcast at 1600Z. U.S. Coast Guard Communications Station Boston, Massachusetts, NMF/NIK, was the primary radio station used for the dissemination of the daily ice bulletins and facsimile charts . Other transmitting stations for the 0000Z and 1200Z ice bulletins included Canadian Coast Guard Radio Station St. John's, Newfoundland/VON; Canadian Forces Meteorological and Oceanographic Center (METOC) Halifax, Nova Scotia/CFH; and U.S. Navy LCMP Broadcast Stations Norfolk/NAM; Thurso, Scotland; and Keflavik, Iceland.

Canadian Forces METOC, Halifax/CFH, as well as AM Radio Station Bracknell, United Kingdom/GFE, are radiofacsimile broadcasting stations which used International Ice Patrol limits in their broadcasts. Canadian Coast Guard Radio Station St. John's/ VON and U.S. Coast Guard Communications Station Boston/NIK provided special broadcasts.

The International Ice Patrol transmissions requested that all ships transiting the area of the Grand Banks report ice sightings, weather, and sea surface temperatures via the above communications/radio stations. Response to this request is shown in Table 5, and Appendix A lists all contributors. Commander, International Ice Patrol extends a sincere thank you to all stations and ships which contributed.

Environmental Conditions 1987 Season

The wind direction along the Labrador and Newfoundland coasts can affect the iceberg severity of each year. The mean wind flow can influence iceberg drift. Dependent upon wind intensity and duration, icebergs can be accelerated along or driven out of the main flow of the Labrador Current. Departure from the Labrador Current normally slows their southerly drift, and in many cases speeds up their rate of deterioration.

The wind direction and air temperature affect the iceberg severity of each year in an indirect way by influencing the extent of sea ice. Sea ice protects the icebergs from wave action, the major agent of iceberg deterioration. If the air temperature and wind direction are favorable for the sea ice to extend to the south and over the Grand Banks of Newfoundland, the icebergs will be protected longer as they drift south. When the sea ice retreats in the spring, large numbers of icebergs will be left behind on the Grand Banks. Also, if the time of sea ice retreat is delayed by below normal air temperatures, the icebergs will be protected longer, and a longer than normal ice season can usually be expected. The opposite is true if the southerly sea ice extent is minimal, or if above normal temperatures cause an early retreat of sea ice from the Grand Banks.

The following discussion summarizes the environmental conditions along the Labrador and Newfoundland coasts for the 1987 ice year. The Gander Airport Weather Office provided the data for Table 6.

January: The mean pressure distribution in Figure 3 shows the Icelandic Low was southwest of its mean position, with stronger than normal pressure gradients surrounding it. The resulting stronger northerly flow brought more Polar Continental air to Labrador causing colder, drier than normal conditions, and more Polar Maritime air to Newfoundland causing colder, wetter conditions (Table 6). The Grand Banks conditions were probably similar to the Newfoundland conditions, colder, wetter than normal.

February: The Icelandic Low remained intense in February and shifted farther to the southwest, bringing a northeasterly flow to Labrador and Newfoundland (Figure 4). The conditions in Labrador were warmer and wetter than normal, while the temperatures on Newfoundland were about normal with above normal precipitation (Table 6). These conditions were caused by the northeasterly flow bringing in large amounts of Polar Maritime air to the region. This maritime air would have a warmer temperature and more moisture than the continental air usually influencing Labrador's weather.

March: The Icelandic Low returned to its usual position and nearly normal intensity for March (Figure 5). In addition to the Icelandic Low, a low pressure trough extended from the Grand Banks south. Conditions in Nain and Gander returned to nearly normal while Goose Bay was drier than normal and St. John's was colder and wetter than normal (Table 6). The northwesterly flow brought dry polar air to Goose Bay instead of the maritime air it is usually influenced by. The low pressure trough off the Grand Banks brought moisture to St. John's from the south. The conditions on the Grand Banks were probably similar to those at St. John's, colder and wetter than normal.

April: The Icelandic Low was more intense than normal for April, and the position of the Bermuda High was more to the northwest than normal (Figure 6). This pressure distribution brought a southwesterly flow to Newfoundland, and a westerly flow to Labrador. The conditions at Newfoundland were warmer and wetter than normal, while the conditions on Labrador were warmer and drier than normal (Table 6). These conditions were caused by the southwesterly flow bringing warmer, moister, maritime air to Newfoundland,

and the westerly flow bringing warmer, drier, continental air to Labrador, instead of the Polar Maritime air usually influencing Newfoundland and Labrador. The conditions over the Grand Banks were likely warmer, wetter, than normal due to the southwesterly flow again bringing warm, moist, air to the Grand Banks from the south.

May: A ridge of high pressure extended across the North Atlantic in May (Figure 7). The resulting southwesterly flow around this ridge brought air from farther south than normal to Newfoundland. This warm, moist air brought warmer than normal temperatures to Newfoundland and southern Labrador (Table 6). The conditions on the Grand Banks were likely to be warmer and moister than normal in May. The colder, wetter, than normal weather at Nain (Table 6) was caused by the low pressure system off of the Labrador coast bringing Polar Maritime air to northern Labrador rather than the warmer, drier, continental air usually influencing the region.

June: With the Bermuda High still farther west than normal in June, the flow of air to Newfoundland was more out the west than normal (Figure 8). This brought cooler, drier, continental air to Newfoundland rather than the warm, moist, maritime air usually coming to the region from south. This resulted in cooler, drier, than normal weather in St. John's and Gander (Table 6). Labrador was also under the influence of the continental air mass, as it usually is, and nearly normal conditions were reported in Nain and Goose Bay.

July: The pressure distribution in July was nearly normal (Figure 9). This distribution brought normal temperatures to Newfoundland (Table 6). The colder, wetter, than normal conditions in northern Labrador were caused by the area of low pressure off of Greenland bringing the cold, but wet, Polar Maritime air to the region rather than the warmer, drier, continental air which normally influences northern Labrador in July.

August: A low pressure trough formed north of Labrador in August (Figure 10). The resulting flow was northerly, rather than the the normal southwesterly flow. This caused conditions in Newfoundland and southern Labrador to be colder and drier than normal (Table 6).

September: September saw the return of the Icelandic Low, deeper than normal, and the diminishing of the Bermuda High (Figure 11). The westerly flow over Newfoundland and Labrador was nearly normal. Conditions on Newfoundland were colder than normal, while the conditions on Labrador were warmer than normal (Table 6).

NOTE: Temperature and precipitation data for Nain, Labrador, are compared to 1985 values in Table 6. The reporting station at Hopedale, Labrador, was closed in 1984 and the Nain station opened. A historical mean for Nain does not exist.

Table 6. Environmental Conditions for the 1987 IIP Year.

	Station	Temp °C Monthly Mean	Temp °C Diff. from Norm.	Total Precipitation (mm)	% of Normal Precipitation	% of Normal Snowfall
OCT 1986	Nain	-1.7	-4.1	42.3	67.4%	
	Goose	0.4	-2.3	88.9	116.1%	87.9%
	Gander	3.8	-2.2	113.4	108.3%	198.4%
	St. John's	5.4	-1.5	157.2	108.0%	50.0%
NOV	Nain	-11.0	-7.8	31.0	54.0%	
	Goose	-10.3	-6.5	71.7	95.3%	152.8%
	Gander	-1.4	-3.2	138.7	129.3%	351.6%
	St. John's	0.7	-2.7	203.1	125.0%	306.1%
DEC	Nain	-14.9	-4.2	29.3	51.7%	
	Goose	-14.4	-1.4	38.1	52.4%	64.1%
	Gander	-5.6	-1.8	68.0	62.8%	82.5%
	St. John's	-3.9	-2.4	80.8	50.1%	77.7%
JAN 1987	Nain	-16.5	-0.7	20.6	33.1%	
	Goose	-17.2	-0.8	14.6	19.6%	26.3%
	Gander	-8.2	-2.0	163.2	149.6%	201.8%
	St. John's	-5.5	-1.6	174.4	111.9%	158.7%
FEB	Nain	-12.9	2.2	178.0	355.3%	
	Goose	-11.6	2.9	131.5	217.0%	257.3%
	Gander	-6.3	0.5	129.1	129.5%	153.8%
	St. John's	-5.0	-0.5	175.1	125.0%	177.5%
MAR	Nain	-11.2	-0.7	60.5	109.2%	
	Goose	-8.1	0.5	35.3	48.9%	42.5%
	Gander	-3.9	-0.4	99.7	90.6%	27.1%
	St. John's	-3.4	-1.1	149.7	113.5%	78.2%
APR	Nain	-1.8	3.1	23.5	50.5%	
	Goose	2.3	4.0	28.5	46.6%	13.4%
	Gander	2.4	1.5	100.7	108.0%	27.6%
	St. John's	2.0	0.8	120.9	104.6%	3.8%
MAY	Nain	1.1	-0.3	58.0	114.4%	
	Goose	6.5	5.3	46.9	73.5%	39.7%
	Gander	7.7	1.5	90.6	129.4%	3.1%
	St. John's	7.4	2.0	79.8	78.4%	10.8%
JUN	Nain	6.4	0.0	44.4	69.5%	
	Goose	11.7	0.4	83.7	89.9%	0%
	Gander	11.1	-0.7	59.6	74.2%	0%
	St. John's	9.8	-1.1	37.9	44.3%	0%
JUL	Nain	8.8	-1.7	110.6	130.9%	
	Goose	15.7	-0.1	105.2	100.1%	*
	Gander	17.3	0.8	10.5	15.2%	*
	St. John's	15.5	0.0	50.8	61.1%	*
AUG	Nain	9.2	-0.5	83.6	121.7%	
	Goose	14.0	-5.3	76.8	74.4%	*
	Gander	15.5	-0.1	51.4	52.8%	*
	St. John's	14.5	-0.8	70.9	58.3%	*
SEP	Nain	7.3	1.4	76.4		
	Goose	10.9	1.8	92.3	109.2%	*
	Gander	10.4	-5.2	68.0	83.7%	*
	St. John's	11.2	-4.7	112.8	100.7%	*

* No snowfall recorded during this month.

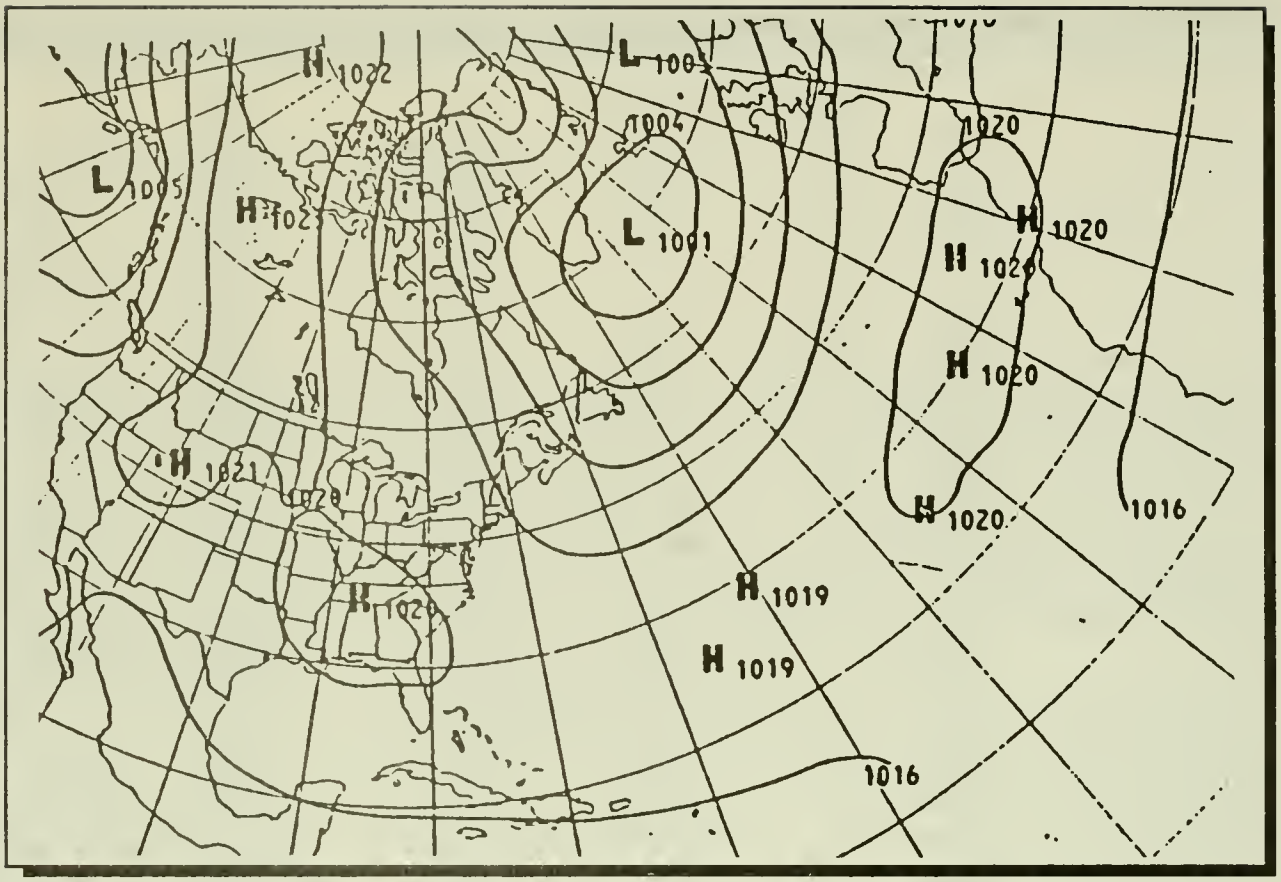

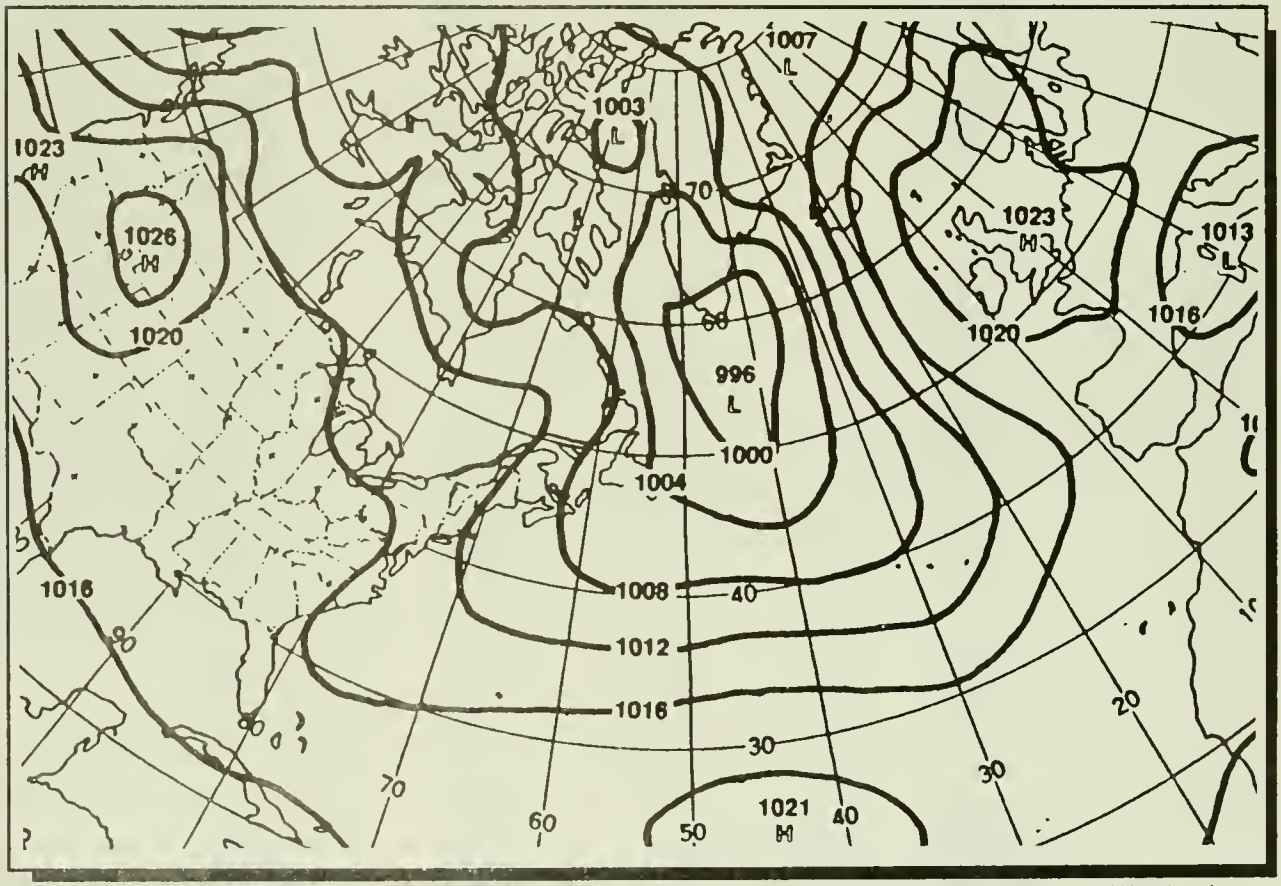

Figure 3. Comparison of January 1987 monthly mean surface pressure in mb (bottom, from Mariner's Weather Log, 1987b) with January historical average, 1948-1970 (top).

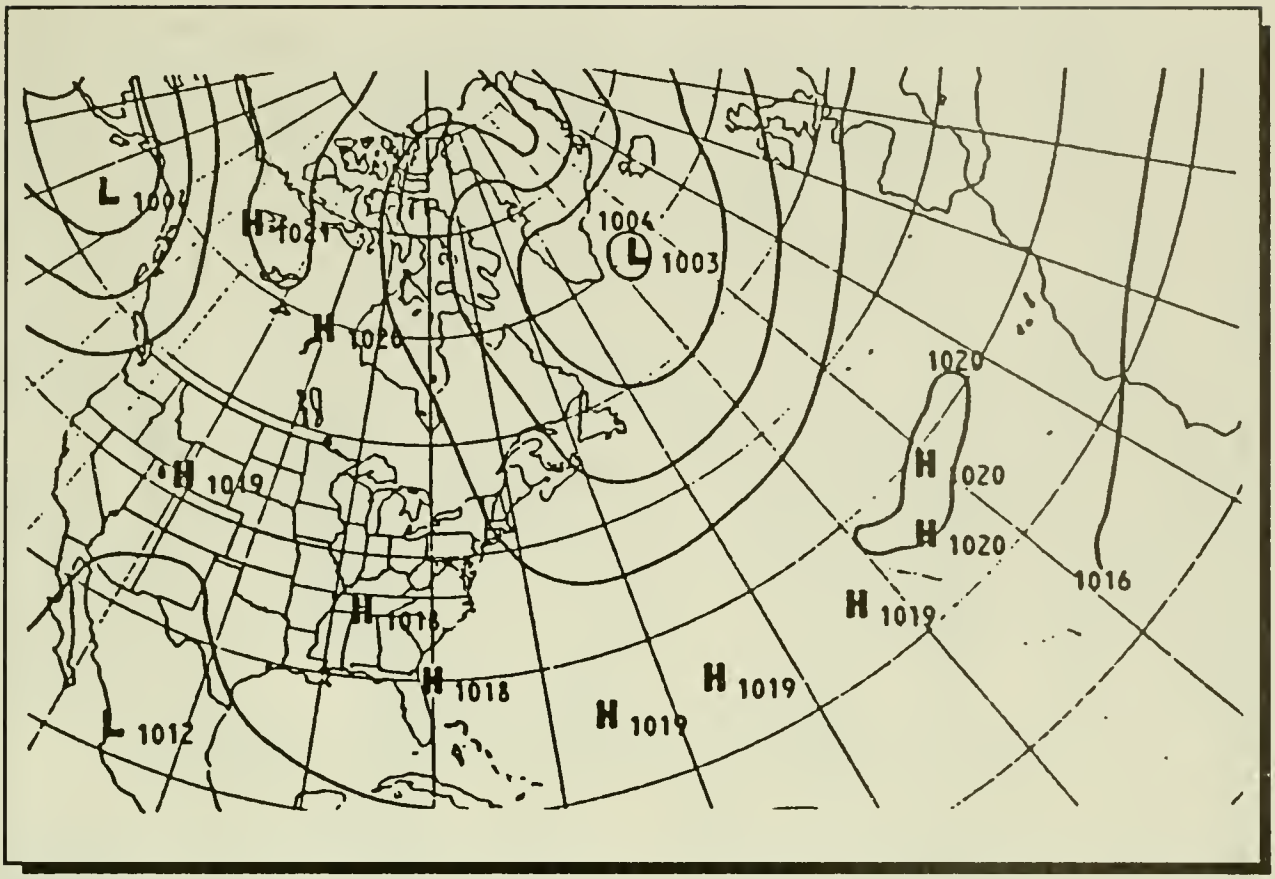

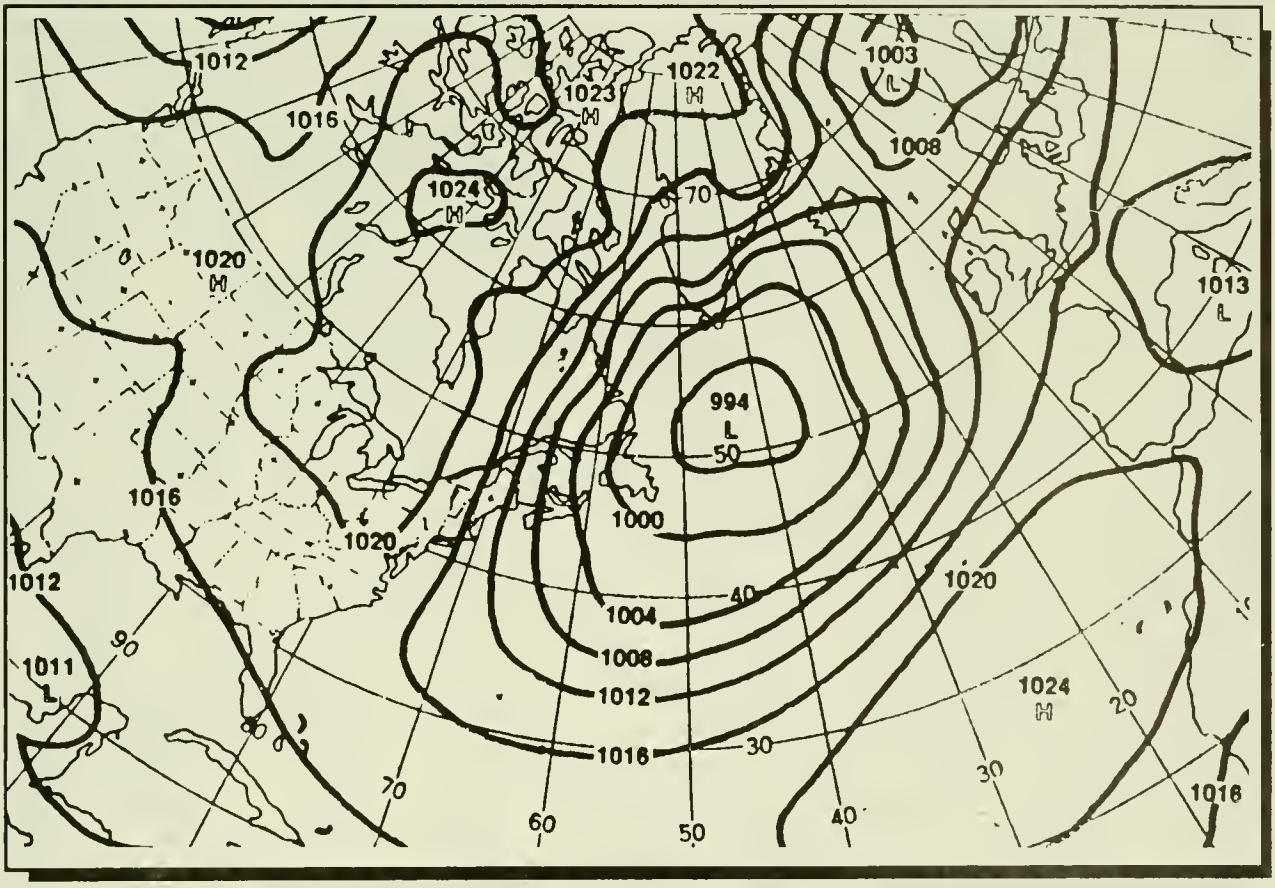

Figure 4. February 1987 (from Mariner's Weather Log, 1987b).

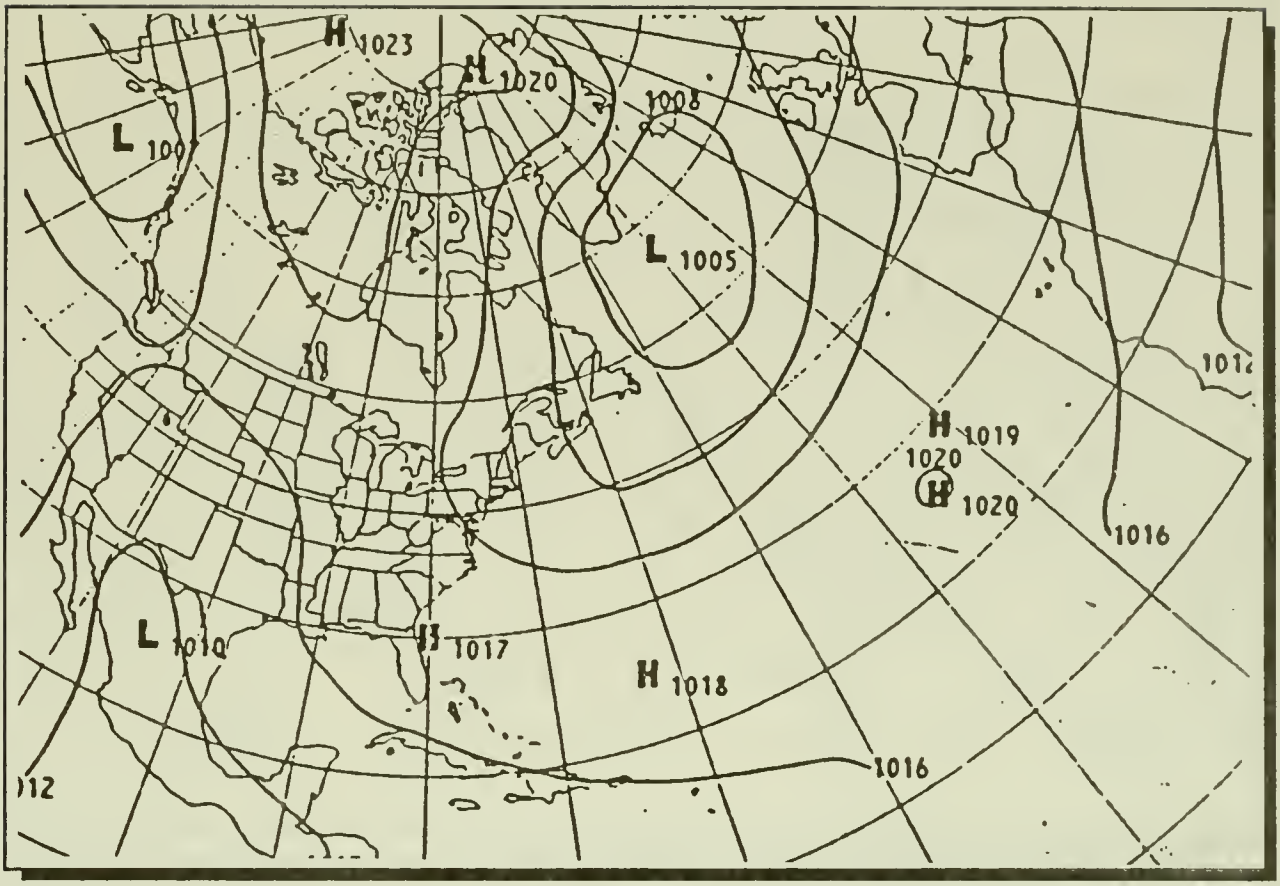

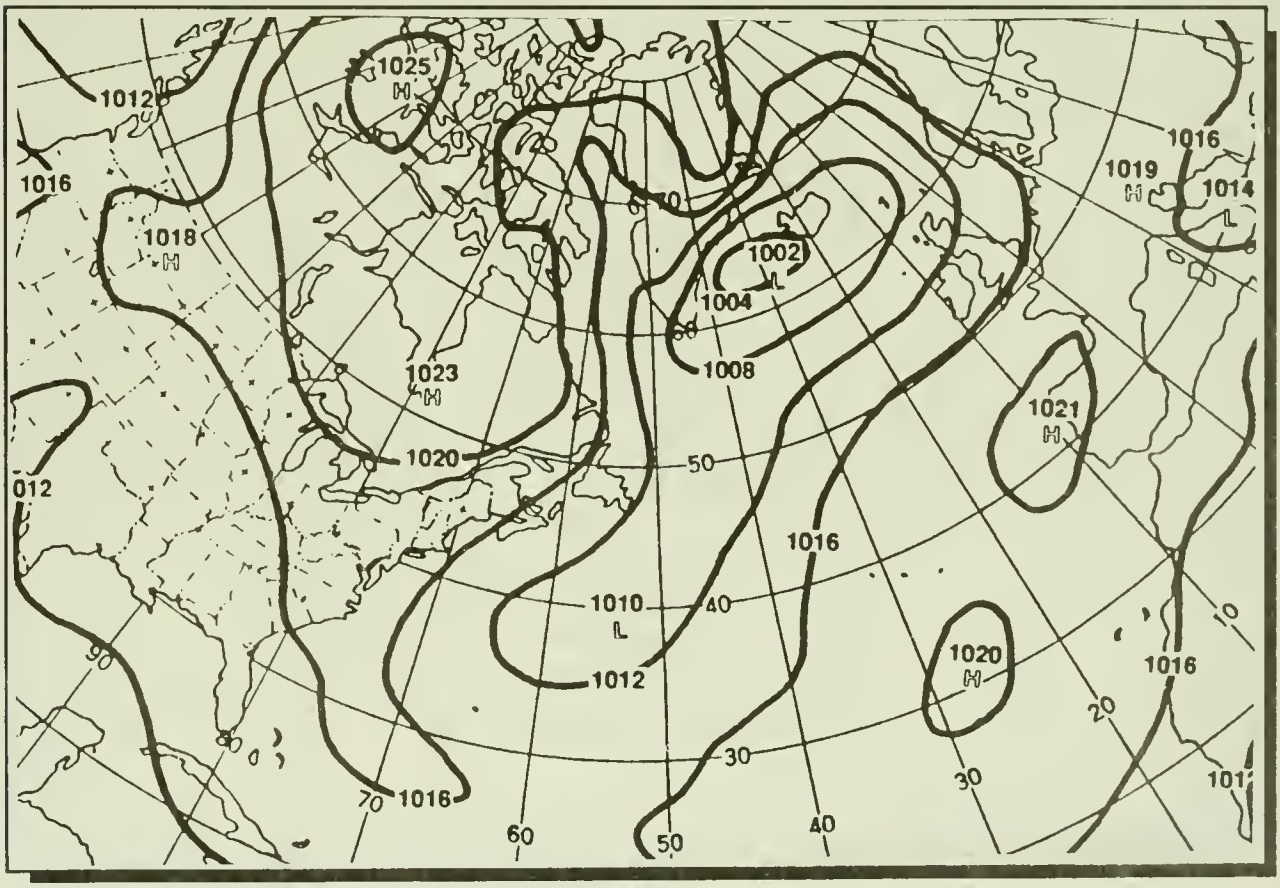

Figure 5. March 1987 (from Mariner's Weather Log, 1987b).

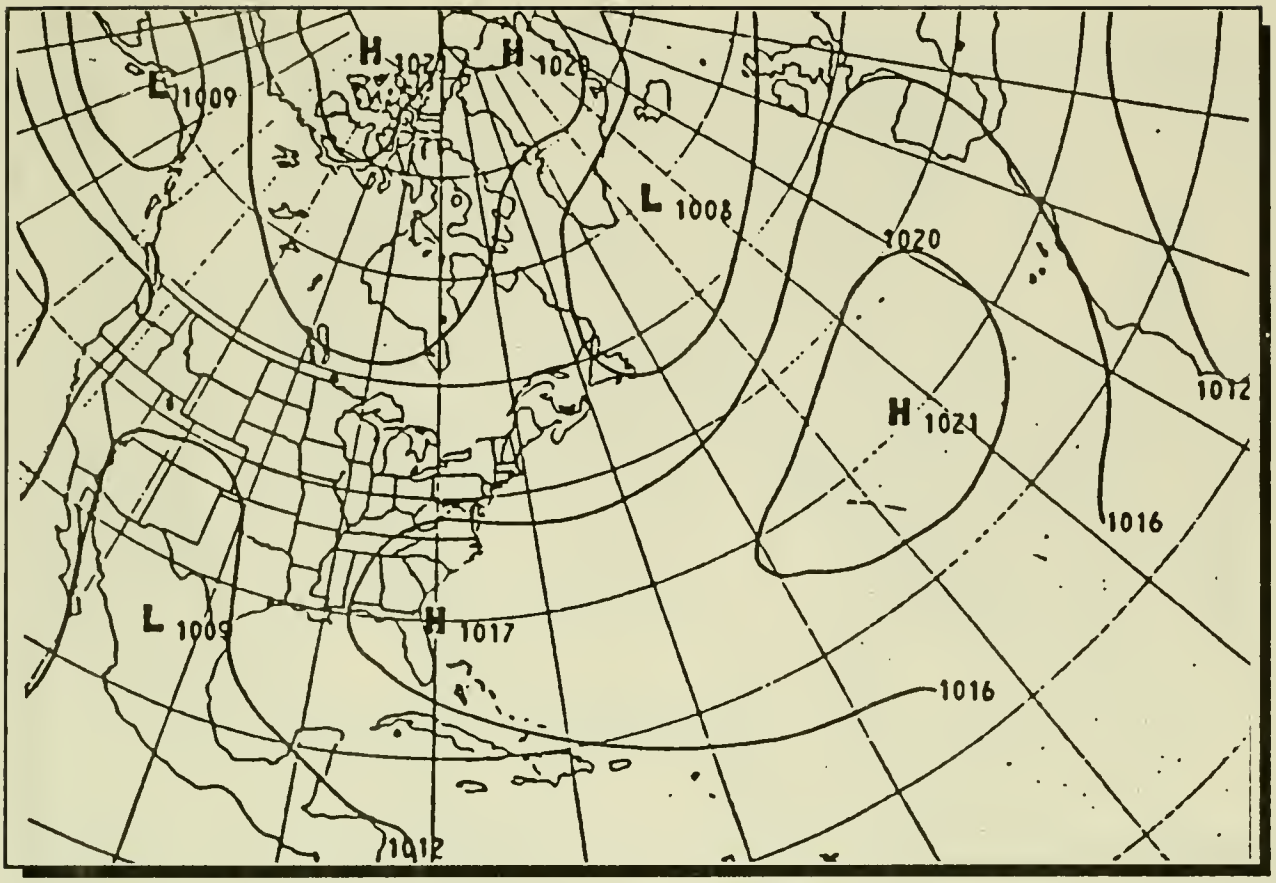

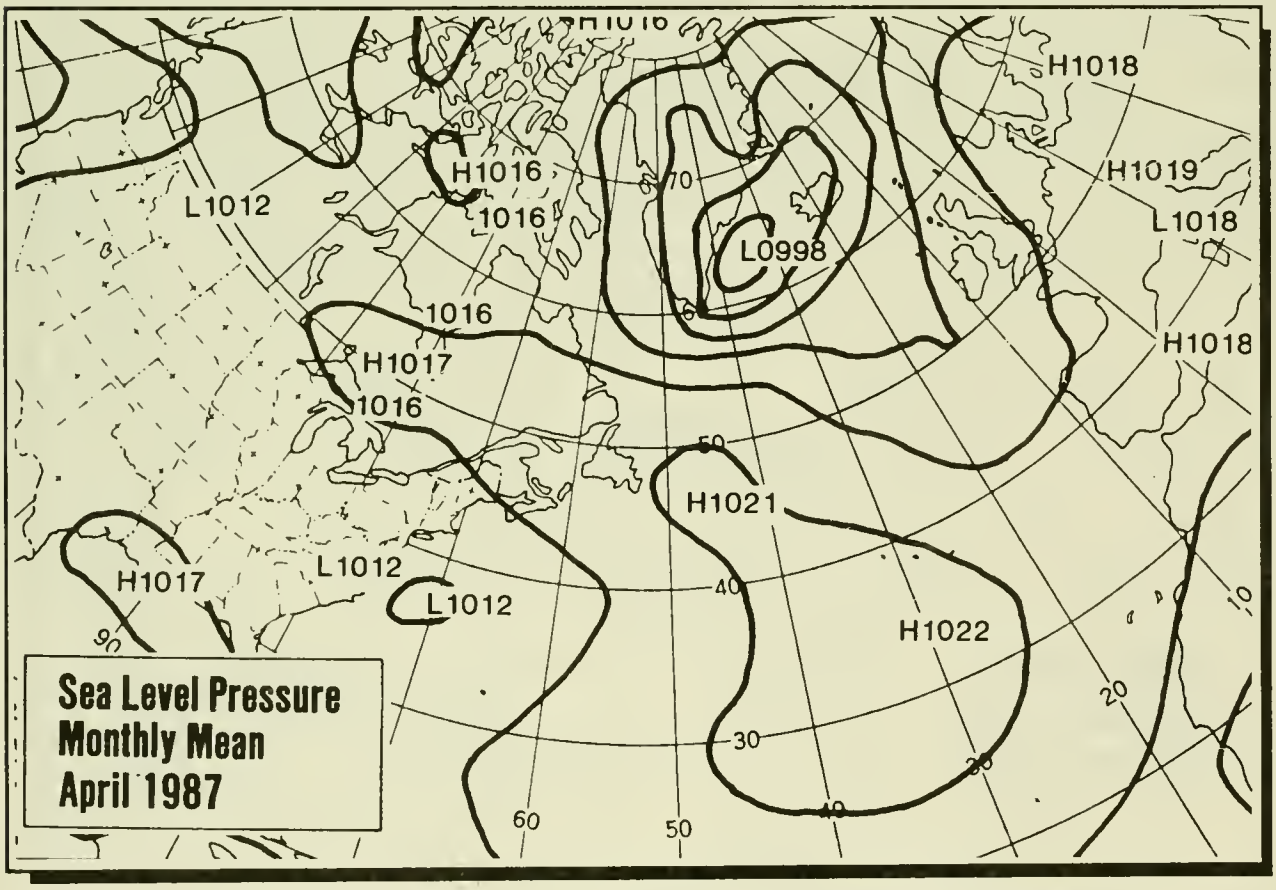

Figure 6. April 1987 (from Mariner's Weather Log, 1987c).

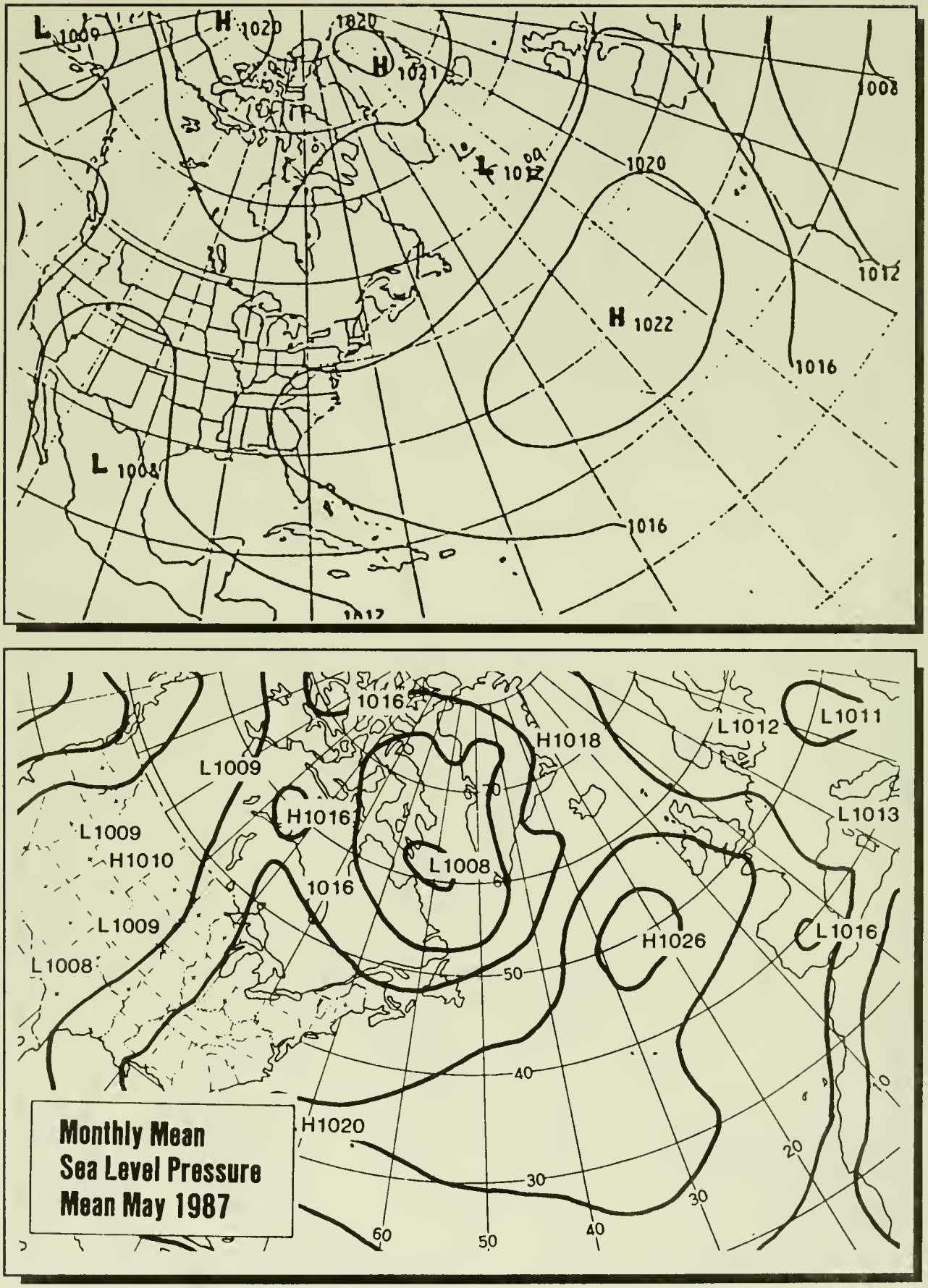

Figure 7. May 1987 (from Mariner's Weather Log, 1987c).

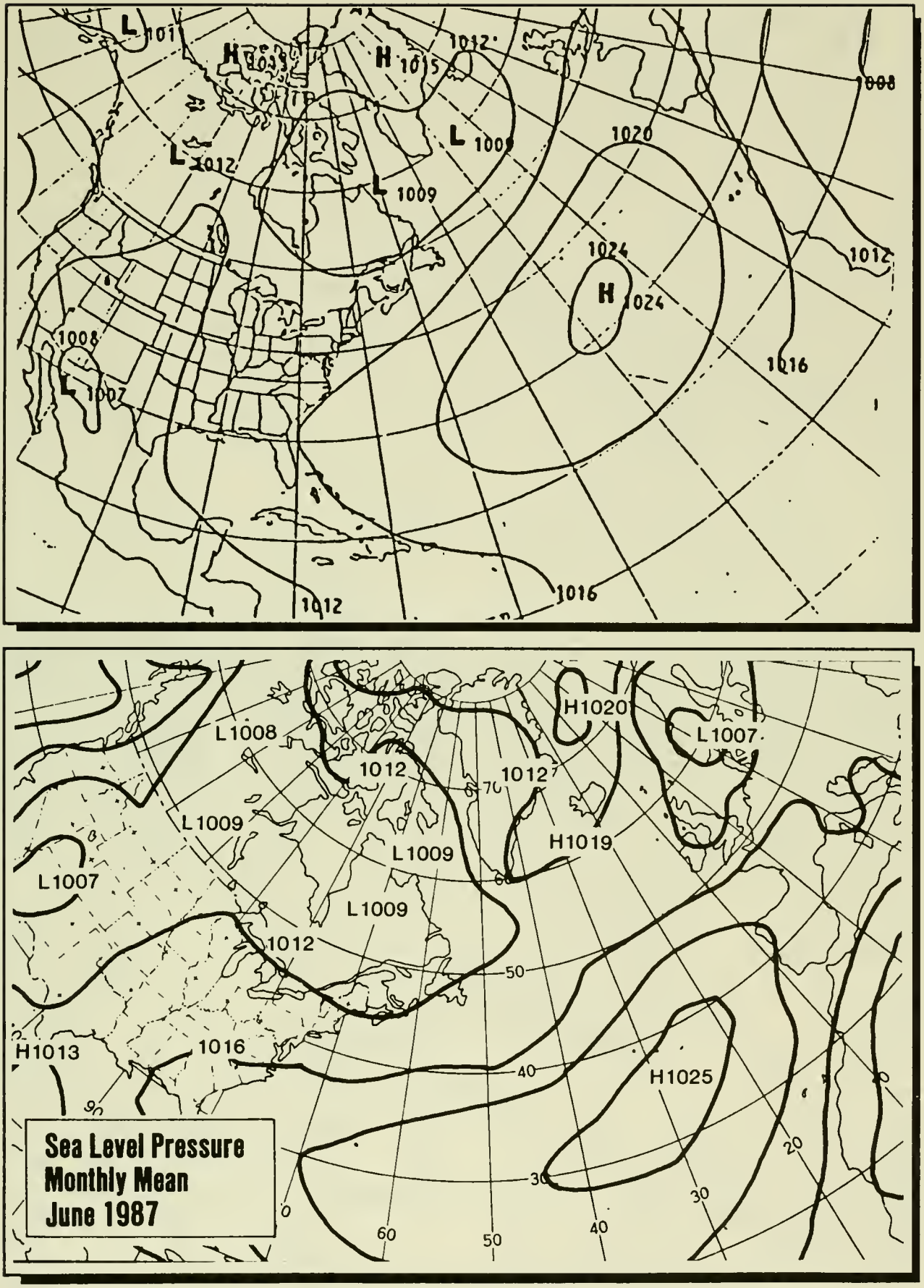

Figure 8. June 1987 (from Mariner's Weather Log, 1987c).

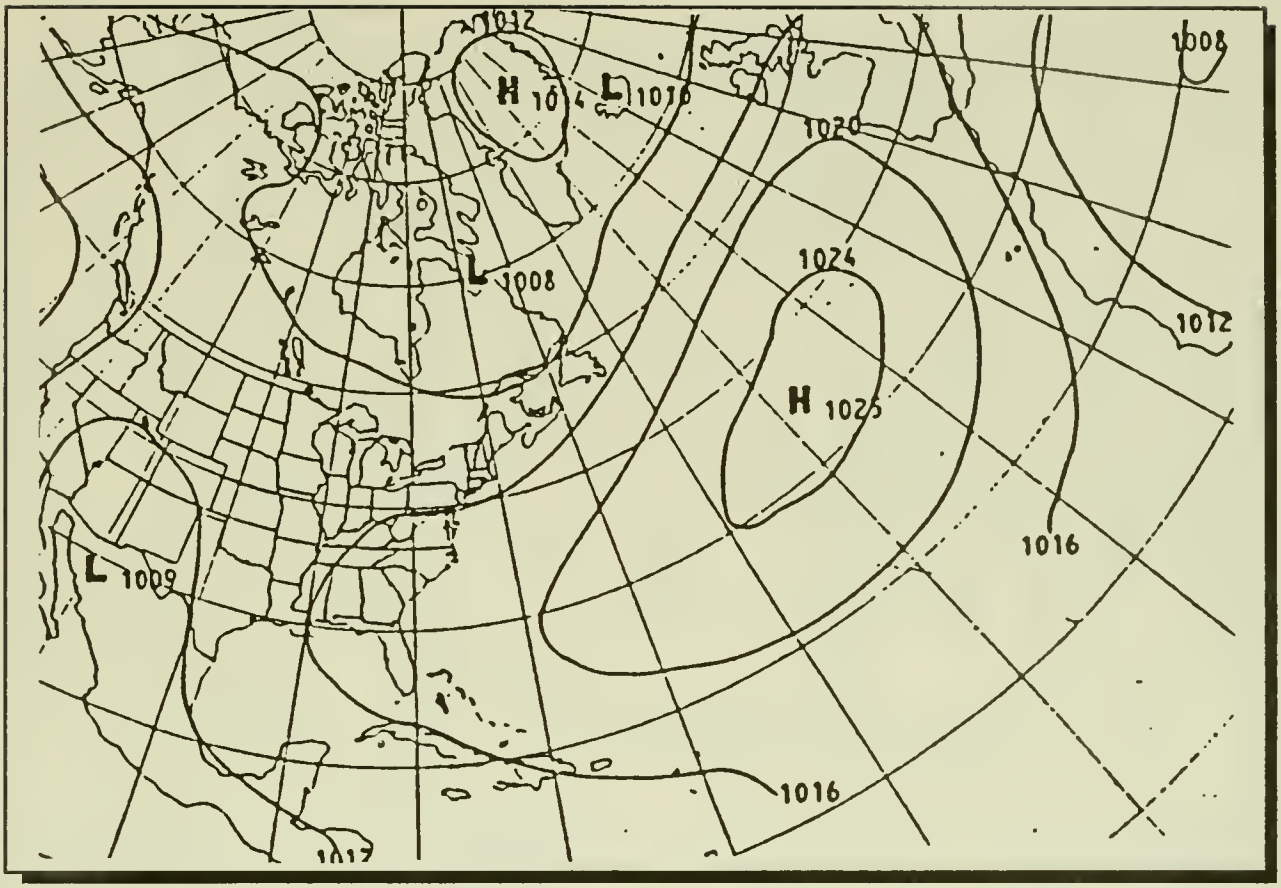

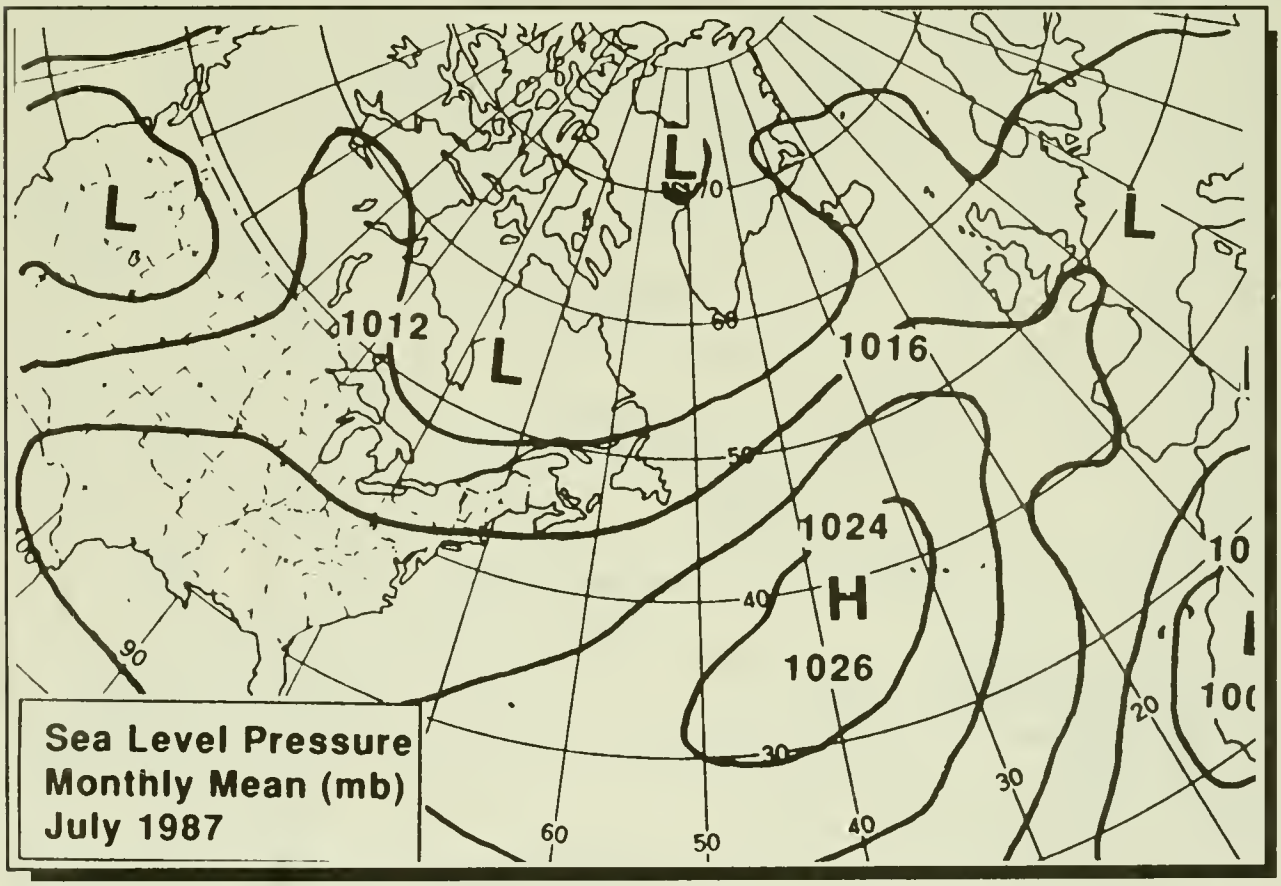

Figure 9. July 1987 (from Mariner's Weather Log, 1988).

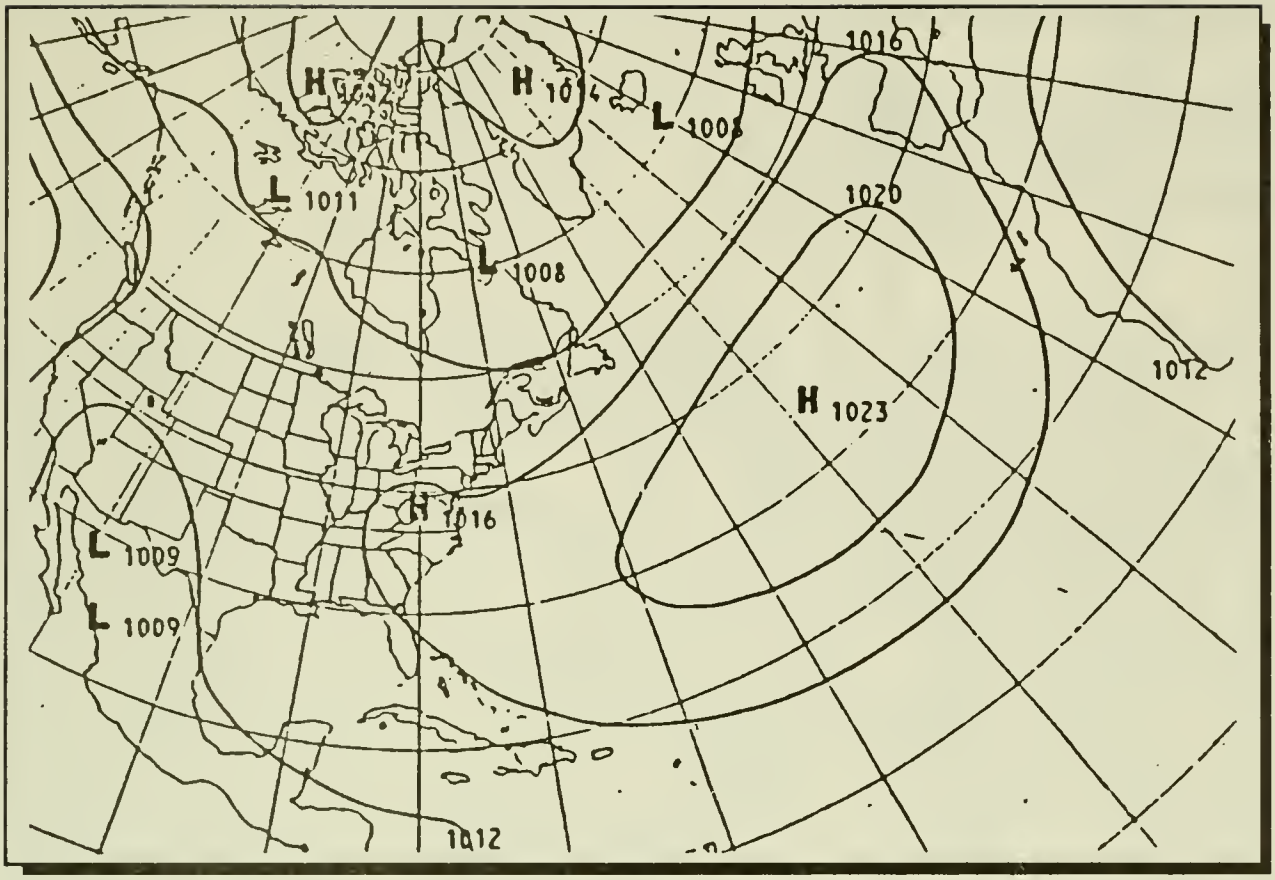

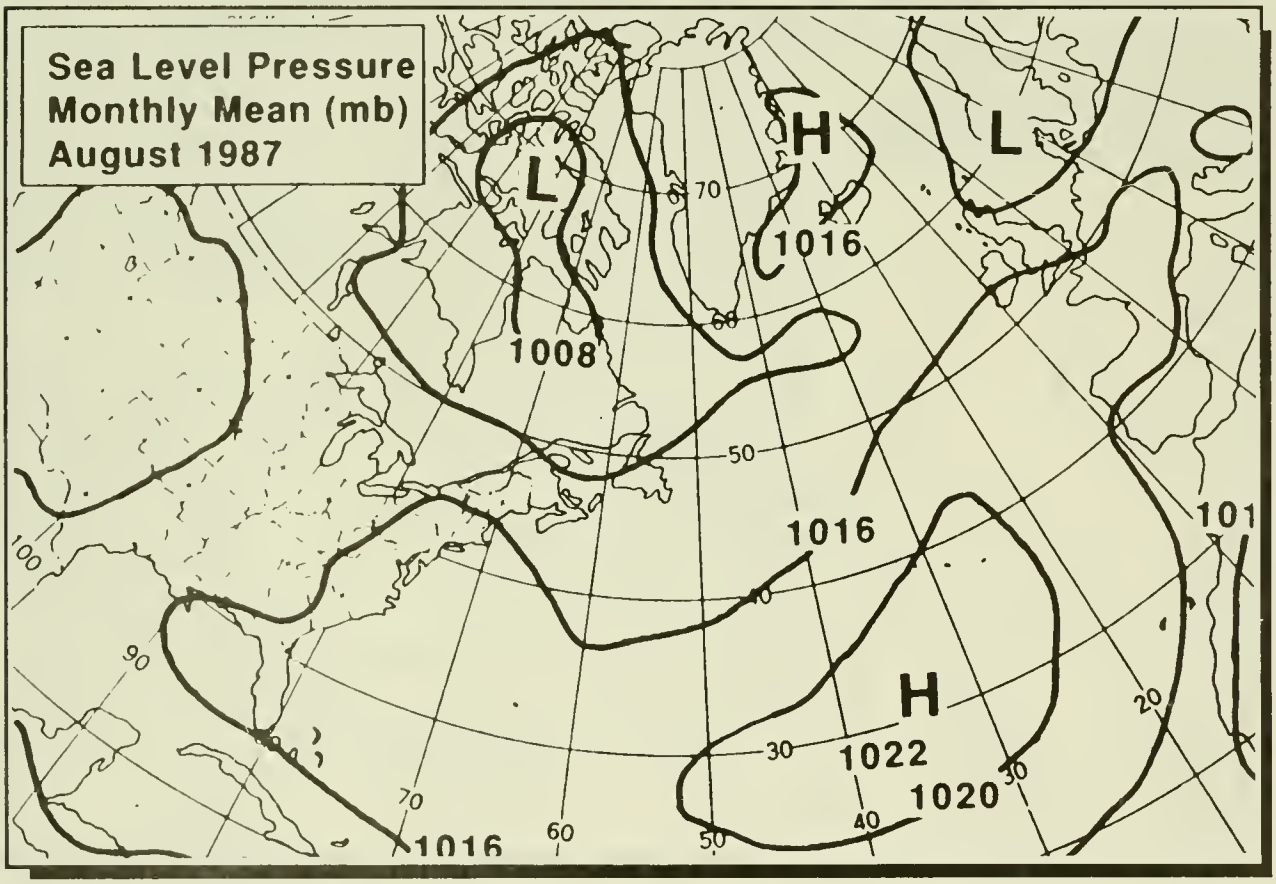

Figure 10. August 1987 (from Mariner's Weather Log, 1988).

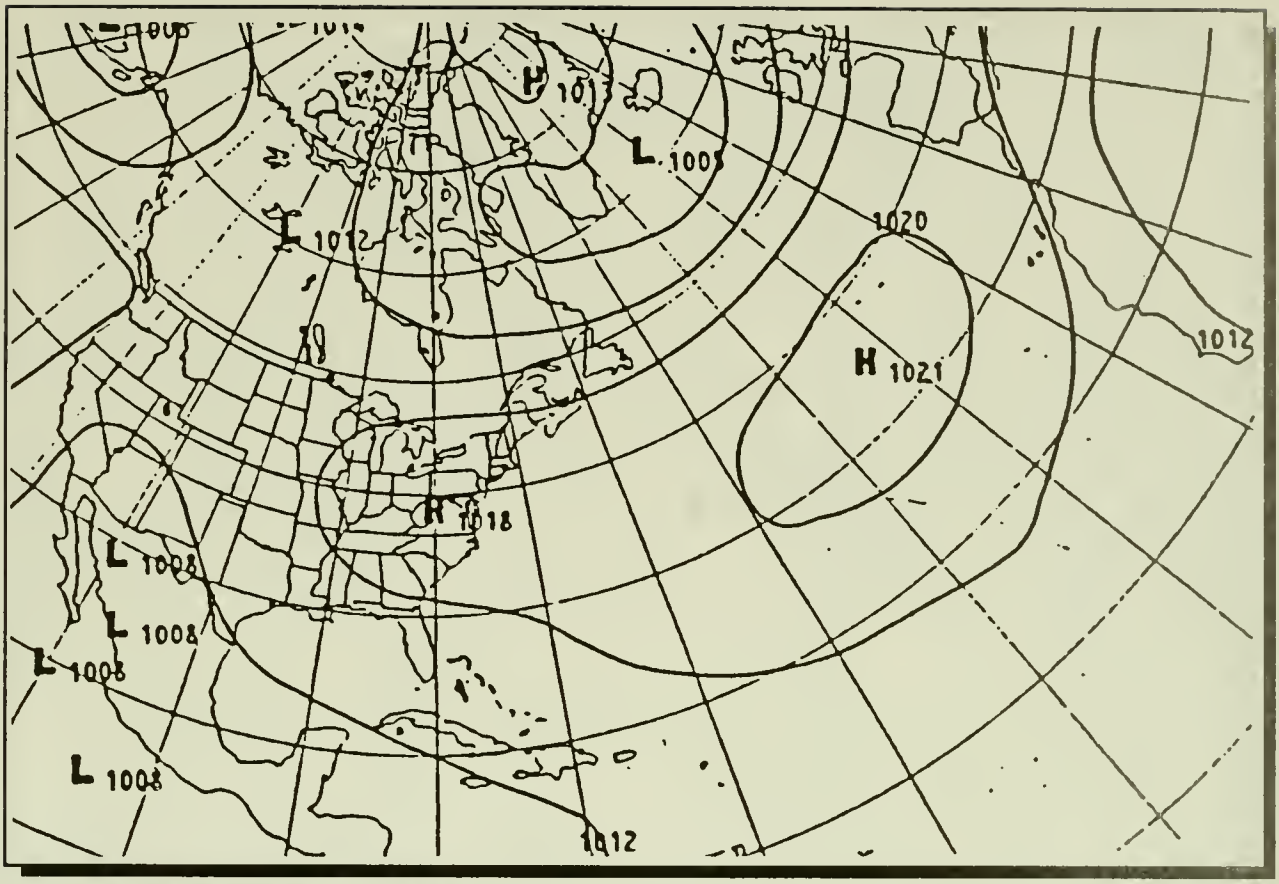

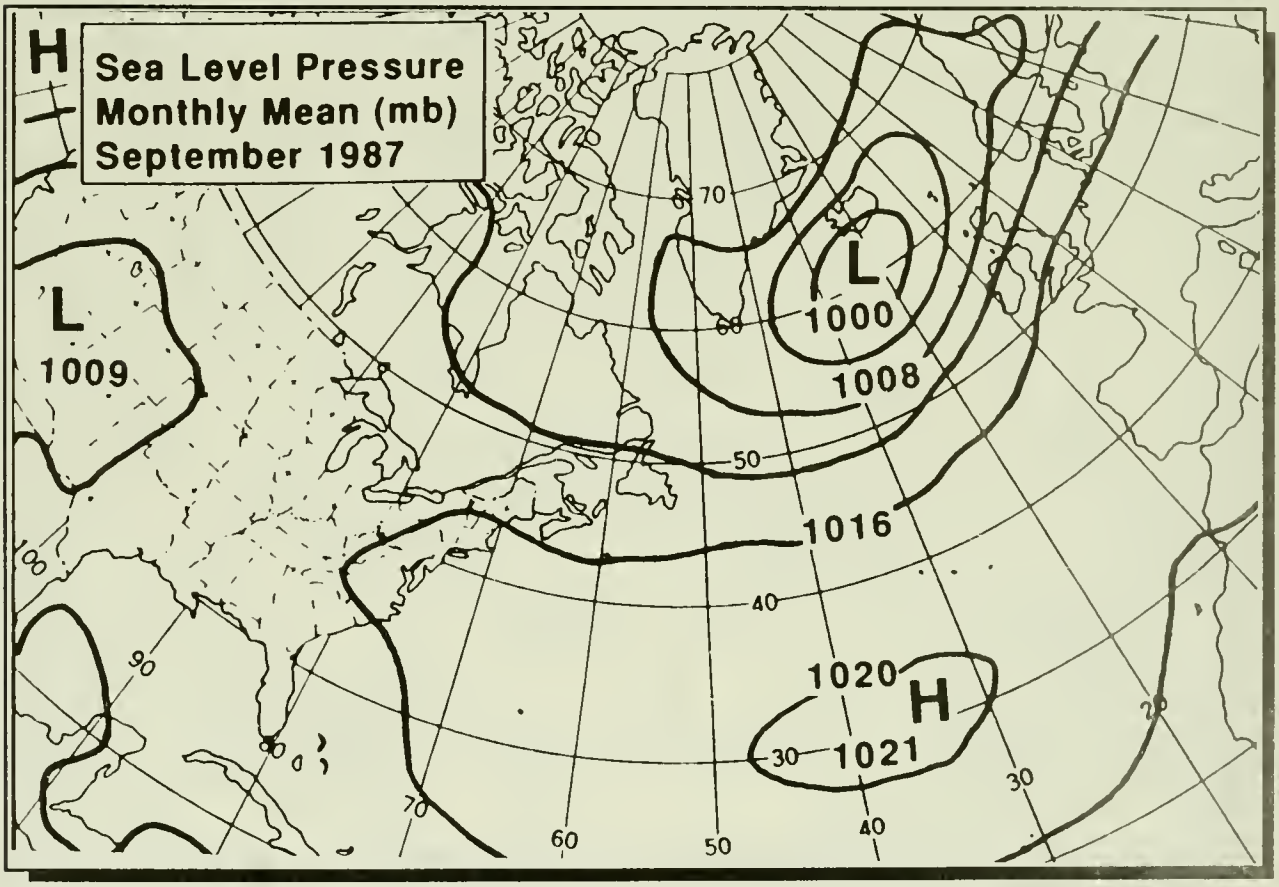

Figure 11. September 1987 (from Mariner's Weather Log, 1988).

Ice Conditions 1987 Season

The following discussion summarizes the sea ice and iceberg conditions along the Labrador and Newfoundland coasts and on the Grand Banks of Newfoundland for the 1987 ice year. The sea ice type and concentration information used in this discussion came from the Monthly Thirty Day Ice Forecast for Northern Canadian Waters published monthly by the Atmospheric Environment Service (AES) of Canada and the Southern Ice Limit published twice-monthly by the U.S. Navy-NOAA Joint Ice Center. Information on the maximum, mean, and minimum sea ice extent was obtained from Naval Oceanography Command, 1986.

October 1986: No sea ice was seen south of 65°N in October, which is normally the case (Figure 12). There were no icebergs reported south of 52°N in October.

November 1986: In mid-November, new, young, and thin first-year sea ice began to form in Ungava Bay, Hudson Strait, and Davis Strait (Figure 13). The mean extent of sea ice in November is confined to the southern tip of Baffin Island with the maximum sea ice extent covering Hudson Strait, and Ungava Bay. Ice conditions in November 1986 were close to the maximum conditions. An unusually deep Icelandic Low (Mariner's Weather Log, 1987a) brought below normal temperatures to Labrador (Table 6) which enhanced the sea ice growth. There were 8 icebergs reported south of 52°N in November.

December 1986: Aided by continued below normal temperatures (Table 6), the sea ice edge continued to be farther south than the mean and close to the maximum extent of sea ice. In mid-December, thin first-year, young and new sea ice were just north of the Strait of Belle Isle (Figure 14). Concentrations were generally 8-10 tenths. There were 9 icebergs reported south of 52°N in December; 5 of these icebergs were south of 48°N.

January 1987: In mid-January, new and young sea ice were north of the Avalon Peninsula and along the eastern coast of Newfoundland (Figure 15). The Strait of Belle Isle was now ice covered with new and young sea ice. The sea ice again extended beyond the mean limits of sea ice, but did not extend to the maximum limits of sea ice extent. By the end of January, the sea ice growth and spread was 2-3 weeks ahead of normal (AES, 1987). This above average sea ice growth can again be attributed to below normal temperatures in Labrador and Newfoundland (Table 6). There were 5 icebergs reported south of 52°N in January; 2 of these were south of 48°N.

February 1987: By mid-February, a tongue of 9-10 tenths first-year sea ice extended along the Labrador coast, into the Strait of Belle Isle, and along the eastern coast of Newfoundland down to the Avalon Peninsula (Figure 16). Young, thin first-year, and first-year sea ice were west of Newfoundland with concentrations of 9-10 tenths. The extent of sea ice in February was close to the mean extent. The increase in temperatures to warmer than normal in Labrador and near normal on Newfoundland (Table 6) returned the sea ice extent to near normal. There were 14 icebergs observed south of 52°N in February; all of these icebergs were south of 48°N.

March 1987: The 1987 International Ice Patrol season opened on March 12. Figure 24 shows the iceberg distribution at the beginning of the season. In mid-March, thin first-year sea ice advanced from the Avalon Peninsula south over the Grand Banks (Figure 17). The sea ice edge was again close to its mean extent. Towards the end of March, drastic changes in the sea ice extent occurred. Figure 26 shows the sea ice pushed off the Grand Banks with all the remaining sea ice confined to close to the east and south coast of Newfoundland. The iceberg distribution on March 30 showed a marked shift to the west compared to March 15 (Figure 25). Between March 15 and March 30, the prevailing winds were easterly (AES 1987), forcing the sea ice and icebergs westward. There were 57 new icebergs south of 52°N in March; 48 of these icebergs were south of 48°N. At the end of March, there were 25 icebergs on plot (Figure 26).

April 1987: The unusual sea ice distribution created by the easterly winds at the end of March continued into April. There was no sea ice on the Grand Banks or the west coast of Newfoundland (Figure 18). The southern coast of Newfoundland, usually ice free, had 9-10 tenths of sea ice. The extent of sea ice was still near average for April . The iceberg distribution on April 15 (Figure 27) only extended to 47°W. By April 30, the iceberg distribution extended to 43°W (Figure 28). There were 117 new icebergs south of 52°N; 76 of these were south of 48°N. There were 142 icebergs on plot at the end of April (Figure 28).

May 1987: In mid-May, the southern and eastern coasts of Newfoundland became ice-free as the sea ice retreated northward (Figure 19). A large polynya (an area of open water surrounded by ice) formed along the Newfoundland and Labrador coasts between 50 and 55°N. This polynya was formed from southwesterly winds pushing the ice off-shore (AES, 1987). Above average temperatures on Newfoundland and southern Labrador had accelerated the sea ice retreat in these regions. As the sea ice retreated northward, large numbers of icebergs were released to drift southward. With 236 new icebergs south of 52°N, May was the heaviest month for new icebergs. Only 29 of these icebergs were south of 48°N. Only a few of these icebergs drifted with the Labrador Current through Flemish Pass. There were 158 icebergs on plot the end of May (Figure 30).

June 1987: By mid-June, the ice edge had retreated to Goose Bay (Figure 20). This is the typical pattern of retreat in June (Naval Oceanographic Command, 1986). The number of new icebergs south of 52°N was again high in June. There were 215 new icebergs south of 52°N in June; 127 of these were south of 48°N. By mid-June, a large number of icebergs had drifted onto the Grand Banks (Figure 31). Most of these icebergs were gone by the end of June with most of the remaining icebergs north of 48°N (Figure 32). There were 64 icebergs on plot the end of June (Figure 32).

July 1987: The sea ice edge continued to retreat northward, but at a slower rate than normal. By mid-July, the sea ice edge has usually retreated to Baffin Island, with some sea ice also persisting in Ungava Bay. In mid-July 1987, however, the sea ice edge was still down along the Labrador Coast (Figure 21). The temperatures in July on Labrador were colder than normal (Table 6) and these cooler temperatures may have caused the sea ice edge to retreat slower than it would have normally. There were 25 new icebergs south of 52°N; 15 of these were south of 48°N. There were 10 icebergs on plot the end of July (Figure 34). The 1987 International Ice Patrol season was closed on July 31,1987.

August 1987: The retreat of the sea ice edge to just north of Frobisher Bay in August left Hudson Strait and most of Davis Strait ice free (Figure 22). There were 57 icebergs reported south of 52°N in August; 2 of these were south of 48°N.

September 1987: The only sea ice observed south of 65°N in September was near Frobisher Bay (Figure 23).

Figure 12.

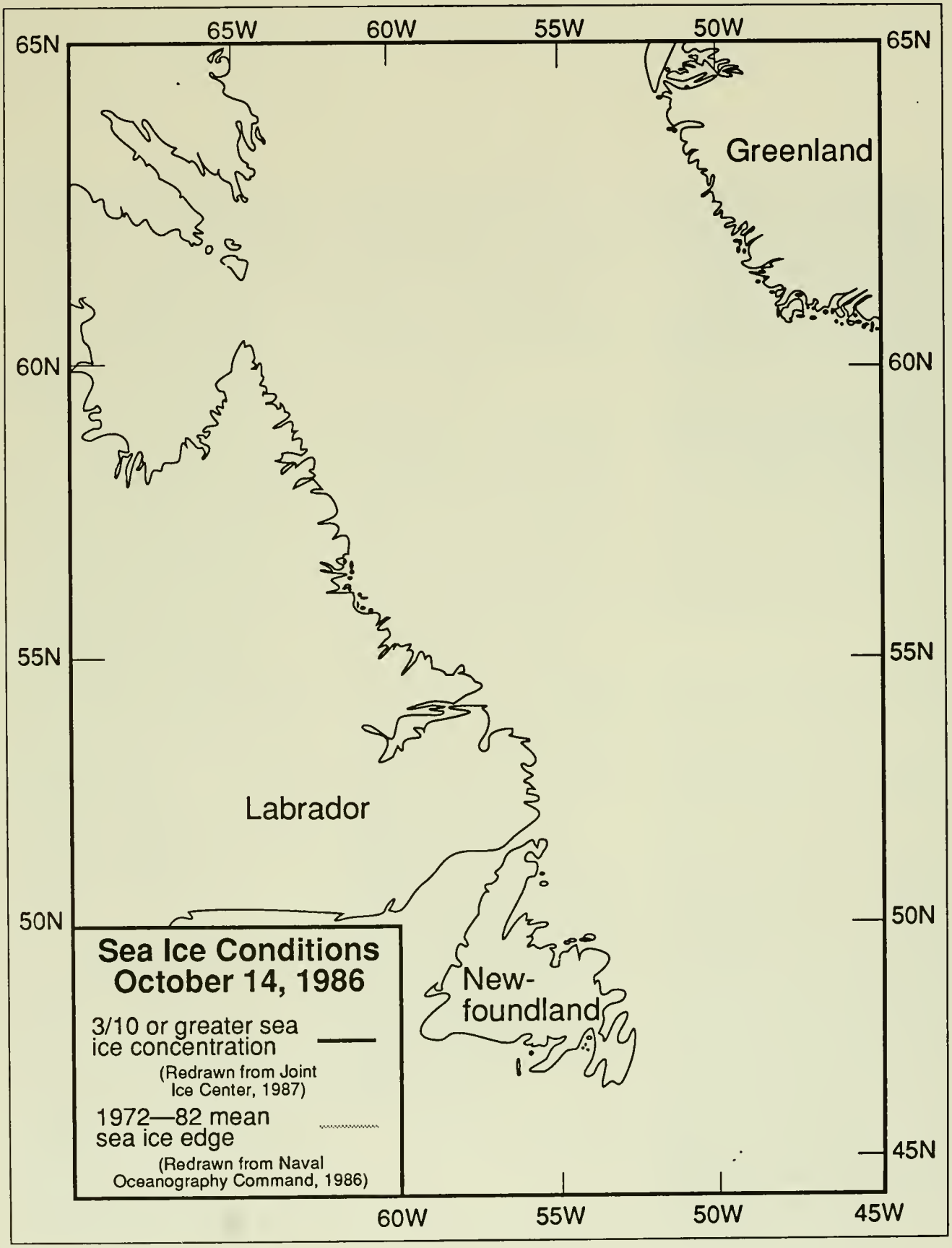
65W
60W
55W
50W
65N
60N
55N
50N
45N
Greenland
Labrador
New-
foundland
Sea Ice Conditions
October 14, 1986
3/10 or greater sea ice concentration
(Redrawn from Joint Ice Center, 1987)
1972—82 mean sea ice edge
(Redrawn from Naval Oceanography Command, 1986)
60W
55W
50W
45W

Figure 13.

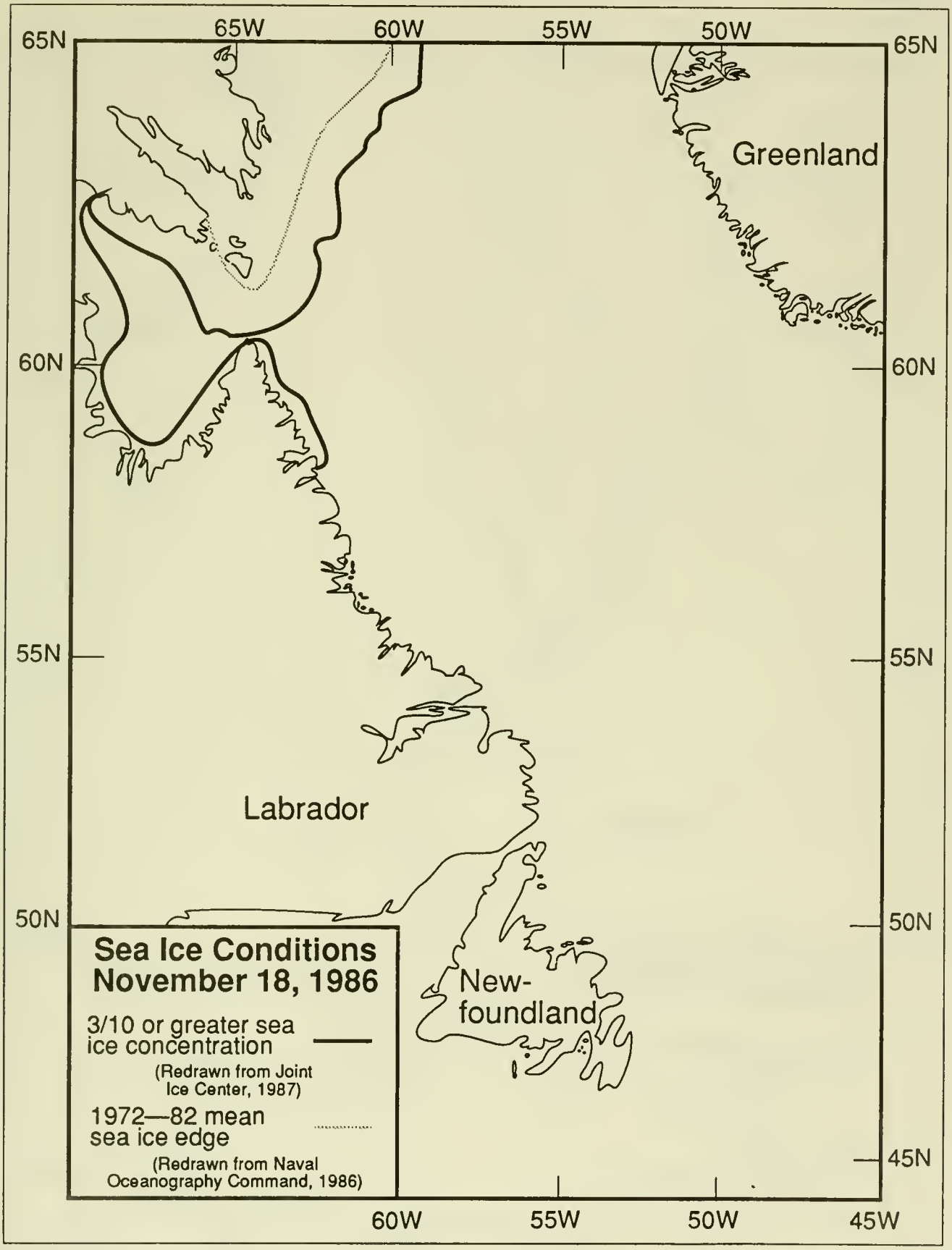
65N
65W
60W
55W
50W
65N
Greenland
60N
60N
55N
55N
Labrador
50N
50N
New-
foundland
45N
60W
55W
50W
45W
Sea Ice Conditions
November 18, 1986
3/10 or greater sea ice concentration
(Redrawn from Joint Ice Center, 1987)
1972—82 mean sea ice edge
(Redrawn from Naval Oceanography Command, 1986)

Figure 14.

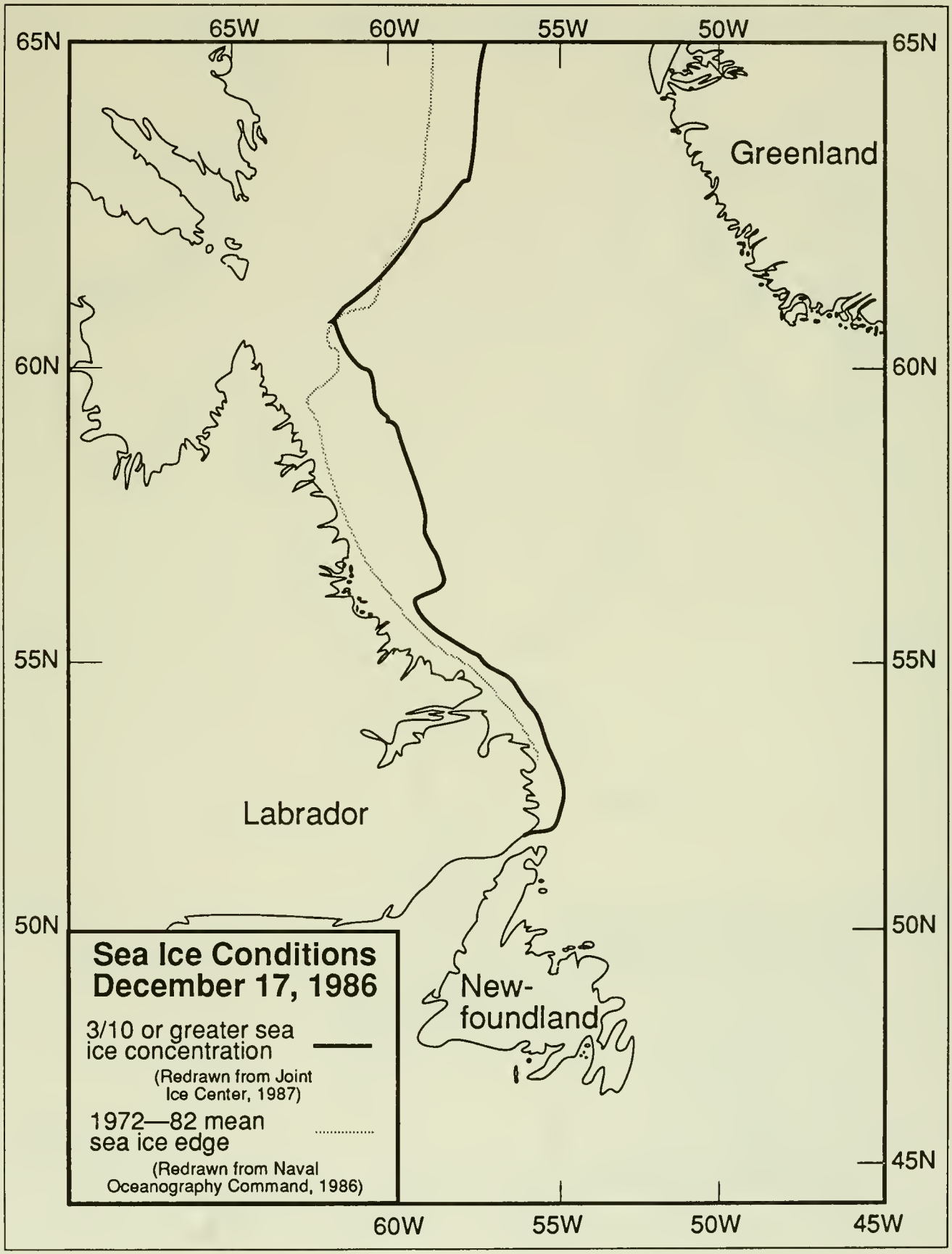
65W
60W
55W
50W
65N
60N
55N
50N
45N
Greenland
Labrador
New-
foundland
Sea Ice Conditions
December 17, 1986
3/10 or greater sea ice concentration
(Redrawn from Joint Ice Center, 1987)
1972—82 mean sea ice edge
(Redrawn from Naval Oceanography Command, 1986)
60W
55W
50W
45W

Figure 15.

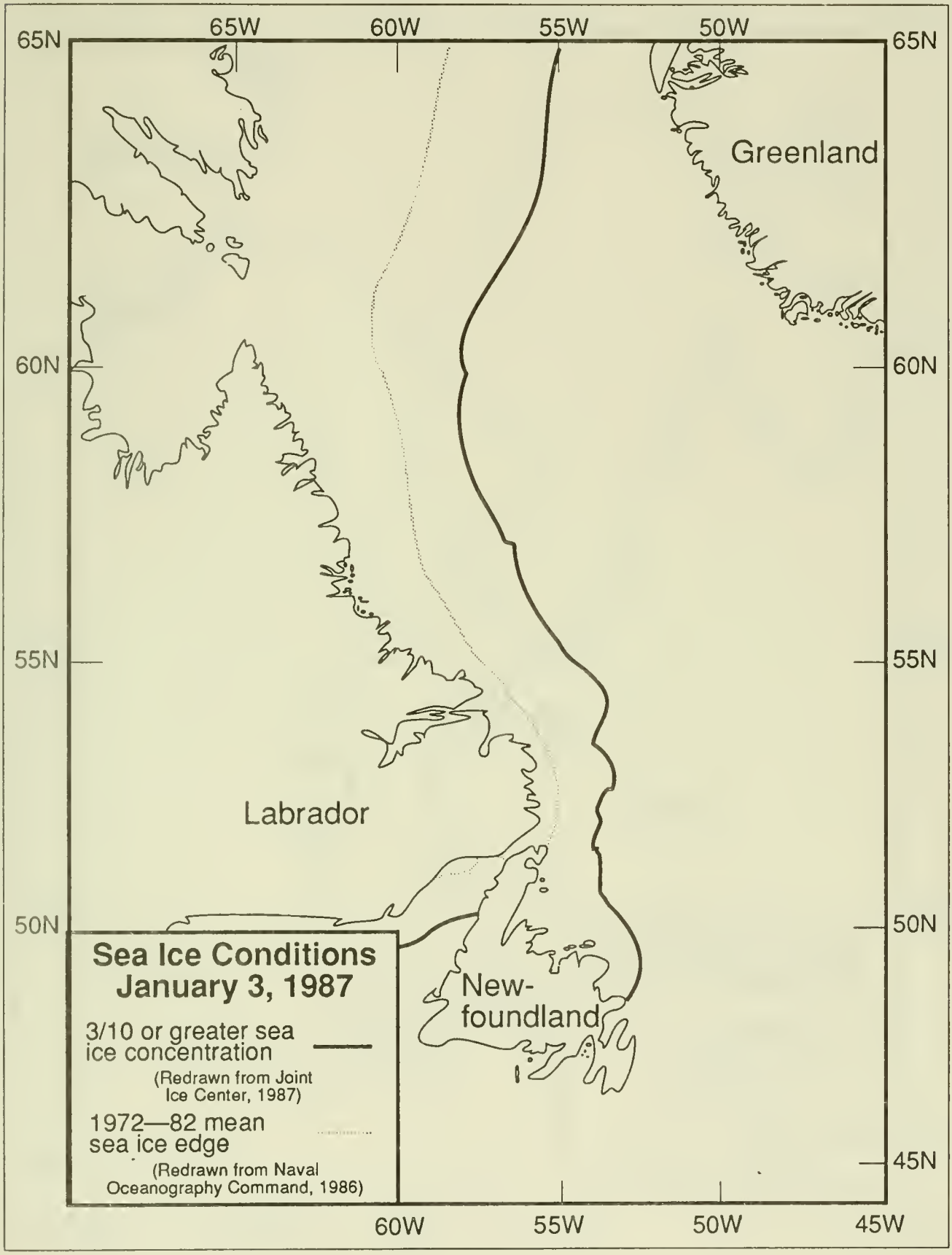
65W
60W
55W
50W
65N
60N
55N
50N
45N
Greenland
Labrador
New-
foundland
Sea Ice Conditions
January 3, 1987
3/10 or greater sea ice concentration
(Redrawn from Joint Ice Center, 1987)
1972—82 mean sea ice edge
(Redrawn from Naval Oceanography Command, 1986)
60W
55W
50W
45W

Figure 16.

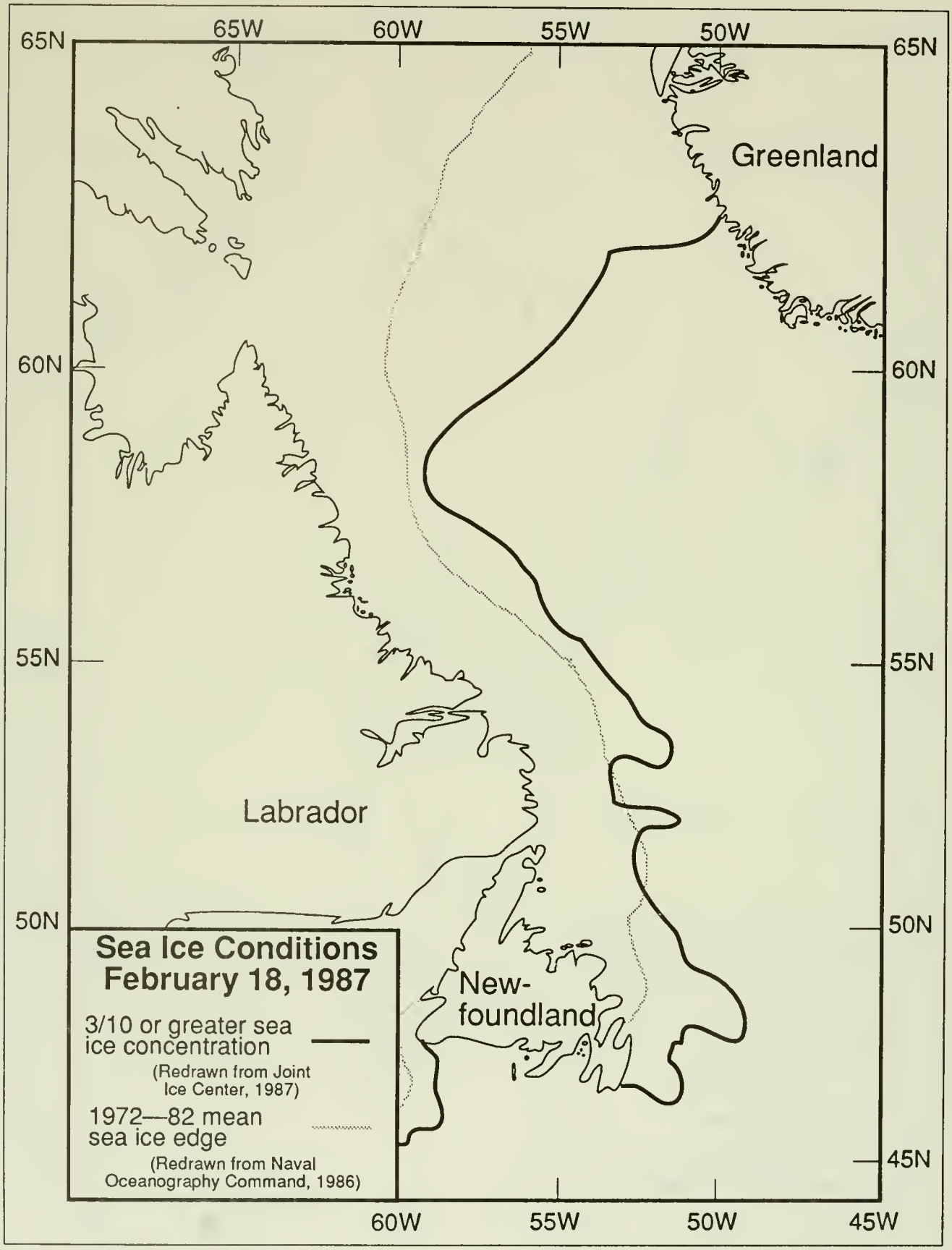
65W
60W
55W
50W
65N
60N
55N
50N
45N
Greenland
Labrador
New-
foundland
Sea Ice Conditions
February 18, 1987
3/10 or greater sea ice concentration
(Redrawn from Joint Ice Center, 1987)
1972—82 mean sea ice edge
(Redrawn from Naval Oceanography Command, 1986)
60W
55W
50W
45W

Figure 17.

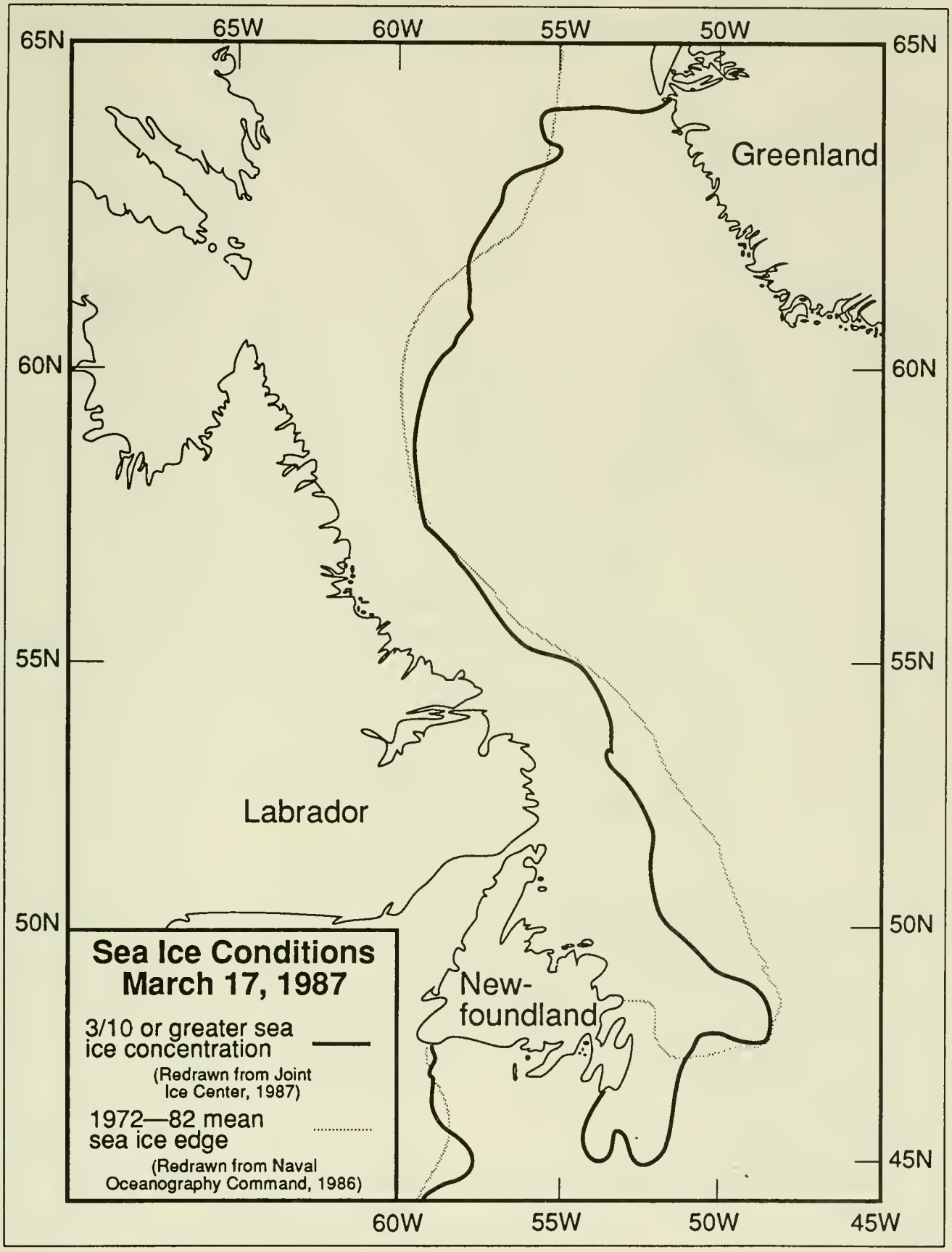
65N
65W
60W
55W
50W
65N
Greenland
60N
60N
55N
55N
Labrador
50N
50N
Sea Ice Conditions
March 17, 1987
3/10 or greater sea ice concentration
(Redrawn from Joint Ice Center, 1987)
1972—82 mean sea ice edge
(Redrawn from Naval Oceanography Command, 1986)
New-
foundland
45N
60W
55W
50W
45W

Figure 18.

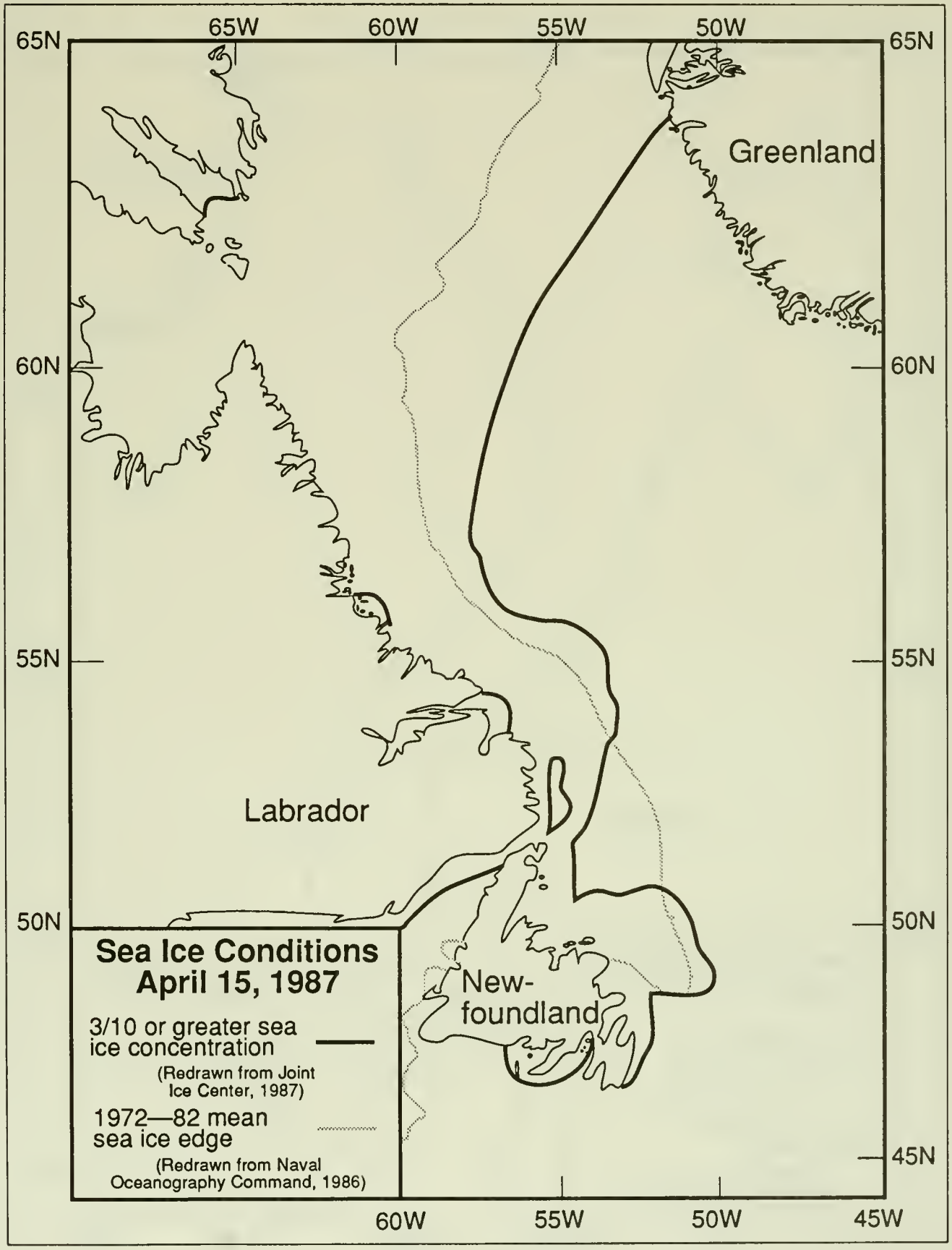
65N
65W
60W
55W
50W
65N
Greenland
60N
60N
55N
55N
Labrador
50N
50N
Sea Ice Conditions
April 15, 1987
3/10 or greater sea ice concentration
(Redrawn from Joint Ice Center, 1987)
1972—82 mean sea ice edge
(Redrawn from Naval Oceanography Command, 1986)
New-
foundland
45N
60W
55W
50W
45W

Figure 19.

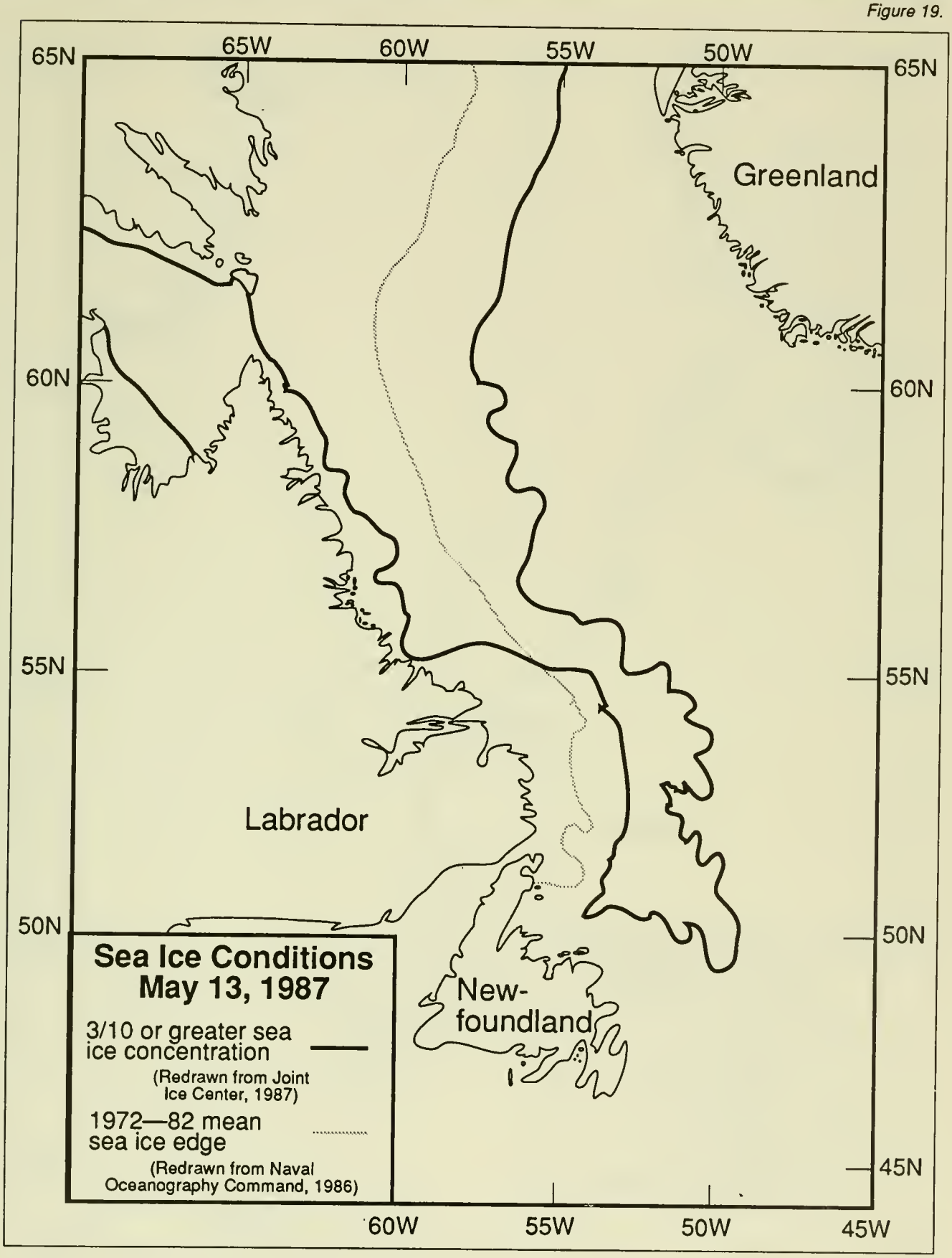
65N
65W
60W
55W
50W
65N
Greenland
60N
60N
55N
55N
Labrador
50N
50N
New-
foundland
45N
60W
55W
50W
45W
Sea Ice Conditions
May 13, 1987
3/10 or greater sea ice concentration
(Redrawn from Joint Ice Center, 1987)
1972—82 mean sea ice edge
(Redrawn from Naval Oceanography Command, 1986)

Figure 20.

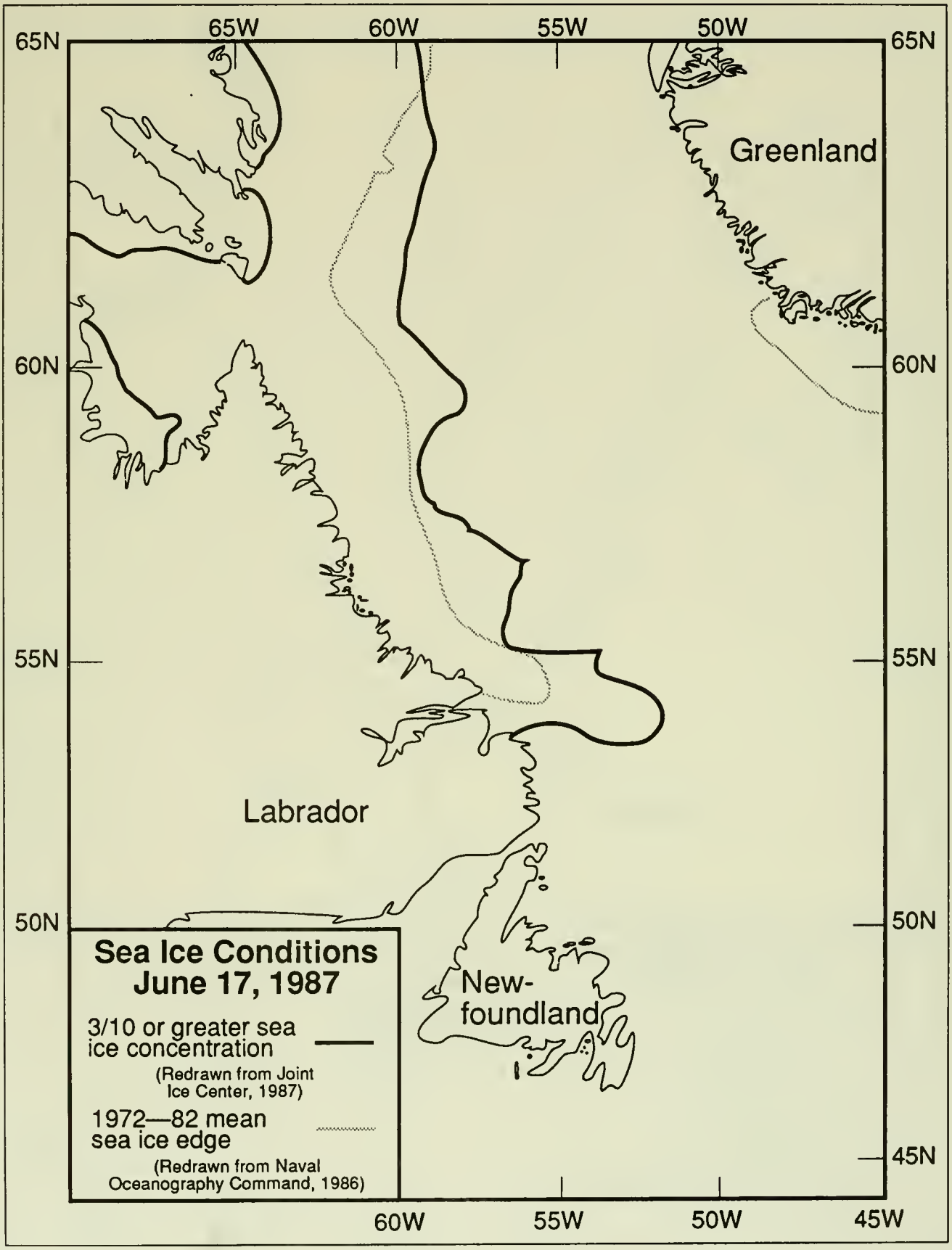
65W
60W
55W
50W
65N
60N
55N
50N
45N
Greenland
Labrador
New-
foundland
Sea Ice Conditions
June 17, 1987
3/10 or greater sea ice concentration
(Redrawn from Joint Ice Center, 1987)
1972—82 mean sea ice edge
(Redrawn from Naval Oceanography Command, 1986)
60W
55W
50W
45W

Figure 21.

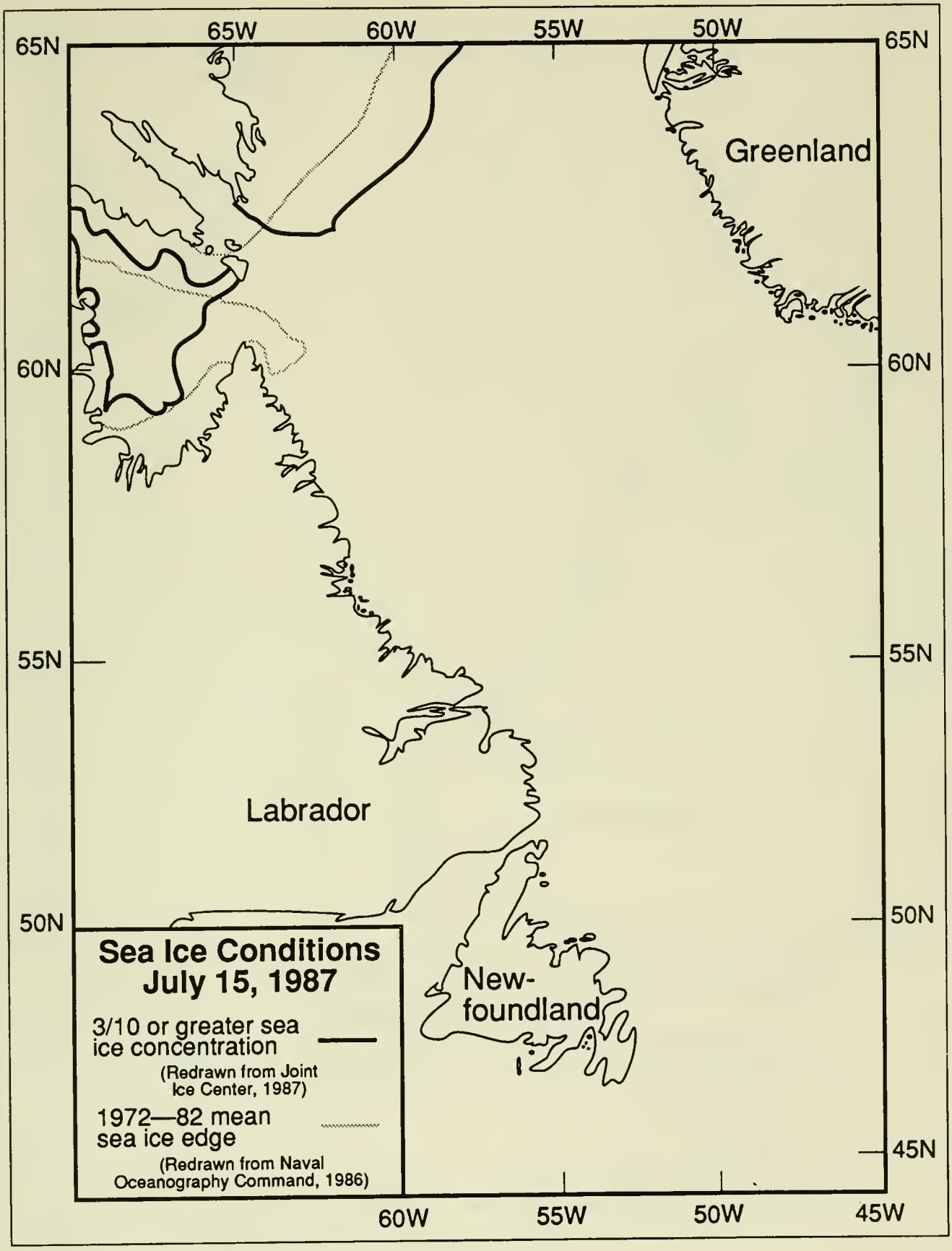
65W
60W
55W
50W
65N
60N
55N
50N
45N
Greenland
Labrador
New-
foundland
Sea Ice Conditions
July 15, 1987
3/10 or greater sea ice concentration
(Redrawn from Joint Ice Center, 1987)
1972—82 mean sea ice edge
(Redrawn from Naval Oceanography Command, 1986)
60W
55W
50W
45W

Figure 22.

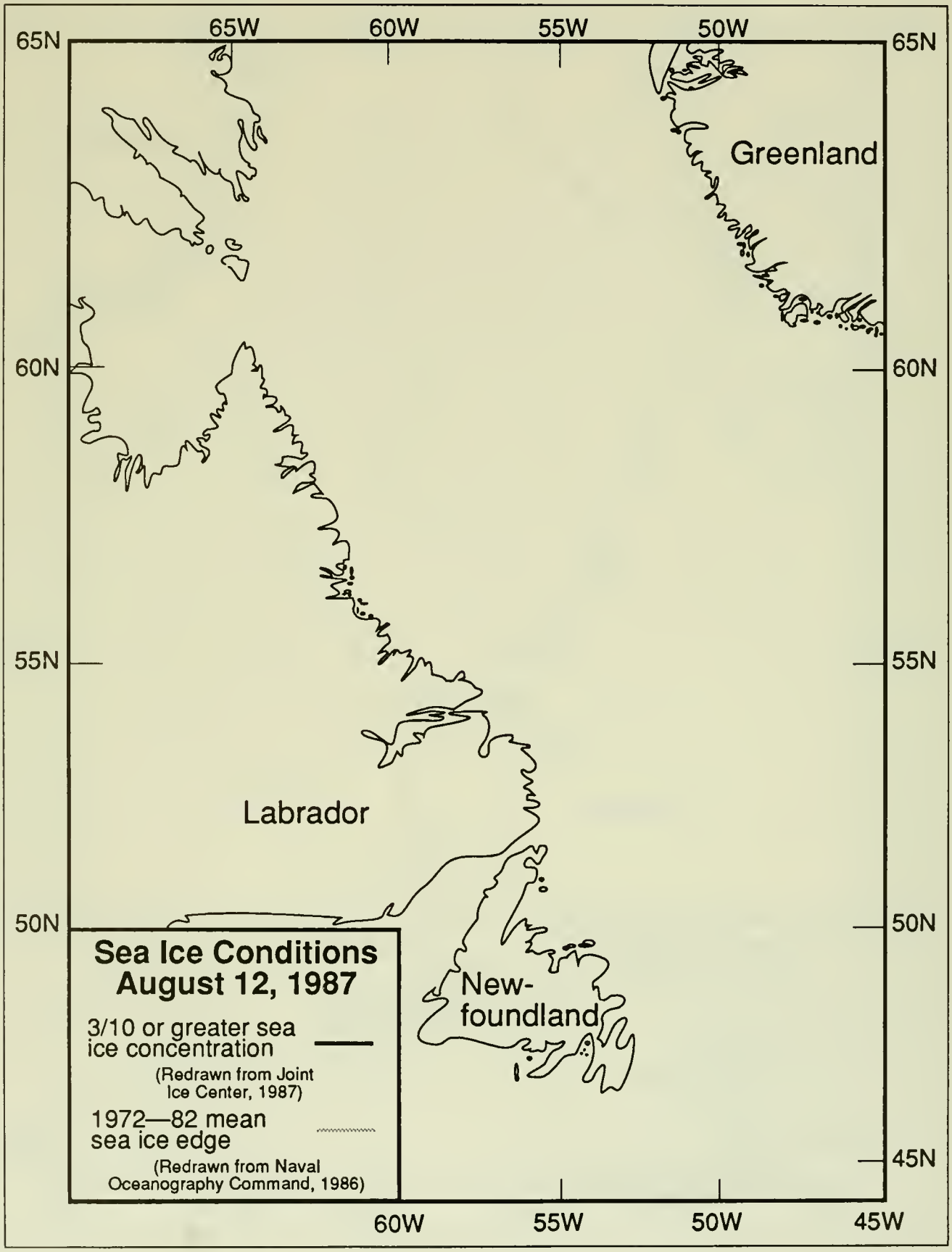
65W
60W
55W
50W
65N
60N
55N
50N
45N
Greenland
Labrador
New-
foundland
Sea Ice Conditions
August 12, 1987
3/10 or greater sea ice concentration
(Redrawn from Joint Ice Center, 1987)
1972—82 mean sea ice edge
(Redrawn from Naval Oceanography Command, 1986)
60W
55W
50W
45W

Figure 23.

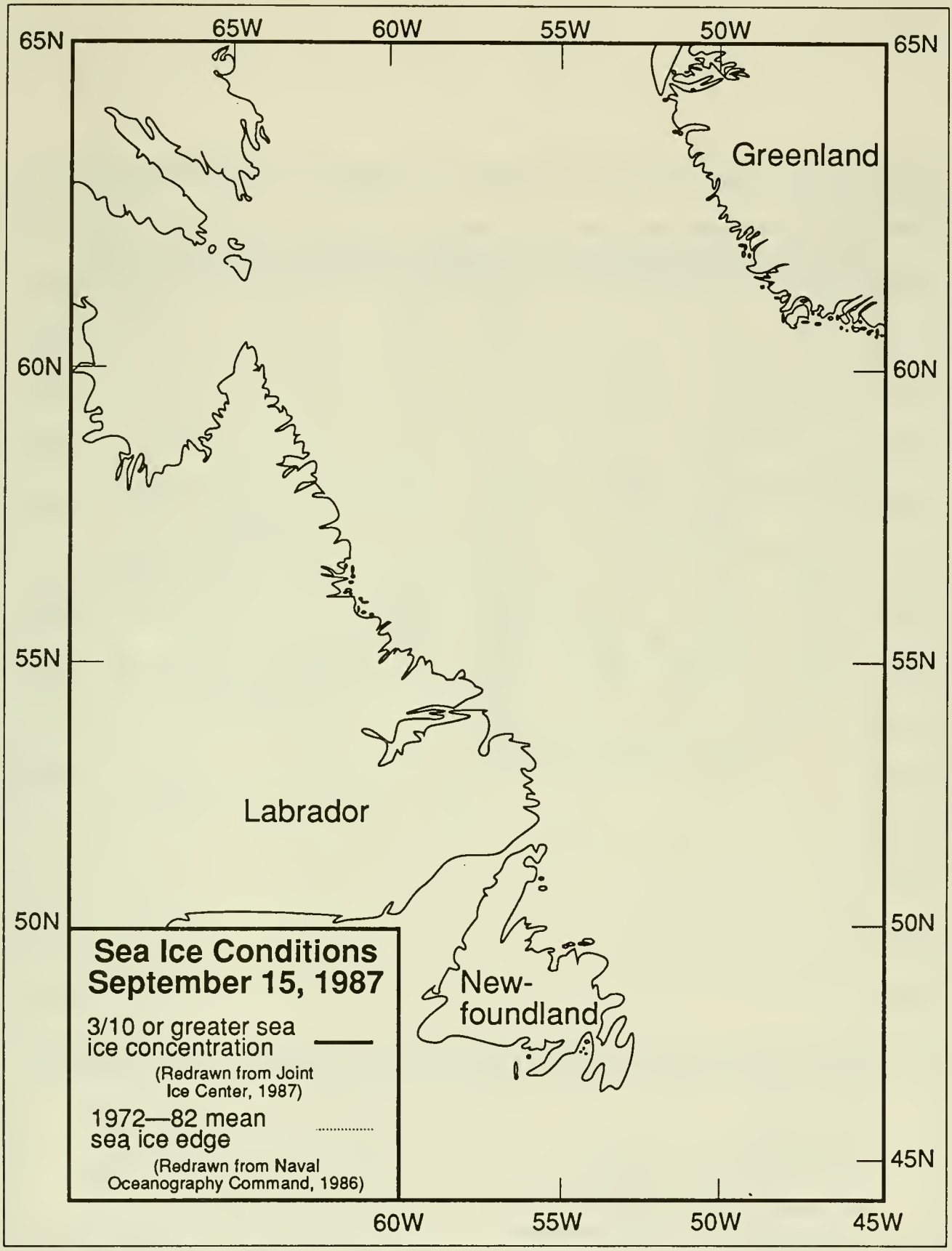
65N
65W
60W
55W
50W
65N
Greenland
60N
60N
55N
55N
Labrador
50N
50N
Sea Ice Conditions
September 15, 1987
3/10 or greater sea ice concentration
(Redrawn from Joint Ice Center, 1987)
1972—82 mean sea ice edge
(Redrawn from Naval Oceanography Command, 1986)
New-
foundland
45N
60W
55W
50W
45W

Figure 24. Graphic Depiction of International Ice Patrol Plot for 1200 GMT March 12, 1987, Based on Observed and Forecast Conditions.

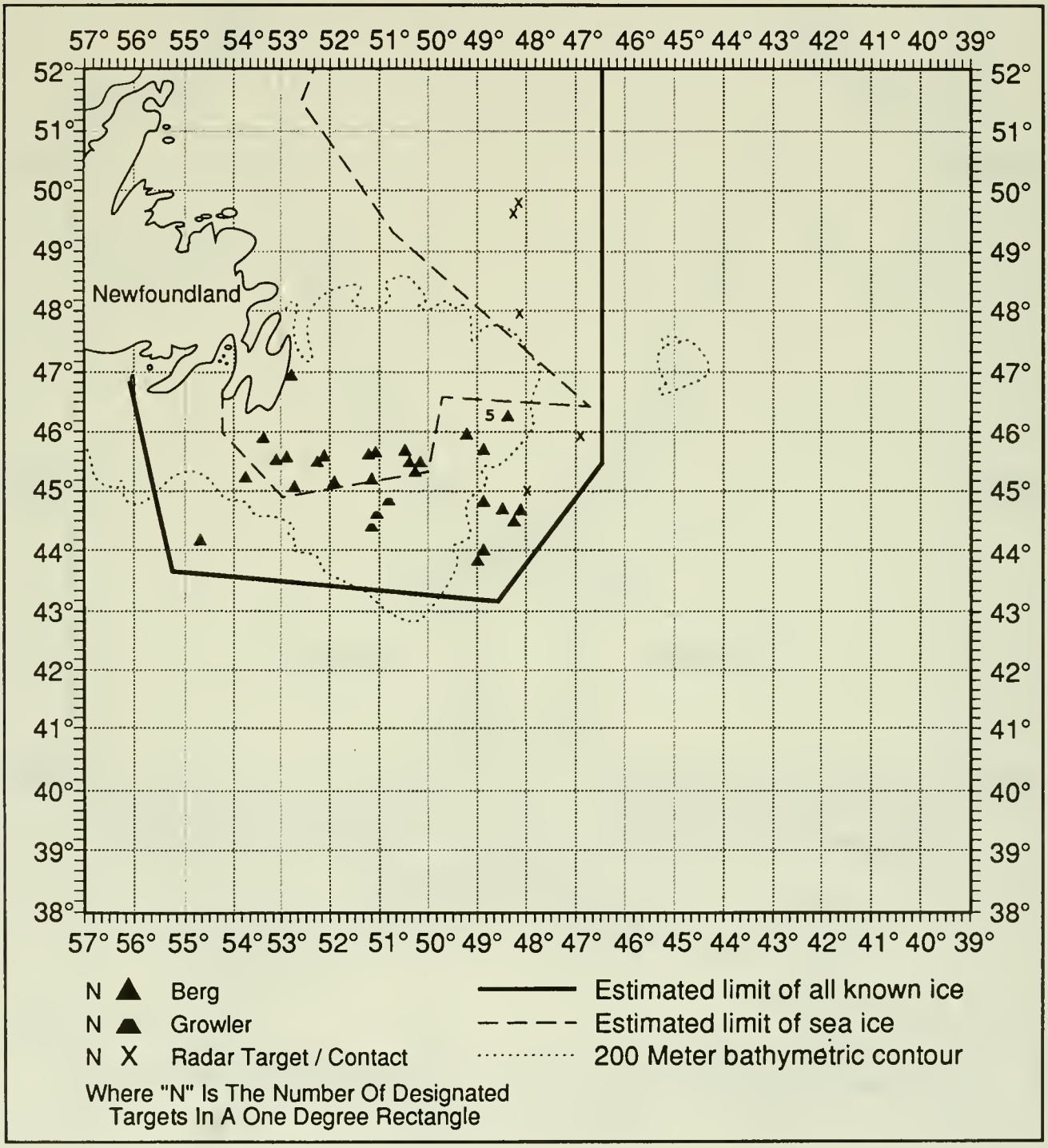

Figure 25. Graphic Depiction of International Ice Patrol Plot for 1200 GMT March 15, 1987, Based on Observed and Forecast Conditions.

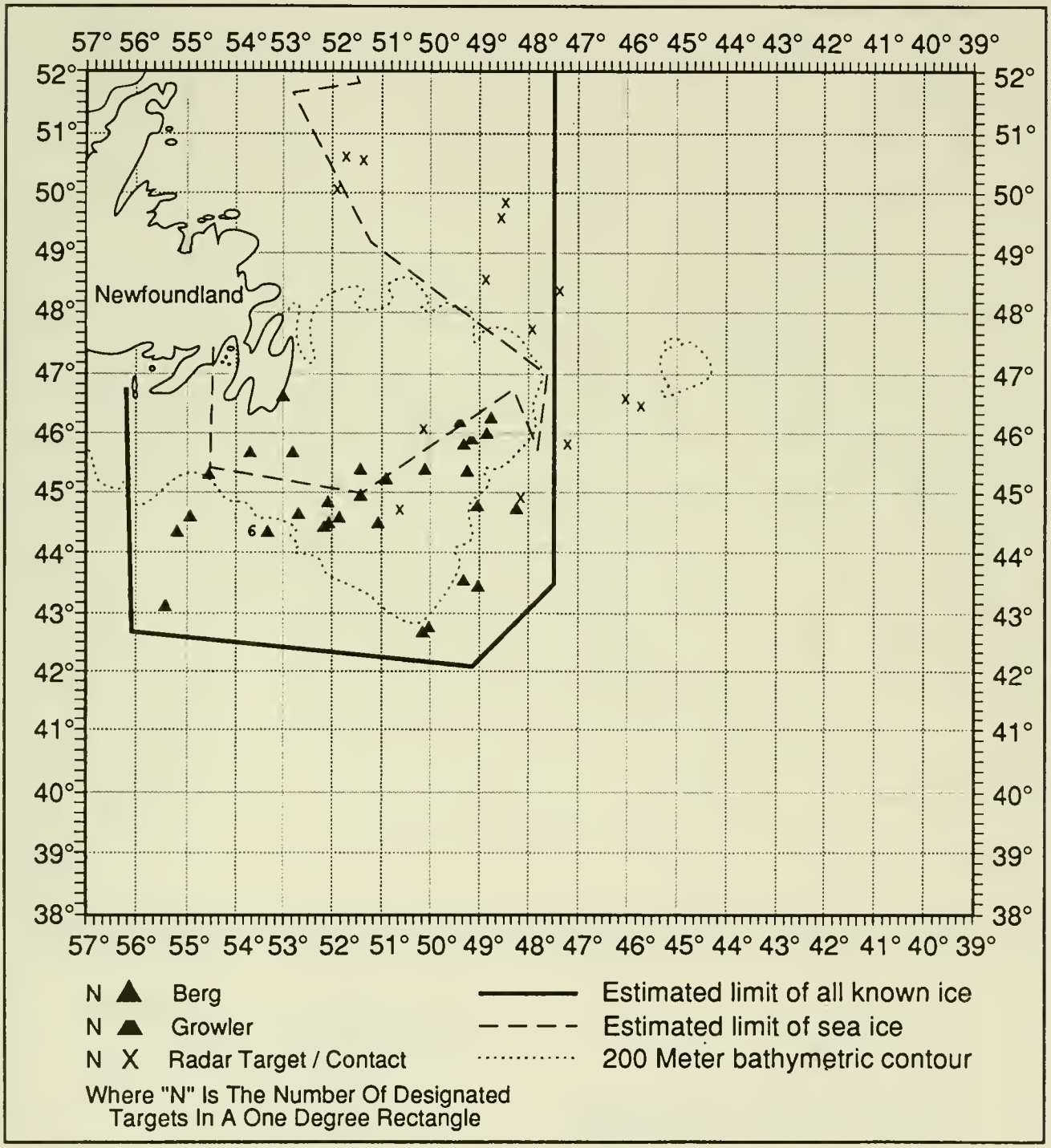

Figure 26. Graphic Depiction of International Ice Patrol Plot for 1200 GMT March 30, 1987, Based on Observed and Forecast Conditions.

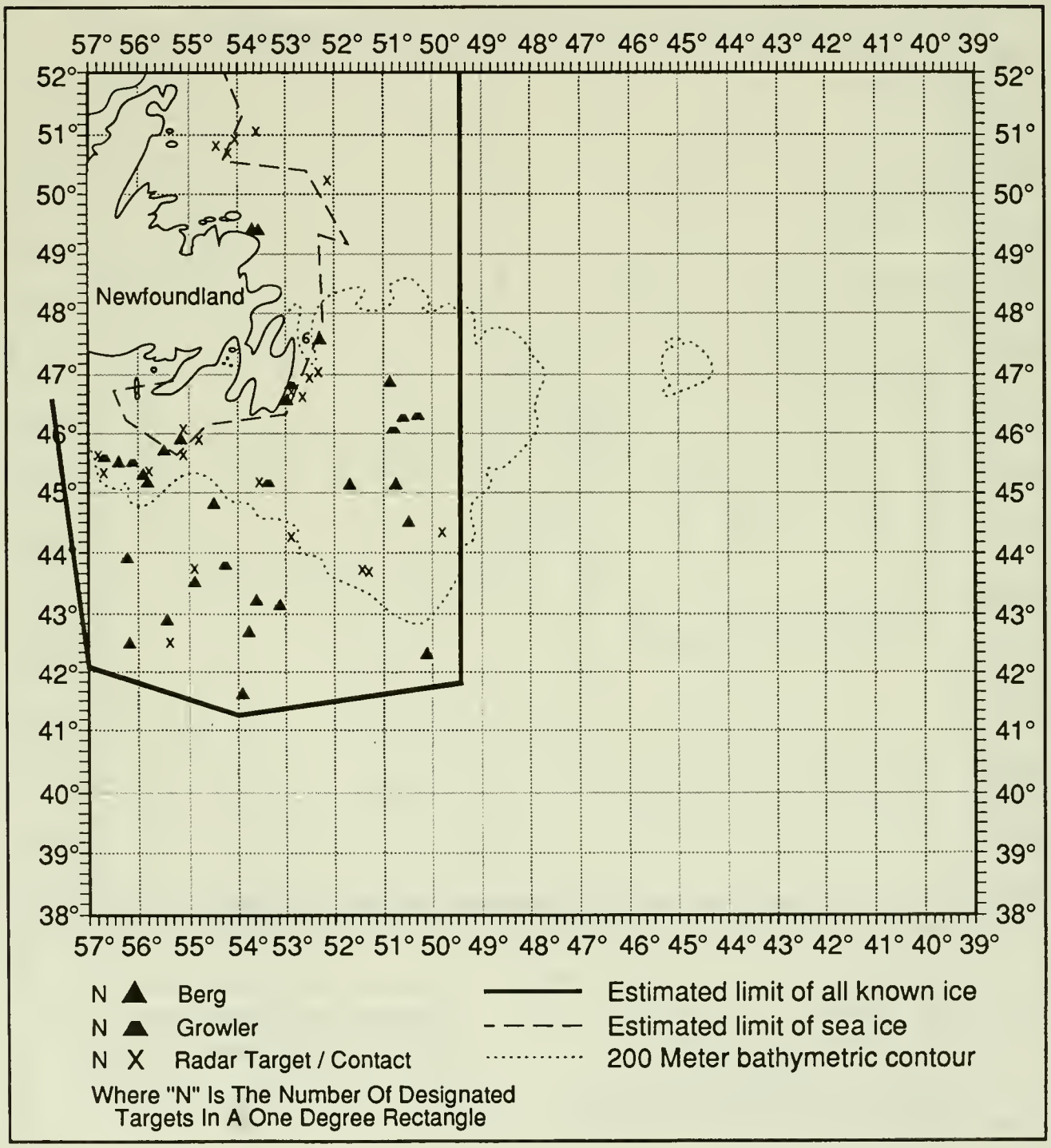

Figure 27. Graphic Depiction of International Ice Patrol Plot for 1200 GMT April 15, 1987, Based on Observed and Forecast Conditions.

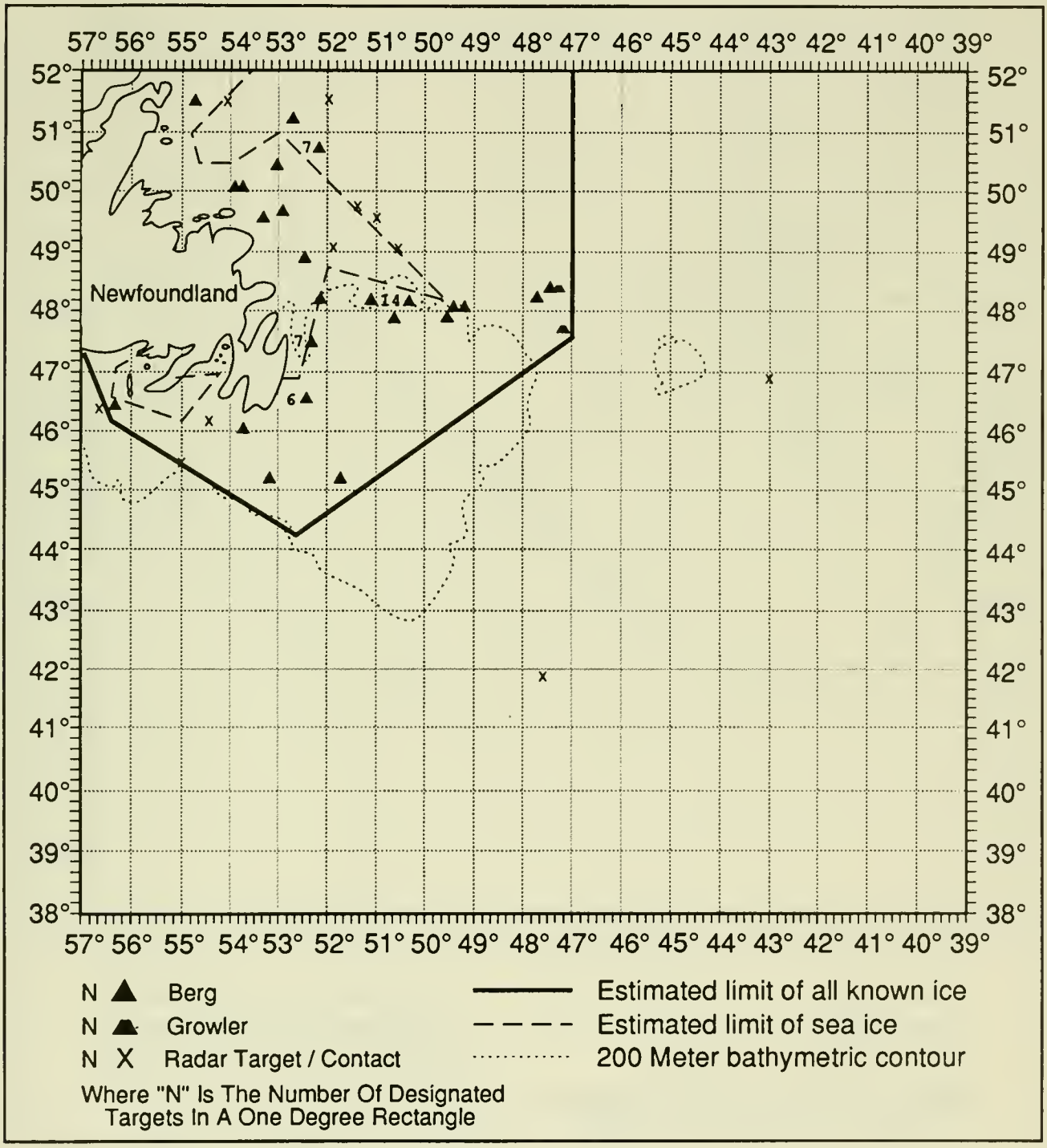

Figure 28. Graphic Depiction of International Ice Patrol Plot for 1200 GMT April 30, 1987, Based on Observed and Forecast Conditions.

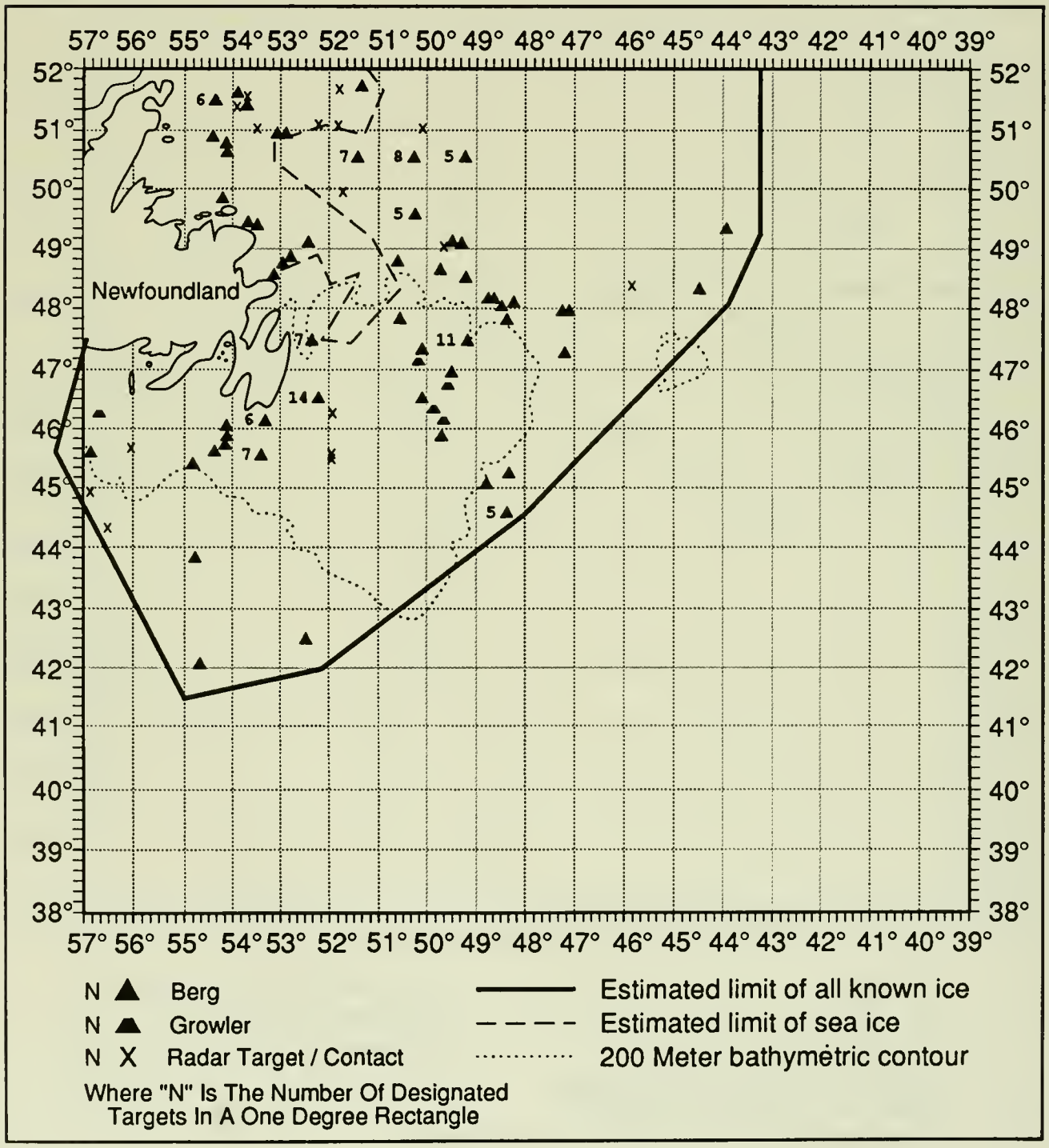

Figure 29. Graphic Depiction of International Ice Patrol Plot for 1200 GMT May 15, 1987, Based on Observed and Forecast Conditions.

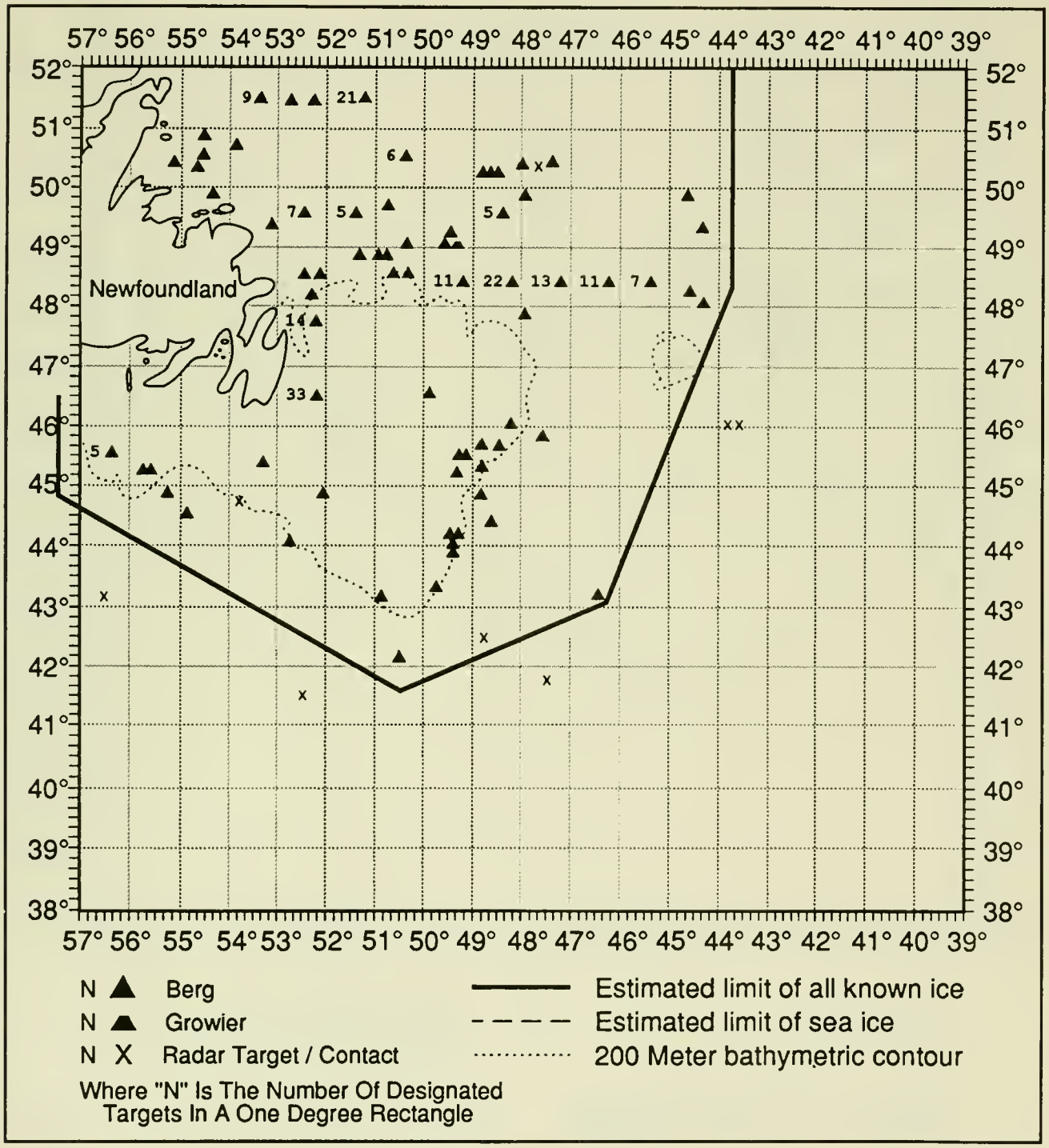

Figure 30. Graphic Depiction of International Ice Patrol Plot for 1200 GMT May 30, 1987, Based on Observed and Forecast Conditions.

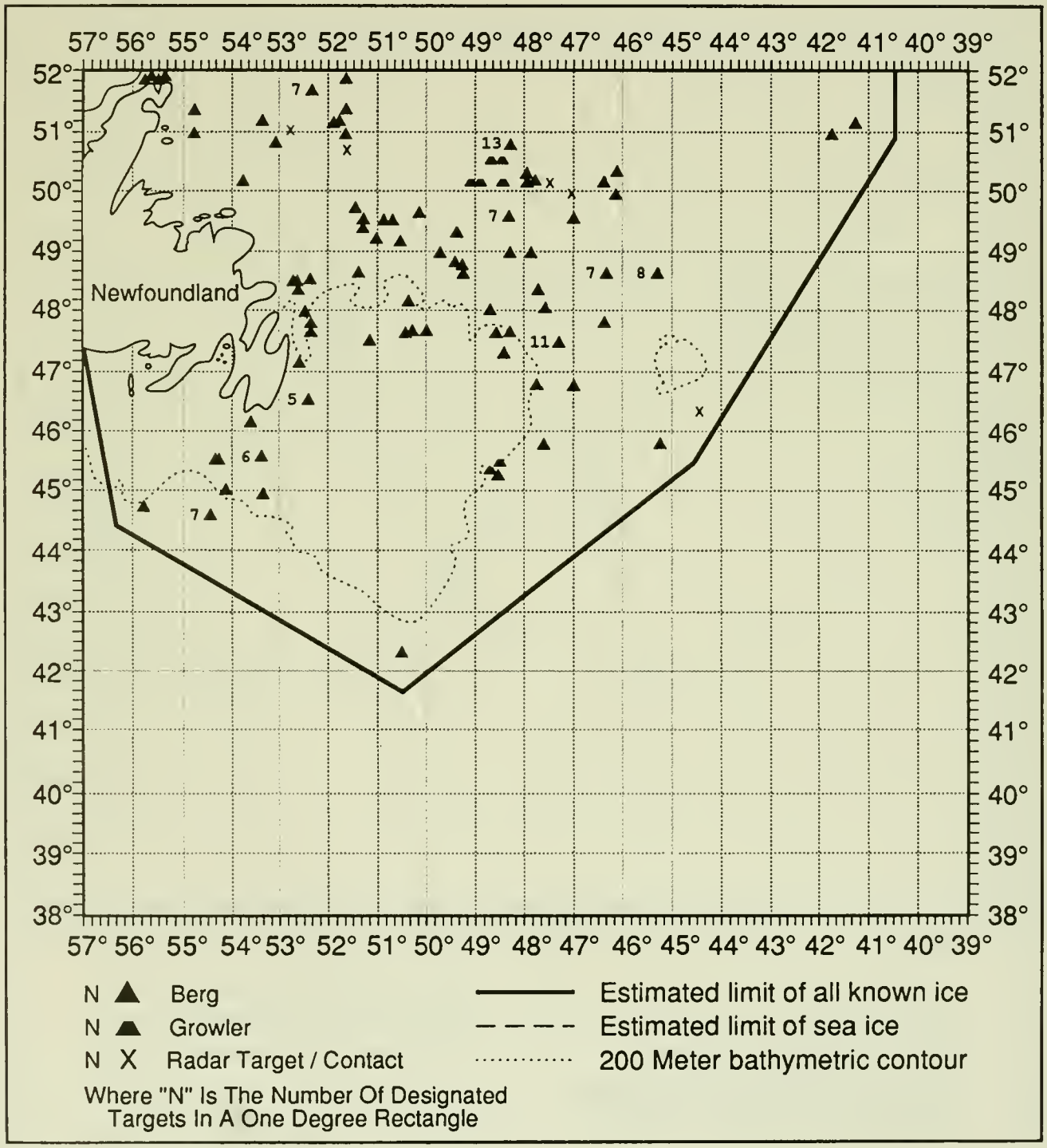

Figure 31. Graphic Depiction of International Ice Patrol Plot for 1200 GMT June 15, 1987, Based on Observed and Forecast Conditions.

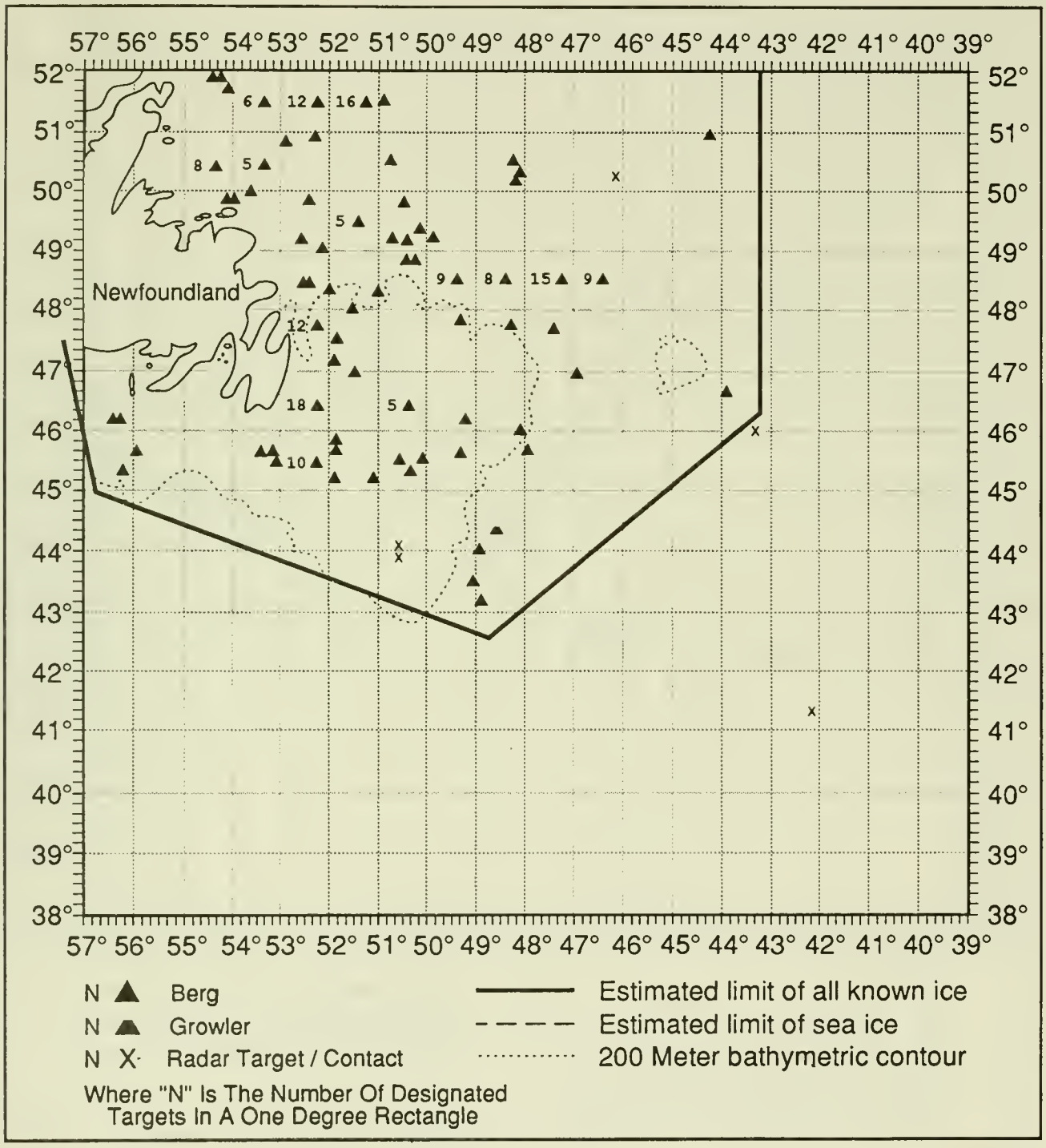

Figure 32. Graphic Depiction of International Ice Patrol Plot for 1200 GMT June 30, 1987, Based on Observed and Forecast Conditions.

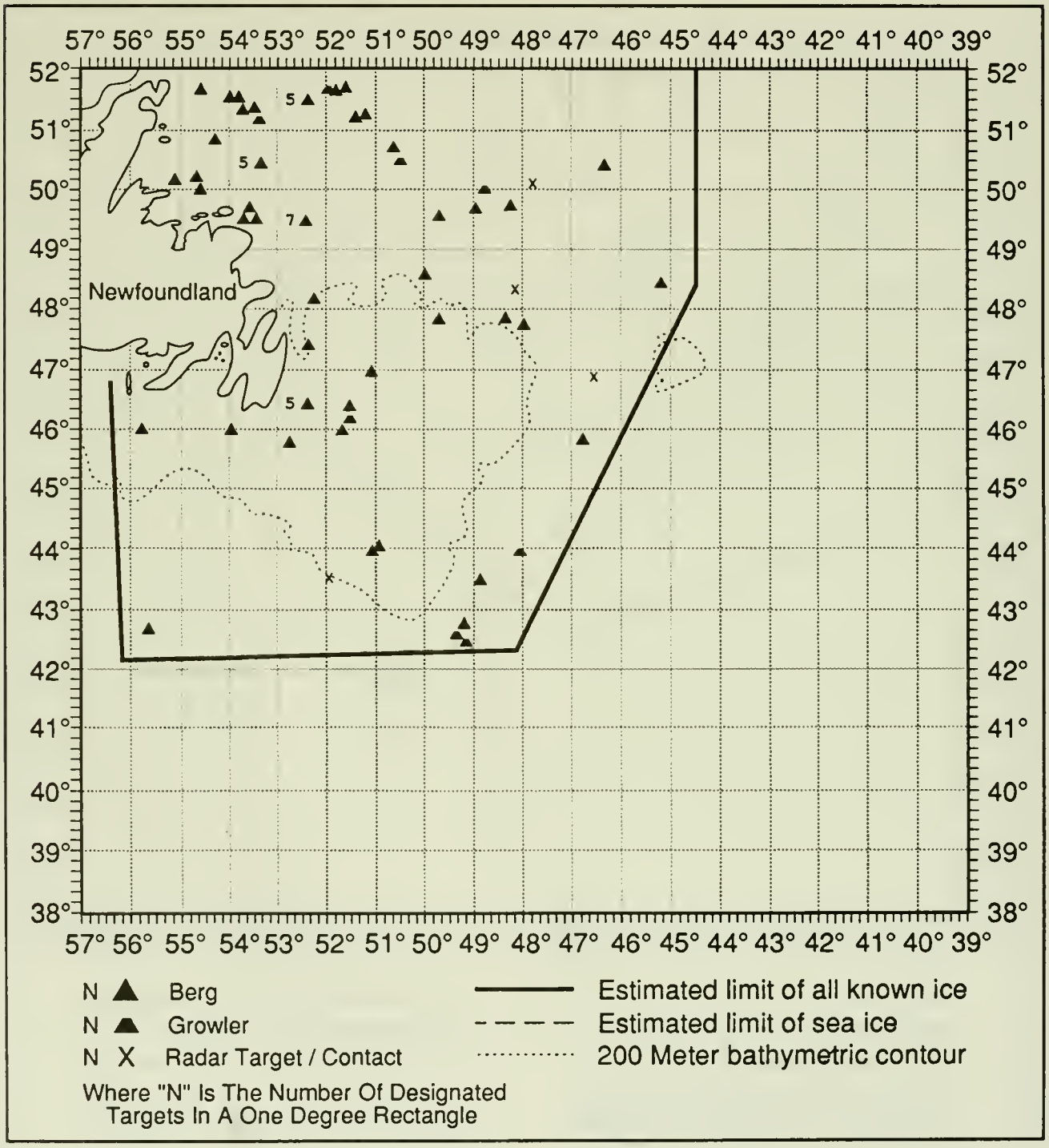

Figure 33. Graphic Depiction of International Ice Patrol Plot for 1200 GMT July 15, 1987, Based on Observed and Forecast Conditions.

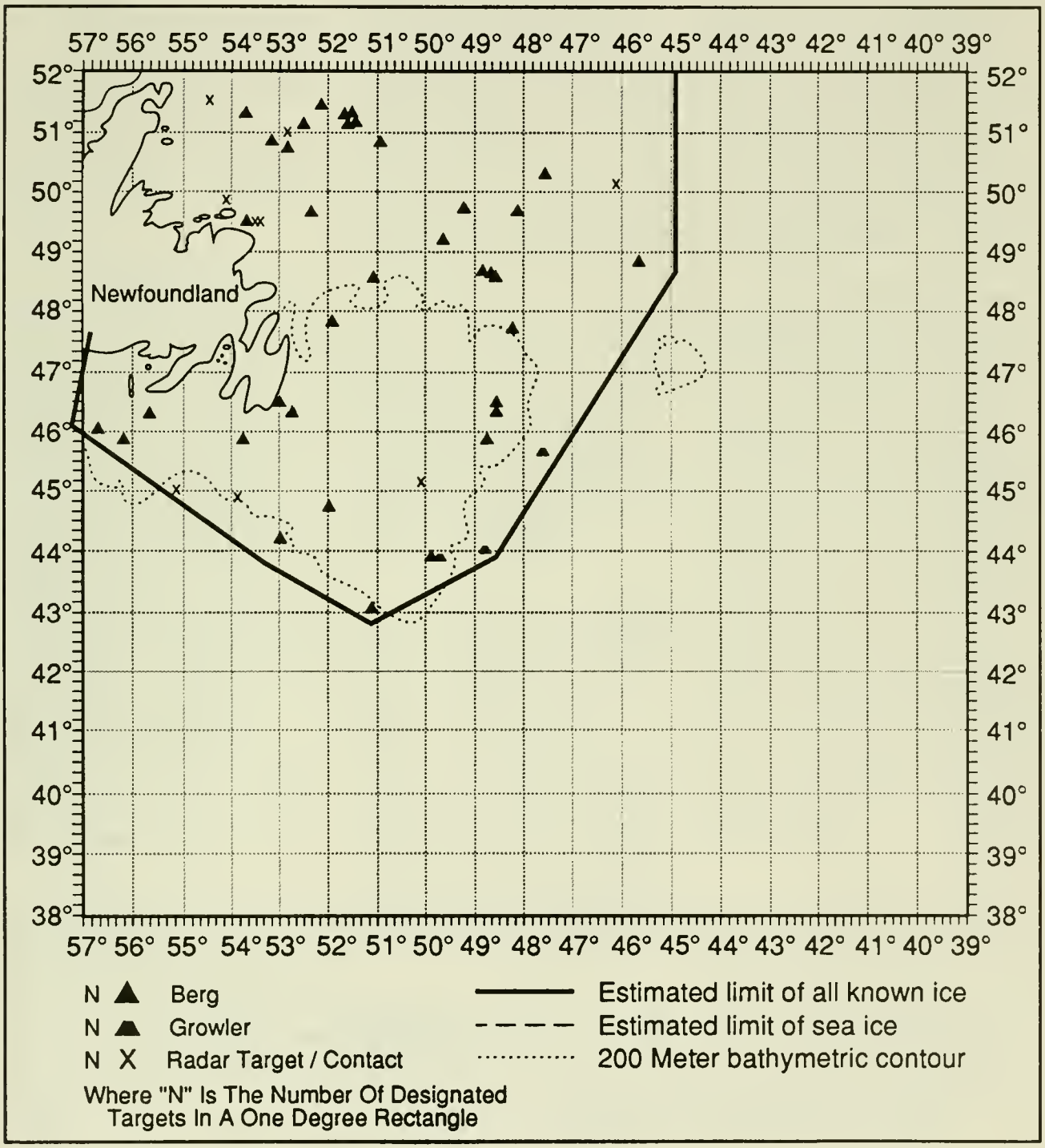

Figure 34. Graphic Depiction of International Ice Patrol Plot for 1200 GMT July 30, 1987, Based on Observed and Forecast Conditions.

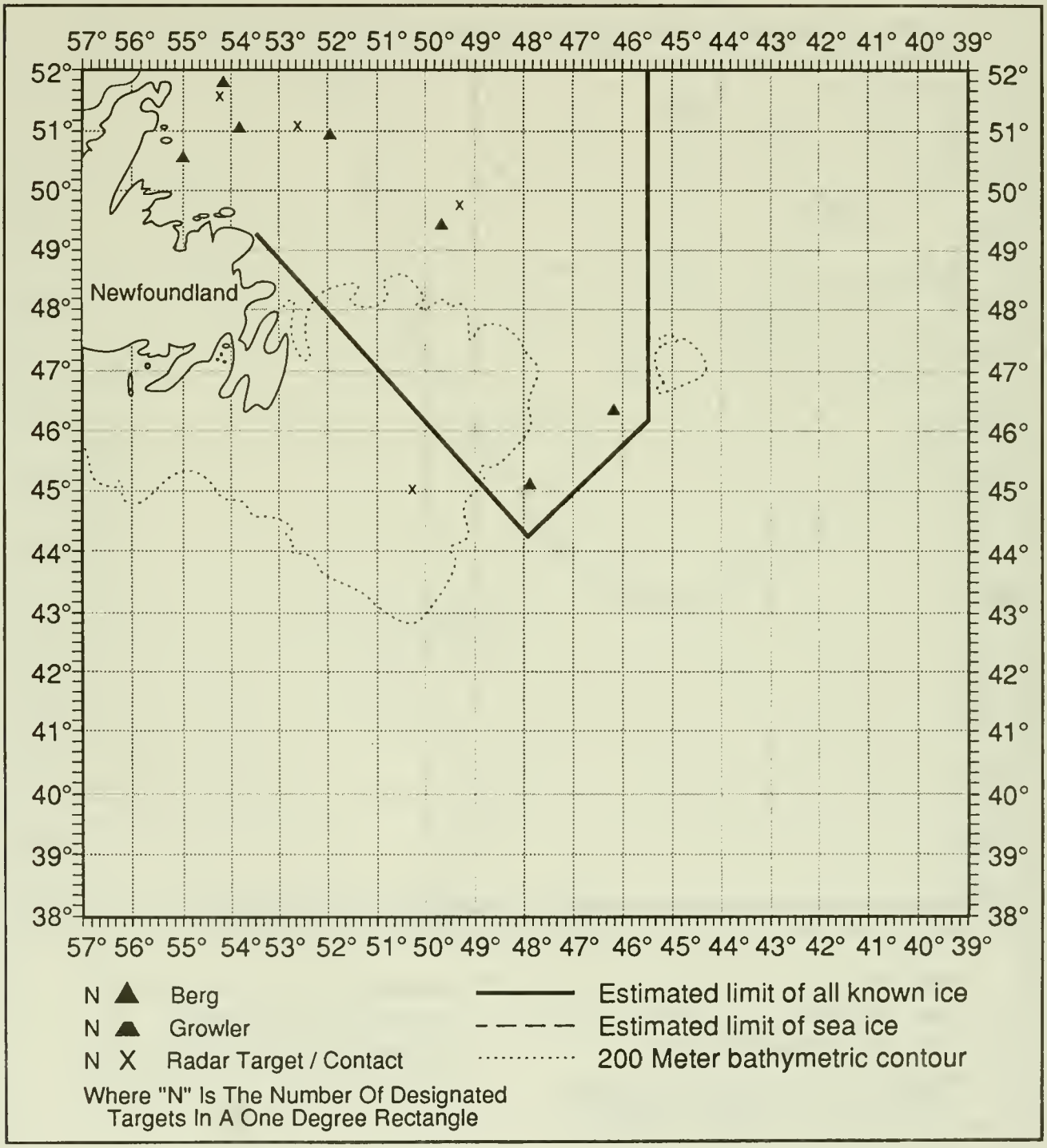

Discussion of Ice and Environmental Conditions

The number of icebergs that pass south of 48°N in the International Ice Patrol area is the measure by which the International Ice Patrol has judged the severity of each year since 1913 (Appendix B). With 318 icebergs south of 48°N, the severity of 1987 was below the 1913-1986 average (Appendix B).

Since the number of icebergs calved each year by Greenland's glaciers is in excess of 10,000 (Knutson and Neill, 1978), a sufficient number of icebergs exist in Baffin Bay during any year. Therefore, annual fluctuations in the generation of Arctic icebergs are not a significant factor in the number of icebergs passing south of 48°N annually. The number of icebergs passing south of 48°N each season is determined by the supply of icebergs available to drift south onto the Grand Banks, as well as factors affecting iceberg transport (currents, winds, and sea ice) and the rate of iceberg deterioration (wave action, sea surface temperature, and sea ice).

Sea ice impedes the transport of icebergs by winds and currents and protects icebergs from wave action, the major agent of iceberg deterioration. Although it slows current and wind transport of icebergs, sea ice is itself an active medium, for it is continually moving toward the ice edge where melt occurs. Therefore, icebergs in sea ice will eventually reach open water unless grounded. The melting of sea ice itself is affected by snow cover (which slows melting) and air and sea water temperatures. As sea ice melt accelerates in the spring and early summer, trapped icebergs are rapidly released and are then subject to normal transport and deterioration.

The Labrador Current, aided by northwesterly winds in winter, is the main mechanism transporting icebergs south to the Grand Banks. In addition to transporting icebergs south, the relatively cold waters of the Labrador current slow the deterioration of icebergs in transit.

Sea ice conditions were above normal for the first part of the 1987 season. The sea ice edge was farther south than normal in December and January, and at its mean location in February. This would have the affect of protecting the icebergs longer and releasing them farther south than normal. These ice conditions would normally lead to a season of average or above average iceberg severity.

The AES/IIP preseason surveys in January and February indicated an adequate supply of icebergs available to drift south onto the Grand Banks (Osmer and McRuer, 1987).

Based on the sea ice conditions and availability of icebergs, International Ice Patrol was expecting an average to above average season. The question of how and why the iceberg season develops as it does is always of interest to International Ice Patrol. This is particularly true when the season does not develop as expected, as happened in 1987.

In February, the sea level pressure distribution indicated the mean flow pattern for the month was northeasterly rather than northwesterly. This would result in an unfavorable drift to the west, out of the Labrador Current and against the Labrador coast. The icebergs would get grounded or trapped in the many bays and inlets along the Labrador coast. The easterly winds in March pushed all the sea ice off the Grand Banks, and packed it against the Newfoundland coast. Again, the winds in March were unfavorable for iceberg drift. The icebergs were pushed out of the Labrador Current, and along the coasts of Labrador and Newfoundland.

In summary, it appears that in spite of adequate supply of icebergs and favorable sea ice conditions, an average or above average 1987 iceberg season failed to occur because wind conditions were not favorable in February and March for the transport of icebergs south of 48°N.

References

Alles, M.F., and M.A. Alfultis. A Mobile Oceanographic Data Collection System, International Ice Patrol Technical Report, In Press.

Anderson, I. Iceberg Deterioration Model, *Report of the International Ice Patrol in the North Atlantic, 1983 Season, CG-188-38*, U.S. Coast Guard, Washington D.C., 1983.

Atmospheric Environment Service (AES), Thirty Day Ice Forecast for Northern Canadian Waters, January 1987.

Atmospheric Environment Service (AES), Thirty Day Ice Forecast for Northern Canadian Waters, March 1987.

Atmospheric Environment Service (AES), Thirty Day Ice Forecast for Northern Canadian Waters, May 1987.

Knutson, K.N. and T.J. Neill, *Report of the International Ice Patrol Service in the North Atlantic Ocean for the 1977 Season, CG-188-32*, U.S. Coast Guard, Washington D.C., 1978.

Mariners Weather Log, Spring 1987, Vol. 31, Number 2, 1987a.

Mariners Weather Log, Summer 1987, Vol. 31, Number 3, 1987b.

Mariners Weather Log, Fall 1987, Vol 31, Number 4, 1987c.

Mariners Weather Log, Winter 1988, Vol. 32, Number 1, 1988.

Murphy, D.L. and I. Anderson. Evaluation of the International Ice Patrol Drift Model, *Report of the International Ice Patrol in the North Atlantic, 1985 Season, CG-188-40*, U.S. Coast Guard, Washington D.C., 1985.

Naval Oceanography Command, Sea Ice Climatic Atlas: Volume II Arctic East, 1986.

Navy-NOAA Joint Ice Center, Naval Polar Oceanography Center, Southern Ice Limit, Published Bi-monthly, 1987.

Osmer, S. R. and H. McRuer, 1987 Preseason Iceberg Survey and Season Prediction, Proc. Oceans '88, Oct. 1987, Halifax, N.S.

Acknowledgements

Commander, International Ice Patrol acknowledges the assistance and information provided by the Atmospheric Environment Service (AES) of Environment Canada, the U.S. Naval Fleet Numerical Oceanography Center, U.S. Naval Eastern Oceanography Center, and the U.S. Coast Guard Research and Development Center.

We extend our sincere appreciation to the staffs of the Canadian Coast Guard Radio Station St. John's, Newfoundland/ VON, Ice Operations St John's, Newfoundland, Air Traffic Control Gander, Newfoundland, Canadian Forces Gander and St. John's, Newfoundland, and the Gander Weather Office, and to the personnel of U.S. Coast Guard Air Station Elizabeth City, US Coast Guard Communications Station Boston, USCGC BITTERSWEET, and USCGC TAMAROA for their excellent support during the 1987 International Ice Patrol season.

It is also important to recognize the efforts of the personnel at the International Ice Patrol: LCDR S. R. Osmer, LCDR W. E. Hanson, Dr. D. L. Murphy, LT I. Anderson, LT N. B. Thayer, LT M. A. Alfultis, MSTCS G. F. Wright, MSTC M. F. Alles, YN1 S. A. Cooper, MST1 P. O. Pelletier, MST1 M. G. Barrett, MST2 D. A. Hutchinson, MST2 D. D. Beebe, MST2 W. A. Henry, MST2 K. A. Austin, MST3 P. B. Reilley, and MST3 C. F. Weiller.

Appendix A
List of Participating Vessels, 1987

VESSEL NAME	FLAG	SST	ICE	REPORTS
ABITIBI MACADO	FED. REP. OF GERMANY			4
ABTARTICO	PORTUGAL			1
ACADIAN GAIL	CANADA			1
ACADIAN TEMPEST	CANADA			1
ADA GORTHON	SWEDEN			3
AFRICAN EVERGREEN	LIBERIA	1		
AFRICAN GARDENIA	LIBERIA	10		
AGIATHALASSINI	PANAMA	1		2
AIFANOURIOS	LIBERIA	17		
AKRANES	ICELAND			1
ALBERRY	SAUDI ARABIA	3		
ALBRIGHT EXPLORER	UNITED KINGDOM			1
ALBRIGHT PIONEER	UNITED KINGDOM			1
ALGERIAN	SWEDEN	5		
ALMARE SETTIMA	ITALY			1
ALMESSILAH	KUWAIT	16		2
AMERICANA	ITALY			1
APOLLO	UNITED KINGDOM	1		
ARABELLA	GREECE			1
ARCTIC	CANADA			2
ARGUS TRAUCHER	LIBERIA	9		
ARKA	UNKNOWN			3
ARMERIA	JAPAN	1		1
ASTOR	ST. VINCENT THE GRENADINES			3
ATLANTIC	NETHERLANDS			1
ATLANTIC AMITY	UNITED KINGDOM	1		1
ATLANTIC LINK	BAHAMAS			3
ATLSGA	SWEDEN			1
BAFFIN	CANADA	2		
BALAO	LIBERIA	7		1
BALTIC	CYPRUS			7
BALTIC SUN	NETHERLANDS	1		1
BARBER NARA	SWEDEN			1
BARON	PANAMA			1
BARTLETT	CANADA			5
BELLE ETOILE	MAURITUIS			1
BIENDIE	LIBERIA	1		
BIRDIE	AUSTRALIA	5		
BISHAH	SAUDIA ARABIA	5		

VESSEL NAME	FLAG	SST	ICE REPORTS
BITTERSWEET	USA	3	1
BLUE PINE	PANAMA		2
BOKA	JAPAN	4	
BOKHTARMA	PEOPLES REP. OF CHINA		1
BONNY	BAHAMAS	8	
BRIDGEWATER	FED. REP. OF GERMANY		2
BRITISH STEEL	UNITED KINGDOM		1
BROOMPARK	UNITED KINGDOM		1
CANMAR AMBASSADOR	CANADA		8
CANMAR (DART) EUROPE	BELGIUM		4
CANADIAN EXPLORER	UNITED KINGDOM		1
CAPETAN HALARIS	UNKNOWN		1
CAPE BYRON	FED. REP. OF GERMANY		1
CAPE ROGER	CANADA		1
CARMEN MARE	GREECE	39	
CAST CARIBOU	LIBERIA	1	2
CAST HUSKEY	UNITED KINGDOM		2
CAST MUSKOX	UNITED KINGDOM		1
CAST OTTER	UNITED KINGDOM		1
CAST POLAR BEAR	LIBERIA	10	4
CAVELIER DELASSALLE	FRANCE		1
CECELIA DESGAGNES	CANADA		1
CHARLOTTE BASTIAN	FED. REP. OF GERMANY		3
CHIPPEWA	LIBERIA	1	1
CHERRY VALLEY	USA		2
CIECERO	CANADA		4
COASTAL CANADA	CANADA		4
CZANTORIA	POLAND	1	4
DAMODAR DR. A. BLOCK	INDIA		1
DANAU MARU	JAPAN		1
DART AMERICA	PANAMA		2
DART ATLANTIC	UNITED KINGDOM		2
DART BRITAIN	UNITED KINGDOM		1
DONNY	SWEDEN		1
DORTHE OLDENDORFF	SINGAPORE		4
DUESSELDORF EXPRESS	FED. REP. OF GERMANY		2
DUKE OF TOPSAIL	UNITED KINGDOM		1
DOZE VALE	BRAZIL	8	
EASTERN UNICORN	PANAMA	7	7
ECAREG LIRIA	SPAIN		1

VESSEL NAME	FLAG	SST	ICE REPORTS
EDCO	EGYPT		1
EIRMNES	LIBERIA		1
ENERCHEM FUSION	CANADA		5
ENSORTFONAH	BELGIUM		1
ESSICAMILLA	SINGAPORE		1
ESSO PROVIDENCE	LIBERIA		2
EUROPEGASUS	LIBERIA		1
EUTERPE	CYPRUS		1
EVRYALOS	GREECE	1	2
FAIR SPIRIT	LIBERIA	3	
FALCON	LIBERIA	1	
FALKOFN	SWEDEN		1
FEDERAL CALUMET	SWEDEN		1
FEDERAL FUJI	JAPAN		2
FEDERAL POLARIS	JAPAN		1
FEDERAL ST. CLAIR	LIBERIA		1
FINNARCTIS	UNITED KINGDOM		1
FINN FALCON	UNITED KINGDOM		12
FINNFIGHTER	FINLAND	2	2
FINNPOLARIS	UNITED KINGDOM	7	5
FINNSNES	LIBERIA		1
FLAME	CYPRUS		1
FRED J. AGNICH	CANADA		1
FROST CASTOR	CYPRUS	1	
FURIA	LIBERIA	3	
GALASSIA	ITALY	15	
GAUDREAU	CANADA		1
GENERAL GARCIA	PHILIPPINES		1
GENERAL VARGAS	PHILIPPINES		1
GRAND COURT	USSR		2
GRAND KNIGHT	USSR		1
GRAND PRINCE	UNKNOWN		1
GRENFELL	CANADA		4
GROSEWATER	CANADA		2
GULF HARVEST	PANAMA		1
HANSEATIC	PANAMA		1
HARITAS	CYPRUS	5	
HELENA OLDENDORFF	PANAMA		2
HELLESPONT MARINER	GREECE		1
HELLESPONT VALOUR	GREECE	6	

VESSEL NAME	FLAG	SST	ICE REPORTS
HENRI TE' LLIER	CANADA		1
HEXMARRDO	UNITED KINGDOM	1	1
HIGH AEUT	SINGAPORE		4
HOFSJOKULL	ICELAND		4
HOLCAN MAAS	URUGUAY		1
HUAL TRAPPER	PANAMA	5	
HUBERT GAUCHER	CANADA		1
HUDSON	CANADA		5
ICE LACKENKY	UNITED KINGDOM		2
ICE TECHNO VENTURE	CANADA		2
IMPERIAL BEDFORD	CANADA		2
IMPERIAL QUEBEC	CANADA		2
INGRID GORTHON	BAHAMAS		1
IRONMASTER	PANAMA		3
IRVING OURS POLAIRE	CANADA		16
IRVING WOOD	UNITED KINGDOM		4
ISHIKARIMARU	JAPAN	10	1
JACKMAN	CANADA		6
JESSIE STOVE	SINGAPORE	11	
JOHANNA SCHULTE	CYPRUS	3	3
JOKULFELL	ICELAND		3
JUGOAGENT	UNKNOWN		1
KANGUK	CANADA		2
KATTEGAT	PHILIPPINES		1
KAZIMIERZ PULASKI	SUDAN		1
KHUDOYHNIK PAKHOMOV	USSR		1
KHUDOYHNIK ROMAS	USSR		4
KOELN EXPRESS	FED. REP. OF GERMANY	1	2
KOLL BJORG	NORWAY	2	
KRISTINA LOGOS	USSR		1
KRITI CORAL	GREECE		3
LABRADOC	CANADA		1
LA CHENE	CANADA		2
LADY HIND	BELGIUM	11	2
LAKENBY	UNITED KINGDOM		1
LAKESTAR	CYPRUS	2	
LAPPONIA	BAHAMAS	1	1
LAURENCE H. GIANELLA	UNKNOWN		1

VESSEL NAME	FLAG	SST	ICE REPORTS
LEBRAVE	UNKNOWN		2
LECEDREN	CANADA		3
LECH	AUSTRIA	2	2
LEERORT	FED. REP. OF GERMANY	3	
LEONARD J. COWLEY	UNKNOWN		5
LIBERTY BELL VENTURE	LIBERIA		1
LIPNO	CZECHOSLAVIA	8	
LONE VENTURE	CANADA		1
LONG CHALLENGER	LIBERIA	2	
LOTILA	BAHAMAS		1
L. ROCHETTE	CANADA		1
LUCIEN PAGUIN	CANADA		6
LUCKY MAN	CYPRUS	1	1
LUDOLF OLDENDORFF	SINGAPORE		1
MAERSK SEBAROK	SINGAPORE	1	1
MAHONE BAY	CANADA		2
MALOJA	CYPRUS		4
MANCHESTER CHALLENGE	UNITED KINGDOM		7
MANGA	UNITED KINGDOM		2
MARIA AUXILIDORA	BRAZIL		1
MARIA G L	GREECE		1
MARIN	LIBERIA		2
MARINE PACKER	CANADA		1
MASHUMARU	JAPAN	6	
MEDALLION	DENMARK		4
MELA	PANAMA		1
METRO STAR	CANADA		2
ML JET	YUGOSLAVIA		2
MOCHIZUKI	JAPAN		1
MOSIL ORE	LIBERIA		1
MT BONNY	BAHAMAS	3	
MUO	ST. VINCENT	1	1
MUSKOX	UNITED KINGDOM		1
MYRSINIDI	LIBERIA		1
NADEZHDA OBUKHOVA	USSR		1
NARWHAL	UNITED KINGDOM		6
NELVANA	LIBERIA	2	2
NEMEMCHA	ALGERIA		
NEPTUNE JADE	SINGAPORE		1
NORDHEIDI	SINGAPORE		5
NORDIC SUN	LIBERIA		1

VESSEL NAME	FLAG	SST	ICE REPORTS
NORDMARK	SINGAPORE		2
NORD PACIFIC	SINGAPORE	10	2
NORDSTAR	SINGAPORE		3
NORLANDIA	FED. REP. OF GERMANY		1
NORTHERN ENTERPRISE	BERMUDA		1
NORTHERN PRINCESS	CANADA		1
NORTHWIND	USA	11	2
NORWIND	NETHERLANDS	2	1
NOSAC LAKAYAMA	LIBERIA	1	
NURNBERG EXPRESS	FED. REP. OF GERMANY		9
OKANAGAN	CANADA	1	1
OLIVIA	BRAZIL		1
ORIENTAL RUBY	JAPAN	1	1
ORIENT PIONEER	LIBERIA		1
ORLANDO	LIBERIA		1
PENALARA	FRANCE	2	2
PENNY LUCK	UNKNOWN		1
PEONIA	LIBERIA		2
PLACENTIA BAY	CANADA		8
POLAR BEAR	LIBERIA	2	
PONIA	HONDURAS		1
PRIMOSTEN	YUGOSLAVIA	1	3
PRODUCT SPLENDOR	UNITED KINGDOM	4	1
PROTECTEUR	CANADA	6	
PUHOS	BAHAMAS		1
RAVIDAS	INDIA		1
REED VOYAGER	PANAMA		6
RIVER PRINCESS	LIBERIA	1	1
ROBERT MAERSK	DENMARK	3	1
RODRIGOTORREABLA	BRAZIL	7	
ROVER	USA	1	
SAINT DIMITIRIOS	LIBERIA	6	
SAINT LAWRENCE	PAKISTAN		1
SAINT VASSILLOS	CYPRUS	1	
SAMBURG	USSR		2
SAM JOHN PIONEER	PANAMA		1
SAMUEL L COBB	USA	10	8
SANDNESS	PANAMA		2
SANTA MALFALDO	PORTUGAL		1

VESSEL NAME	FLAG	SST	ICE REPORT
SEASTAR 2	CYPRUS		1
SELKIRK SETTLERR	CANADA		1
SENTIS	UNITED KINGDOM	3	
SIR H. GILBERT	CHILE		9
SIR ROBERT BOND	CANADA		4
SKIDEGATE	CANADA		10
SOREN TOUBRO	INDIA	6	3
SOVETSK	USSR		1
SPYROS A. LEMOS	GREECE		1
STALWART	USA	4	
STARWORLD	UNITED KINGDOM		1
STEFAN BATORY	POLAND		4
STEFAN STARZYNSKI	POLAND		2
STILLANOVA	NETHERLANDS		1
STOLT CASTLE	LIBERIA		2
STOLT CROWN	LIBERIA		2
STOLT SAPPHIRE	LIBERIA	4	2
STOLT SPAN	LIBERIA		1
STOLT SYDNESS	LIBERIA	3	
STUTTGART EXPRESS	FED. REP. OF GERMANY		1
SUMMIT	LIBERIA		3
TAMAROA	USA	5	1
TAVERNER	CANADA		1
TEAM FROSTA	SINGAPORE	5	
TEVERA	CYPRUS	1	
THAMES	LIBERIA		1
TILIA GORTHOU	SWEDEN		1
TOKI ARROW	NORWAY	1	1
TORONTO	BERMUDA	1	
TRINITY BAY	CANADA		4
UNDERWOOD	USA	6	
VADASTEINUR	DENMARK		1
VALOR	PHILIPPINES		1
VAYGACH	USSR		1
VESALIUS	BELGIUM		1
VICTORIUS	PANAMA		2
VIKING OSPREY	BAHAMAS		1
VIKTOR TKACHYOV	USSR		2
VISHVA PALLAV	INDIA		1
VOLOS	LIBERIA	3	

VESSEL NAME	FLAG	SST	ICE REPORT
WESER HARBOUR	FED. REP. OF GERMANY		1
WEST BRIDGE	LIBERIA		2
WILFRED TEMPLEMAN	CANADA		3
WINONA	LIBERIA		1
WOODLAND	CANADA		4
YAYAMARIA	CYPRUS		1
YOUNG SHINKO	JAPAN	3	
YUKOVA	LIBERIA		2
ZAGREB	YUGOSLAVIA		1
ZANDAM	INDIA		1
ZANDBERG	CANADA		1
ZAWRAT	POLAND		1
ZIEMIA LUBELSKA	POLAND		1
ZIEMIA OLSZTYNSKA	POLAND		3
ZIEMIA OPOLSKA	POLAND	3	
ZIEMIA TARNOWSKA	POLAND		1
ZIM KEELUNG	ISRAEL		1

Appendix B

Iceberg Populations South of 48° N Since 1900

LT Michael A. Alfultis, USCG

Since its beginning, the International Ice Patrol has maintained an annual count of the number of icebergs crossing latitude 48°N. Each year the number of icebergs south of 48°N is used by International Ice Patrol to gauge the potential threat to North Atlantic shipping, and, therefore, the opening and closing date of each Ice Patrol Season.

Table B-1 provides a monthly breakdown of the estimated number of icebergs crossing 48°N each year since 1900. This updates the historical iceberg statistics last published in the 1977 Ice Patrol Bulletin No. 63. Table B-1 is in a slightly different format from that published previously. Recently, International Ice Patrol began using as its ice year the period from October through September rather than the calendar year or the period September through August, as was done in the past. The data published in 1977 have been updated to reflect this, and the iceberg counts since 1977 added.

The monthly counts are broken into four eras, 1900-1912, 1913-1945, 1946-1982, and 1983-1987. The first era is the pre-International Ice Patrol period when icebergs sighted by commercial shipping were reported to the U. S. Hydrograhic Office. During the next era, the International Ice Patrol estimated the iceberg distribution from surface observations made from U. S. Coast Guard cutters and commercial vessels transiting the area. Visual reconnaissance from aircraft became International Ice Patrol's primary method for iceberg detection during the third era. During the final era, the Side-Looking Airborne Radar (SLAR) provided International Ice Patrol with an all-weather capability to detect icebergs. Iceberg sightings provided by commercial shipping have been, and continue to be, an important source of information to International Ice Patrol.

International Ice Patrol defines those ice years with less than 300 icebergs crossing 48°N as light or low ice years; those years with 300 to 600 icebergs crossing 48°N as average or intermediate ice years; those years with 600 to 900 icebergs crossing 48°N as heavy or severe ice years; and those ice years with more than 900 icebergs crossing 48°N as extreme ice years.

Figure B-1 is a bar graph of icebergs crossing 48 N since 1912. The variability in the record is readily seen. The factors that determine this variability are the supply of icebergs available to drift onto the Grand Banks, those affecting iceberg transport (currents, winds, and sea ice), and those affecting deterioration (wave action, sea surface temperature, and sea ice). These factors are often unpredictable. During the 1987 season, short term changes in the mean wind flow dramatically affected the iceberg distribution, and changed the character of an anticipated severe iceberg season to barely an average season (318 icebergs).

Table B-1. Iceberg Populations South of 48° N Since 1900.

ICE YEAR	OCT	NOV	DEC	JAN	FEB	MAR	APR	MAY	JUN	JUL	AUG	SEP	ANNUAL TOTAL
Pre-International Ice Patrol													
1900	0	0	0	10	0	0	5	32	33	6	1	1	88
1901	1	0	0	1	0	0	4	13	29	22	6	5	81
1902	1	2	5	3	0	1	1	13	5	16	1	0	48
1903	1	0	0	0	2	400	166	151	52	23	7	0	802
1904	0	0	1	0	0	12	63	82	89	14	3	2	266
1905	0	0	0	3	2	168	373	109	100	50	9	8	822
1906	8	0	15	14	11	77	49	133	87	18	16	0	428
1907	0	0	0	0	1	11	162	248	138	64	11	0	635
1908	0	0	3	1	0	7	39	82	51	2	2	20	207
1909	15	3	0	0	55	147	134	321	181	121	45	19	1,041
1910	1	0	0	0	0	0	34	10	3	3	0	0	51
1911	0	0	0	0	8	41	112	72	77	21	40	3	374
1912	0	8	14	1	0	34	395	345	159	63	19	0	1,038
TOTAL 1900-1912	27	13	38	33	79	898	1,537	1,611	1,004	423	160	58	5,881
AVERAGE 1900-1912	2	1	3	2	6	69	118	124	77	32	12	4	452
Surface Patrol Vessels													
1913	0	3	0	2	4	37	109	292	71	14	4	7	543
1914	0	6	4	1	41	32	27	419	71	22	46	52	721
1915	13	1	6	14	72	67	96	97	71	28	17	5	487
1916	0	1	0	0	0	0	0	25	29	0	0	0	55
1917	0	0	0	0	0	13	3	3	9	10	0	0	38
1918	0	0	0	0	0	12	23	26	37	27	34	22	181
1919	1	14	3	3	4	5	25	75	56	26	36	69	317
1920	2	12	4	6	43	20	5	211	86	18	5	18	430
1921	19	10	4	17	5	43	210	198	175	53	24	4	762
1922	10	1	6	0	3	35	71	245	83	21	11	6	492
1923	27	21	0	0	3	28	65	83	42	10	3	2	284
1924	0	0	0	3	0	6	2	0	0	0	0	0	11
1925	0	0	0	0	3	5	8	58	22	13	0	0	109
1926	0	0	0	0	3	15	58	168	85	4	6	2	341
1927	3	1	0	4	10	26	93	153	95	5	3	0	393
1928	0	0	0	0	0	14	156	190	87	55	5	0	507
1929	4	4	0	0	0	45	332	460	376	107	1	0	1,329
1930	0	18	12	14	116	87	89	101	62	3	1	1	504
1931	1	0	0	0	0	2	1	10	0	0	0	0	14
1932	0	0	0	0	1	43	321	90	58	1	0	0	514
1933	0	0	0	0	2	4	12	162	36	0	0	0	216
1934	0	0	0	1	0	0	245	228	87	14	1	0	576

Table B-1 (Continued).

ICE YEAR	OCT	NOV	DEC	JAN	FEB	MAR	APR	MAY	JUN	JUL	AUG	SEP	ANNUAL TOTAL
1935	0	0	0	0	0	46	177	501	134	11	3	0	872
1936	0	0	3	0	0	0	8	14	0	0	0	0	25
1937	0	0	0	20	53	121	124	137	14	1	0	0	470
1938	0	0	0	2	3	38	212	286	110	13	0	0	664
1939	0	0	0	0	0	22	173	471	150	28	6	0	850
1940	0	0	0	0	0	0	0	1	0	0	0	0	1
1941	0	1	0	0	0	0	1	1	0	0	0	0	3
1942	0	0	0	0	0	30	0	0	0	0	0	0	30
1943	0	0	0	0	0	25	90	298	270	150	7	0	840
1944	0	0	0	0	0	31	319	213	106	30	1	0	700
1945	0	0	0	0	6	352	253	256	92	109	15	0	1,083
TOTAL 1913-1945	80	93	42	87	372	1,204	3,308	5,472	2,514	773	229	188	14,362
AVERAGE 1913-1945	2	3	1	3	11	36	100	166	76	23	7	6	435
Visual Aircraft Reconnaissance													
1946	0	0	0	0	2	67	98	168	88	7	0	0	430
1947	0	0	0	3	1	2	5	11	26	15	0	0	63
1948	0	0	0	0	0	60	210	185	68	0	0	0	523
1949	0	0	0	0	0	1	23	20	3	0	0	0	47
1950	0	0	0	0	12	61	183	135	58	7	0	1	457
1951	1	2	0	0	3	2	0	0	0	0	0	0	8
1952	0	0	1	0	0	0	12	2	0	0	0	0	15
1953	0	0	0	0	0	21	11	18	6	0	0	0	56
1954	0	0	0	1	16	47	165	65	16	2	0	0	312
1955	0	0	0	0	0	10	32	14	5	0	0	0	61
1956	0	0	0	0	0	9	13	34	21	3	0	0	80
1957	0	0	0	3	43	41	172	265	288	113	6	0	931
1958	0	0	0	0	0	0	0	0	0	1	0	0	1
1959	0	0	0	0	0	14	266	180	186	43	0	0	689
1960	0	2	3	3	0	0	41	161	44	4	0	0	258
1961	0	0	0	0	6	60	30	16	1	0	1	0	114
1962	1	0	1	0	0	14	72	21	10	3	0	0	122
1963	0	0	0	0	0	4	20	0	1	0	0	0	25
1964	0	0	0	0	3	88	225	19	28	5	1	0	369
1965	0	0	0	0	1	19	33	22	1	0	0	0	76
1966	0	0	0	0	0	0	0	0	0	0	0	0	0
1967	0	0	0	0	0	25	134	209	65	8	0	0	441
1968	0	0	0	0	0	0	104	44	60	14	4	4	230
1969	0	0	0	0	0	0	0	35	17	1	0	0	53
1970	0	0	0	0	0	0	5	2	70	8	0	0	85

Table B-1 (Continued).

ICE YEAR	OCT	NOV	DEC	JAN	FEB	MAR	APR	MAY	JUN	JUL	AUG	SEP	ANNUAL TOTAL
1971	0	0	0	0	0	31	4	20	7	11	0	0	73
1972	0	0	0	0	40	185	501	559	225	48	26	4	1,588
1973	0	0	6	54	110	134	212	159	151	19	1	0	846
1974	0	0	0	0	1	99	345	446	266	168	61	1	1,387
1975	0	0	0	0	24	41	10	20	5	0	0	0	100
1976	0	0	0	0	0	33	13	67	35	3	0	0	151
1977	0	0	0	0	3	7	12	0	0	0	0	0	22
1978	0	0	0	0	0	5	28	35	7	0	0	0	75
1979	0	0	0	0	5	20	81	34	9	3	0	0	152
1980	0	0	0	1	3	7	0	9	4	0	0	0	24
1981	0	0	0	0	0	48	10	5	0	0	0	0	63
1982	0	0	0	0	0	17	61	13	94	3	0	0	188
TOTAL 1946-1982	2	4	11	65	273	1,172	3,131	2,993	1,865	489	100	10	10,115
AVERAGE 1946-1982	0	0	0	2	7	32	85	81	50	13	3	0	273
Aircraft SLAR Reconnaissance													
1983	0	0	2	9	165	124	339	465	168	76	4	0	1,352
1984	0	0	0	0	0	101	953	484	227	335	93	9	2,202
1985	3	11	7	2	57	129	208	205	247	123	39	32	1,063
1986	0	0	0	0	3	40	60	59	24	18	0	0	204
1987	0	0	5	2	14	48	76	29	127	15	2	0	318
TOTAL 1983-1987	3	11	14	13	239	442	1,636	1,242	793	567	138	41	5,139
AVERAGE 1983-1987	0	2	3	3	48	88	327	248	159	113	28	8	1,027
TOTAL 1900-1987	112	121	105	198	963	3,716	9,612	11,318	6,176	2,252	627	297	35,497
AVERAGE 1900-1987	1	1	1	2	11	42	109	129	70	26	7	3	403
TOTAL 1913-1987	85	108	67	165	884	2,818	8,075	9,707	5,712	1,829	467	239	29,616
AVERAGE 1913-1987	1	1	1	2	12	38	108	129	69	24	6	3	395

Figure B-1.

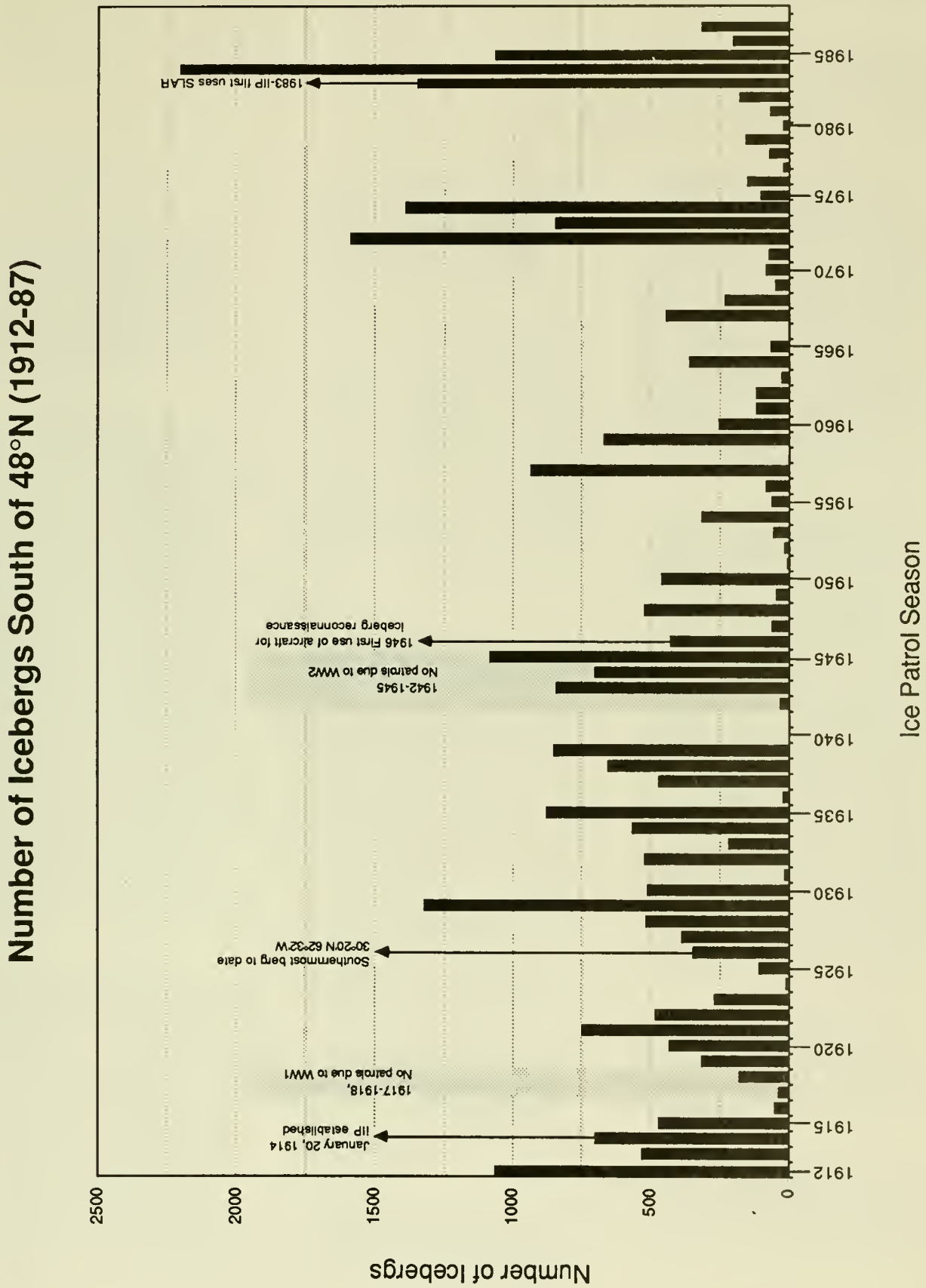
Number of Icebergs South of 48°N (1912-87)
Number of Icebergs
2500
2000
1500
1000
500
0
1912
1915
1920
1925
1930
1935
1940
1945
1950
1955
1960
1965
1970
1975
1980
1985
Ice Patrol Season
January 20, 1914
IIP established
1917-1918,
No patrols due to WW1
Southernmost berg to date
30°20'N 62°32'W
1942-1945
No patrols due to WW2
1946 First use of aircraft for
iceberg reconnaissance
1983-IIP first uses SLAR

Appendix C

1987 International Ice Patrol Drifting Buoy Program

Donald L. Murphy
LT Neal B. Thayer, USCG

INTRODUCTION

This report documents the operational portion of the 1987 drifting buoy program of the International Ice Patrol. The program, which began in 1976, supports Ice Patrol operations and research.

Eighteen separate buoy deployments were made in 1987. Of these, nine were launched from Ice Patrol reconnaissance aircraft and the data used primarily for operational purposes (Summy and Anderson, 1983 and Summy, 1982). The remainder were deployments from U.S. Coast Guard vessels conducting Ice Patrol research cruises. Most of the latter were drift tracks of short duration, with the buoy being recovered at the end of each experiment. Two of the aircraft-deployed buoys were launched by Ice Patrol off northern Labrador as part of a Canadian Atmospheric Environment Service (AES) test of their iceBerg Analysis and Prediction System (BAPS).

Ice Patrol sponsored two oceanographic research cruises in 1987. The first, (IIP 87-1) from 27 April to 20 May, was conducted aboard USCGC BITTERSWEET (WLB 389). The objective of IIP 87-1 was to investigate the ability of IIP's side-looking airborne radar (SLAR) to detect warm-core eddies. Six separate buoy deployments were made during this research. Of these, two buoys were not recovered at the end of the experiment, and their data were used for operational purposes. The buoy tracks during the cruise period are discussed in Appendix D of this Bulletin.

The second 1987 Ice Patrol research cruise (IIP 87-2) was an iceberg drift and deterioration study conducted aboard USCGC TAMAROA (WMEC 166), from 8 June to 27 June. TAMAROA deployed three buoys, all of which were recovered at the end of the experiment. The results of this cruise are discussed in Appendix E.

With the exception of the buoys deployed solely for research, Ice Patrol enters all of its buoy data onto the Global Telecommunications System (GTS). Although Ice Patrol is directly interested in sea surface temperature and position data only when the buoys are within its operations area, the buoys frequently leave the area and move eastward across the North Atlantic. Tracking the buoys eastward serves the dual purpose of providing useful oceanographic data to the world oceanographic community and providing the opportunity to recover a buoy when it beaches or crosses the path of a ship willing to recover it. Approximately one buoy per year is recovered and returned to Ice Patrol for reuse.

All of the buoys used in 1987 had a 3 meter long spar hull with a 1 meter diameter flotation collar. Each buoy was equipped with a 2 by 10 meter window-shade drogue attached to the buoy with a 50 meter tether of 1/2" (1.3 cm) nylon. The center of the drogue was at 58 m. In addition, each buoy had a temperature sensor mounted approximately 1 m below the waterline, a drogue tension monitor, and a battery voltage monitor. The sea surface temperature is accurate to approximately 1°C.

The drogue sensor data should be viewed with some caution. Although recent experience (Anderson, 1986) suggests that the sensor reliably reports drogue status, it sometimes fails. In some cases the buoy's drift track can provide evidence of drogue separation. For example, an abrupt increase in variability with a period of several days might suggest that the drogue has detached and the buoy drift is being affected by the wind and wind-driven currents. However, short of relocating and recovering the buoy, there is no way to know with certainty that the drogue remained attached for the period of interest.

The data from the buoys are acquired and processed by Service ARGOS. Ice Patrol queries and stores the data files once daily.

Table C-1 summarizes the 18 buoy deployments in 1987. This table reflects the status of all the buoys as of 31 December 1987.

Table C-1. Summary of the 18 buoy deployments in 1987. This Table reflects the status of all buoys as of 31 December 1987.

Buoy ID	Date Deployed	Deployment Platform	Deployment Position	Recovered/Stopped Transmitting
4511a	07 MAY	BITTERSWEET	43°59'N 48°09'W	11 MAY (1)
4511b	17 MAY	BITTERSWEET	43°13'N 47°43'W	ACTIVE
4528	15 AUG	HC-130	60°00'N 61°43'W	ACTIVE
4536	07 MAY	BITTERSWEET	43°39'N 48°12'W	09 DEC
4545a	04 MAR	HC-130	47°48'N 48°45'W	05 MAY (2)
4545b	05 MAY	BITTERSWEET	45°14'N 48°46'W	11 MAY
4545c	17 MAY	BITTERSWEET	44°40'N 49°00'W	20 MAY
4545d	15 JUN	TAMAROA	51°06'N 53°28'W	19 JUN
4547a	07 MAY	BITTERSWEET	44°10'N 48°10'W	11 MAY
4547b	15 JUN	TAMAROA	51°06'N 53°28'W	20 JUN
4553	25 JUN	HC-130	52°44'N 51°55'W	ACTIVE
4554	25 MAR	HC-130	50°00'N 50°40'W	28 MAY
4555	25 MAR	HC-130	48°20'N 48°26'W	03 JUL
4556	14 APR	HC-130	48°20'N 49°19'W	19 JUN
4558	14 JUN	TAMAROA	51°14'N 53°20'W	20 JUN
4559	06 JUN	HC-130	49°40'N 50°52'W	06 AUG (3)
4560	06 MAY	HC-130	49°00'N 50°36'W	ACTIVE
4562	15 AUG	HC-130	59°13'N 60°18'W	ACTIVE

Notes:

(1) A letter behind a buoy number indicates that the buoy was deployed more than once during the year.

(2) Buoy 4545 was recovered by USCGC BITTERSWEET on 5 May at position 45°42' N, 49°21'W. The missing drogue was replaced and the buoy redeployed on 5 May.

(3) Buoy 4559 was picked up by an unknown vessel on 6 August. The buoy track from that point headed toward Europe at approximately 12 knots.

BUOY DEPLOYMENT FROM AIRCRAFT

Ice Patrol has deployed satellite-tracked buoys from HC-130's since 1979. The buoy is strapped into an air-deployment package and launched out the rear door of an HC-130 flying at an altitude of 500 feet (150 m) at 150 knots (77 m/s). The air-deployment package consists of a wooden pallet and a parachute, both of which separate from the buoy after it enters the water. The parachute riser is cut by a cable-cutter that is activated by a battery that energizes when immersed in salt water. The pallet separates when salt tablets dissolve and release straps holding the buoy to the pallet. The buoy then floats free and the drogue falls free and unfurls.

Nine buoys were air-deployed in 1987. Of these, three pallets (4528, 4553, and 4559) failed upon entry into the HC-130's airstream. When this occurs, the buoy and drogue usually survive intact, but frequently the wires to the parachute cutter break. This means that the parachute remains attached to the buoy hull and can act as a near-surface drogue. Aerial inspections and shipboard recoveries of buoys have shown that the parachutes collapse and become entangled with the buoy hull or the upper part of the drogue tether. It is not likely that these failures contaminated the drift data significantly.

BUOY DEPLOYMENT STRATEGY

It is not possible to obtain adequate temporal and spatial coverage of the Ice Patrol operations area (40-52N, 39-57W) over a 5 or 6-month period with a few (< 12) buoys. As a result, the buoy deployment strategy focuses on the current that is the major conduit of icebergs into the North Atlantic shipping lanes, the southward-flowing off-shore branch of the Labrador Current. The goal is to monitor this current for the entire ice season by keeping one or two buoys in it at all times. With two exceptions (4511 and 4536), all of the 1987 buoys were deployed in the Labrador Current. The two exceptions were deployed in and near a warm-core eddy that was affecting the flow of the Labrador Current near 44°N. No buoys entered, nor were any deployed, in the inshore branch of the Labrador Current. Previous attempts at deployments in this near-shore region resulted in short drift tracks because the buoys became entangled in fishing gear and were recovered by fishermen.

DATA PROCESSING

Most of Ice Patrol's buoy position data fall within the standard location accuracy (LeTran and Liabet, 1987) provided by Service ARGOS. The data are reported to 0.001° of latitude and longitude, which far exceeds this standard location accuracy. For 46°N, the center latitude of the Ice Patrol operations area, the positions are accurate to 0.003° of latitude and 0.005° of longitude. The raw position data are unevenly-spaced in time, with virtually no data from the period from 00Z to 004Z each day. This null period is due to the orbits of the NOAA satellites. Approximately 10 fixes are determined each day for each of the buoys.

Although the data are relatively noise free, all records are scanned before processing to ensure quality control. First, duplicate positions and positions with time separations of 30 minutes or less are deleted. Then, positions < 700 m from adjacent positions are deleted, unless the deletion results in a time separation of 4 or more hours.

The error-free position data are then fitted to a cubic spline curve to arrive at an evenly-spaced record with an interval of 3 hours. This process results in a slight reduction in the number of fixes per day (from 10 to 8). Next, the position records are filtered using a low-pass cosine filter with a cut-off of 1.16 X 10-5 Hz (one cycle per day). This filter removes most tidal and inertial effects. Finally, the buoy drift speeds are calculated at three-hour intervals using a two-point backward differencing scheme.

Most of the trajectory plots presented in this report are from the filtered records. Also presented for each buoy is a plot of

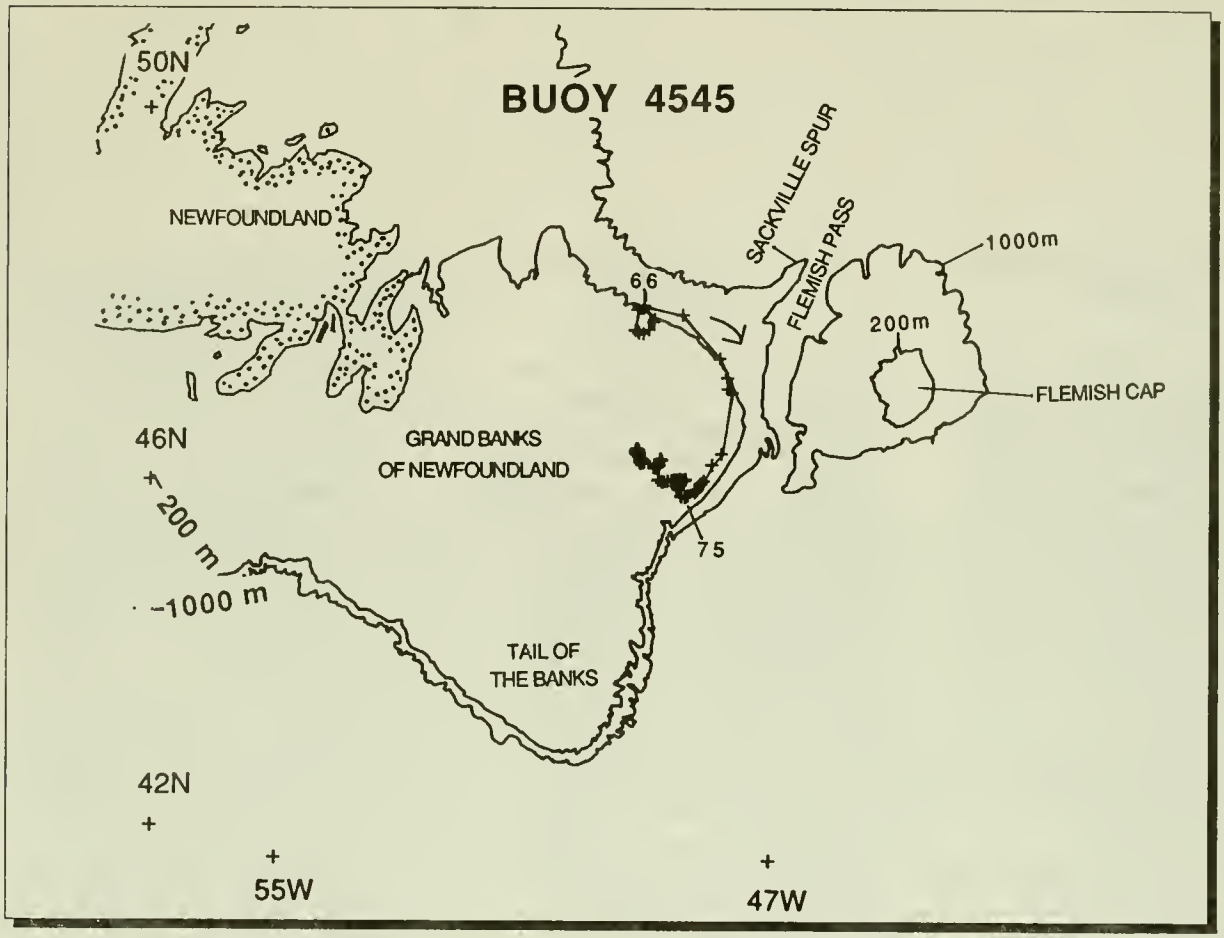

Figure C-1. Trajectory of Buoy 4545.

the time history of the U (east is positive) and V (north is positive) components of velocity from the filtered records. Finally, a time history of the raw sea surface temperature data is plotted for each buoy. The dates used in all of the plots are year-dates, which are numbered sequentially from January 1. In the text, the year-dates are included parenthetically.

BUOY TRAJECTORIES

In the following sections each buoy trajectory is discussed separately, presented in chronological order by deployment date. Only the operational buoys are discussed. This includes two buoys that were deployed from BITTERSWEET and allowed to drift free at the end of the experiment and two buoys purchased by, and deployed for, AES. Buoys 4547 and 4558 were used only during the research cruises. Their data are reported in Appendices D and E.

The intent of the following discussions is to summarize each buoy's performance and the data that it contributed to Ice Patrol operations. It is not intended to be an exhaustive data analysis. The buoy data from the area east of 39°W, the eastern boundary of the Ice Patrol operations area, are not presented. All of the data from the IIP drifting buoy program are archived at the IIP office in Groton, Connecticut.

BUOY 4545

Buoy 4545 (Figure C-1, C-2) was deployed and recovered four times in 1987 (Table C-1), but only one deployment was for operational use. On 4 March (63) it was air-deployed at 47-45N, 48-45W. It provided position and temperature data for 63 days until it was recovered on 5 May (125) at 46-42N, 49-21W by USCGC BITTERSWEET during IIP 87-1. During the entire period, the drogue sensor showed that the drogue remained attached; however, when the buoy was recovered only the 50 m nylon drogue tether and the chain bridle that supports the drogue were attached to the buoy. The chain was badly abraided, suggesting that it had dragged

across the bottom. The position data presented and discussed in this section are the raw data, not filtered. The record was short and the data return from the buoy immediately after its deployment was poor (2-3 fixes per day) so much of the interesting data would be lost filling the filter.

Buoy 4545 was deployed near the 200 m isobath. During the first 48 hours after deployment, it moved onto the Grand Banks and made an anticyclonic loop with a diameter of about 35 km. Typical buoy speeds during this period were 30-40 cm/s. For the next 10 days (7 - 16 March, 66-75) it moved southward through Flemish Pass, near and parallel to the 200 m isobath. Buoy speeds during this period were 40-50 cm/s and the temperature changed little (-0.8 to -1.4°C).

On 16 March (75), 4545 started to move northwestward onto the continental shelf. By 8 April (98) the buoy had moved into a region where it is likely that the drogue was dragging on the bottom, so the drift data after this date are of little use. The surface temperature continued to increase slowly but persistently. The surface temperature when the buoy was recovered was 3.3°C.

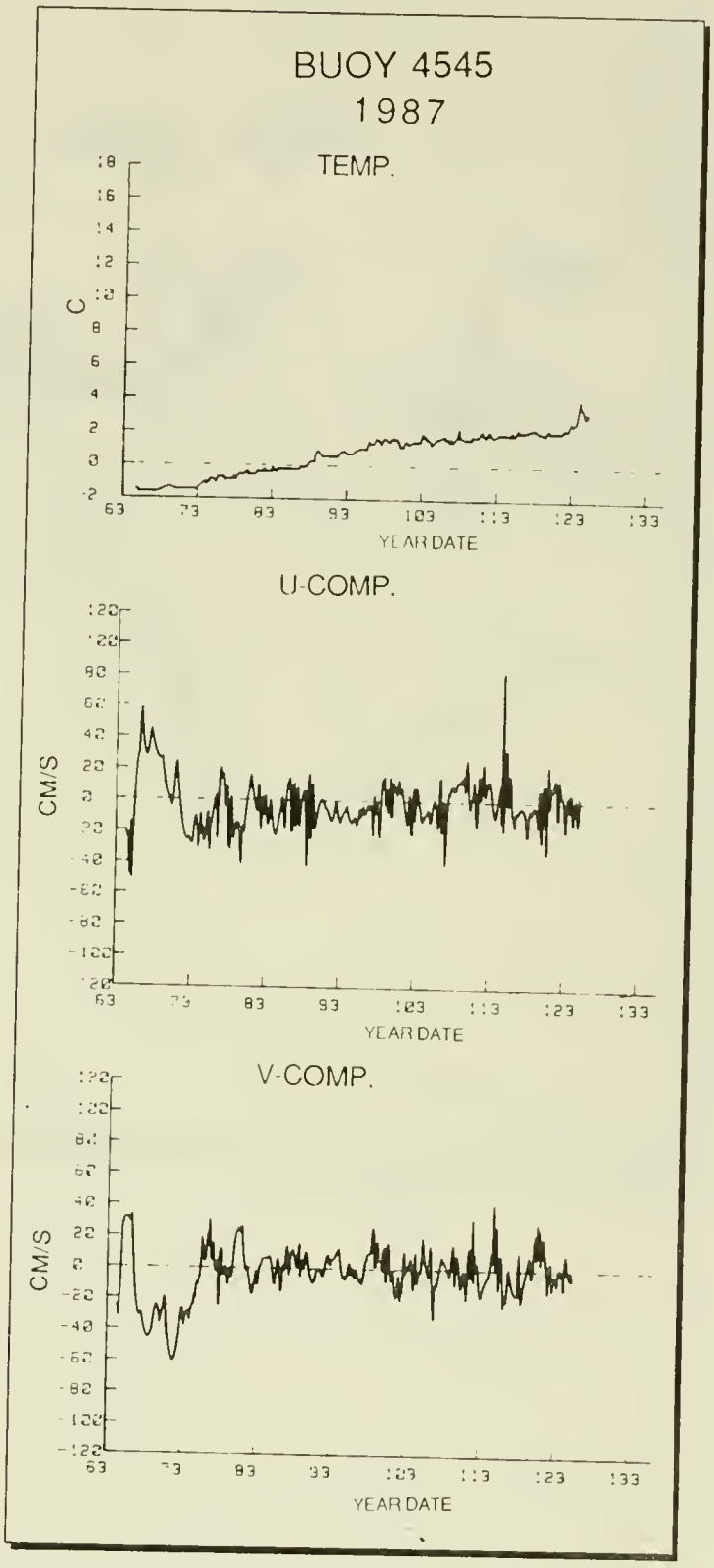

Figure C-2. Temperature, U and V velocity components for buoy 4545.

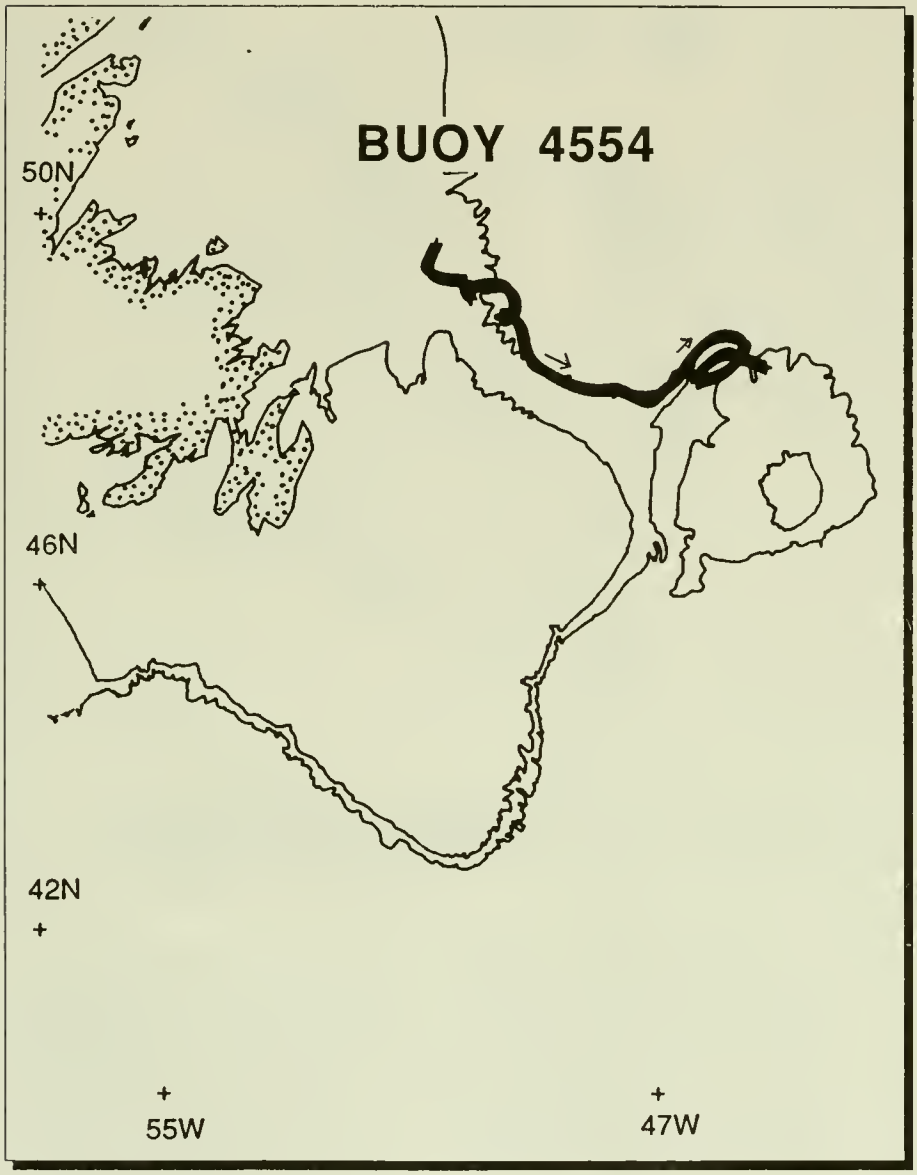

Figure C-3. Trajectory of Buoy 4554.

BUOY 4554

Buoy 4554 (Figure C-3, C-4) was air-deployed at 50-00N, 50-40W on 25 March (84). It transmitted position and temperature data for 65 days, failing on 28 May (148). The buoy's battery voltage and the number of fixes per day were normal until failure. The drogue remained attached during the entire drift period.

After its deployment, 4554 moved southeastward, approximately following the 1000 m isobath. Over this period, the filtered buoy speeds varied over the range of 5 to 30 cm/s. The temperature record is unremarkable, with a slow increase in temperature of from 0 to 6°C over the 65 days (0.1°C/day) of the buoy's life.

At Sackville Spur, 4554 turned to the northeast, after which it made an anticyclonic loop (~50 km diameter). It failed shortly thereafter.

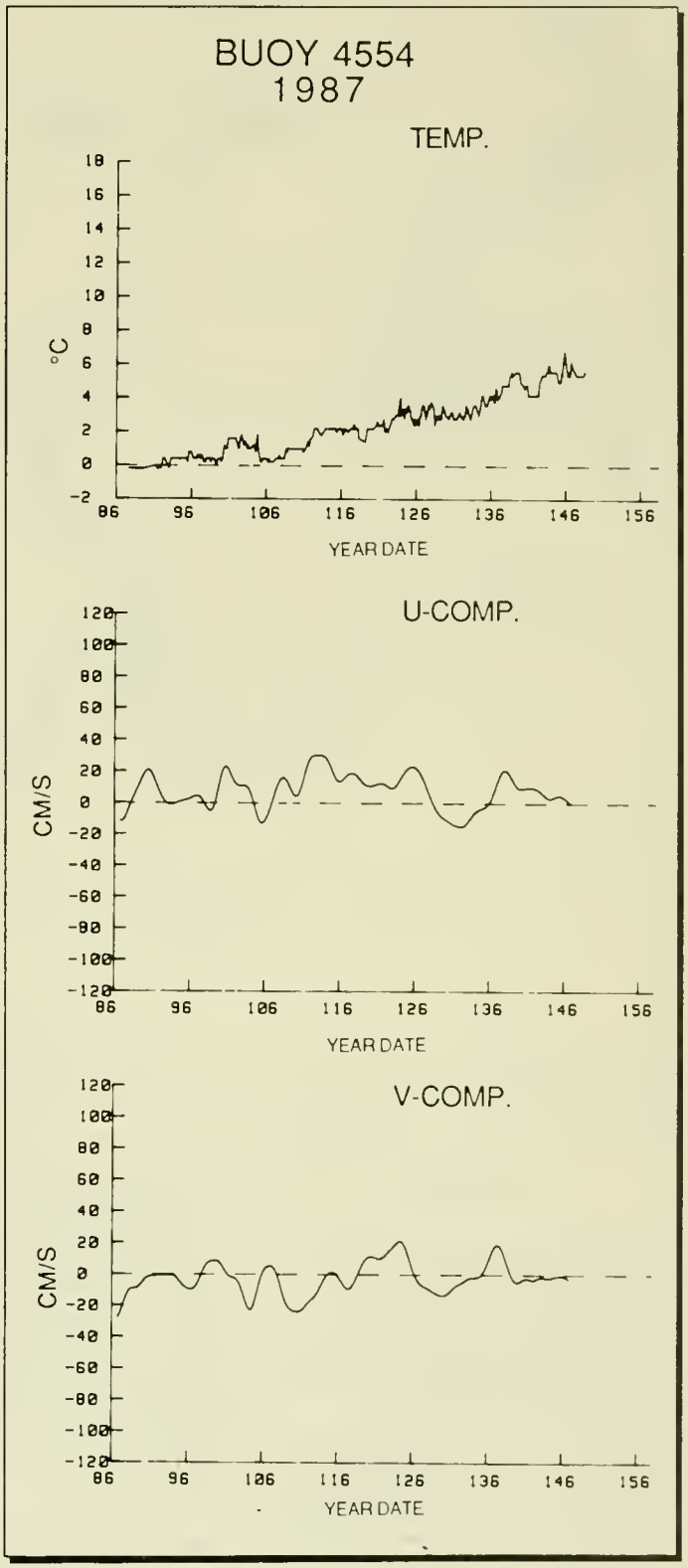

Figure C-4. Temperature, U and V velocity components for buoy 4554.

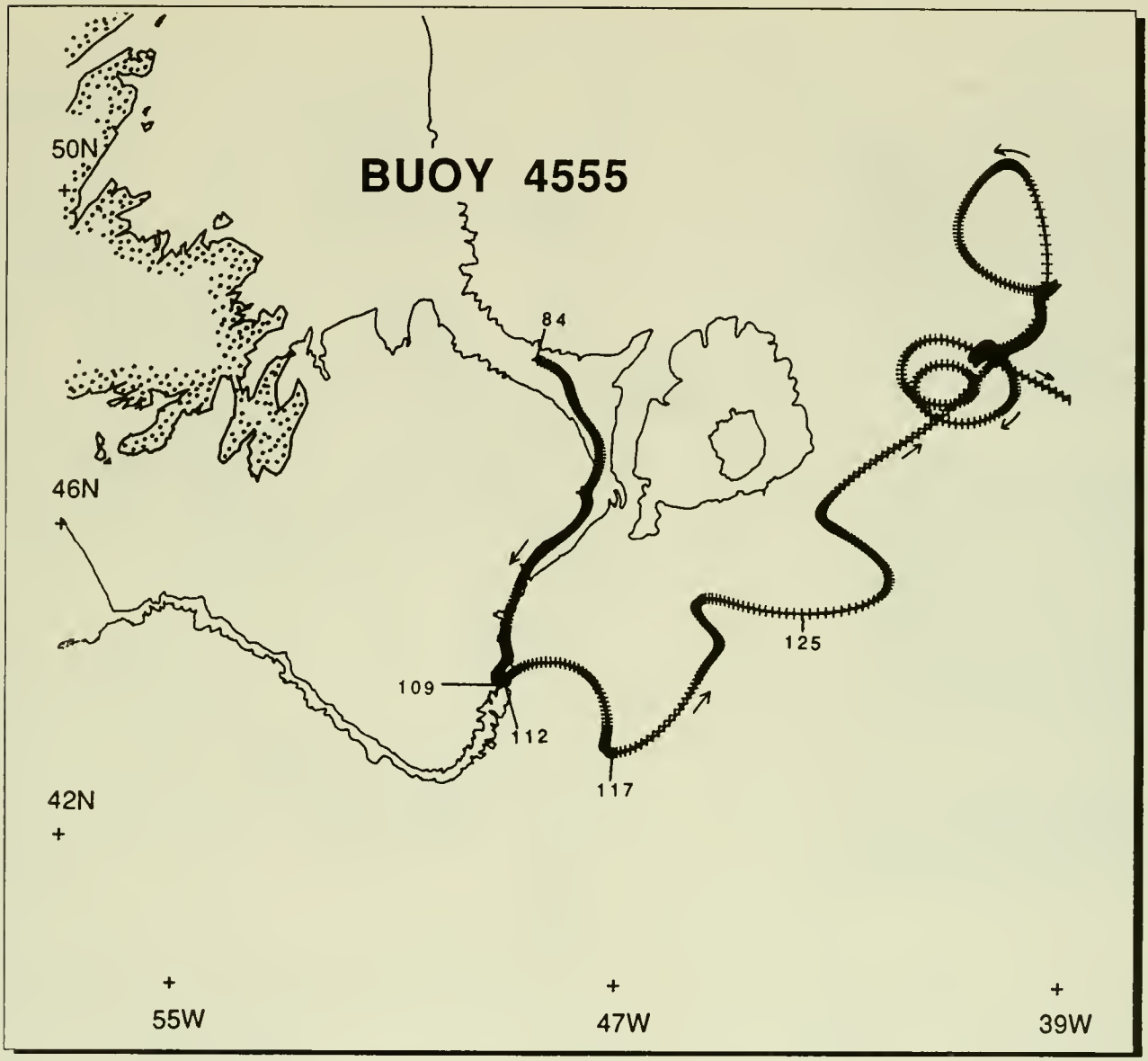

Figure C-5. Trajectory of Buoy 4555.

BUOY 4555

Buoy 4555 (Figure C-5, C-6) was air-deployed at 48-20N, 48-26W on 25 March (84). It remained in the Ice Patrol operations area for 91 days, passing east of 39°W on 23 June (174). The drogue remained attached to the buoy for the entire 91-day drift period, detaching on 29 June (180). Shortly thereafter (3 July, 184), 4555 was recovered by an unknown vessel at 46-28°N, 37-06°W and taken in the direction of Europe.

After deployment, 4555 moved southeastward and then southward through Flemish Pass, approximately following the 200 m isobath. During this 25-day period, from 25 March to 19 April (84-109), the temperature increased slowly from -1.4 to 1.4°C and the speed varied widely (10-50 cm/s).

At approximately 44°N, the trajectory of 4555 changed abruptly under the influence of a warm-core eddy centered at 43-30N, 48-10W. The buoy slowed, reversed direction, and then moved eastward and southward, tracing an anticyclonic path approximately one-half the way around the boundary of the eddy. This occurred over a 6-day period, during which the buoy moved at speeds of 50-70 cm/s. During the period that 4555 was moving around the outside of the eddy, the temperature record shows a considerable variability over the range from 0.8 to 13°C, suggesting that the buoy was

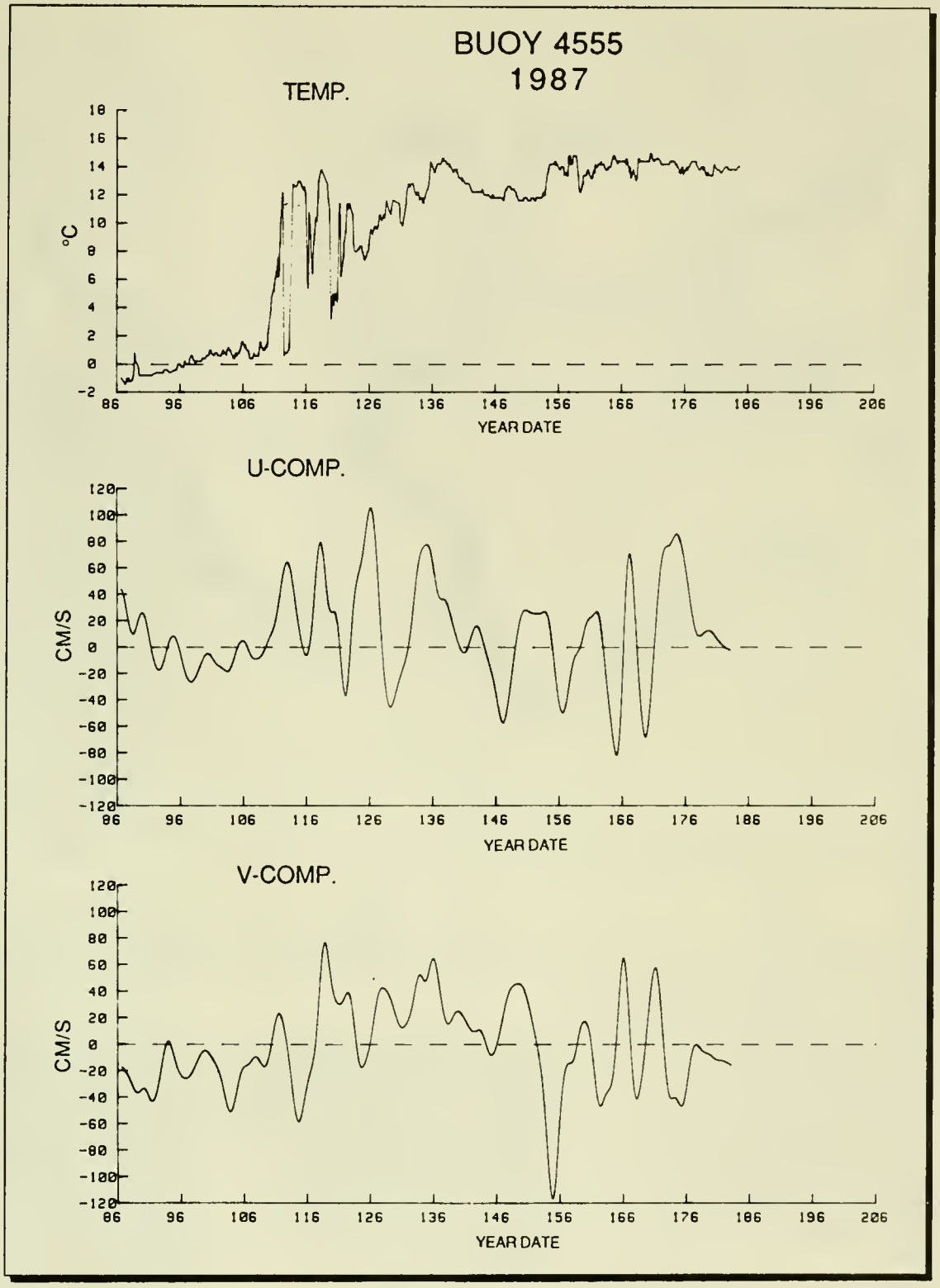

Figure C-6. Temperature, U and V velocity components for buoy 4555.

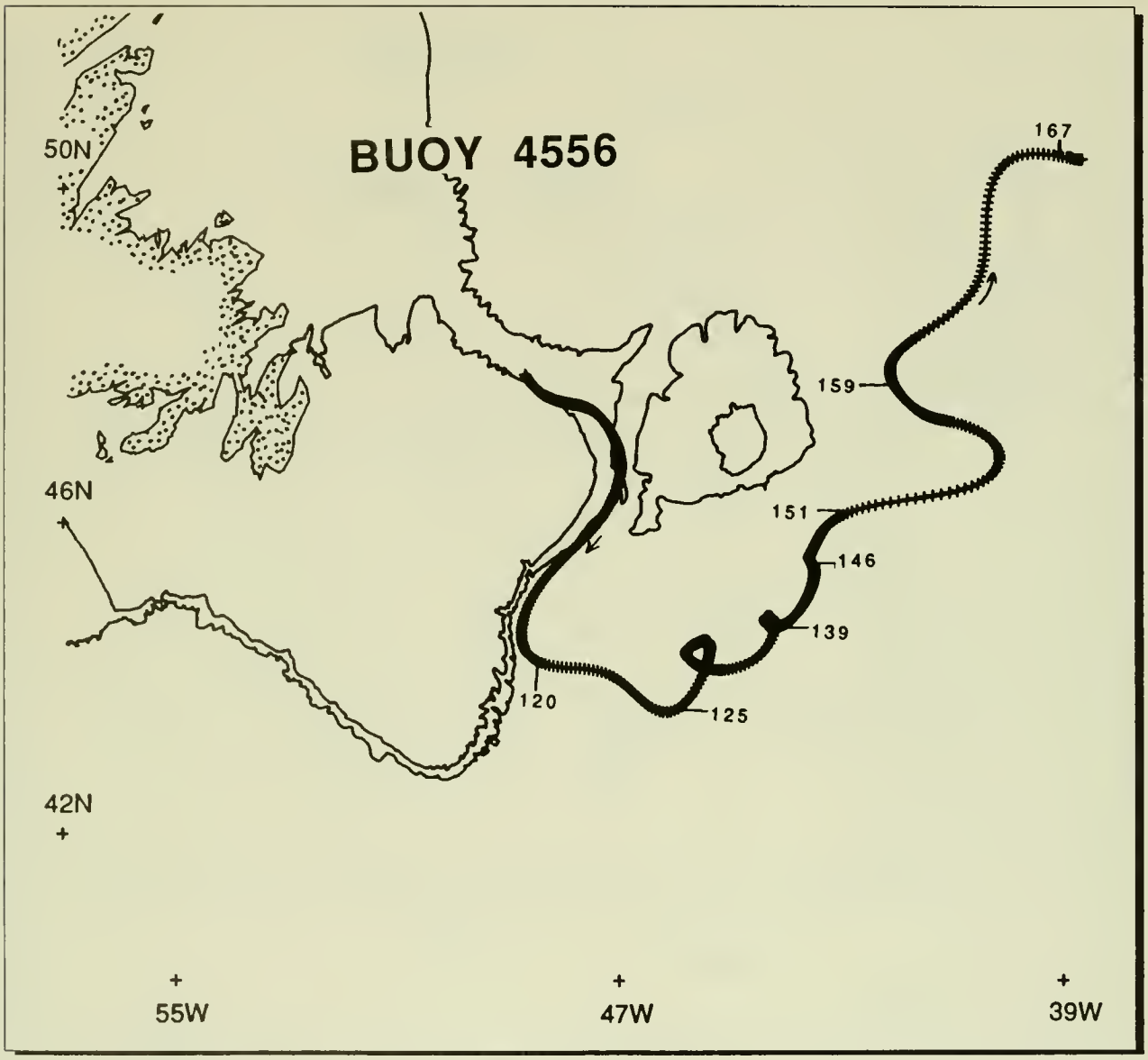

Figure C-7. Trajectory of Buoy 4556.

close to the eddy's boundary. It is likely that the drogue (~58 m) remained in the cold, subsurface core of the Labrador Current while the temperature sensor at the surface was moving through surface waters of various temperatures near the eddy's boundary.

The track of 4555 after it left the vicinity of the eddy was generally northeastward, with wide fluctuations in the filtered speeds. The temperature record shows that the buoy remained in waters greater than 8°C, with most of the readings in the range of 12-14°C. The buoy's subsequent movement is complex, with evidence of eddies and meanders associated with the North Atlantic Current, particularly in the area east of Flemish Cap.

BUOY 4556

Buoy 4556 (Figure C-7, C-8) was deployed from an aircraft on 14 April (104) at 48-20.1N, 49-19.8W. It remained in the Ice Patrol operation area for 63 days, passing east of 39°W on 16 June (167). Three days later (170), the buoy stopped transmitting, although there was no prior indication of a reduction in the buoy's battery voltage or the number of fixes per day. The drogue indicator showed that the drogue detached on 31 May (151), thus it remained attached to the buoy for 48 days.

After its deployment, the buoy moved southward through the Flemish Pass and along the eastern edge of the Grand Banks, approximately following the 1000 m isobath. During this period (14-20 April, 104-120), the average speed was 30-45 cm/s and the sea surface temperature increased slightly from -1.4°C to 0.6°C.

On 30 April (120), 4556 began to move rapidly (50-70 cm/s) to the east, north of the warm core eddy that was surveyed during IIP 87-1. This eastward motion of a buoy deployed in the Labrador Current and encountering a warm core eddy near the eastern edge of the Grand Banks is similar to that observed in 1986 (Murphy et al, 1986). The buoy's motion around the eddy suggests that a portion of the Labrador Current left the eastern edge of the Grand Banks at approximately 44-10N and traced a path partially around the eddy. Buoy 4556's temperature record, which showed a slow increase in temperature (0.6 to 2.0°C), suggests that it did not enter the eddy, instead remaining in the Labrador Current.

On 4 May (124), 4556 started a general northeastward drift, which is typical of many IIP buoys that become entrained in the North Atlantic Current. Over the next twelve days the temperature increased 8°C (2-10°C). This period is also remarkable in that the buoy's trajectory shows that it became entrained in a small (< 40 km in diameter) cyclonic eddy that was propagating northeastward and apparently decreasing in size. The trajectory shows that the buoy made three circuits of the eddy while the eddy moved northeastward at about 5 km/day.

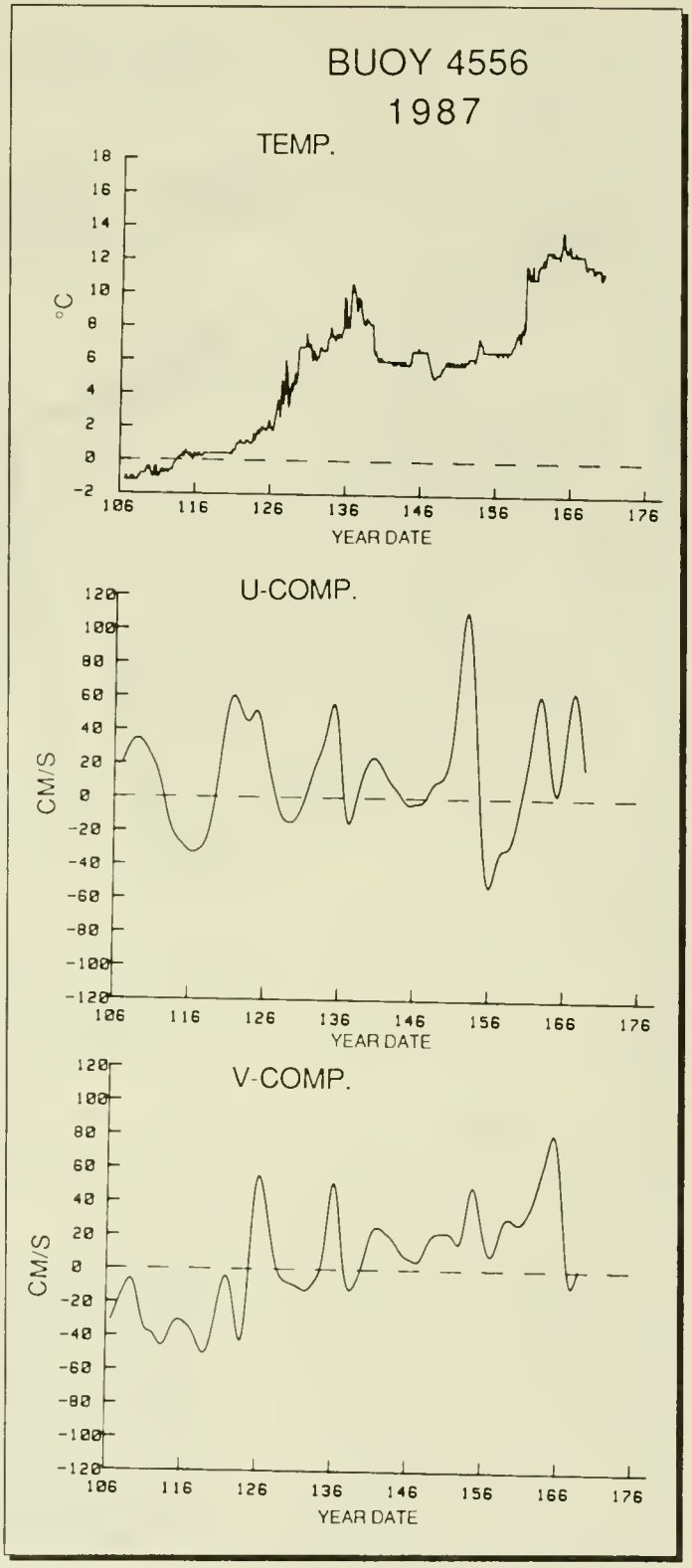

Figure C-8. Temperature, U and V velocity components for buoy 4556.

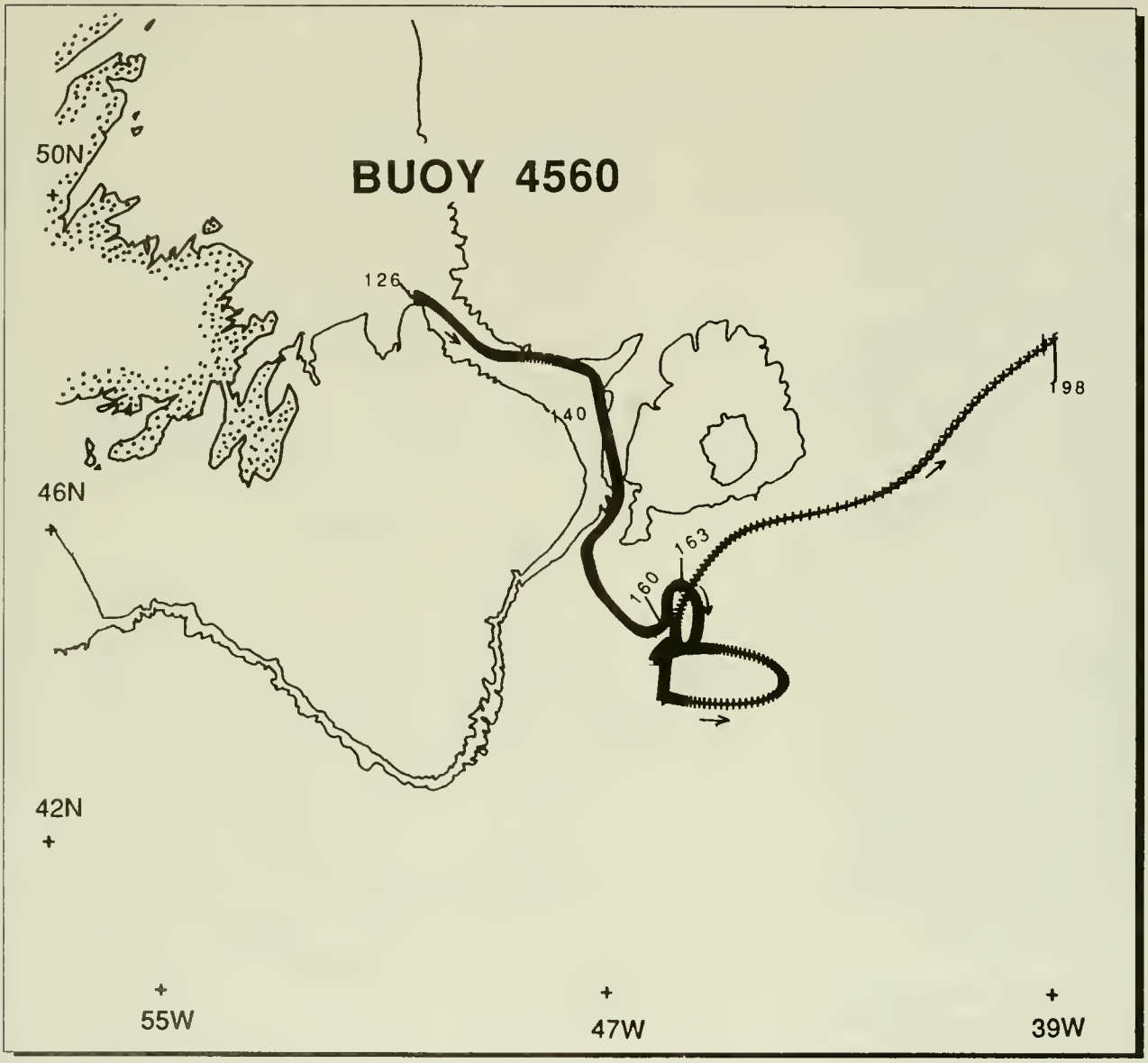

Figure C-9. Trajectory of Buoy 4560.

The temperature record during the period that 4556 was moving in the anticyclonic eddy (125-146) cannot be easily explained. First, the temperature increased from 2-10°C, then it decreased rapidly to 5-6°C. It is possible that the low temperature recordings from 19 May to 8 June (139-159) are the result of a sensor malfunction. However, other than the loss of the drogue on 30 May (150), there is no evidence of a buoy malfunction.

On 8 June (159) the temperature record shows an increase from 8.2 to 11.8°C on successive satellite passes (about three hours apart). Eight days later (167), 4556 crossed east of 39°W. On 19 June (170), 66 days after its deployment, 4556 stopped transmitting.

Buoy 4556 was recovered by the Irish Navy and returned to Ice Patrol in August 1988. It was severely damaged and could not be returned to service.

BUOY 4560

Buoy 4560 (Figure C-9, C-10) was air-deployed on 6 May (126) at 49-00N, 50-36W. It provided data in the Ice Patrol operations area for 73 days, passing east of 39°W on 17 July (198). The drogue remained attached for the entire period, detaching on 17 October (290) 175 days after deployment. The buoy continued to transmit data for the remainder of the calendar year.

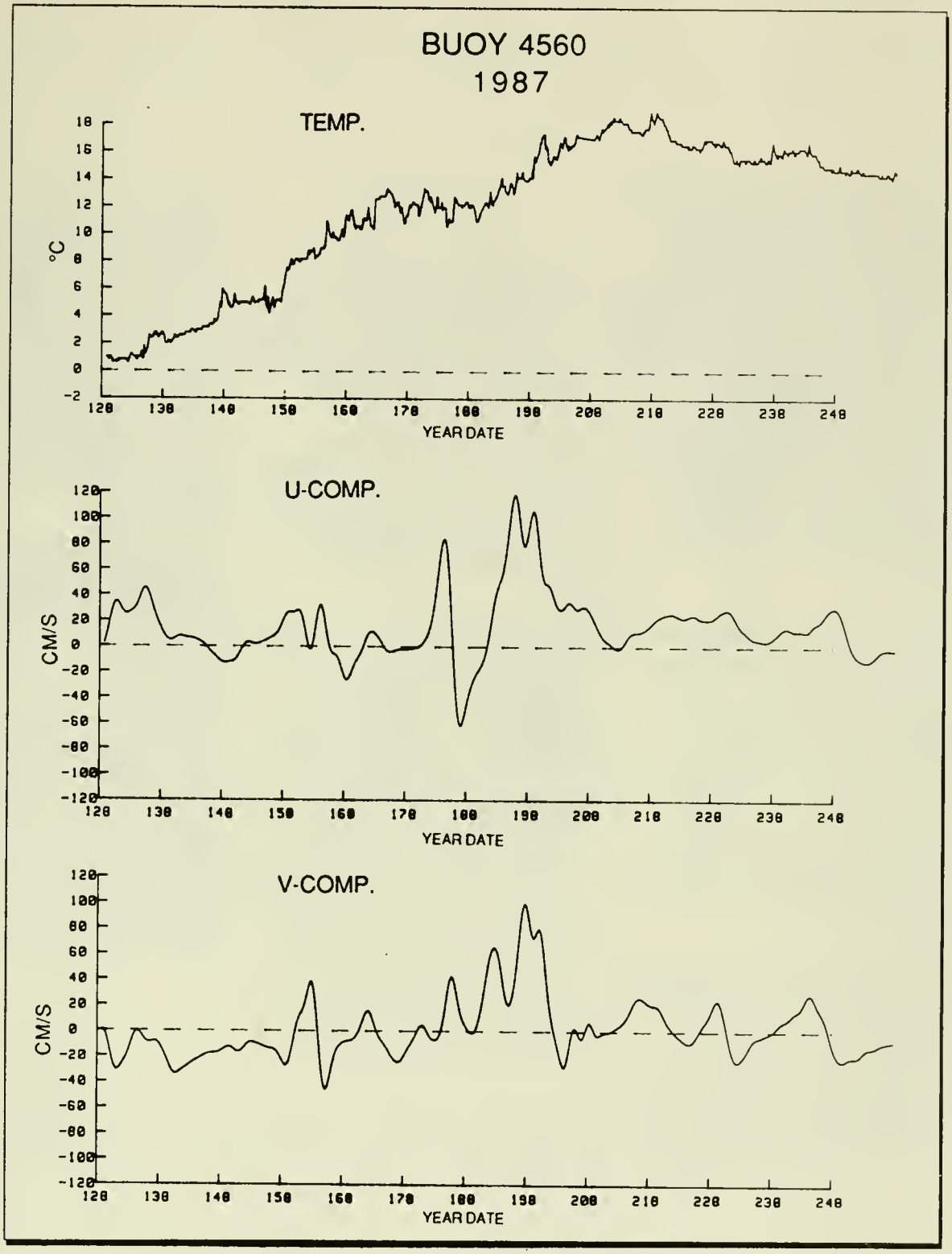

Figure C-10. Temperature, U and V velocity components for buoy 4560.

During the first 14 days following its deployment (6-20 May,126-140), 4560 moved southeastward to the northern part of Flemish Pass. During this period the buoy's speed varied over the range 25-40 cm/s while the temperature increased slightly (1-3°C). The southward motion through Flemish Pass approximately followed the 1000 m isobath. The buoy speed through Flemish Pass varied from 20-35 cm/s, while the temperature remained about 2-3°C.

After departing Flemish Pass, 4560 left the slope and moved slowly (< 20 cm/s) southeastward. During this period the temperature changed little. The buoy trajectory in the region south of Flemish Cap is complex. Buoy 4560 remained in this region for 31 days (9 June-10 July,160-191), during which the surface temperature increased from 8 to 12°C.

On 10 July (191), 4560 began a rapid and persistent movement northeastward with speeds varying over the range of 65-135 cm/s. During this period the surface temperature increased rapidly, from 12 to 16°C.

BUOY 4536

Buoy 4536 (Figure C-11, C-12) was deployed from BITTERSWEET at 43-39N, 48-12W on 7 May (127) in a warm-core eddy. It provided data in the Ice Patrol operations area for 152 days, passing east of 39°W on 5 October (278). The drogue sensor indicated an early drogue failure, with detachment occurring on 20 May (140), 14 days after deployment. The buoy ceased transmitting on 9 December (343).

Buoy 4536 remained in the eddy for only 3 days. The data from that period are presented in Appendix D. The departure of 4536 from the eddy was marked by an abrupt decrease in surface temperature (10.2 to 7.8°C in about 5 hours) and a persistent movement to the east. Over this 5-day period, 11-15 May (131-135), the buoy accelerated form 40 to 110 cm/s and the surface temperature increased from 6 to over 13°C. This motion and temperature increase suggest 4536 entered the North Atlantic Current.

During the next 34 days (17 May - 20 June, 137-171) 4536 remained in the region directly south of Flemish Cap. The buoy's trajectory in this area is complex, with three anticyclonic and one cyclonic loop. At times 4536 moved at over 60 cm/s. The surface temperature varied form 8-12°C. These data suggest an area characterized by North Atlantic Current meanders and eddies.

Over the next 6 days (20-25 June, 171-176), 4536 moved rapidly (70-125 cm/s) eastward and then northward. The temperature over the period remained within 10-13°C. For the remainder of its period in the Ice Patrol operations area (26 June - 5 October, 177-278) 4536 remained north of Flemish Cap. The trajectory is complex but it suggests that the flow in the region was dominated by North Atlantic Current meanders. The temperature varied over the range of 13-18°C.

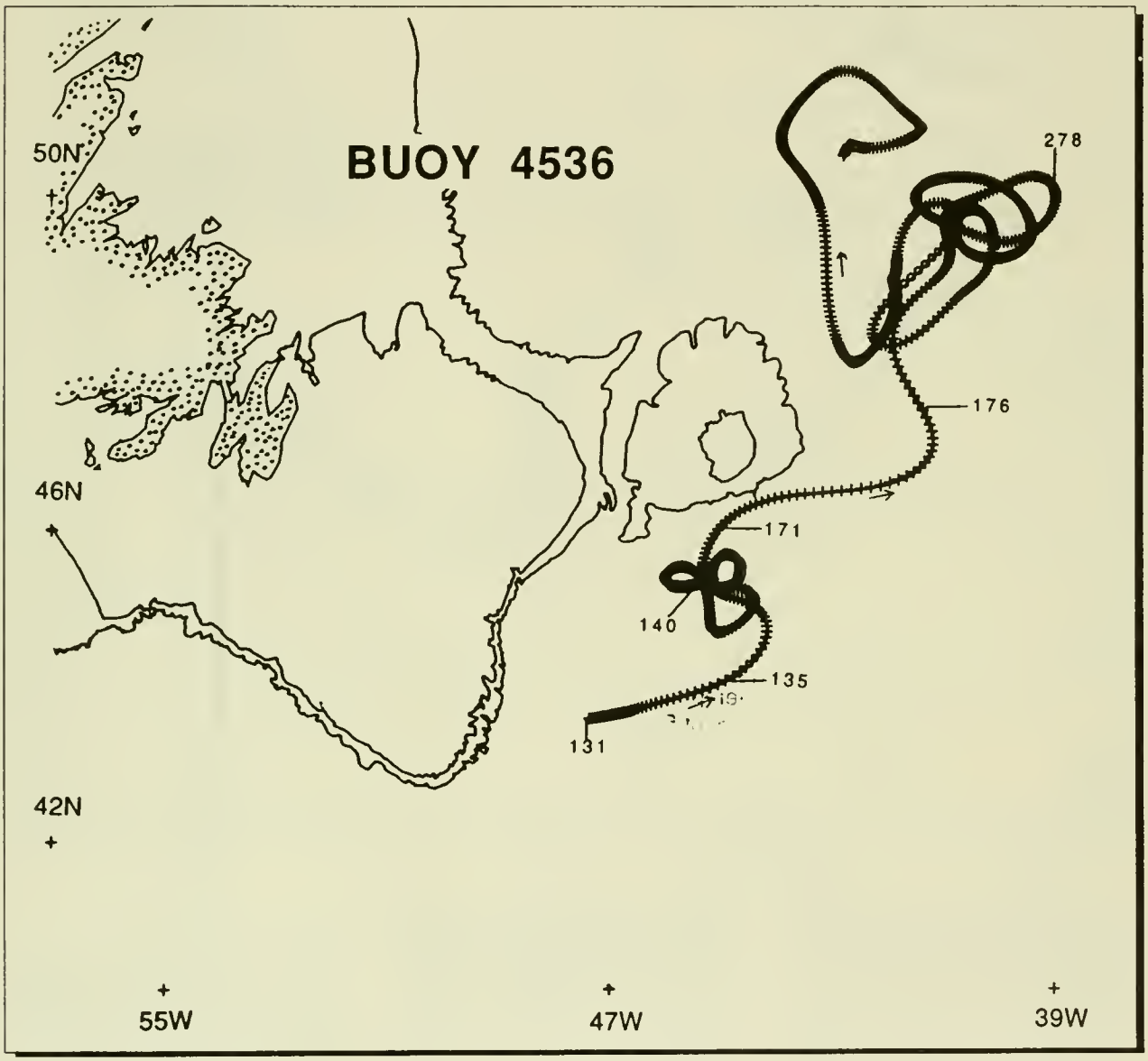

Figure C-11. Trajectory of Buoy 4536.

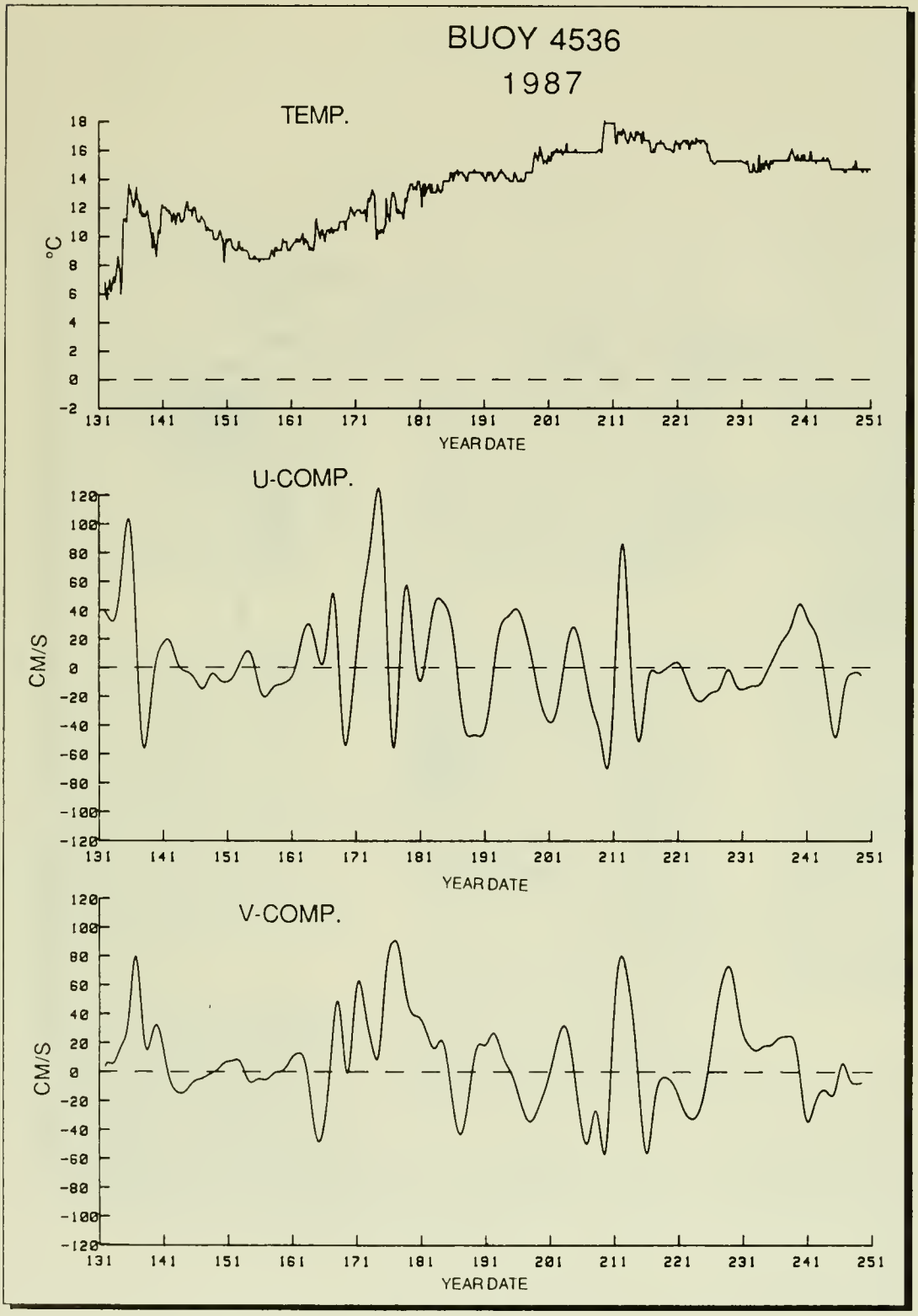

Figure C-12. Temperature, U and V velocity components for buoy 4536.

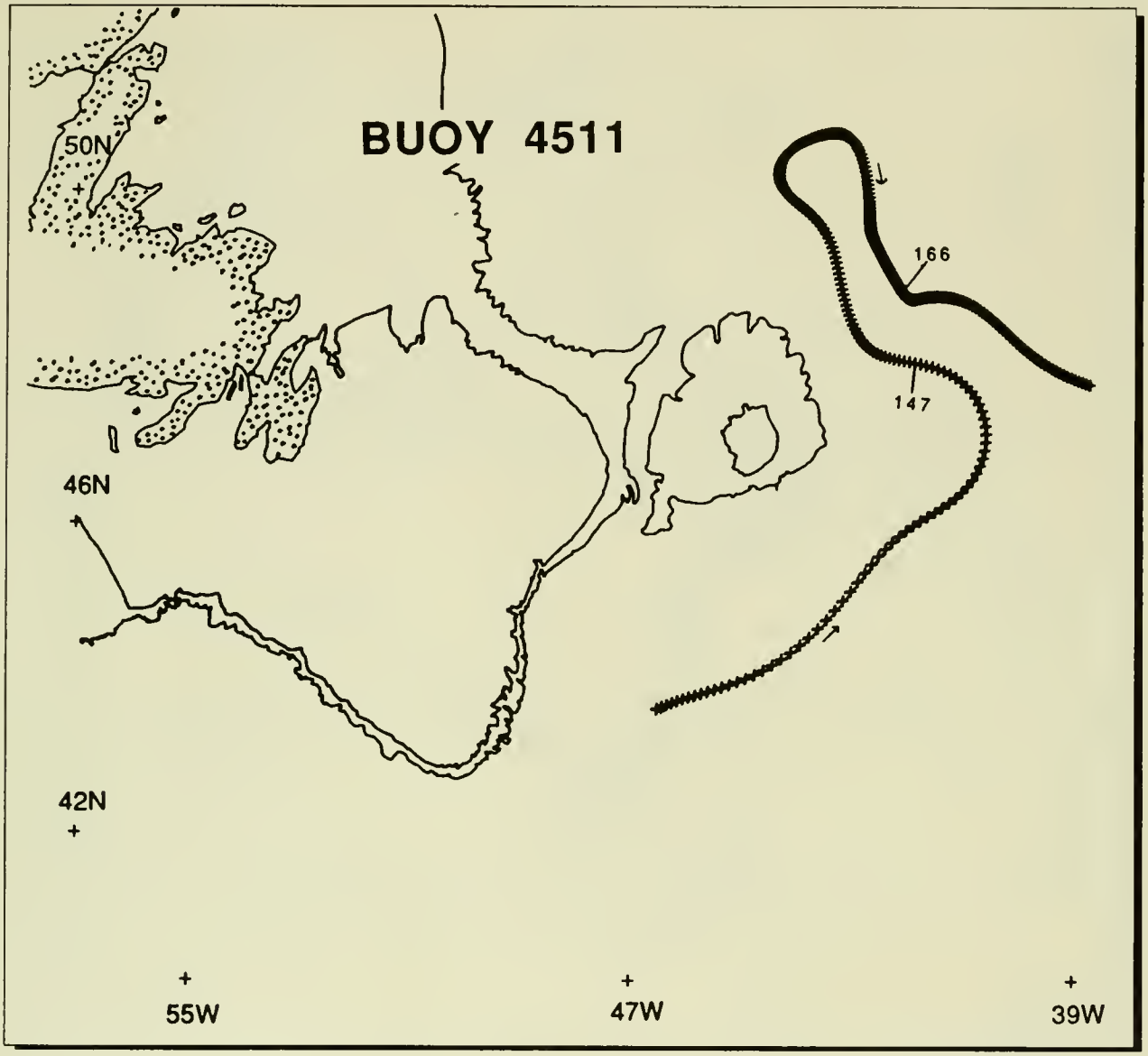

Figure C-13. Trajectory of Buoy 4511.

BUOY 4511

Buoy 4511 (Figure C-13, C-14) was deployed twice in 1987, the second time to collect operational data. On 17 May (137) it was deployed at 43-13N, 47-43W by USCGC BITTERSWEET (WLB 389). It provided 37 days of operational data in the Ice Patrol operations area, before passing east of 39°W on 22 June (173). Due to a data formatting error, no data regarding drogue status was received from the ARGOS processing center after 15 June (166). The earlier data indicate that the drogue was attached until that time. Buoy 4511 continued to transmit data throughout the remainder of 1987 as it moved eastward across the Atlantic Ocean.

Buoy 4511 was deployed south of the eddy surveyed by BITTERSWEET. This shipboard deployment provided an opportunity to compare the sea surface temperature as determined by the buoy and a CTD (conductivity, temperature, and depth) measurement made at the depth of the buoy's temperature sensor. The agreement was excellent. The buoy measured 16.3-16.4°C while the CTD measurement was 16.4°C. The two measurements were taken approximately 15 minutes apart.

After its deployment, 4511 moved persistently and rapidly to the northeast, with speeds, at times, exceeding 150 cm/s. During the

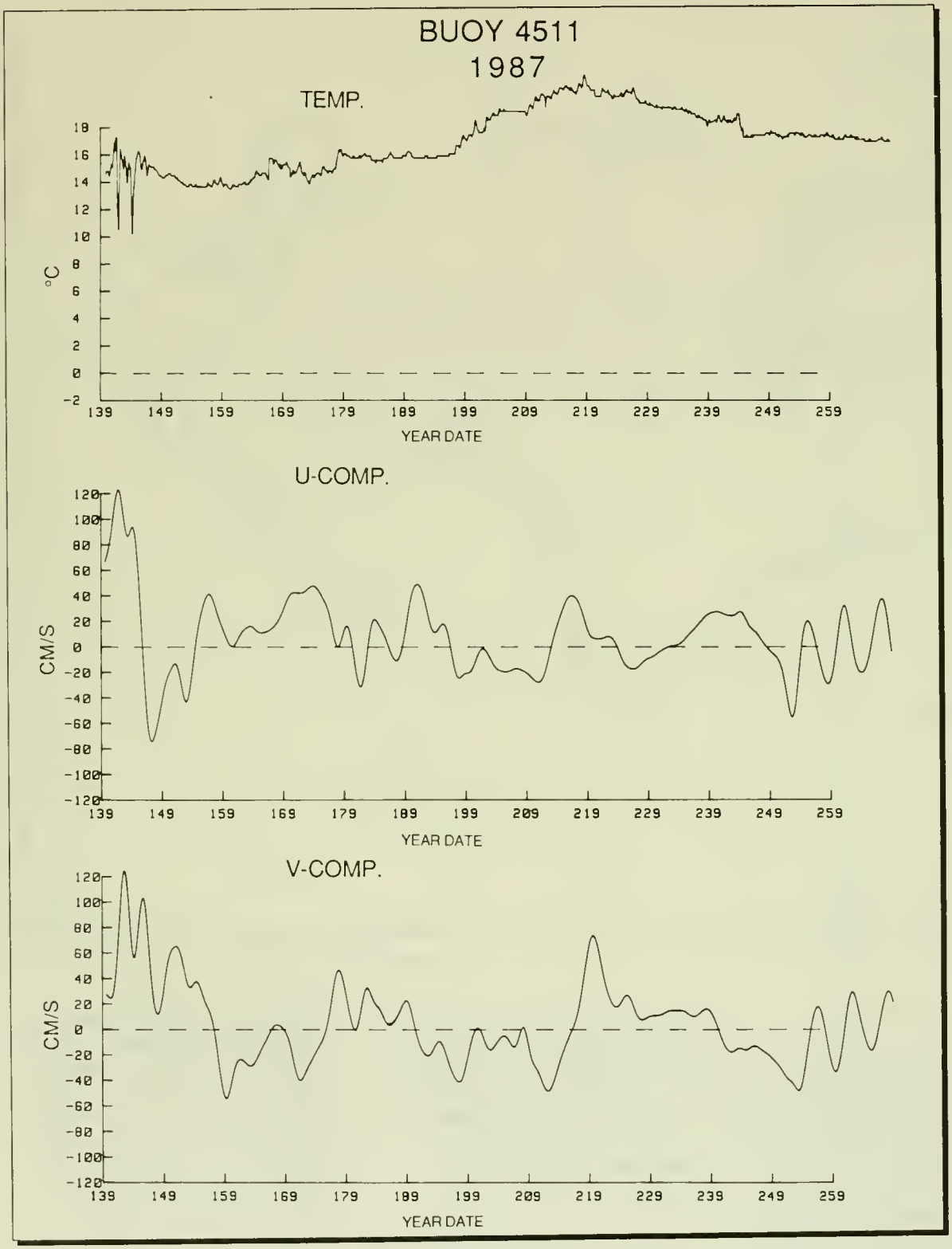

Figure C-14. Temperature, U and V velocity components for buoy 4511.

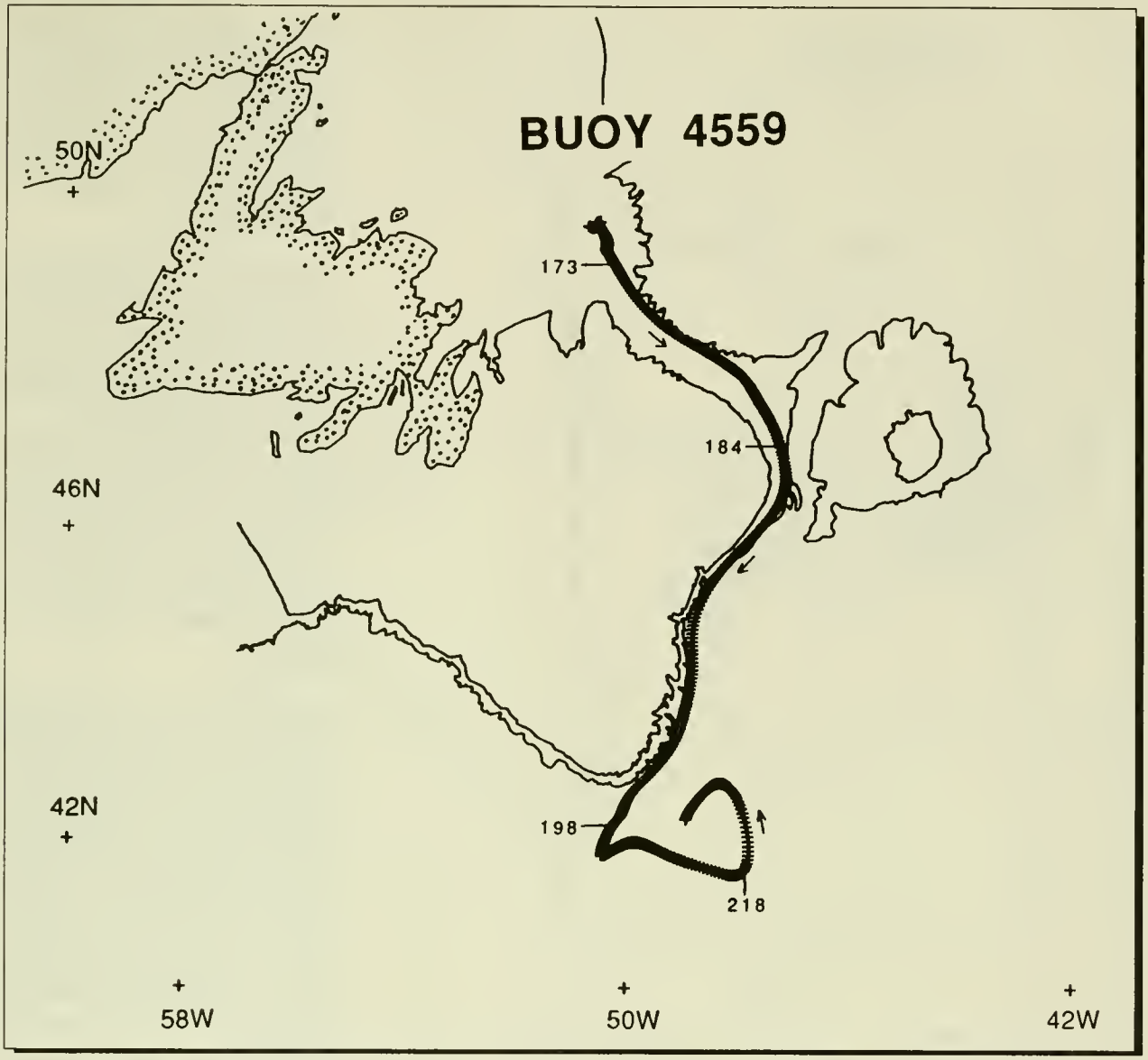

Figure C-15. Trajectory of Buoy 4559.

same period (17-27 May, 137-147), the temperature record shows considerable variability over the range 10-17°C. At the end of this period, 4511 turned abruptly to the northwest and slowed substantially with the typical speeds varying over the range of 20-70 cm/s. It is likely that this motion was due to a northwestward-projecting meander of the North Atlantic Current near Flemish Cap. During this entire period, the temperature remained stable near 14°C.

BUOY 4559

Buoy 4559 (Figure C-15, C-16) was air-deployed at 49-40N, 50-52W on 6 June (157). It provided data in the Ice Patrol operations area for 62 days, during which the drogue remained attached. On 6 August (218) it appears that the buoy was recovered by a vessel. The temperature showed an abrupt 6°C increase to 23.8°C, accompanied by an indication of drogue detachment. Shortly thereafter, the buoy ceased transmitting.

The first 16 days after deployment were characterized by a sluggish (< 20 cm/s) movement to the southeast, with the sea surface temperature remaining in the 2-5°C range. On 12 June (163), six days after its deployment, 4559 was inspected by the Ice Patrol field party aboard TAMAROA at 49-39.9N, 50-32.8W. The drogue was properly deployed, but the parachute had not cut and was fouled around the wooden pallet. The parachute was cut free. On 22 June (173),

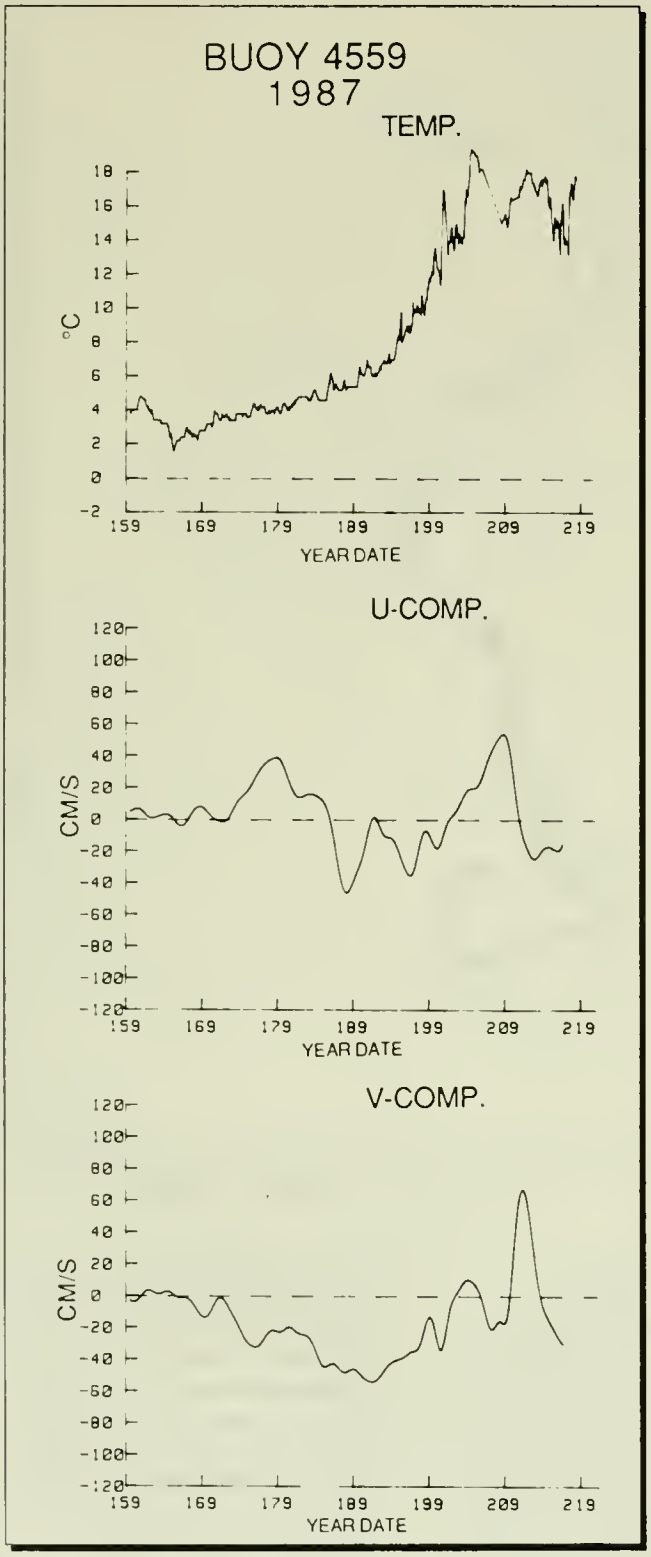

Figure C-16. Temperature, U and V velocity components for buoy 4559.

when the buoy reached the vicinity of the 1000m isobath, 4559 began a more vigorous (30-40 cm/s) southeastward movement along that isobath. During this 11-day period (22 June - 3 July, 173-184) the sea surface temperature changed little.

On 3 July (184), 4559 started to move southward through Flemish Pass. It then moved southward in the Labrador Current along the eastern edge of the Grand Banks, approximately following the 1000 m isobath to the Tail of the Bank with speeds mostly in the 40-60 cm/s range and some peak readings approaching 70 cm/s. During this two-week period (3-17 July, 184-198) the surface temperature increased about 5°C (5 to 10°C).

After leaving the 1000 m isobath at the Tail of the Bank, 4559 moved southward and then eastward. During this period there is a data gap of three days duration due to communications problems within the ARGOS system. Finally, the track of 4559 traced a cyclonic loop with a diameter of approximately 110 km. The surface temperature during this period varied considerably over the range of 14 to 18°C.

BUOY 4553

Buoy 4553 (Figure C-17, C-18) was air-deployed on 25 June (176) at 52-44N, 51-55W. It was the last operational buoy deployed during the 1987 iceberg season. It provided position and sea surface temperature data for 100 days in the Ice Patrol operations area, passing east of 39°W on 22 September (265). It was still transmitting as of 31 December 1987. The drogue sensor showed that the drogue remained attached for

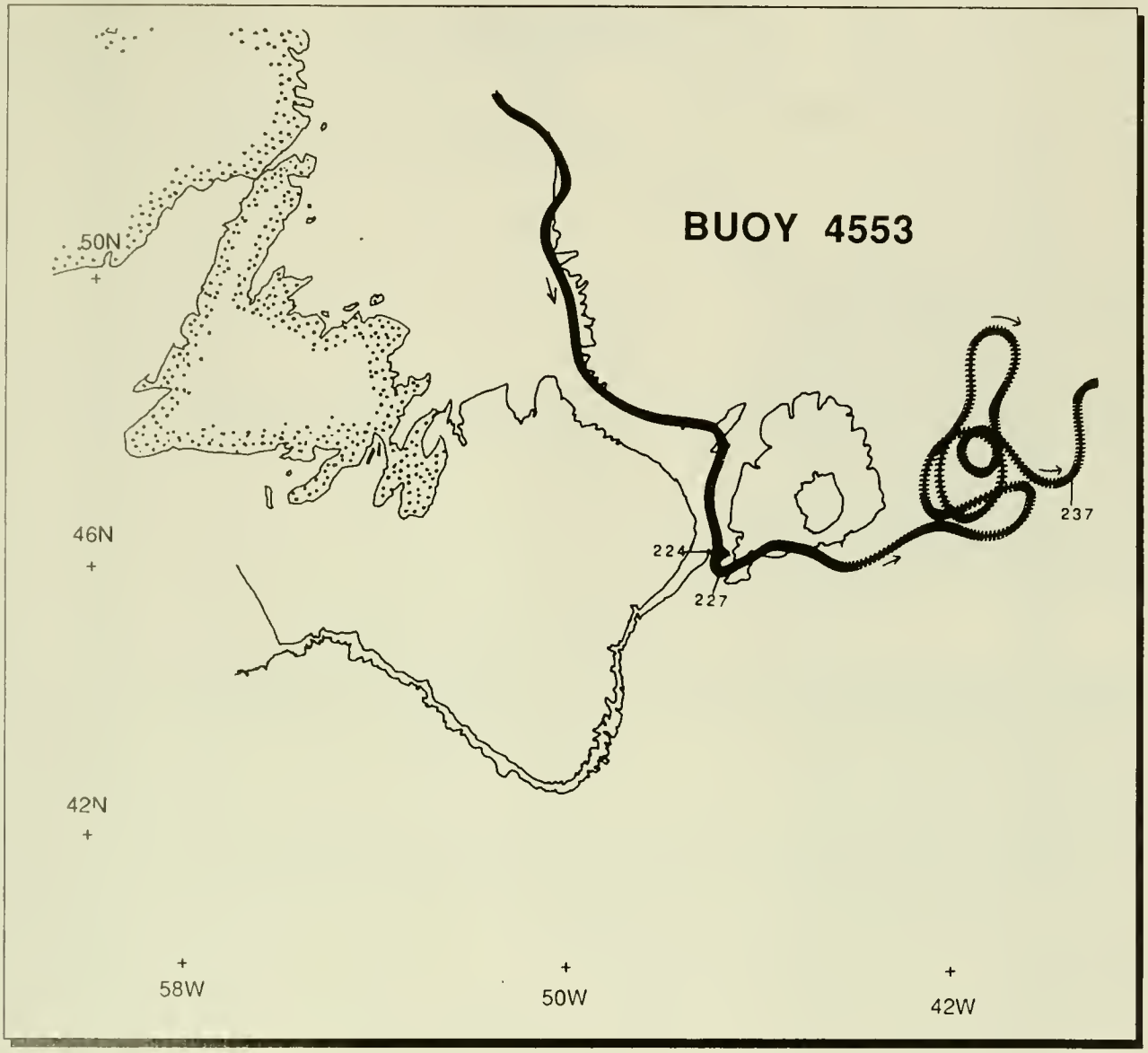

Figure C-17. Trajectory of Buoy 4553

approximately one-half of the 100-day period, detaching on 12 August (224).

Buoy 4553's southeastward motion after deployment almost exactly traces the 1000 m isobath down to 46°N, including the movement southward through Flemish Pass. While moving southward through Flemish Pass, 4553 recorded a 5.2°C increase in temperature over a 21-day period (~.25 deg/day). During this period the buoy's speed varied from near zero to 30 cm/s. It is also during this period that the drogue sensor showed drogue detachment. The detachment of the drogue added no noise to the position record, as might be expected due to wind effects on the above-water portion of the buoy hull.

On 15 August (227) at approximately 46°N, 4553 began an eastward motion south of Flemish Cap. During the next 10 days the temperature continued to increase until it reached about 15°C on 25 August (237), while the buoy moved persistently eastward at 15-35 cm/s. At this point the temperature leveled off and remained within 2°C of 15°C for the remainder of the drift period in the Ice Patrol operations area. At the same time, 25 August (237), the buoy's movement changed substantially. Figure C-18 shows that on this date 4553 entered a region east of Flemish Cap where the flow was vigorous, apparently dominated by eddies and meanders of the North Atlantic Current.

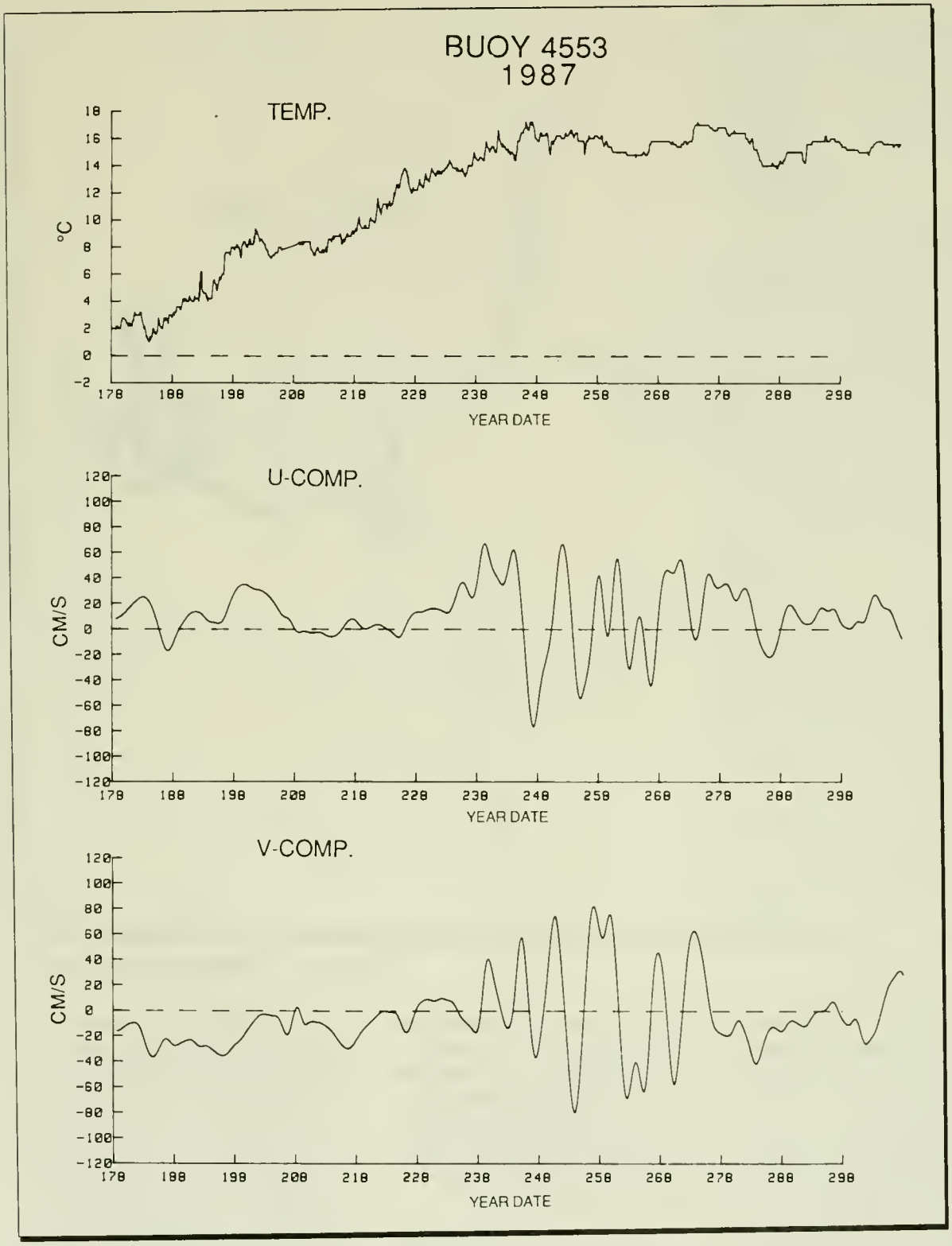

Figure C-18. Temperature, U and V velocity components for buoy 4553.

BUOY 4562

Buoy 4562 (Figure C-19, C-20) was launched from an aircraft on 15 August (227) at 59-13N, 60-18W. It entered the Ice Patrol operations area on 26 November (330) when it passed south of 52°N and transmitted data throughout the remainder of 1987. The drogue sensor indicated drogue detachment on 24 October (297), 70 days after the buoy's deployment.

For the first 28 days (15 August-11 September (227-254)) after its deployment, 4562 moved to the southeast, mostly between the 200 m and 1000 m isobaths. The speeds were in the range of 20 to 55 cm/s, while the temperature remained nearly constant (4-5°C). On 13 September (256), 4562 moved onto Hamilton Bank into water that was too shallow for the buoy's drogue. It remained in that vicinity for about 57 days, during which it moved slowly, with frequent direction changes. About halfway through this period (3 October (276)) the temperature record shows an abrupt decrease in temperature (3°C over 18 hours).

The remainder of 4562's southward movement occurred well inside the 1000 m isobath (3 days). The buoy speeds varied widely (0 to 35 cm/s), while the temperature decreases slowly but persistently from 3°C to 0°C.

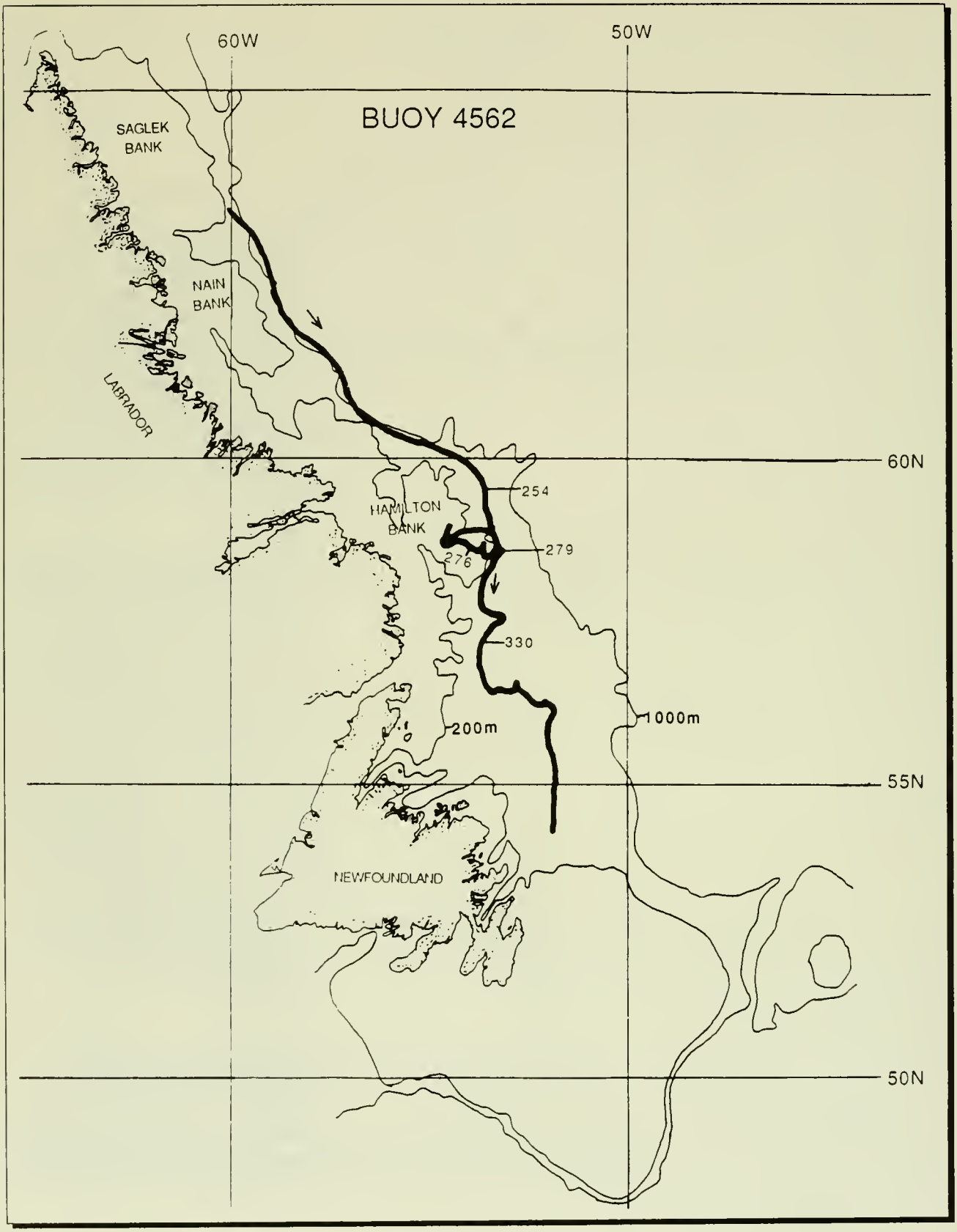

Figure C-19. Trajectory of Buoy 4562.

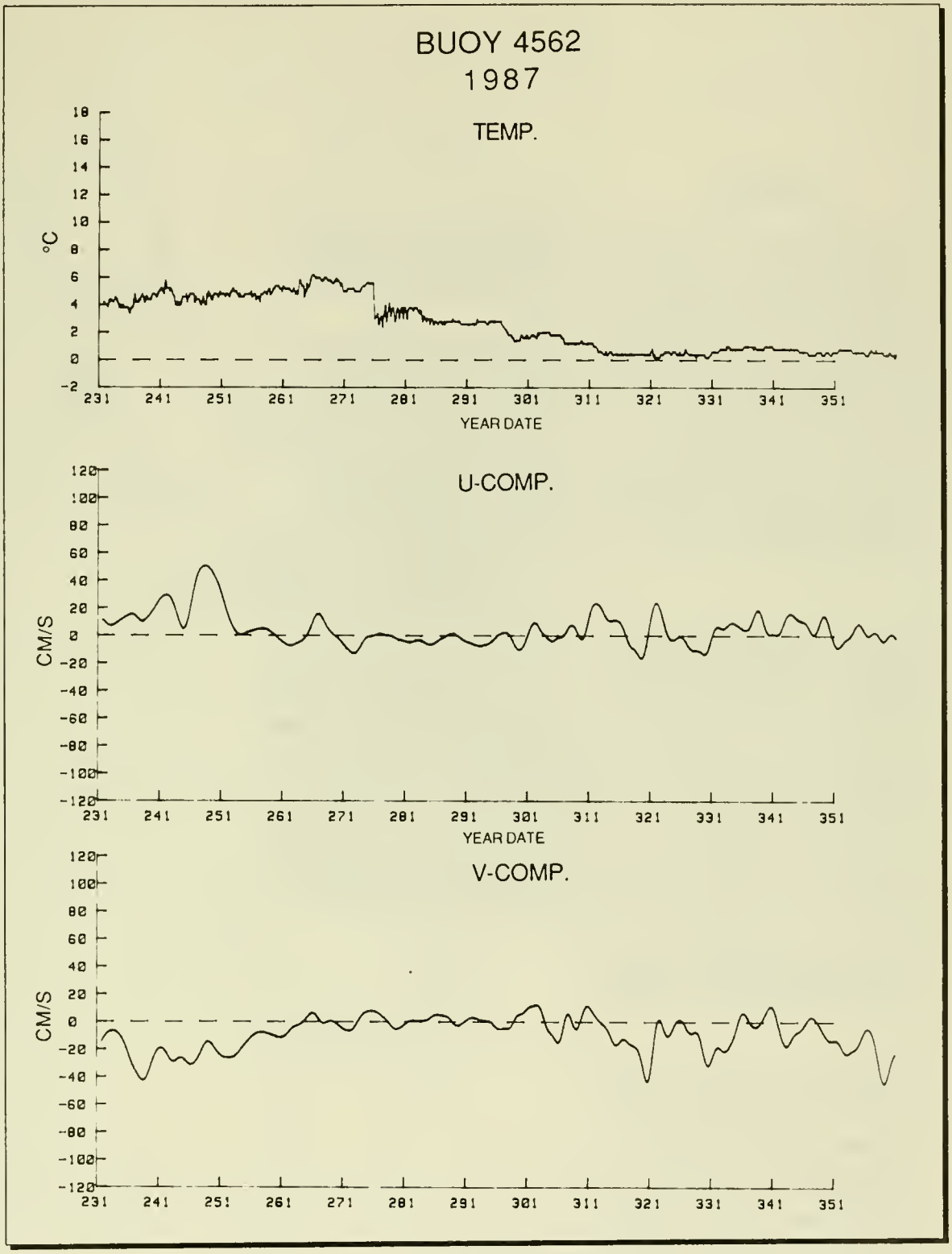

Figure C-20. Temperature, U and V velocity components for buoy 4562.

BUOY 4528

Buoy 4528 (Figure C-21, C-22) was deployed from an aircraft at 60-00N, 61-43W on 15 August (227), after the close of the 1987 iceberg season. Due to a data formatting error, no data regarding the status of the drogue were received from the ARGOS processing center. Buoy 4528 transmitted data throughout the remainder of 1987. It entered the Ice Patrol operations area on 13 October (286) when it crossed south of 52°N.

Buoy 4528 was deployed near the 200m isobath, which it then followed southward to approximately 55°N. Along this track, the buoy's speed varied over the range of 20-30 cm/s. However, there was one 5-day period (1-5 September, 244-248) during which it slowed to about 10 cm/s. This occurred between Saglek and Nain Banks, where the buoy made a small westward excursion. The temperature record during the period, between launch and 55°N, is unremarkable, with a slow increase from 1 to 6°C.

After passing south of 55°N (25 September, 268), 4528 followed the 1000 m isobath for the next 50 days, during which period it moved southward then eastward to a region directly north of Flemish Pass. During this period, the buoy's speed varied mostly over the range of 20-45 cm/s, with two brief periods of slower motion. The temperature record is remarkably constant during the southward motion, but when 4528 began its eastward motion (6 November, 310) the temperature increased rapidly from 3.5 to 6°C.

Buoy 4528 continued its eastward motion, moving to the north of Flemish Cap. Its subsequent motion is complex. First it moved around Flemish Cap, approximately following the 1000 m isobath. Then it apparently became entrained in the North Atlantic Current, as indicated by an abrupt eastward (2 December, 336) then northward motion. During the first part of the period the temperature increased slowly from 6 to 8.5°C, then during a 28-hour period (8-9 December, 342-343) the temperature increased by nearly 8°C. Over the same period the buoy's speed increased from 50 to 85 cm/s. This indicates that the buoy had entered a portion of the North Atlantic Current dominated by meanders and eddies.

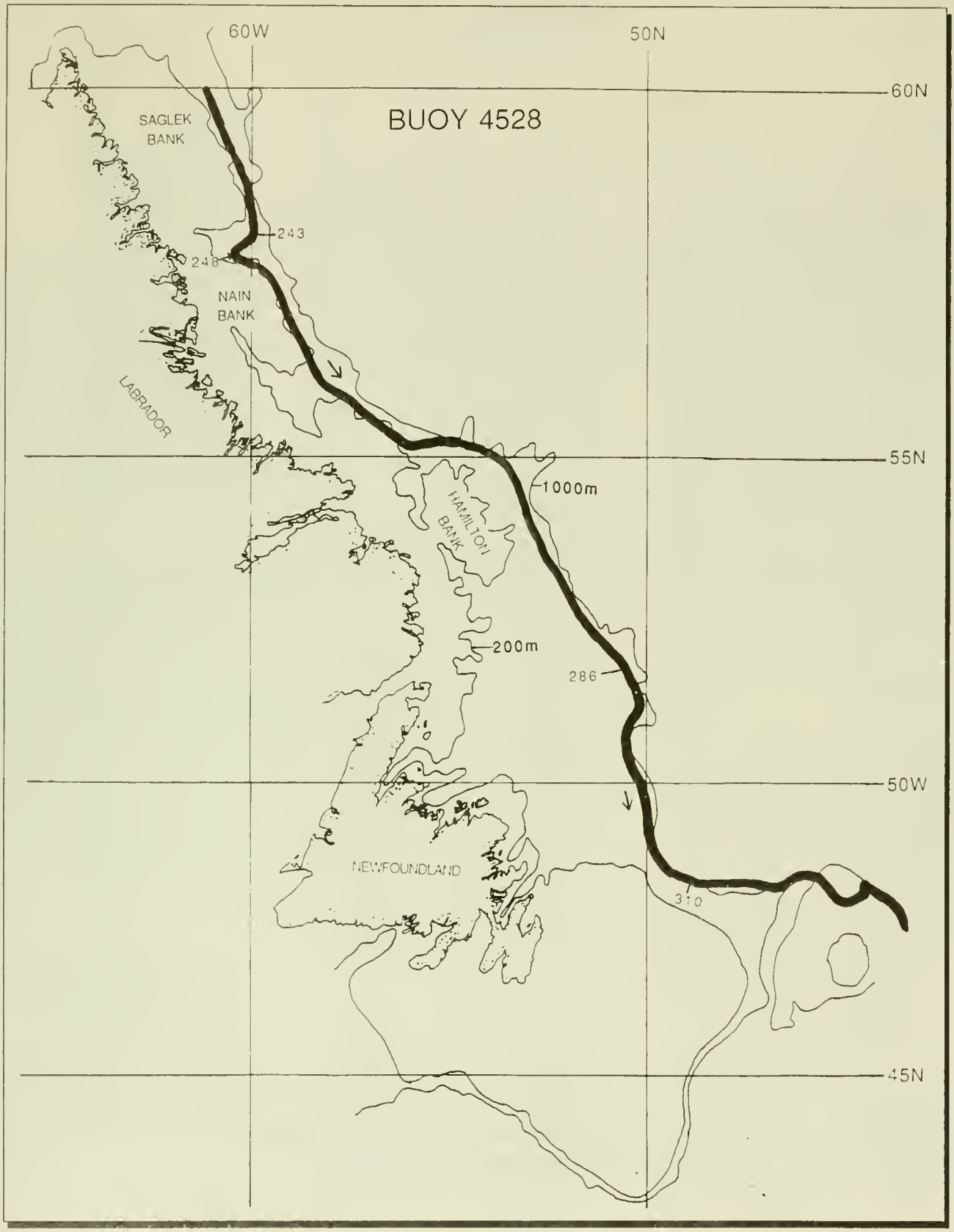

Figure C-21. Trajectory of Buoy 4528.

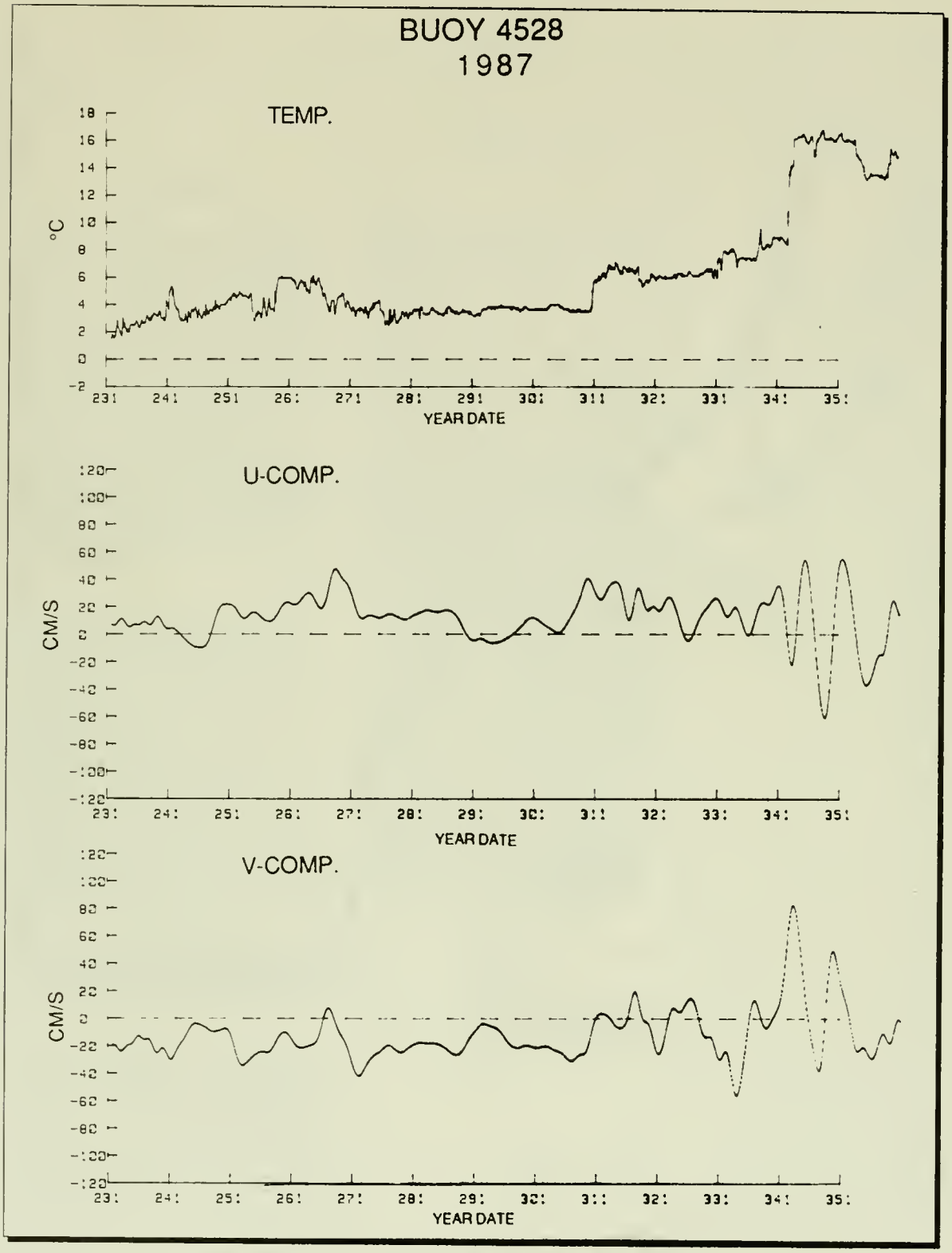

Figure C-22. Temperature, U and V velocity components for buoy 4528.

SUMMARY AND CONCLUSIONS

In 1987 the data return from the buoys was good. The average length of time that a buoy transmitted data from the Ice Patrol operations area was 78 days. According to the drogue sensor data, the average drogue life span was somewhat shorter (70 days), but its survival is well-matched to the requirement that it remain attached during the period the buoy drift is used for operations.

Most buoys transmit data far longer than the 78 days they spend in the Ice Patrol operations area. Five continued to transmit for the remainder of the calendar year. Three buoys were recovered before leaving the area, one by an Ice Patrol research vessel (for redeployment), and two by unknown vessels. Two buoys suffered premature failures, after 65 days and 67 days. It is possible that they were recovered by unknown vessels, but their fate remains uncertain.

The 1987 buoy program did an excellent job of monitoring the Labrador Current, particularly from Flemish Pass southward. The trajectories showed strong bathymetric steering of the current, with most buoys following the continental slope (200-1000 m) southward through Flemish Pass.

Substantial temporal variability in the Labrador Current is also evident in the data. Early in the iceberg season (April - May), two buoys (4555 and 4556) left the slope at 44° and moved rapidly to the east, north of a warm-core eddy at the shelf edge. A similar event occurred in 1986 (Anderson, 1986). Later in the season (July), the track of 4559 suggests that neither the eddy nor any North Atlantic Current meanders were significant factors in the southward movement of the Labrador Current along the slope. After departing Flemish Pass, buoy 4559 moved to the region south of Tail of the Bank (41-50N) in 14 days. This is the most dangerous flow pattern in terms of icebergs moving into the North Atlantic shipping lanes. However, it occurred in July when no icebergs were moving southward through Flemish Pass. Had Ice Patrol relied solely on its historical current data base, which is based on many years of hydrographic data and is time-invarient (Murray, 1979), there would have been no recognition of this observed temporal variability of the Labrador Current.

The 1987 drifting buoy data suggest that the Labrador Current speeds in Ice Patrol historical current data base for the region south of Flemish Pass are too high. [During the iceberg season IIP operations center personnel had to reposition many resighted icebergs upstream from where the drift model had predicted.]

Six buoys passed southward through Flemish Pass, three of which continued their southward movement along the continental slope well south of the pass. In the data base, typical Labrador Current speeds in the area along the slope from 44-46°N are 90-110 cm/s. None of the 1987 buoys recorded speeds as high as this, even for short periods (3 hr). Buoy 4559, which moved from the pass the the Tail of the Bank, recorded the highest speeds, but most were in the 40-60 cm/s range. Ice Patrol has undertaken a program that will make use of all available drifter data to investigate the accuracy of its historical data base. In the regions where sufficient data exist, the data base will be modified to reflect these observations.

No current data were collected on the Grand Bank or in the inshore branch of the Labrador Current in 1987. The distribution of icebergs for this year shows that this is a problem that needs to be addressed. Many icebergs were sighted along the Newfoundland Coast and directly south of the island, a region where the Ice Patrol data base is particularly poor. Little attention has been given to this region. A new generation of smaller, less expensive satellite-tracked buoys is now available. Ice Patrol has been evaluating these buoys and expects to integrate them into the buoy program within the next few years. They will be particularly

useful on the continental shelf and in the near-shore areas where there is a greater risk of unauthorized recovery. They are smaller, more difficult to see, and less of a financial loss when they are recovered by unknown vessels.

REFERENCES

Anderson, I, 1986. TIROS Oceanographic Drifter Tracks on the Grand Banks During the 1986 International Ice Patrol Season. Appendix B, *Report of the International Ice Patrol in the North Atlantic Ocean , Season of 1986, (CG-188-41), Bulletin No. 72.* International Ice Patrol, Avery Point, Groton, CT 06340-6096, U.S.A.

Le Tran, P.Y. and R. Liaubet, 1987. Location: Matching Service To User Needs ARGOS Newsletter No. 30, July 1987. Service ARGOS Inc., 1801 McCormick Drive, Suite 10, Landover, MD 20785 (USA).

Murray, J.J., 1979. Oceanographic Conditions. Appendix B, *Report of the International Ice Patrol Service in the North Atlantic Ocean, Season of 1979 (CG-188-34), Bulletin No. 65.* International Ice Patrol, Avery Point, Groton, CT 06340-6096, U.S.A.

Murphy, D.L., I. Anderson, and N.B. Thayer, 1986. Observations of an Oceanic Front South of Flemish Pass. Appendix C, *Report of the International Ice Patrol in the North Atlantic Ocean, Season of 1986 (CG-188-41), Bulletin No. 72 .* International Ice Patrol, Avery Point, Groton, CT 06340-6096, U.S.A.

Summy, A.D.; "Oceanographic Conditions on the Grand Banks During the 1982 Ice Patrol Season"; Appendix B, *Report of the International Ice Patrol Service in the North Atlantic, Season of 1982 (CG-188-37) Bulletin No. 68.* International Ice Patrol, Avery Point, Groton, CT 06340-6096, U.S.A.

Summy, A.D. and I. Anderson; "Operational Uses of TIROS Oceanographic Drifters by International Ice Patrol (1978 - 1982)", *Proceedings 1983 Symposium on Buoy Technology.* Marine Technology Society, Gulf Coast Section, pp. 246-250.

Appendix D

Observations of a Warm-Core Eddy Near the Grand Banks of Newfoundland

Donald L. Murphy

INTRODUCTION

In April - May 1987, the International Ice Patrol conducted a surface hydrographic and remote sensing study of a warm core eddy near the eastern edge of the Grand Banks of Newfoundland (Figure D-1). The surface vessel was USCGC BITTERSWEET (WLB 389). The primary objective of the study was to improve Ice Patrol's ability to interpret images of the ocean's surface made with its side-looking airborne radar (SLAR).

Imaging radars map the sea surface roughness primarily through Bragg scattering (Robinson, 1985), which for the 3 cm wavelength and incidence angles (45° to 87°) of the Ice Patrol SLAR, results in a sensitivity to wavelengths of 2 cm. These waves are in the capillary-gravity part of the spectrum, thus they are influenced by molecular viscosity, which is a function of sea surface temperature and salinity. The physics of radar returns from the sea surface is receiving increased research attention (see for example, Phillips, 1988 and Donelan and Pierson, 1987) mostly because radar is used to measure oceanic wind distributions. Ice Patrol is interested in using radar images of the sea surface to map the major water-mass boundaries within its operations area.

A previous study (Murphy et al, 1986 and Thayer and Murphy, 1987) showed that the SLAR mapped the location of sharp surface thermal gradients that marked the boundary between a warm-core eddy and the Labrador Current. They found that the warm surface-water within the eddy was always marked by a stronger radar return than the surrounding cooler water. However, they were unable to map the entire boundary around the eddy. A likely explanation of this observation is that their flight patterns permitted only two look angles (with respect to the wind) at the eddy boundary and these were reciprocals of each other. This means that along some portions of the eddy's boundary, the radar was looking along the Bragg wave field rather than into it. This reduces the intensity of the radar return from within the eddy and makes the location of the thermal front difficult to determine.

One of the goals of the 1987 experiment was to improve on the previous experimental design by including four look angles at the eddy in hopes of defining the entire boundary of the feature. In addition, the 1987 experiment provided an opportunity to conduct the surveys under different environmental conditions than those encountered in 1986.

The intent of this report is to describe the experiment that was conducted in 1987 and to present some of the preliminary results. None of the SLAR data are available for presentation at this time, but a portion of the surface-truth data is. This presentation, made before a thorough analysis is completed, is nonetheless worthwhile because it helps understand the oceanographic conditions in the Ice Patrol operations area during 1987. The eddy studied during IIP-87-1 dominated the circulation near the southeastern edge of the Grand Banks early in the season

OBSERVATIONAL PROGRAM

The study site was chosen prior to BITTERSWEET's departure from port based on a satellite infrared image obtained from the National Marine Fisheries Service (NMFS) laboratory at Narragansett, Rhode Island. It showed a warm-core eddy near the eastern slope of the Grand Bank at about 44°N. In addition, data from Ice Patrol operational drifting buoys showed apparent eastward movement in the Labrador Current north of the eddy. Hence, the region had waters of the cold and relatively fresh (< 2°C and < 34.3 ppt) Labrador Current and the warm and more saline (> 12°C and > 35.5 ppt) North Atlantic Current in close proximity. The substantial surface temperature gradients presented a good location to test the SLAR.

Hydrographic Survey

The hydrographic survey was divided into two phases, the first during 5-10 May and the second from 16-20 May. The objective was to survey the eddy and its surroundings twice, in an attempt to describe the evolution of the feature over the entire three-week

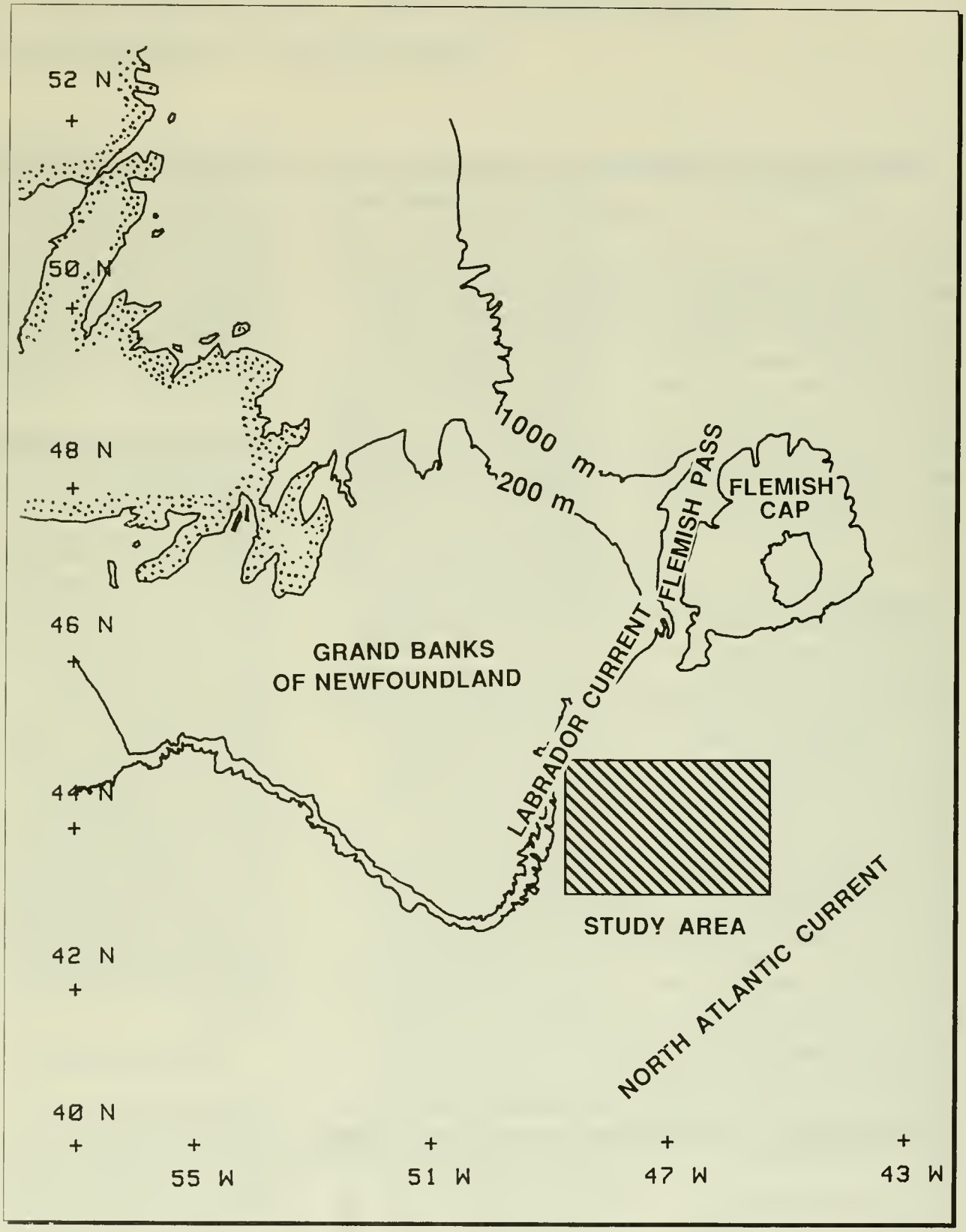

Figure D-1. Schematic of the major current systems near the Grand Banks of Newfoundland. The study area is shown by the shaded rectangle.

study period. In particular, a knowledge of the movement of the thermal fronts over the period of the SLAR surveys is essential when the images are compared to the surface data. The length of each hydrographic phase was limited to no more than 6 days due to the short endurance of the survey vessel.

Phase one consisted of 50 CTD (conductivity, temperature, and depth) stations and 70 XBT stations. This phase consisted of six hydrographic lines, four oriented north-south and two east-west, and one XBT line, a diagonal. The CTD station spacing along the hydrographic lines was 18 km (10 nm), with an XBT cast taken half way between the CTD stations. The station spacing along the XBT line was 9 km (5 nm).

The CTD casts were taken to about 1000 m or to within 50 m of the bottom at stations shallower than 1000 m. To verify CTD results, deep quality control samples were taken at most stations using a Nansen bottle with reversing thermometers. XBT stations were made with T-4 XBT's, which provide a temperature profile to 450 m.

High winds and seas further constricted the time available for sampling during phase two. BITTERSWEET was unable to complete the originally-planned 45 station star pattern, and completed 38 CTD stations and 48 XBT deployments. As in phase one, CTD station spacing was 18 km (10 nm) and XBT casts were conducted about halfway between the CTD stations.

This research cruise marked the first operational use of Ice Patrol's Mobile Oceanography Laboratory (MOL). BITTERSWEET is a buoy tender with no special equipment for oceanographic sampling, thus all sampling and analysis equipment had to be brought aboard for the cruise and removed after its completion.

The MOL consists of a 4.2 X 2.4 X 2.4 m (14 X 8 X 8 ft) steel shipping container, which was attached to brackets welded to BITTERSWEET's buoy deck. The interior of the MOL is fitted with desks and equipment racks containing the computers that retrieve and store data from the CTD and XBT systems, as well as a global positioning system (GPS) receiver.

An electrically-powered, portable oceanographic winch with about 2000 m of 1/4" (0.6 cm) armored hydrographic cable was chained to the buoy deck. The final component of the sampling system was a portable hydrographic platform with a hydraulically operated A-frame, which was placed in the buoy port. All of this equipment can be installed in one day and removed in about four hours.

Drifting Buoys

The drifts of satellite-tracked buoys were used to determine the current speed and direction in the study area. The buoys were 3 meter long spars with a 2 X 10 meter window-shade drogue attached at the end of a 50 meter tether. The accuracy of the position data is about 350 m. The buoys were fitted with temperature sensors (accuracy ~ 1°C) mounted approximately 1 m below the buoy's waterline. Each buoy received about 8 fixes per day.

Eight drift tracks are used for this study. Of these, two are from operational buoys deployed in the Labrador Current well north of the study area by Ice Patrol's reconnaissance aircraft (HC-130). They moved southward along the eastern edge of the Grand Banks (Murphy and Thayer, 1987) and passed through the study area shortly before BITTERSWEET arrived on scene. The remaining drift tracks are from buoys deployed from BITTERSWEET, most of which were recovered after the experiment concluded.

SLAR Surveys

Four SLAR surveys, on 2, 6, 14 and 20 May, mapped the features in the study area. On two dates (15, 18 May) portions of the study area were mapped during routine iceberg patrols. The Ice Patrol SLAR is an X-band (3 cm wavelength), real-aperture radar that produces a continuous 9" (23 cm) analog image on film. When the

aircraft is flown at 8000 ft (2440 m), the radar maps a 50 km wide swath on each side of the aircraft with a blind spot 5 km wide directly under the aircraft. Both antennas are vertically polarized.

Several different flight patterns were used during the survey. The intent of the various patterns was to obtain several different directions of look relative to the wind, in addition to looking at the thermal fronts from various ranges.

RESULTS

The following sections describe some of the data that constitute the surface-truth for the SLAR interpretation experiment. The radar data are currently being analyzed. The surface-truth data presented here are limited to the first phase because it is the more complete of the two data sets and the first to be analyzed.

Hydrography

Figure D-2 shows the surface temperature on the first phase hydrography. A small, warm-core eddy, centered at 43-50N, 48-20W and with a diameter of about 65 km dominates the temperature field in survey area. North of the eddy is cold water (< 3°C) of Labrador Current origin, while warm water (> 12°C) from the North Atlantic Current is evident in the southeastern part of the study area. Although it appears from the surface temperature distribution that the eddy was separate from the North Atlantic Current, their proximity makes it likely that they were interacting.

The greatest surface temperature gradient, about 8°C, is located at the northern boundary between the eddy and the Labrador Current. Over an 18 km distance, the surface temperature changes from less than 3°C to greater than 10°C. It is in this region that the SLAR is most likely to detect a difference in radar return.

A vertical temperature section (Figure D-3) along the center of the 5 north-south transects (A-B on Figure D-2) shows that the 10°C isotherm extends to about 160 m. It also shows the locations where three of the drifting buoys were deployed. Buoy 4536 was deployed in 13°C water near the center of the eddy. Buoy 4547 was deployed in 3-4°C water north of the eddy. Finally, buoy 4511 was deployed near the eddy's northern edge. The center of the drogues for all of the buoys is at ~ 58 m.

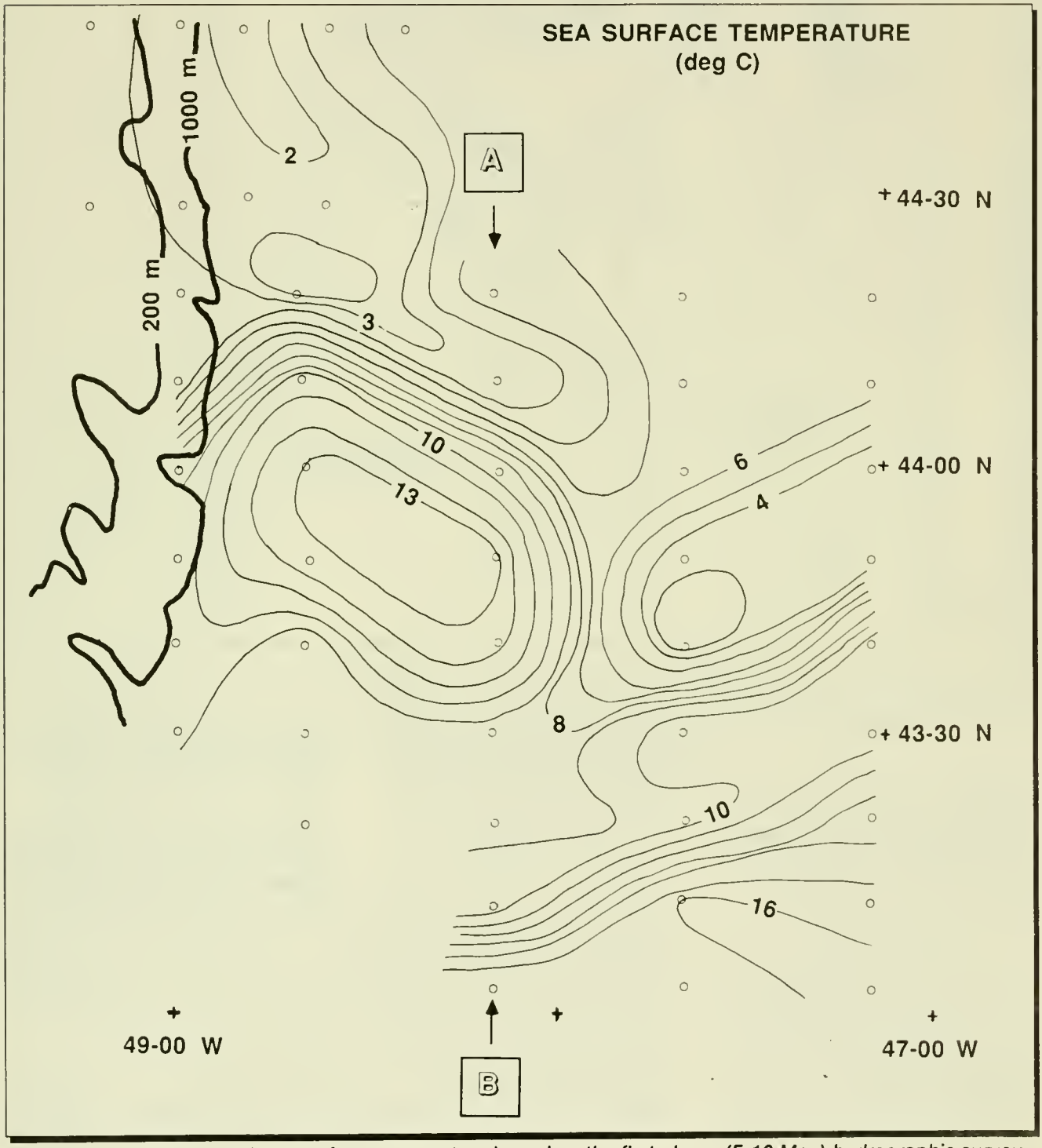

Figure D-2. Distribution of sea surface temperature based on the first phase (5-10 May) hydrographic survey.

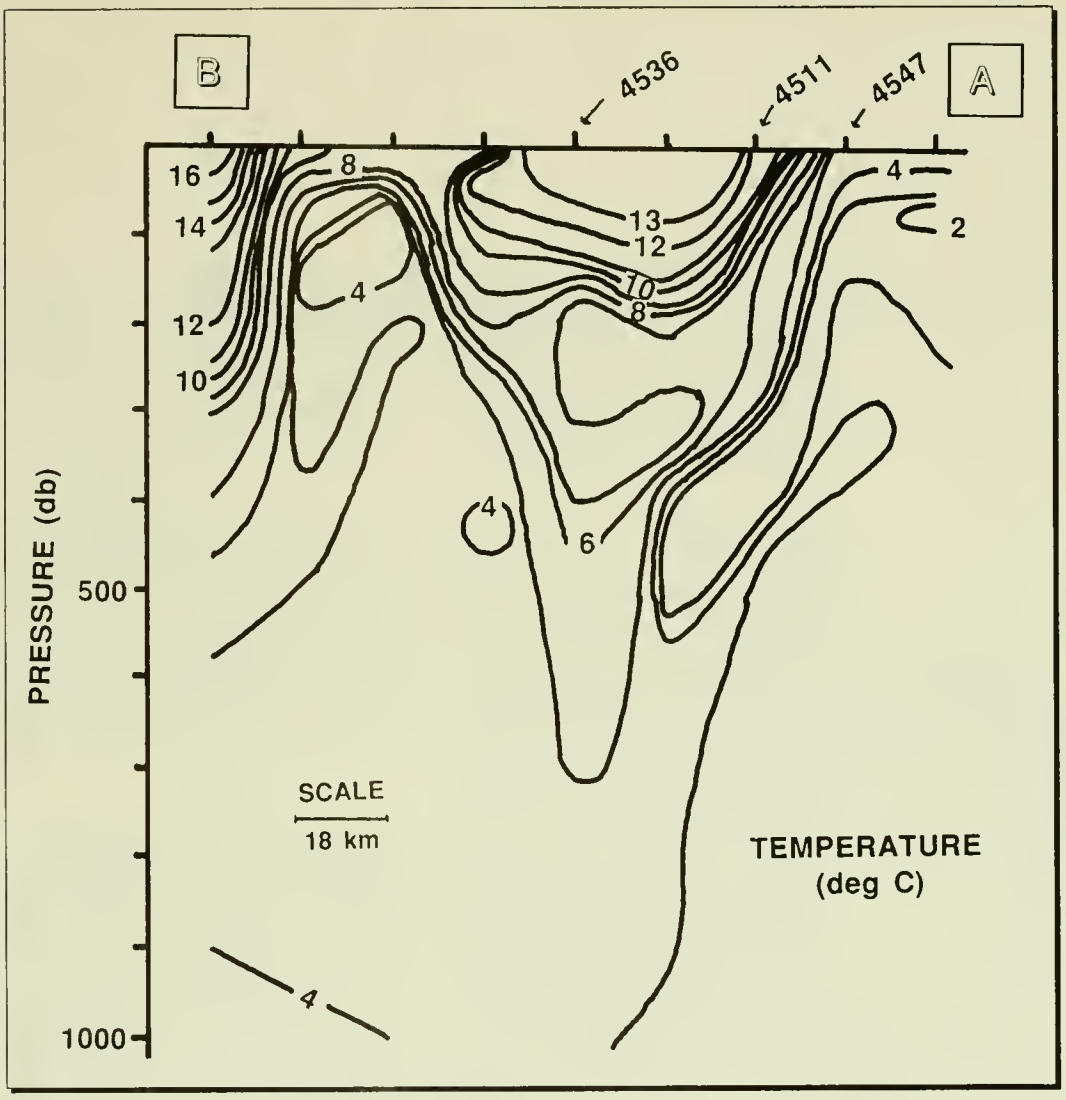

Figure D-3. Vertical distribution of temperature along transect marked A-B in Figure D-2.

Drifters

The drifter data are presented in two plots. The first (Figure D-4) presents trajectories of 4555 and 4556, both of which were Ice Patrol operational drifters deployed in the Labrador Current north of Flemish Pass.

Buoy 4555 arrived in the study area on 20 April, approximately two weeks before the start of the hydrographic survey. Over the next 6 days it traced an anticyclonic path approximately one-half the way around the eddy's boundary. The buoy speeds over this period varied over the range of 50-70 cm/s, while the temperature varied over the range from 0.8 to 13°C, suggesting that the buoy was close to the eddy's boundary.

On 30 April, 4556 entered the study area. Like 4555, buoy 4556 moved rapidly (50-70 cm/s) to the east, north of the eddy. However, buoy 4556's temperature record was quite different, with a slow increase from 0.6 to 2.0°C over the period during which it remained in the area.

Figure D-5 presents the drifter data from the four buoys deployed by BITTERSWEET. They are plotted on a map of the surface dynamic topography (relative to 1000 db) calculated from the first phase (5-10 May) hydrographic survey. The buoy tracks are for the same period as the survey.

Both the dynamic topography and 4536's drift track suggest that the eddy was interacting with the North Atlantic Current. Buoy 4556 did not complete one entire circuit around the eddy before it departed to the east and left the study area.

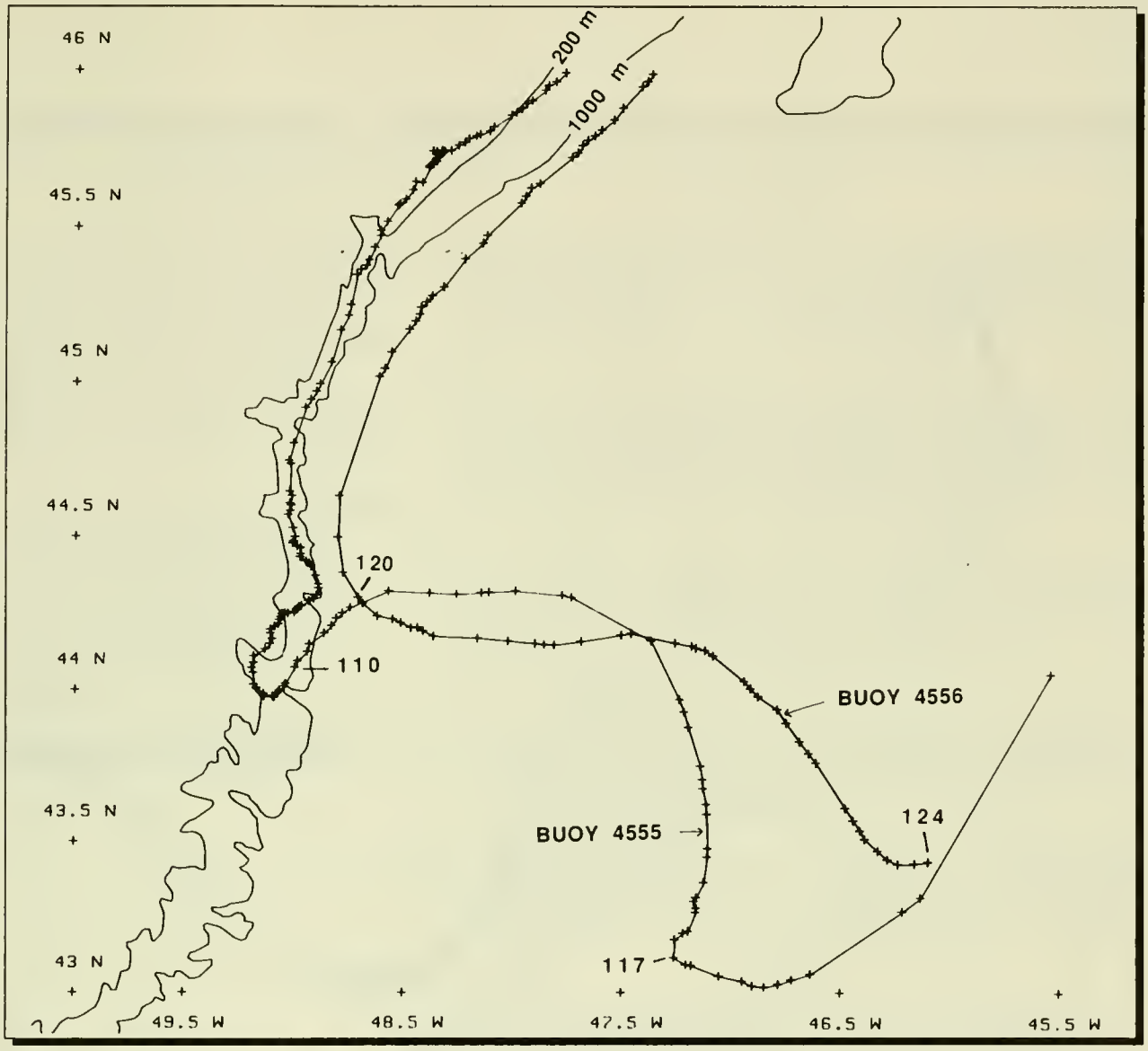

Figure D-4 Trajectories of 4555 and 4556, both of which were deployed north of Flemish Pass.

The track of 4547 is remarkable in that shortly after deployment it moved southward and eventually intersected the path of 4511. The drifter tracks are in general agreement with the surface dynamic topography.

CONCLUSIONS

The data presented here show a small, warm-core eddy centered at 43-50N, 48-20W and interacting with the North Atlantic Current. Although the detailed dynamics of the eddy cannot be resolved by the coarse sampling scheme, its effect on the Labrador Current is clear. During the period that the eddy was close to the continental slope (April-May), a portion of the Labrador Current departed the slope and moved to the east at about 44°N.

The tracks of 4555 and 4556, which were deployed in the Labrador Current but moved eastward off the slope at 44°N, are consistent with the existence of an eddy at this location. The eddy had a major influence on the Labrador Current as early as 20 April, and perhaps before.

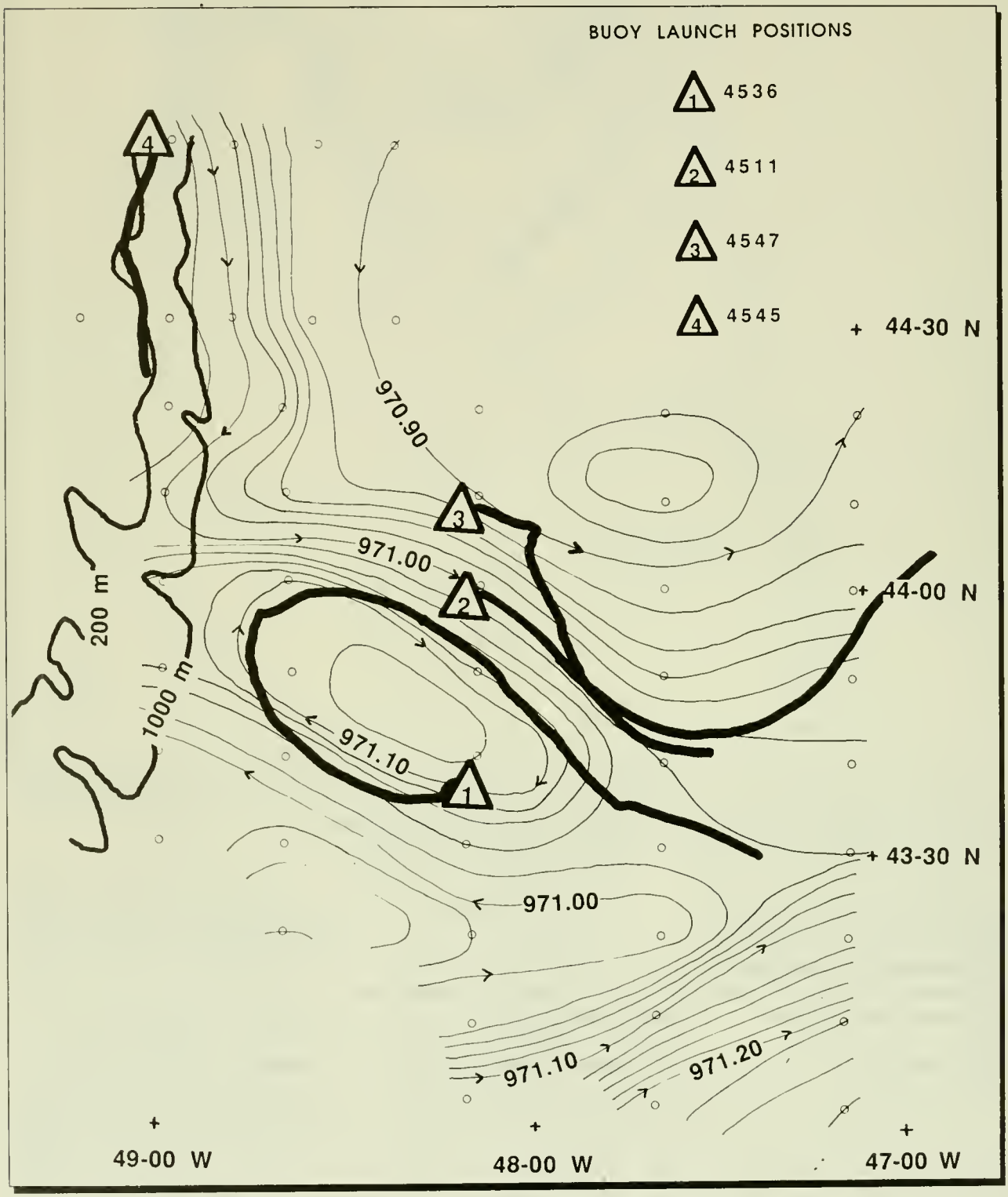

Figure D-5. Trajectories of four buoys (4511, 4536, 4545, and 4547) plotted on a map of the surface dynamic topography (with respect to 1000db) based on the first phase hydrographic survey.

ACKNOWLEDGEMENTS

Sincere appreciation is extended to the Marine Science Technicians of International Ice Patrol who collected and are currently analyzing the data from the experiment described herein. Without their efforts this work could not have been accomplished.

The officers and crews of USCGC BITTERSWEET (WLB 389) and CG 1503 and CG 1504, both of Coast Guard Air Station Elizabeth City, North Carolina enthusiastically supported Ice Patrol's research. Their efforts are greatly appreciated.

REFERENCES

Donelan, M. A. and W. J. Pierson, Jr., 1987. Radar Scattering and Equilibrium Ranges on Wind-Generated Waves With Application To Scatterometry. *Journal of Geophysical Research*, Vol 92 (C5): 4971-5029.

Murphy, D. L., I. Anderson, and N. B. Thayer, 1986. Observations of an Oceanic Front South of Flemish Pass. Appendix C, *Report of the International Ice Patrol in the North Atlantic Ocean, Season of 1986 (CG-188-41), Bulletin No. 72.* International Ice Patrol, Avery Point, Groton, Connecticut 06340 U.S.A.

Murphy, D. L. and N. B. Thayer, 1987. 1987 International Ice Patrol Drifting Buoy Program. Appendix C, *Report of the International Ice Patrol in the North Atlantic Ocean, Season of 1987 (CG-188-42), Bulletin No. 73.* International Ice Patrol, Avery Point, Groton, Connecticut 06340 U. S. A.

Phillips, O. M., 1988. Radar Returns From The Sea Surface - Bragg Scattering And Breaking Waves. *Journal of Physical Oceanography*, Vol 18: 1065-1074.

Thayer, N. B. and D. L. Murphy, 1988. SLAR Observations of Ocean Fronts East of the Grand Banks of Newfoundland. Proceedings of the 11th Canadian Symposium on Remote Sensing, University of Waterloo, Waterloo, Ontario, Canada N2L 3G1. (In press).

Robinson, I. S., 1985. *Satellite Oceanography: An Introduction for Oceanographers and Remote Sensing Scientists.* West Sussex, England: Horwood Limited. 455 pp.

Appendix E

Operational Forecasting Concerns Regarding Iceberg Deterioration

LCDR Walter E. Hanson Jr., USCG

INTRODUCTION

Since 1971, the International Ice Patrol (IIP) has used computer-based drift prediction models to help evaluate the extent of the iceberg danger to North Atlantic shipping in the vicinity of the Grand Banks of Newfoundland. A dynamic model began operational use in 1979 (Mountain, 1980). This model, along with a parametric iceberg deterioration model which began operational use in 1983 (Anderson, 1983), has grown in importance as iceberg reconnaissance has gone to an every other week schedule. During the peak of the iceberg season, April through June, the iceberg danger covers a large area, requiring reconnaissance missions to concentrate on patrolling the limits. Often icebergs go several weeks before being resighted. Resighting icebergs depends heavily on these models effectively predicting drift and deterioration rates. These predictions are also routinely used to set the limit of all known ice, as reported in the IIP bulletins.

As evidenced by the many years of safe passage by trans-Atlantic shipping, the IIP seems to have some skill in determining the extent of the ice danger. (To assess the model's predictions there is a need for accurate data to represent the initial iceberg, interim iceberg, and environmental conditions.) Iceberg drift prediction is highly dependent upon iceberg mass (size and shape). Consequently, the ability to accurately predict changes in iceberg size for the majority of icebergs, which are infrequently resighted, becomes very important.

Between 1983 and 1985, the IIP studied the drift and deterioration of four icebergs. Although no firm conclusions could be drawn from such a small data set, which represented an average drift of 4.5 days, the prediction models did fairly well hindcasting the drift and deterioration when observations were used as inputs (Anderson, 1985). A similar study was performed, using U. S. Coast Guard iceberg data, for the Atmospheric Environment Service of Canada (El-Tahan et al, 1987). The results were mixed. Thus in June 1987, the IIP conducted another cruise to collect similar data for a cluster of icebergs.

The objectives of this study were to compare iceberg deterioration predictions derived from environmental data collected in situ to inputs available from operational data centers. These latter inputs were divided between global and regional scale products.

BACKGROUND

The iceberg deterioration model used by the IIP provides its watch officers with a daily estimate of the "melt" status of each iceberg entered in the drift model. The computer-based application (Anderson, 1983), which computes the melt rate, is derived from White, et al 1980. The model sums the effects of the following processes which are depicted in order of importance in Figure E-1:

- solar radiation;
- buoyant heat convection;
- heat convection caused by iceberg movement relative to the water mass (forced heat convection); and
- waterline wave erosion, followed by calving of the resultant ice overhang.

Based on the 1980 report, warm air heat convection is considered insignificant and not calculated. The report also identified other iceberg deterioration processes; however, they were only partially addressed and difficult to quantify. Consequently those processes are not modelled.

The model calculates melt in terms of length instead of mass. This measure of melt accommodates IIP's operational procedures, in which nearly all iceberg dimensions are reported by size categories. These categories are based primarily on the maximum observed length of the iceberg.

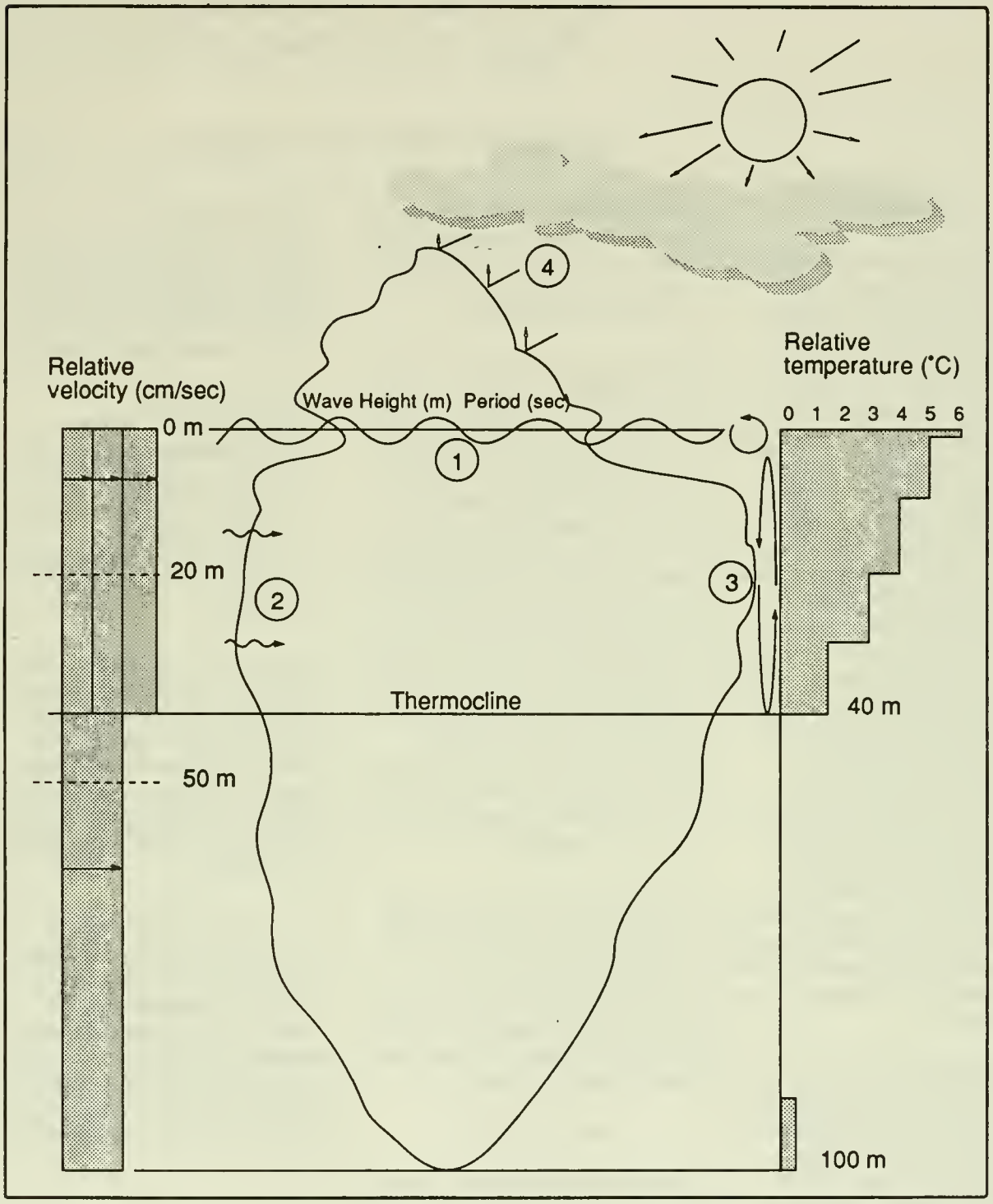

Figure E-1. Modelled Iceberg Deterioration Processes. This figure depicts four processes used by the IIP deterioration model to "melt" icebergs. The four processes, which are labelled in order of importance are: (1) wave erosion; (2) forced heat convection; (3) buoyant heat convection; and (4) solar radiation. The figure also identifies the variable environmental terms used to model each process and their influence on "melt" for the icebergs studied by IIP. These terms are: relative velocity; wave height; wave period; and relative temperature. Other terms used to model iceberg "melt" are: cloud cover, which is constant; and maximum waterline length of the iceberg.

1987 DATA COLLECTION EFFORT

This study collected data on six medium to small icebergs for a period ranging from 2.1 to 6.3 days. The icebergs were studied as they drifted south with the Labrador Current on the northeast Newfoundland Shelf (centered around position 50-45°N, 53-30°W); see Figure E-2. The study was conducted between 15 and 21 June 1987 using the USCGC TAMAROA, a 68m (205 ft) U. S. Coast Guard cutter.

Iceberg above water dimensions were taken during daylight using a camera and reticulated laser rangefinder. Iceberg shape and size were calculated from photographic images scaled according to rangefinder measurements. This required a 360 degree look at each iceberg; measuring and photographing all prominent faces. Measurements were accurate to +/- 8% of the observed dimensions. No underwater iceberg dimensions were measured.

The rangefinder-derived distances were used with visual bearings to fix the icebergs' positions during daylight. At night, radar bearings and ranges were used. The cutter used LORAN-C and SATNAV to fix its position. Positional accuracy for iceberg positions was estimated (by summing system errors) to be +/- 750m. Table E-1 summarizes the observed dimensions and estimated drift of the icebergs.

Hourly environmental observations included: air and sea surface temperature, cloud cover, and wind (at 22.3m). Sea surface temperature was taken by bucket thermometer (error was +/- 0.1°C); wind was measured by the ship's anemometer. Wave height, period and direction were visually estimated every six hours. Visual wave observations were estimated to have an error of +/- 0.5m for wave height; and +/- 2sec for period. Surface currents were inferred from the drift of two satellite-tracked drifters (FGGE-hulled), which had window-shade (2m X 10m) drogues. Both drifters were deployed at the same time near the center of the cluster. One was drogued near the surface (center of the drogue: 8m deep), while the other was drogued at 58m, at the core of the Labrador Current. Temperature vs. depth profiles were taken in the vicinity of each iceberg and transects were made at the beginning and end of the study to determine iceberg drift in relation to the

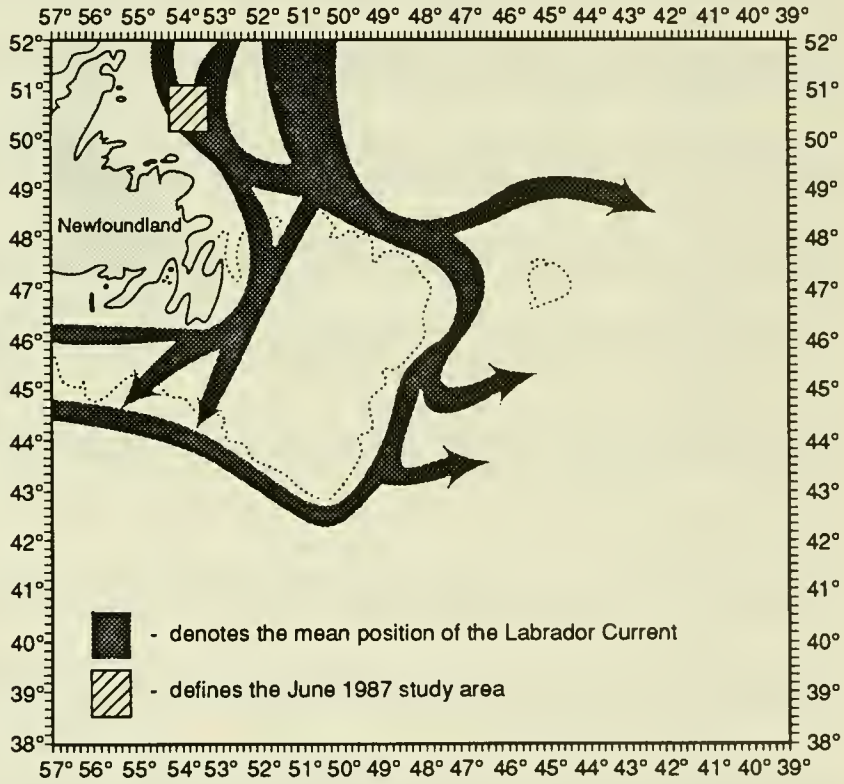

Figure E-2. International Ice Patrol Study Area. This figure depicts the area in which iceberg drift and deterioration is operationally modelled by IIP. The 200m bathymetric contour is shown to describe the Grand Banks of Newfoundland and Flemish Cap.

Table E-1: Observed Size, Shape, and Estimated Drift of Icebergs.

Elapsed Days	Maximum Dimensions (in meters) Length	Height	Shape	Interpolated 12-hourly Speed (cm/sec)	Direction (T)
Berg #620					
0.0	43	11	Wedged		
0.6				19	231
0.9	41	10	Pinnacled		
1.1				18	201
1.6				22	209
1.7	36	11	Domed		
2.1				35	186
2.6				45	171
2.9	41	12	Pinnacled		
3.1				32	165
3.6				46	193
4.0	52	27	Pinnacled		
4.1				38	192
4.6				24	127
4.8	58	7	Pinnacled		
Berg #744					
0.0	32	7	Domed		
0.1				6	295
0.6				20	295
0.8	77	18	Pinnacled		
1.1				8	229
1.6				37	140
2.0	55	16	Pinnacled		
2.1				45	138

Elapsed Days	Maximum Dimensions (in meters) Length	Height	Shape	Interpolated 12-hourly Speed (cm/sec)	Direction (T)
Berg #747					
0.0	114	24	Wedged		
0.9	70	24	Wedged		
1.0				16	234
1.5				13	183
1.7	96	25	Wedged		
2.0				18	163
2.5				33	150
2.9	86	28	Pinnacled		
3.0				41	146
3.5				32	154
4.0				25	173
4.5				23	142
4.7	115	22	Pinnacled		
5.0				21	107
5.5				6	065
6.0	96	23	Pinnacled	14	118
6.3	86	27	Pinnacled		
6.5				33	131
Berg #784					
0.0	89	31	Pinnacled		
0.8				23	121
1.0	110	49	Pinnacled		
1.3				28	153
1.8				36	166
2.0	107	43	Pinnacled		
2.3				44	168
2.8				38	178
3.0	112	24	Pinnacled		
3.3				35	182
3.8	117	43	Pinnacled	21	185
4.3				4	147
4.8				9	274
4.9	113	33	Pinnacled		
5.3				3	275

Table E-1 (Continued).

Elapsed Days	Maximum Dimensions (in meters) Length	Height	Shape	Interpolated 12-hourly Speed (cm/sec)	Direction (T)
0.0	97	37	Pinnacled		
0.4				26	355
0.8	94	32	Drydock		
0.9				12	293
1.4				21	191
1.9	92	30	Drydock	35	169
2.4				37	143
2.8	84	25	Drydock		
2.9				43	136
3.4				31	145
3.9				15	164
4.4				11	182
4.8	71	7	Domed		
4.9				15	164
Berg #787					
0.0	81	34	Pinnacled		
0.3				49	169
0.8				52	194
1.1	75	23	Pinnacled		
1.3				34	192
1.6	57	25	Pinnacled		
1.8				22	208
2.3				10	250
2.8				8	152
3.1	59	23	Pinnacled		
3.3				21	308

Labrador Current. The measurements were made to a depth of about 300m using T-4 eXpendable BathyThermographs (XBT).

Having only one observation platform to monitor the drift and deterioration of six icebergs, which were within a circle of approximately 55km radius, made both compiling environmental factors affecting each iceberg and verifying iceberg identity difficult. The distance between the cutter and each iceberg determined the applicability of environmental observations. Table E-2 summarizes the distances between observations and icebergs. The average distance wave data were collected from each iceberg was 48km; wind and weather data, 61km; and sea temperature data, 7km. These distances were computed from the interpolated positions of each iceberg for 0000Z and 1200Z as derived from a cubic spline.

The spatial separation of the wind and wave observations is much smaller than the 250km data grid-spacing on which global environmental products are prepared by FLENUMOCEANCEN for IIP use (COMNAVOCEANCOM, 1986). Because the study area was at least 105km offshore, the wind and wave fields were assumed to be spatially uniform.

In mapping the sea surface temperature, the icebergs were in a tongue-like feature of cold water which protruded southeastward. The feature, which measured about 18km across, complicated the data analysis, since the temperature field could not be assumed uniform. As a compromise, only observations within 9km of an iceberg's position were accepted. Because of this restriction and having only one observation platform, the data sets for some icebergs were incomplete. The temperature values necessary to model deterioration were linearly interpolated from these data sets.

Table E-2: Distance of Observations from Individual Icebergs.

Type of Data Collected		Distance (in km) From Iceberg		
	Wind	Min	Max	Avg
Berg#	620	3	104	49
	744	9	71	45
	747	9	121	69
	784	1	136	60
	785	1	111	52
	787	13	103	49
	Sea Surface Temperature	Min	Max	Avg
Berg#	620	3	15	7
	744	3	14	9
	747	1	11	7
	784	0	16	9
	785	1	7	4
	787	4	9	6
	Wave	Min	Max	Avg
Berg#	620	14	53	31
	744	1	76	52
	747	73	127	106
	784	1	31	16
	785	0	61	17
	787	11	107	65

THE ICEBERGS STUDIED

Six non-tabular icebergs were studied. Five were classified medium in size; one was small (#620). Most icebergs did not deteriorate enough to change size. The numbers (e.g. #620) refer to the sequential numbering system that IIP uses to identify individual icebergs during the course of the ice season. These are the same numbers used in archived IIP iceberg data at the World Data Center for Glaciology, Boulder, Colorado.

Although the icebergs did not change size category during the course of the study, all were deteriorating rapidly. Because of the recurring presence of growlers and bergy bits in the vicinity of all icebergs except #620 and #744, calving was assumed to be a major factor in the cluster's deterioration. Table E-3 describes the amount of calved ice in the vicinity of each iceberg during daily sizing measurements. The study could not document all calving for any one iceberg since no iceberg was observed around-the-clock. However, two events were documented: iceberg #784 on 19 June; and #747 on 21 June. Because of the warm water (greater than 3°C), the brash melted between daily observations. Bergy bits and growlers which did not fully melt between observations were tracked (in one case up to 18 hours), to keep calving statistics for the cluster from being inflated.

Only icebergs #785 and #787 appeared stable throughout the study period. Stability in this context meant that the iceberg length and height constantly decreased. Figure E-3 describes the areal dimensions for these icebergs at the beginning and end of the study period. Most of the icebergs changed shape during the study, probably from rolling. Iceberg #784 rolled while the cutter was nearby on 19 June. In this case, the rolling caused height to double although length increased insignificantly (5%).

Table E-3. Total Amount of Calved Ice Observed Daily in the Vicinity of Icebergs.

	Iceberg #					
Date (June)	620	744	747	784	785	787
14	fog	-	-	-	-	-
15	0	fog	fog	fog	brash	
16	4G	0	brash	0	brash	
17	0	brash	4G+1B	0	4G	3G+1B
18	0	-	-	8G+1B	3G	5G+2B
19	0	-	1G+1B	5G	-	1G
20	-	-	-	0	2B	fog
21	-	-	5G	-	-	-

fog - observations obscured by dense fog

(-) - no observation made during 24-hour period

G - growler, which is less than 1m high and/or 5m long

B - bergy bit, which is larger than a growler, but less than 5m high and/or 15m long

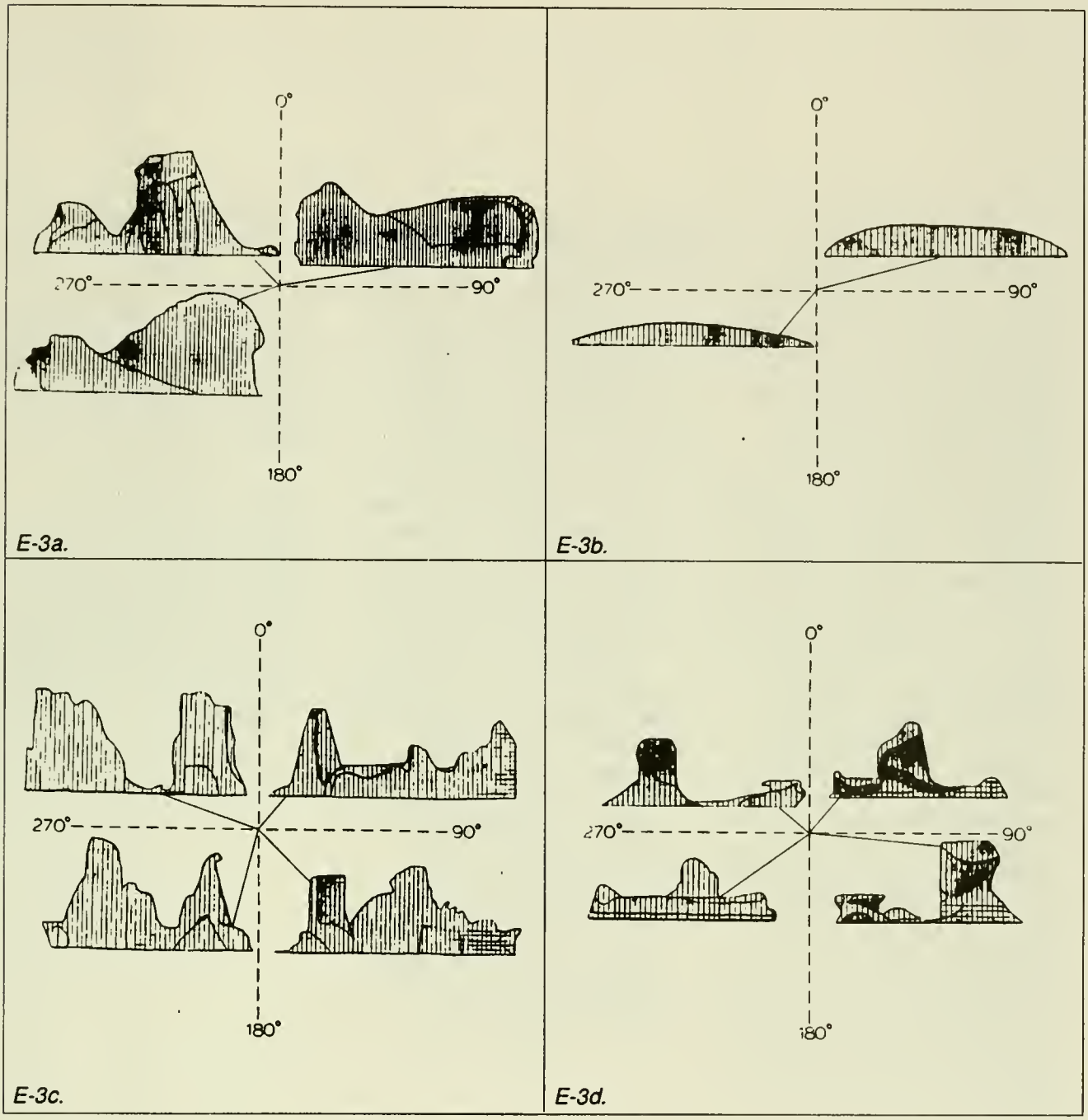

Figure E-3. Areal Dimensions of Icebergs.
These figures describe the major faces of two medium-sized, non-tabular icebergs studied during June 1987. The initial and final dimensions of each iceberg are presented. The scale is the same for all figures (1 unit = 3.1m (10 ft)). The orientation of each face to true North is also shown. The faces depicted in the initial and final sizing are dissimilar.

Figure E-3a. depicts the inital dimensions of iceberg #785 (maximum height = 37m, maximum length = 97m); Figure E-3b shows the same iceberg 4.8 days later (maximum height = 7m, maximum length = 71m).

Figure E-3c depicts the initial dimensions of iceberg #787 (maximum height = 34m, maximum length = 81m); Figure E-3d shows the same iceberg 3.1 days later (maximum height = 23m maximum length = 59m).

THE WATER COLUMN

The cluster of icebergs was in a tongue of the Labrador Current as evidenced from both sea surface temperatures and the XBT profiles (see Figure E-4). The tongue of Labrador water had a cold (-1°C) core at 60m, below a shallow thermocline at 40m. Surface temperatures ranged between 3.4 and 7.6°C. Temperatures of -1°C or colder, that would preclude melt (White et al, 1980), existed from 40m to 90m in the eastern portion of the study area, and from 40m to 160m in the western portion. XBT casts taken in the vicinity (within 28km) and within 6 hours of the 0000Z interpolated iceberg's positions were used to estimate the average heat available in the water column to melt the iceberg. When there was no XBT cast near a particular iceberg within six hours of 0000Z, the temperature information was calculated by linearly interpolating in time. The water temperature, relative to -1°C, was averaged over 10m intervals over the estimated draft of the iceberg. Iceberg draft was estimated as 3.95 times the average sail height observed during the study (Robe, 1975).

From analyzing temperature profiles taken about four days apart, this tongue of the Labrador Current had advected south 74km. The advection of the cold core at 60m agrees well with the deep-drogued drifter. Its drift indicated a predominantly southerly flow (186°T at 21cm/sec) for 4 days (from 15 June/0000Z through 19 June/0000Z), then an easterly flow (112°T at 12cm/sec) for the last 1.5 days of drift. The westward displacement of the thermal field above the thermocline agreed well with the shallow-drogued drifter. From 15 June/0000Z to 17 June/1600Z the drift was 193°T at 27cm/sec. From 17 June/1600Z until recovered on 20 June/1243Z, the drifter showed a steady deceleration, averaging 206°T at 9cm/sec. Figure E-5 summarizes the drifts of all icebergs and drifters and shows the XBT transects used to describe the thermal characteristics of the water column. All of the drifters recorded sea temperature at 1m depth between 3 and 5°C, which agreed well with the bucket thermometer measurements.

DETERIORATION MODEL EVALUATION CRITERIA

The deterioration processes were evaluated based on observations compiled for the four medium, non-tabular icebergs #747, #784, #785, and #787 which had estimated drafts from 98 to 146m. This cluster was studied for 5 days.

Based on in situ temperature, icebergs #747 and #787 had insignificant melt from convective processes below 40m depth. Therefore the buoyant and forced heat convection contributions below 40m depth were calculated and evaluated for only icebergs #784 and #785.

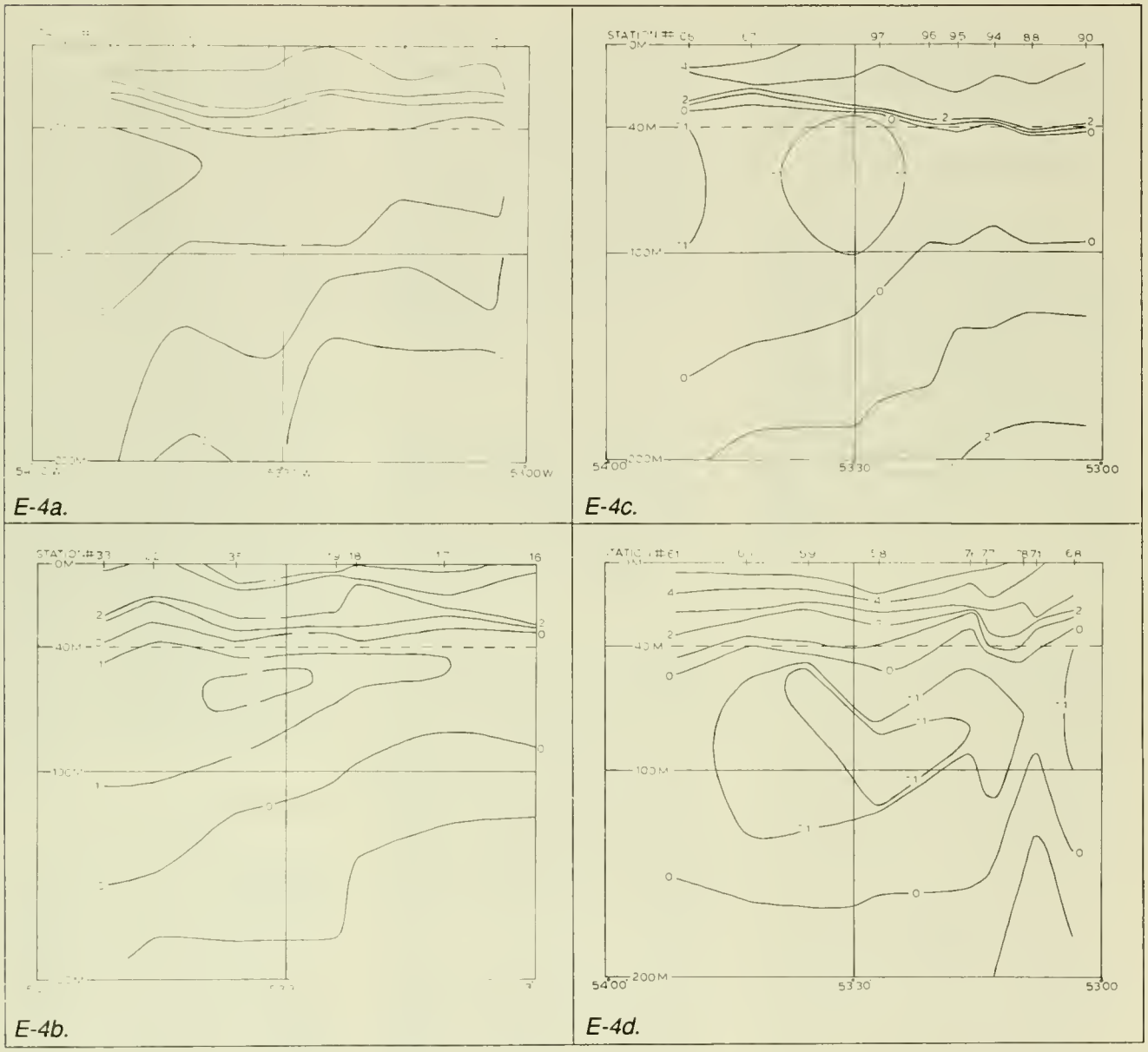

Figure E-4. Thermal Structure of the Water Column.
These figures depict the thermal structure along four eXpendable BathyThermograph transects taken during the IIP June 1987 study. These transects were nearly orthogonal to the flow of the Labrador Current. The XBT positions are noted by cast numbers along the top of each figure. The geographic positions of the transects are shown in Figure E-5. Figure E-4a depicts transect A1, which was measured between 0645Z June 15 and 0631Z June 16. Figure E-4b depicts transect B1, which was measured between 1949Z June 14 and 0151Z June 16. Figures E-4c and E-4d represent transects taken about 4 days later approximately 74km downstream from the A1 and B1 transects. Figure E-4c depicts transect A2, which was measured between 0819Z June 19 and 1234Z June 20. Figure E-4d depicts transect B2, which was measured between 0429Z and 2008Z June 19.

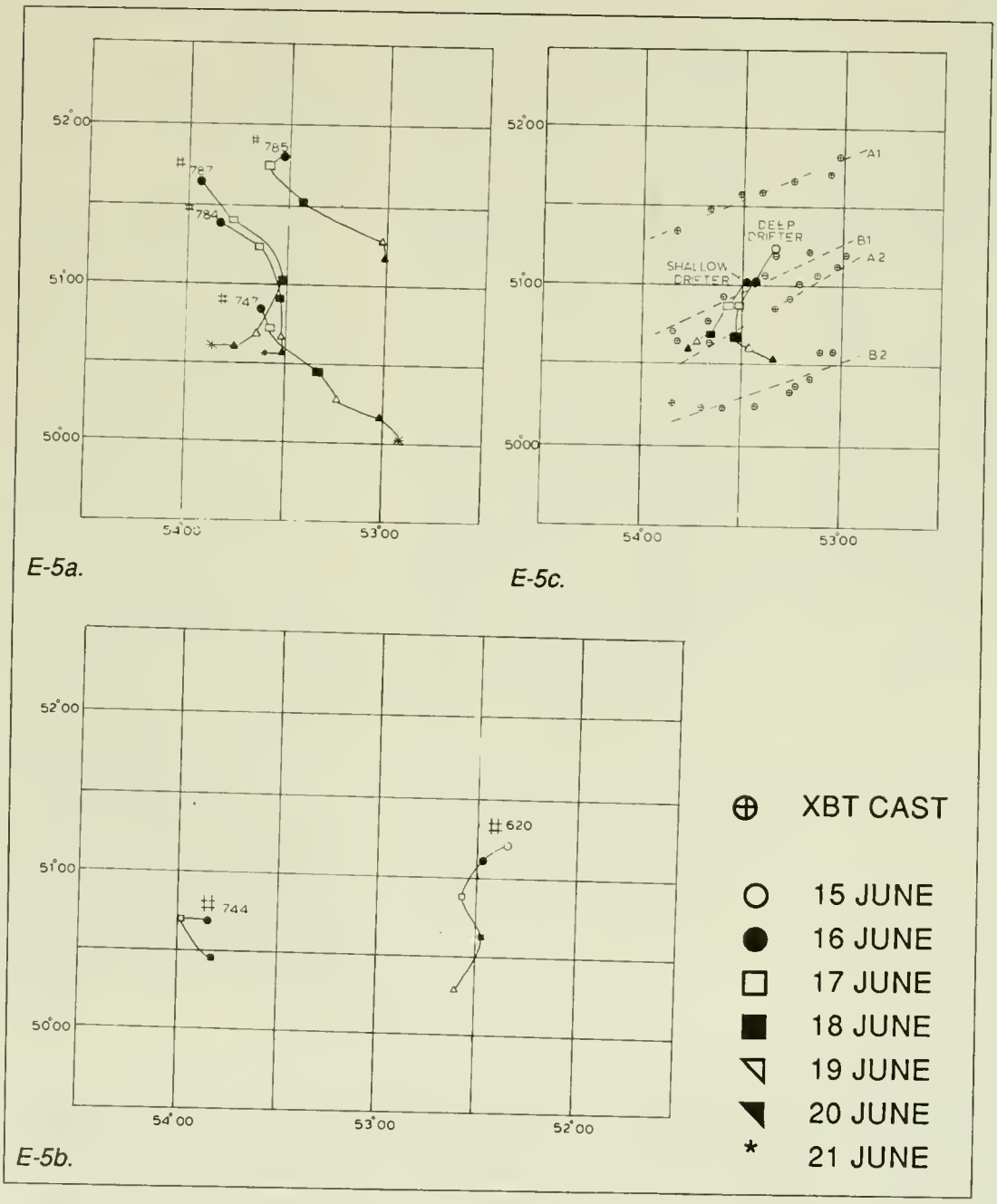

Figure E-5. Iceberg and Bathythermograph (XBT) Position Data.
Figures E-5a and E-5b show the interpolated 0000Z positions for the six icebergs studied during June 1987. The icebergs in Figure E-5a were used to evaluate the deterioration model; the icebergs in Figure E-5b were not. Figure E-5c shows the interpolated 0000Z positions for the shallow and deep-drogued drifters and the positions of the four XBT transects described in Figure E-4.

The rest of this paper evaluates modelled iceberg deterioration by examining environmental terms used in the formulae. The environmental assumptions regarding each melt process are also reviewed. Building on White's research (White et al, 1980), various observed thermal and velocity parameters are independently compared to determine which of each best represent the terms in the formulae. Using Anderson's operational computer model (Anderson, 1983), melt estimates are calculated from operational data center inputs. Figure E-6 depicts the contribution of each deterioration process to illustrate its relative importance and the changes in contribution caused by using different parameters to represent terms in formulae. The implications of error estimates for various model inputs on IIP operations are then discussed.

WARM AIR CONVECTION

Melt from warm air convection is ignored in the model. For March through mid-May, no melt is estimated for air convection. For July through September, the average melt is estimated at 8cm/day, assuming an average daily air temperature of 10°C and average wind of 37km/hr.

The daily average air temperature warmed during the study period from 6°C on 15 June to 8°C on 21 June. The average wind speed for the study period was 33km/hr. Warm air heat convection was estimated at 4cm/day.

Climatological average air temperatures for the IIP region could be used to make monthly melt estimates. Likewise, daily global-scale air temperature values could be requested from an operational data center; however, this level of effort for a relatively insignificant deterioration process seems impractical for operational forecasting purposes.

SOLAR RADIATION

The modelled melt due to solar radiation is fixed at 2cm/day, which represents the minimum melt rate for the period March through August (Anderson, 1983). The model assumes cloudy conditions.

The daylight (0800Z to 2400Z) was obscured (100%) by cloud cover or fog every day of the study except for the afternoon of 17 June and morning of 19 June. For those half day periods the skies were partly (averaged 50%) cloudy. Assuming a 35% albedo for an iceberg, the average melt rate for the June study period was 4cm/ day (White et al, 1980).

The model could be adapted to the monthly melt estimates derived by White, although the benefit would be minimal. Likewise, global-scale radiation estimates could be requested from operational data centers (COMNAVOCEANCOM, 1986); however, the level of effort to identify those periods of clear skies would only provide an additional melt of 2cm/day.

Again this level of effort for a relatively insignificant deterioration process seems impractical for operational forecasting purposes.

WATER TEMPERATURE

The model uses sea surface temperature to estimate both buoyant and forced convection contributions to iceberg melt. The melts due to buoyant and forced convection were computed as a function of observed sea surface temperature (T_o) and as a function of the in-situ temperature of the water column integrated over the estimated draft of the iceberg ($\int T_o$).

Buoyant Vertical Convection

Buoyant convection is considered solely dependent upon the "relative" temperature between a near vertical wall of ice and the water column. The cluster's average daily melt due to buoyant convection using $\int T_o$ was estimated at 2cm/day with average values for individual icebergs ranging from 1cm/day (#787) to 3cm/day (#785). The melt rate as a function of T_o averaged 7cm/day greater; with daily differences ranging from +3cm/day (#787/21 June) to +11cm/day (#747/20 June). These differences were associated with surface temperatures which were approximately 1.5°C warmer than the averaged temperature for the first ten meters of the water column.

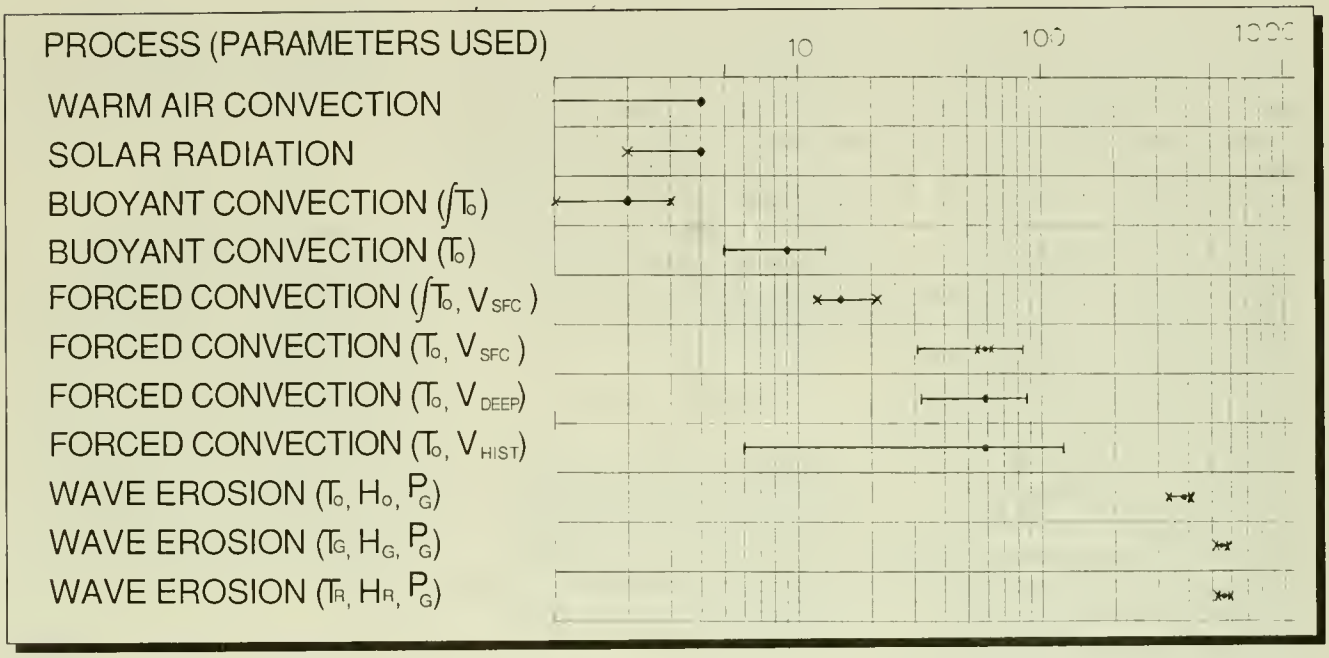

Figure E-6. COMPARISON OF ICEBERG DETERIORATION PROCESSES. This figure graphically describes both the significance of each process and the affects that different parameters have on the "melt" contribution for these processes. The "melt" contributions, which are denoted by a (•), are the five-day average for a cluster of four medium-sized, non-tabular icebergs. An (X) denotes the minimum and maximum five-day average for an individual iceberg. A (I) denotes the minimum and maximum daily "melt" for an individual iceberg.

T_o = *Observed sea surface temperature*
$\int T_o$ = *In situ temperature as a function of depth*
T_G = *Global-scale sea surface temperature product*
T_R = *Regional-scale sea surface temperature product*
H_o = *Observed significant wave height*
H_G = *Global-scale significant wave height*
H_R = *Regional-scale significant wave height*
P_G = *Global scale primary wave period product*
V(sfc) = *Differential velocity between iceberg and surface-drogued drifter*
V(deep) = *Differential velocity between iceberg and deep-drogued drifter*
V(hist) = *Differential velocity between iceberg and historical current field*

Forced Heat Convection

Forced convection is primarily dependent upon the relative temperature between iceberg and the water flowing past the iceberg. The cluster's average daily melt due to forced convection using $\int T_o$ was approximately 15cm/day with average values for individual icebergs ranging from 12cm/day (#787) to 21cm/day (#785). The melt rate as a function of T_o averaged 47cm/day greater; with daily differences ranging from +17cm/day (#784/20 June) to +69cm/day (both #747 and #784 on 18 June). These differences were associated with surface temperatures which were about 0.9°C warmer than the averaged temperature for the first ten meters of the water column.

Combined Effect in Using Sea Surface Temperature

By using sea surface temperature to derive the relative temperature term, the waterline loss could be overestimated by 20 to 80cm/day. This error represents summer conditions (surface warming). Errors for the period March through mid-May should be significantly smaller. Although the error associated with summer sea surface temperatures appears significant, it is an order of magnitude less than the sum of all modelled deterioration processes.

Subsurface temperature values can be requested from operational data centers; however, the quality of the analyses are highly dependent upon the availability of bathythermograph data. More daily observations occur in the IIP region for surface than for subsurface temperature. Additionally, the thermal structure of the water column depicted by data center products often have an accuracy no better than the temperature differences between surface and near surface values (Clancy et al, 1987). Using a subsurface temperature profile would mean substituting a known small bias in melt rate for errors which could vary as described. It would also mean a two- to four-fold increase in data input. For these reasons, IIP could not justify requesting and using subsurface temperature fields from operational data centers.

RELATIVE VELOCITY

Forced convection is also a function of relative velocity between the iceberg and the surrounding water column. The model equates relative velocity to the difference between iceberg drift and the IIP historical current in the iceberg's vicinity. The wind-induced component of the current is ignored.

Melt rates for forced convection using relative velocities derived from different current inputs were compared. The shallow-drogued drifter was assumed to represent the velocity of the water mass between the surface and the 40m thermocline, that portion of the water column which contributed most to iceberg deterioration. The relative velocity between each iceberg and the following were calculated as inputs to the model: shallow- and deep- drogued drifters, and the IIP's "master" historical current field velocity, which for the entire study area was 160°T at 23cm/sec. The deep-drogued drifter represents real-time current data which, when available, is used to "modify" the historical current. (Summy et al, 1983) Sea surface temperature was used to compute the relative temperature term. The melt rates derived using the deep-drogued drifter and "master" current as inputs were compared to the melt rate derived from the shallow-drogued drifter input.

The average daily melt due to forced convection, using iceberg drift relative to the shallow-drogued drifter, was estimated at 59cm/day with average values for individual icebergs ranging from 55cm/day (#785) to 62cm/day (#747). The melt rate as a function of iceberg drift relative to the deep-drogued drifter ranged from 25cm/day slower (#747/19 June) to 38cm/day faster (#784/20 June). Using the "master" historical current, the melt rate ranged from 53cm/day slower (#747/19 June) to 63cm/day faster (#784/20 June).

These differences in melt equated to velocity differences between the shallow-drogued drifter and the deep-drogued drifter (i.e. the "modified" current) and between the shallow-drogued drifter and the "master" current of +/- 9cm/sec

and +/- 16cm/sec respectively. In comparing the melts due to forced convection between the "master" and "modified" currents, the real-time input serves to reduce the daily differences for each iceberg by nearly half. The meteorological conditions during the study also helped to reduce the daily differences in melt between using the shallow- and deep-drogued drifter velocities. Rapid changes in the weather prevented wind direction from remaining constant (within a 60° arc of the compass) for periods longer than 27 hours; wind shifts averaged every 12 hours. Consequently, the sum of the differences for each iceberg never exceeded +/- 70cm for the study period, or an averaged error of +/- 21cm/day.

These statistics probably represent the minimum errors. In the IIP region 5- to 7-day wind events occur. An effort to control the growth of these errors may be appropriate. Wind-induced components of the current could be extracted from the dynamic iceberg drift model and substituted for the existing input. This is perceived to be a moderate level of effort for the IIP.

WAVE EROSION: GLOBAL VS REGIONAL SCALE PRODUCTS

Wave erosion, which is induced by heat convection from the turbulent maximum orbital velocity caused by the wave field surrounding the iceberg, is computed by the model. This convection is proportional to wave height (H) times relative temperature (T), and inversely proportional to wave period (P). The model assumes the effects of the wave field are non-directional, implying that the iceberg is melted uniformly from all directions (White et al, 1980). This assumption probably overestimates melt due to wave erosion. Regardless, its melt contribution is up to ten times greater than melt by forced convection, and around 100 times greater than buoyant convection. The applicability and accuracy of the environmental parameters used to model wave erosion thus greatly affect the daily melt rate estimated by the model.

The model computes T from sea surface temperature. Significant wave height and a primary wave period, which is that period associated with peak energy observed in the full wave spectrum, are currently used by the model for H and P respectively. Sea surface temperature is assumed to be the best parameter from which the relative temperature term for wave erosion is calculated, and it is readily available from data centers. Data center products representing H are significant wave height, sea height, or swell height, and products representing P are peak periods for the full, sea, or swell energy spectra (Clancy, 1987). When the model was implemented in 1983, the wave parameters currently used were the only ones available.

Table E-4 shows the differences between our observations and those analysis values produced by operational data centers: U. S. Navy Fleet Numerical Oceanography Center, Monterey, CA (FLENUMOCEANCEN); and Canadian Forces Meteorological and Oceanographic Center, Halifax, Nova Scotia (METOC). The global-scale (250km grid-spacing) analyses were produced by FLENUMOCEANCEN using its computerized Expanded Ocean Thermal Structure (EOTS) analysis and Global Spectral Ocean Wave Model (GSOWM) (COMNAVOCEANCOM, 1986). The regional-scale (estimated from 50 to 100km grid-spacing) analyses were produced by METOC Halifax. METOC depends on human interpretation of surface thermal observations and uses a parametric ocean-wave model (MacDonald et al, 1987) which is qualitatively blended with ship observations. All data center values were interpolated to each iceberg's 0000Z position. All values are for 0000Z, except for the METOC sea state analyses, which were analyzed at 1800Z. The METOC 1800Z sea state analysis normally contains more ship observations than the METOC 0000Z analysis, thereby improving the quality of the 1800Z analysis.

FLENUMOCEANCEN and METOC sea surface temperature products differed. The FLENUMOCEANCEN-produced temperatures averaged 1.3°C colder than the observed values for the cluster; the METOC-produced

temperatures were 0.6°C colder. Averaged differences between observations and FLENUMOCEANCEN products for individual icebergs ranged from 1.9°C (#784) to 0.6°C (#785) colder. The differences listed in Table E-4 which are greater than the reported system error are due to the presence of sub-scalar thermal features. In this case, iceberg #747 and #784 had crossed the surface thermal front between the colder Labrador water and the warmer Newfoundland Shelf water.

Little difference existed between the wave height products by FLENUMOCEANCEN and METOC. The FLENUMOCEANCEN-produced wave heights averaged 0.9m higher than the observed height for the cluster; the METOC-produced height was 0.8m higher. Daily differences between observed and predicted wave heights for individual icebergs ranged: from 0.3m (all/17 June) to 1.5m (#785/20 JUNE) for FLENUMOCEANCEN products; and from 0.2m (all 19 June) to 1.2m (all/18 June) for METOC products. The wave period differences in Table E-4 which exceeded system error may be based partly on the limitations of visual observations and the expertise of each observer.

The cluster's average daily melt due to wave erosion using observed values was estimated at 379cm/day with average values for individual icebergs ranging from 330cm/day (#785) to 408 cm/day (#747). The cluster's average daily melt rate using FLENUMOCEANCEN (global-scale) products averaged 152cm/day faster. Individual icebergs' average melt ranged from 144cm/day (#784) to 200cm/day (#785) faster. The cluster's average daily melt using METOC (regional-scale) products averaged 195cm/day faster. Individual iceberg's average melt ranged from 149cm/day (#785) to 218cm/day (#787) faster.

Table E-4. Average Difference Between Data Center Products and Observations.

		OBSERVED - FLENUMOCEANCEN			OBSERVED - METOC	
Date 0000Z	# of Icebergs	SST (°C)	Wave HT (m)	Wave PD (sec)	SST (°C)	Wave HT (m)
15 JUN	2	+1.1	-1.2	-8 (2)	+0.5	-0.9
16JUN	5	+0.7	-0.9	-5 (5)	+1.0	-0.6
17 JUN	5	+0.3	-0.3	-5 (5)	+0.5	-0.6
18 JUN	6	+1.0	-0.9	-4	+0.2	-1.2
19 JUN	5	+1.5 (2) *	-0.9	-2	-0.1	-0.3
20 JUN	4	+1.8 (2)	-1.2	-4 (1)	+0.2	-0.9
21 JUN	3	+2.5 (2)	-0.6	-2	+0.7	-1.2

**Note: Numbers in parentheses indicate number of times a value was outside the following error bounds:*

SST +/- 1.6°C *Wave Height +/- 1.8 m* *Wave Period +/- 4 sec*

The higher melt estimate derived from using either FLENUMOCEANCEN or METOC products was a function of their higher wave height analyses. The melt estimate using FLENUMOCEANCEN products appeared better than METOC because the underestimation of the temperature analyses offset the overestimation in the wave height analyses. The model's sensitivity to wave height makes that term just as important as the temperature term.

The significant overestimation of wave erosion justifies IIP seeking better temperature and wave data from operational data centers. Regional-scale temperature analyses are available and could reduce the variable error associated with features (i.e. the Labrador Current) which are sub-scaler to the analysis grid. Unfortunately, no digital product is presently available for regional-scale wave analyses. However, the global-scale sea height and associated peak period may reduce the bias evident in the global-scale significant wave height data. Any shift to new inputs should be evaluated by IIP to determine the combined effect of input errors before their final acceptance for operational use.

SUMMARY

Table E-5 summarizes the deterioration processes examined by this paper. For this ensemble of medium-sized, non-tabular-shaped icebergs, a daily melt rate was estimated by the model to be 4.0 m/day. Using FLENUMOCEANCEN products, the melt rate was overestimated by 1.7 m/day. METOC products overestimated the melt by 2.2 m/day. These melt estimates are of the same magnitude as the iceberg sizing error. Because of the short duration of the study, no firm conclusions could be drawn from the observed iceberg measurements. Icebergs #785 and #787, which were the only icebergs to constantly decrease in length and height throughout the study period, appeared to have melted faster than the predictions based on the optimum, observed environmental parameters. Melt predictions based on data center products were within measurement error bounds.

Sea surface temperature appears to be a suitable input for calculating the relative temperature term. In this study the use of sea surface temperature to solely represent the relative temperature term vice using temperature versus depth to represent the term for buoyant and forced convection, caused the melt rate to be overestimated by 12%. Global-scale thermal products cannot adequately represent the Labrador Current. Regional-scale temperature products currently available can improve the resolution of the temperature data.

Oversimplification by IIP of methods used to derive the relative velocity between icebergs and the surrounding water contributed to an error of up to 16% of total melt. Because the wind-induced component of the ocean surface layer (between the surface and 50m depth) is computed in the IIP iceberg drift model, this velocity component could be added to the "modified" or historical surface current. The resultant current value could then be used to compute relative velocity to reduce the magnitude of this error.

Wave height overestimation causes daily melt to be overestimated. This significant (about 38% of total melt) error in determining the wave erosion contribution probably compensates for the model's inability to represent all deterioration processes. New wave products that have recently become available should improve the melt estimate due to wave erosion.

The iceberg sizing method and study time constraints made comparisons of model estimations to observed lengths inconclusive. Either a better method must be used in future studies or studies must be extended over much longer periods (14-21 days). Given the potential for errors associated with operational reconnaissance, which depends heavily on arbitrary size classifications, and the inability to model all deterioration processes, the IIP policy to require icebergs to deteriorate 175% of their original length is prudent.

Table E-5: Average Melt Rate for Various Inputs.

MODEL TERMS	PARAMETERS USED				
Relative Temperature	$\int T_O$	T_O	T_O	T_G	T_R
Relative Velocity	V(sfc)	V(sfc)	V(deep)	V(sfc)	V(sfc)
Wave Height	H_O	H_O	H_O	H_G	H_R
Wave Period	P_O	P_O	P_O	P_G	P_R
DETERIORATION PROCESSES	**MELT RATE (cm/day) USING ABOVE PARAMETERS**				
Warm Air Convection	4	4	4	2	2
Solar Radiation	4	4	4	0	0
Buoyant Radiation	2	9	9	6	8
Forced Convection	15	62	6-122	33	41
Wave Erosion	379	379	379	531	574
Total Average Melt	404	458	402-520	572	625

T_O = Observed sea surface temperature
$\int T_O$ = In situ temperature as a function of depth
T_G = Global-scale sea surface temperature product
T_R = Regional-scale sea surface temperature product
H_O = Observed significant wave height
H_G = Global-scale significant wave height
H_R = Regional-scale significant wave height
P_G = Global-scale primary wave period product
V(sfc) = Differential velocity between iceberg and surface-drogued drifter
V(deep) = Differential velocity between iceberg and deep-drogued drifter

ANDERSON, I., 1983. Iceberg Deterioration Model. *Report of the International Ice Patrol in the North Atlantic Ocean, Season of 1983, (CG-188-38)*, p 67-73.

ANDERSON, I., 1985. Oceanographic Conditions On The Grand Banks During The 1985 IIP Season. *Report of the International Ice Patrol in the North Atlantic Ocean, Season of 1985, (CG-188-40)*, p 56-67.

CLANCY, R. M., B. L. SAMUELS, and K. D. POLLACK, 1987. Technical Description Of The Optimum Thermal Interpolation System (OTIS): A Model For Oceanographic Data Assimilation. Fleet Numerical Oceanography Center Tech Note 422-86-02, 22 May 1987. pp 110.

CLANCY, R. M., 1987. Real-Time Applied Oceanography At The Navy's Global Center. *Marine Technology Society Journal*, Vol 21, No 4, December 1987, p 33-46.

EL-TAHAN, M., S. VENKATESH, and H. EL-TAHAN, 1987. Validation and Quantitative Assesment Of The Deterioration Mechanisms Of Arctic Icebergs. *Journal of Offshore Mechanics and Arctic Engineering*, February 1987, Vol 109, p 102-108.

MACDONALD, K. A., and S. CLODMAN, 1987. The AES Parametric Ocean-Wave Forecast System. *Proceedings of the International Workshop on Wave Hindcasting Forecasting. Report 065.* Environmental Studies Revolving Funds, Ottawa, pp 119-132.

MOUNTAIN, D. G., 1980. On Predicting Iceberg Drift. *Cold Region Science and Technology*, Vol I (3/4), p 273-282.

ROBE, R. Q., 1975. Height To Drift Ratios Of Icebergs. *Proceedings of the Third International Conference on Port and Ocean Engineering Under Arctic Conditions*, 11-15 August 1975, Vol I, p 407-415.

SUMMY, A. D. and I. ANDERSON, 1983. Operational Uses Of TIROS Oceanographic Drifters By the International Ice Patrol (1978-1982). *Proceedings 1983 Symposium On Buoy Technology*, 27-29 April 1983, p 246-250.

WHITE, F. M., M. L. SPAULDING, and L. GOMINHO, 1980. Theoreti cal Estimates Of The Various Mechanisms Involved In Iceberg Deterioration In The Open Ocean Environment. Report CG-D-62-80, U. S. Coast Guard Research and Development Center, Groton, Connecticut 06340-6096, pp126.

Numerical Environmental Products Manual, Vol II, August 1986 Prepared under authority of Commander, Naval Oceanography Command, Stennis Space Center, Mississippi 39525, pp 200.

Appendix F

Evaluation of Shipboard Visual Estimation of Iceberg Size

LCDR Walter E. Hanson, USCG

INTRODUCTION

During 1987, approximately 21 per cent of all sightings entered into the International Ice Patrol (IIP) computer were from visual ship observations. Shipping has each year contributed a significant number of visual sightings. Many studies have assessed the ability of ships to detect icebergs, primarily by radar (Budinger, 1960; Ryan et al, 1985; and Harvey et al, 1986). However, little information is known about the sizing accuracy of visual sightings. Consequently, the 1987 iceberg IIP iceberg deterioration study, described in Appendix E, presented an opportunity to evaluate the ability of shipboard observers to visually estimate iceberg size.

This study evaluates visual sizing efforts which had neither the aid of visual cues (i.e. an object in close proximity for size comparison) nor the aid of stadimeter or sextant. This sizing technique may mirror that of the shipping community. The icebergs studied by IIP were primarily medium-sized, non-tabular shaped. This category of iceberg seems to be the most often sighted by shipping.

BACKGROUND

The IIP uses iceberg size and shape in sighting reports to predict their drift and deterioration. For operational purposes, only seven different categories of icebergs are modelled (Mountain, 1980). They are:

- Growler
- Small, Non-Tabular
- Small, Tabular
- Medium, Non-Tabular
- Medium, Tabular
- Large, Non-Tabular
- Large, Tabular

Drift and deterioration predictions are computed twice daily using computerized models. Iceberg size is used differently by the two models.

In the drift model, the size and shape parameters together select one of seven profiles. Each profile is a different cross-sectional representation of above-surface and sub-surface area. The profile represents the average dimensions for icebergs in that size and shape category. The iceberg is drifted based on the forces acting upon the profile. The profile is not changed until a new size and/or shape is specified.

In the deterioration model, the size and shape parameters together select one of seven waterline lengths. The model calculates "melt" in terms of length instead of mass. Each of the seven lengths is assumed to be the maximum value for the particular size and shape category. Environmental conditions and waterline length are then used as inputs for the daily "melt" of the iceberg.

DATA COLLECTION

The USCGC TAMAROA, a 68 m (205 ft) U. S. Coast Guard cutter, was used for the 6.3 day study. Visual observations were made from the bridge wing; height of eye was 10.8 m. Two IIP ice observers, who each had at least two years of aerial iceberg reconnaissance experience, made the observations.

Iceberg above the waterline dimensions were measured during daylight (from 0800Z to 2400Z) in all weather and light conditions. Table F-1 shows the hours when iceberg sizing occurred. Iceberg shape and size were both estimated by the ice observers and calculated from photographic images scaled according to rangefinder measurements. This required a 360 degree look at each iceberg; measuring and photographing all prominent faces. Measurements were accurate to +/- 8% of the observed dimensions; see Table F-1.

The cutter circled each iceberg twice; once to identify the prominent faces; and during the second pass, to make measurements. When perpendicular to each face the true bearing and laser-derived distance to it were recorded, a

Table F-1. TIMES OF ICEBERG SIZING MEASURMENTS. Dates and times to the nearest hour when icebergs were sized are listed. Iceberg numbers refer to the sequential numbering system that IIP uses to track individual icebergs during the course of the ice season.

ICEBERG # DATE/TIME	620	747	744	784	785	787
14 June	22Z	-	-	-	-	-
15	19Z	00Z/21Z	23Z	16Z	08Z	-
16	15Z	17Z	19Z	13Z	09Z	-
17	20Z	21Z	23Z	17Z	12Z	16Z
18	22Z	-	-	16Z	11Z	18Z
19	18Z	16Z	-	10Z	-	08Z
20	-	-	-	13Z	09Z	18Z
21	-	00Z/08Z	-	-	-	-

photograph taken, and the scalar dimensions recorded. (Scalar dimensions were converted to length and height after all the field work was completed.) At the end of the second pass, the ice observers collectively estimated the iceberg's maximum height and length. No visual cue, like a ship's boat or another vessel, was available to help size the iceberg; only the horizon, when weather permitted. Neither stadimeters nor sextants were used.

Iceberg size measurements were conducted within 1900 m of each iceberg; distances for each observation are listed in Table F-2. These distances were dependent upon weather and the ability to view/measure the entire face of the iceberg through the reticulated binoculars.

STUDY FINDINGS

Thirty-one visual estimations of both height and length were compared to measured dimensions. The results indicated that the trained observer tended to underestimate both length and height.

All but one of the visually-estimated lengths were less than the measured length; see Figure F-1a. For this set, a linear regression indicated the estimated length was about 56 per cent of the measured length. The data set's linear correlation was 0.72.

The observers better estimated height. All but seven of the visually-estimated heights were less than the measured height; see Figure F-1b. For this set, the regression indicated the estimated height was about 66 per cent of the measured height. The correlation was 0.81.

CONCLUSIONS

Visual observations made close to medium-sized, non-tabular icebergs without the aid of measurement devices (i.e. stadimeters, sextants, or reference objects) may underestimate their size. Therefore, if an iceberg appears on the border between two size categories, the IIP recommends assigning the iceberg to the larger of the two size categories. Given the difficulty in properly estimating size, IIP encourages the use of all measurement devices at one's disposal.

Table F-2. DISTANCE AT WHICH ICEBERG SIZING MEASUREMENT MADE. The beginning and ending distance in meters from the iceberg are listed.

ICEBERG # DATE/TIME	620	747	744	784	785	787
14 June	890-620	-	-	-	-	-
15	490-310	1880-1160	300-260	517-390	960-710	-
		580-380				
16	1060-870	1190-940	1280-930	1130-710	780-550	-
17	720-550	1070-700	1350-690	1210-990	1270-990	1350-980
18	1040-750	-	-	1340-1050	1020-860	1230-710
19	1370-580	1140-850	-	1450-810	-	700-540
20	-	-	-	1430-870	790-570	560-420
21	-	1360-860	-	-	-	-
		1780-570				

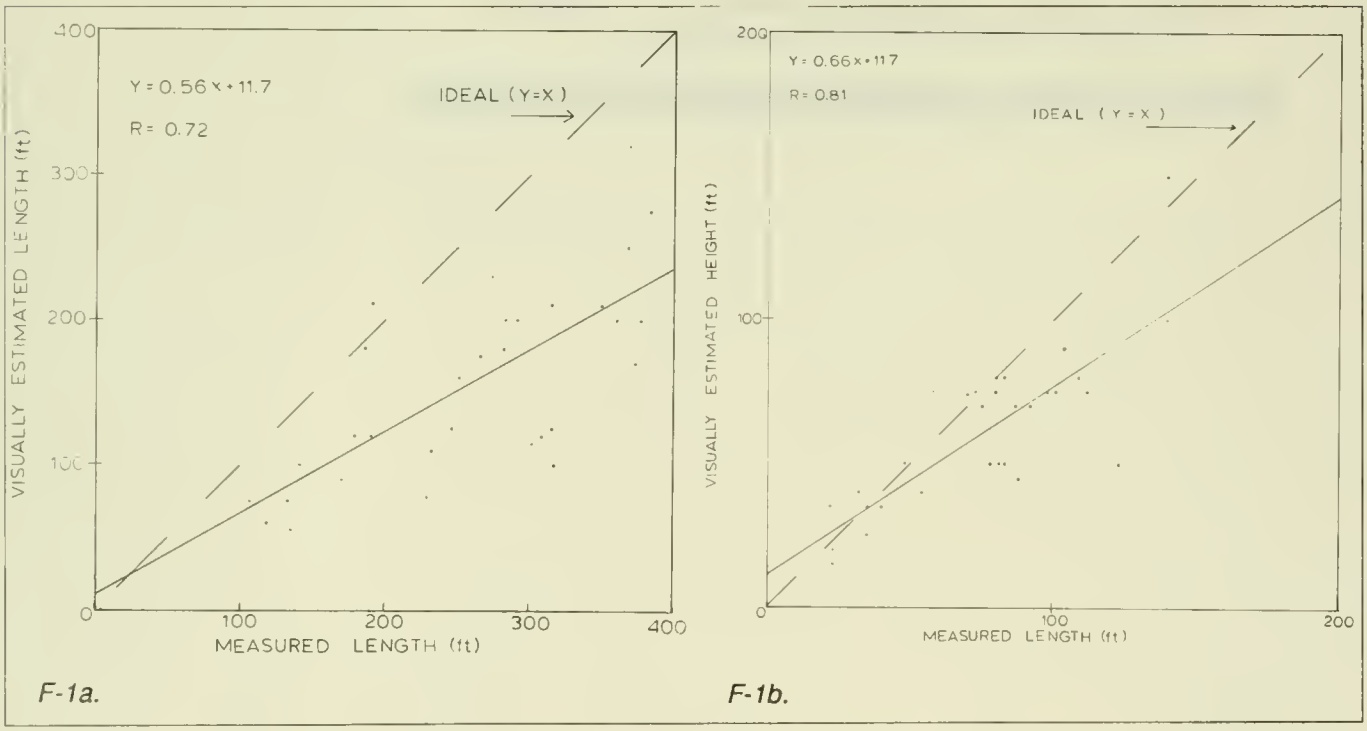

Figure F-1. VISUAL ESTIMATION VS. ACTUAL MEASUREMENTS. These scatter diagrams show the estimated and the measured dimensions of icebergs sized during the IIP June 1987 iceberg deterioration study. The linear regression is the solid line; its equation (in which Y = estimated feet and X = measured feet) and its correlation coefficient are in the upper lefthand corner. The ideal condition (estimated = measured) is shown by the dashed line.

Figure F-1a compares estimated vs measured lengths; Figure F-1b compares heights.

REFERENCES

Budinger, T. F., 1960. Iceberg Detection by Radar. *International Ice Observation And Ice Patrol Service In The North Atlantic Ocean, Season of 1959*, Bulletin No. 45, p 49-97.

Ryan, J. P., M. J. Harvey, and A. Kent, 1985. Assessment Of Marine Radars For The Detection Of Ice And Icebergs. Environmental Studies Revolving Funds Report 008, Ottawa pp 127.

Harvey, M. J. and J. P. Ryan, 1986. Further Studies On The Assessment Of Marine Radars For The Detection Of Icebergs. Environmental Studies Revolving Funds Report 035, Ottawa pp 82.

Mountain, D. G., 1980. On Predicting Iceberg Drift. *Cold Region Science And Technology*, Vol I (3/4) p 273-282.

U. S. GOVERNMENT PRINTING OFFICE 1989/601-414/00022

4221 035